



**Max-Planck-Institut
für Kolloid- und Grenzflächenforschung**



A model for sigma factor competition in bacterial cells

Dissertation

zur Erlangung des akademischen Grades

“doctor rerum naturalium”

(Dr. rer. nat.)

in der Wissenschaftsdisziplin “Theoretische Biologische Physik”

eingereicht an der

Mathematisch-Naturwissenschaftlichen Fakultät

der Universität Potsdam

angefertigt in der

Abteilung Theorie und Bio-Systeme

am Max-Planck-Institut für Kolloid- und Grenzflächenforschung

von

Marco Mauri

Potsdam, Juni 2014

This work is licensed under a Creative Commons License:
Attribution 4.0 International
To view a copy of this license visit
<http://creativecommons.org/licenses/by/4.0/>

Published online at the
Institutional Repository of the University of Potsdam:
URL <http://publishup.uni-potsdam.de/opus4-ubp/frontdoor/index/index/docId/7209/>
URN <urn:nbn:de:kobv:517-opus4-72098>
<http://nbn-resolving.de/urn:nbn:de:kobv:517-opus4-72098>

*A mio nonno Carlo, con amore.
Grazie per avermi stretto la mano
così a lungo*

Abstract

Bacteria respond to changing environmental conditions by switching the global pattern of expressed genes. In response to specific environmental stresses the cell activates several stress-specific molecules such as sigma factors. They reversibly bind the RNA polymerase to form the so-called holoenzyme and direct it towards the appropriate stress response genes. In exponentially growing *E. coli* cells, the majority of the transcriptional activity is carried out by the housekeeping sigma factor, while stress responses are often under the control of alternative sigma factors. Different sigma factors compete for binding to a limited pool of RNA polymerase (RNAP) core enzymes, providing a mechanism for cross talk between genes or gene classes via the sharing of expression machinery. To quantitatively analyze the contribution of sigma factor competition to global changes in gene expression, we develop a thermodynamic model that describes binding between sigma factors and core RNAP at equilibrium, transcription, non-specific binding to DNA and the modulation of the availability of the molecular components.

Association of housekeeping sigma factor to RNAP is generally favored by its abundance and higher binding affinity to the core. In order to promote transcription by alternative sigma subunits, the bacterial cell modulates the transcriptional efficiency in a reversible manner through several strategies such as anti-sigma factors, 6S RNA and generally any kind of transcriptional regulators (e.g. activators or inhibitors). By shifting the outcome of sigma factor competition for the core, these modulators bias the transcriptional program of the cell. The model is validated by comparison with *in vitro* competition experiments, with which excellent agreement is found. We observe that transcription is affected via the modulation of the concentrations of the different types of holoenzymes, so saturated promoters are only weakly affected by sigma factor competition. However, in case of overlapping promoters or promoters recognized by two types of sigma factors, we find that even saturated promoters are strongly affected.

Active transcription effectively lowers the affinity between the sigma factor driving it and the core RNAP, resulting in complex cross talk effects and raising the question of how their *in vitro* measure is relevant in the cell. We also estimate that sigma factor competition is not strongly affected by non-specific binding of core RNAPs, sigma factors, and holoenzymes to DNA. Finally, we analyze the role of increased core RNAP availability upon the shut-down of ribosomal RNA transcription during stringent response. We find that passive up-regulation of alternative sigma-dependent transcription is not only possible, but also displays hypersensitivity based on the sigma factor competition. Our theoretical analysis thus provides support for a significant role of passive control during that global switch of the gene expression program and gives new insights into RNAP partitioning in the cell.

Zusammenfassung

Bakterien reagieren auf Änderungen in ihren Umgebungsbedingungen indem sie global das Genexpressionsprogramm umschalten. Die Zelle aktiviert, als spezifische Reaktion auf Stressbedingungen, mehrere charakteristische Moleküle wie zum Beispiel die Sigmafaktoren. Diese binden reversibel an die RNA Polymerase (RNAP), mit der sie einen Komplex bilden das sogenannte Holoenzym und steuern sie als Reaktion auf den Stress zu den entsprechenden Genen. In exponentiell wachsenden *E. Coli* Zellen wird das Meiste der Transkription von einem sogenannten Haushaltssigmafaktor organisiert. Wohingegen Stressreaktionen häufig von alternativen Sigmafaktoren kontrolliert werden. Die verschiedenen Sigmafaktoren konkurrieren um einen begrenzten Pool von RNAP Coreenzymen, womit die Expression einzelner Gene oder Genklassen beeinflusst wird, da sie sich die Maschinerie teilen. Um den Beitrag der Sigmafaktorkonkurrenz an der gesamten Veränderung der Genexpression quantitativ zu analysieren, haben wir ein theoretisches Modell entwickelt, welches das Binden von Sigmafaktoren mit RNAP Coreenzymen im Gleichgewicht, die Transkription, das nichtspezifische Binden an die DNA sowie die Modulation verfügbarer molekularer Komponenten beschreibt.

Normalerweise wird die Assoziation des Haushaltssigmafaktors mit dem RNAP Coreenzym begünstigt durch dessen grosse Anzahl und die hohe Bindungsaffinität. Daher nutzen bakterielle Zellen verschiedene, reversible Strategien um die Transkription durch alternative Holoenzyme zu fördern. Dazu gehören Anti-Sigmafaktoren, 6S RNA und generell beliebige Transkriptionsregulatoren (z.B.: Aktivatoren oder Repressoren). Sie beeinflussen das Transkriptionsprogramm der Zelle indem sie das Resultat der Sigmafaktorkonkurrenz um die RNAP Coreenzyme zugunsten eines der Sigmafaktoren verschieben. Das Modell kann validiert werden durch Vergleiche mit *in vitro* Konkurrenzexperimenten, die exzellente Übereinstimmung zeigen. Wir können feststellen, dass die Transkription durch Konzentrationsänderungen der verschiedenen Holoenzyme beeinflusst wird, daher ist der Effekt der Sigmafaktorkonkurrenz klein bei saturierten Promotoren. Was sich jedoch ändert bei sich überlappenden Promotoren oder Promotoren, die von zwei verschiedenen Sigmafaktoren erkannt werden. In diesen Fällen sehen wir einen grossen Effekt.

Transkription führt zu effektiv abgesenkter Affinität zwischen den zugehörigen Sigmafaktoren und den RNAP Coreenzymen, was zu komplizierten Verhalten führt und die Frage aufwirft, inwieweit *in vitro* gemessene Effekte in der Zelle wiederzufinden sind. Wir können den Einfluss nichtspezifischen Bindens der RNAPs, der Sigmafaktoren und der Holoenzyme an die DNA abschätzen. Als letztes analysieren wir die Konkurrenz während der "Stringent Response". Hierbei wird die Transkription der ribosomalen RNA unterbrochen was die Anzahl der freien RNAP Coreenzyme stark erhöht. Wir sehen, dass das passive Hochregeln des alternativen sigmafaktorabhängigen Transkriptionsprogramms durch Sigmafaktorkonkurrenz möglich und sogar hypersensitiv ist. Unsere theoretische Analyse zeigt, dass die passive Kontrolle in diesem Fall eine signifikante Rolle im globalen Umschalten des Transkriptionsprogramms spielt und liefert neue Erkenntnisse zur RNAP Partitionierung in der Zelle.

Short summary for non-specialists

One way in which cells adapt to adverse environmental conditions is by changing their composition and structure. The information to perform this task is stored into classes of “genes”, that are read by the RNA polymerase through the process of transcription. To switch the global pattern of expressed genes in response to specific environmental stresses, the cells (and specifically bacteria) activate several specific molecules named sigma factors. They reversibly bind to the RNA polymerase and direct it towards the appropriate stress response genes. During the phase of growth, the majority of the transcriptional activity is carried out by the so-called housekeeping sigma factor, while stress responses are often the control of alternative sigma factors. In the cell the amount of RNA polymerase is limited, for this reason housekeeping and alternative sigma factors have to compete to bind it. The outcome of this competition provides an important mechanism for the global switch of the transcriptional program and thus for the survival of the organism during conditions of stress. The effect on the the genes of sharing RNA polymerase among different sigma factor species has not yet been completely understood. Besides that, competition can be affected in a complex way by several regulatory molecules that are present inside the cell. To shed light on this mechanism, we have studied the influence of the sigma factor competition for binding to the RNA polymerase on the gene expression by using a theoretical (thermodynamic) model. Here, we show that such competition provides a (passive) system for a positive regulation of the stress genes and thus for bacterial adaptation. Moreover, our model, by providing a quantitative description of the system, can be used to address others competitive processes in the cell and to help design biological devices in the field of synthetic biology.

Publications related to this thesis

- A model for sigma factor competition in bacterial cells.
M. Mauri and S. Klumpp
PLoS Comp. Biol. 10, e1003845 (October 2014)

Author contributions. The project was planned by M. Mauri and S. Klumpp. The theoretical analysis was carried out by MM. The paper was written by MM and SK.

This paper is based on the following sections of this thesis: 1.4, 2, 3.4, 3.3, 4, 4.1, 4.2.2, 4.3, 5, Appendix A.

Contents

1	Introduction	1
1.1	Bacterial transcription	2
1.2	Sigma factor competition	3
1.3	Stringent response	7
1.4	Motivation and overview	9
2	Model for sigma factor competition	11
2.1	One sigma factor species binding to RNAP	13
2.2	Sigma factors competition for binding RNAP	16
2.3	Comparison with the experiments	23
2.4	Summary	27
3	Modulation of sigma factor competition by regulatory factors	29
3.1	Anti-sigma factors	30
3.1.1	Anti-sigma factor binding to cognate sigma factor	30
3.1.2	Modulation of competition by anti-sigma factor	31
3.1.3	Anti-anti-sigma factors	32
3.2	6S RNA	34
3.2.1	Binding of 6S RNA to the housekeeping holoenzyme	34
3.2.2	Modulation of sigma factor competition by 6S RNA	35
3.3	Non-specific DNA binding	37
3.3.1	Non-specific binding with of one sigma factor species	38
3.3.2	Modulation of sigma factor competition by non-specific DNA binding	39
3.4	Transcript elongation	41
3.4.1	Transcript elongation with one sigma factor species	42
3.4.2	Modulation of competition by transcript elongation	45
3.5	Transcript elongation - Extensions	48
3.5.1	RNAP may slide to find the promoter target	49
3.5.2	Modulation of transition to open complex	50
3.5.3	Shared promoter/overlapping promoters	51

3.5.4	Transcriptional pauses and promoter clearance	51
3.5.5	Transcription factors: repressors and activators	53
3.5.6	Tethered sigma factor to core during elongation	55
3.5.7	Sigma factor may rebind to the elongating complex	57
3.5.8	Terminators and anti-terminators of transcription	59
3.6	Competition and regulatory factors	61
3.7	Summary	63
4	Stringent response	65
4.1	Increased core availability	66
4.2	Response factor	68
4.2.1	Definition	68
4.2.2	Free binding case	71
4.2.3	Response factor in the presence of regulatory factors	72
4.2.4	Response factor R_E	73
4.3	Cumulative effects of an increased amount of cores and alternative sigma factors on the competition	74
4.4	Synthesis rate	76
4.5	Different stringent/stress response scenarios	80
4.6	RNAP partitioning	82
4.7	ppGpp may weaken binding affinity between housekeeping sigma factor and core RNAP	84
4.8	Summary	86
5	Summary and outlook	91
5.1	Summary and discussion	91
5.2	Outlook	96
A	Values of the parameters used in the simulations	99
A.1	Average volume	99
A.2	RNAPs and sigma factors	99
A.3	Holoenzyme dissociation constants	103
A.4	Anti-sigma factors	108
A.5	6S RNA	108
A.6	Non-specific binding	109
A.7	Specific binding to promoters and elongation	111
B	Competition between two sigma factor species to bind to RNAP - Analytical results	113
B.1	Case I	114
B.2	Case II	115

B.3	Case III	115
B.4	Union of cases I, II, and III	116
B.5	Case IV	117
B.6	Case V	118
B.7	Case VI	119
B.8	Case VII	120
B.9	Union of cases V, VI, and VII	120
B.10	Case VIII	121
C	Analytical results in the presence of regulatory factors	123
C.1	Anti-sigma factor	123
C.1.1	Anti-sigma factor during sigma factor competition	123
C.2	6S RNA	127
C.2.1	6S RNA in the presence of the only σ^{70}	127
C.2.2	6S RNA during sigma factor competition	128
C.3	Non-specific binding	132
C.3.1	Response factor with one sigma factor species	132
C.3.2	Non-specific binding during sigma factor competition	132
C.4	Transcript elongation	133
C.4.1	Holoenzyme formation with one sigma factor species	133
C.4.2	Transcript elongation during sigma factor competition	134
C.5	Onset of sigma factor competition	134
D	Response factor	137
D.1	R_X	137
D.2	R_E during sigma factor competition	138
D.3	$R_{\sigma^{Alt}}$ during sigma factor competition	141
E	Values of the parameters used in the simulations of the shift from exponential growth to stationary phase	143
E.1	RNAPs and sigma factors	145
E.2	6S RNA	145
E.3	Specific binding to promoters and elongation	145
E.4	Non-specific binding	147
E.5	Results of the simulations	148
	List of symbols	149
	Acknowledgements	153
	Bibliography	155

Chapter 1

Introduction

This thesis studies the effects of competition between sigma factors for binding the limited amount of RNA polymerases on the global switches of the genetic expression program in bacteria. Sigma factors are environmental-sensitive detachable subunits of the RNA polymerase, needed for initiation of gene transcription.

Bacteria are the structurally simplest and the most abundant form of life on Earth. They are unicellular organisms characterized by the absence of nucleus or membrane-bound organelles within the cell membrane. Genetic information is stored in DNA, a double stranded nucleic acid composed of subunits called nucleotides. The direction of the genetic information's flow in the cell is described by the central dogma of molecular biology [1, 2], illustrated in the diagram of Figure 1.1. The fundamental processes consist of DNA replication, that makes another copy of the genome by using the DNA polymerase enzyme, of transcription, where the enzyme RNA polymerase (RNAP) produces a primary transcript RNA (usually single stranded nucleic acid) by using as template one strand of the DNA, and translation, in which the ribosomes synthesize

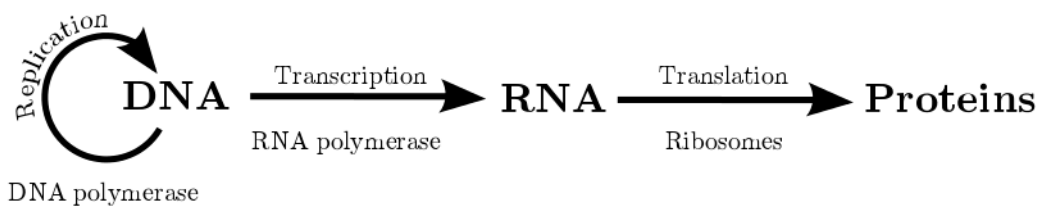


Figure 1.1: The central dogma states that the DNA genetic information can be inherited (the DNA polymerase replicates the DNA) or transferred (the RNA polymerase transcribes DNA into RNA that is translated into proteins by ribosomes) but the flow of information from DNA to protein is irreversible.

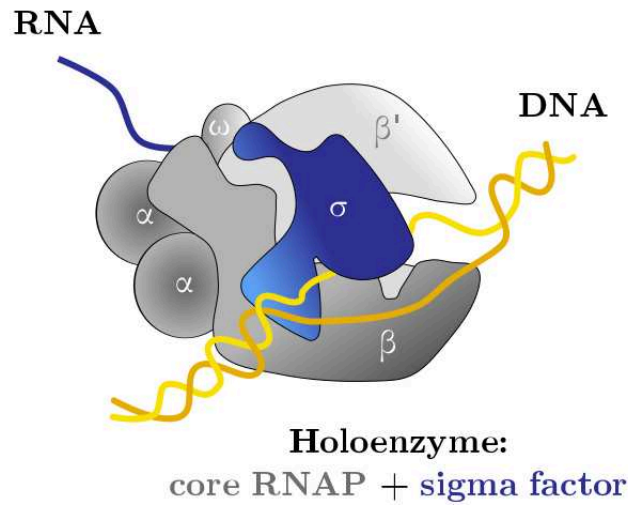


Figure 1.2: The holoenzyme is made up of a core RNA polymerase (in grey, with subunits β , β' , ω and two α , for a total molecular weight of 400 kDalton) and a sigma factor (in blue). During the transcription, the RNAP unwinds the double stranded DNA that slides through the active sites and is transcribed into a single stranded RNA.

the polypeptide chain consisting of amino acid residues that forms the proteins. This mechanism, basically, converts the contents of the genome into functional proteins that implement the cellular tasks. A DNA sequence necessary either for the synthesis of a protein, or that codes a specific RNA (*e.g.* tRNA, rRNA), is called a gene. In the following, we are interested just in two major species of RNA: messenger RNA (mRNA), that codes for proteins, and ribosomal RNA (rRNA), that forms the basic structure of the ribosomes. Groups of genes whose products have related functions and which are transcribed as a unit are called operons. Operons are controlled by the same promoter, a specific region of DNA from which the RNAP initiates the transcription process.

1.1 Bacterial transcription

Bacterial stress response. Bacteria survive successfully in many different - and often changing - environments. Adaptability implies the coding of all the equipment necessary to survive under these conditions. However, since biosynthesis is costly, the bacterial cell must on the one hand produce only those tools that are required in a specific condition and on the other hand cleverly distribute finite transcription (and also translation) machinery among different processes, that in turn request them.

Transcription. Even though the regulation of the genetic information flow can take place at any stage, transcription is a primary mechanism for the cellular decision making because it is the point at which the cell decides the expression of different genes and, as consequence, regulates protein production. The bacterial RNA polymerase is the enzyme that synthesizes the RNA by using the DNA as a template. The complete RNAP or holoenzyme consists of multiple subunits, shown in Figure 1.2: the core enzyme ($\alpha_2\beta\beta'\omega$) and an environment-sensitive unit, the sigma factor (σ). The β and β' subunits form the enzyme's active center that accounts for the RNA catalysis, where the DNA slides through, the nucleotide triphosphate (NTP) accommodates in the active sites and the nascent RNA leaves the enzyme. The sigma protein is a transcription initiation factor that associates reversibly to the core and alters the specificity of the RNAP for the promoter and thus is responsible for the recognition of a specific cognate promoter class. In this way sigma factors regulate globally the transcription in bacterial cell.

The transcription cycle consists of basically three stages, illustrated in green in Figure 1.3: initiation, elongation and termination. During initiation, the RNAP recognizes the promoter and forms a closed complex with the double-stranded DNA, then locally unwinds the DNA helix to form the open complex (transcription bubble). The new state is energetically favored compared to the initial binding and, hence, does not require any ATP hydrolysis. In the initiation phase, the RNAP and the DNA undergo reversible structural changes; single-stranded DNA acts as template for complementary base pairing with the incoming ribonucleotides and the RNAP makes short transcripts while it is still bound to the promoter, often experiencing successive rounds of abortive initiations. When the holoenzyme succeeds in clearing the promoter, during early elongation, the interaction between the core RNAP and the sigma factor weakens and σ is stochastically released [3]. The translocation of the RNA polymerase with the transcription bubble and the RNA chain formation characterizes the elongation process, that ends when the enzyme encounters and recognizes a termination sequence. Upon termination, the elongation complex dissociates into DNA template, RNA chain and free RNAP that can reassociate with a free sigma factor to form a holoenzyme and begin again the process of transcription. The release of sigma factor during each round of transcription provides the central mechanism for RNAP reprogramming and cognate promoter regulation [4].

1.2 Sigma factor competition

Sigma factor. A housekeeping sigma factor is required for most transcription during growth (σ^{70} in *Escherichia coli* and σ^A in *Bacillus subtilis*), while other sigma factors act as master regulators during stress responses such as heat shock or entry to stationary phase (σ^H and σ^S , respectively in *E. coli*) or for developmental programs

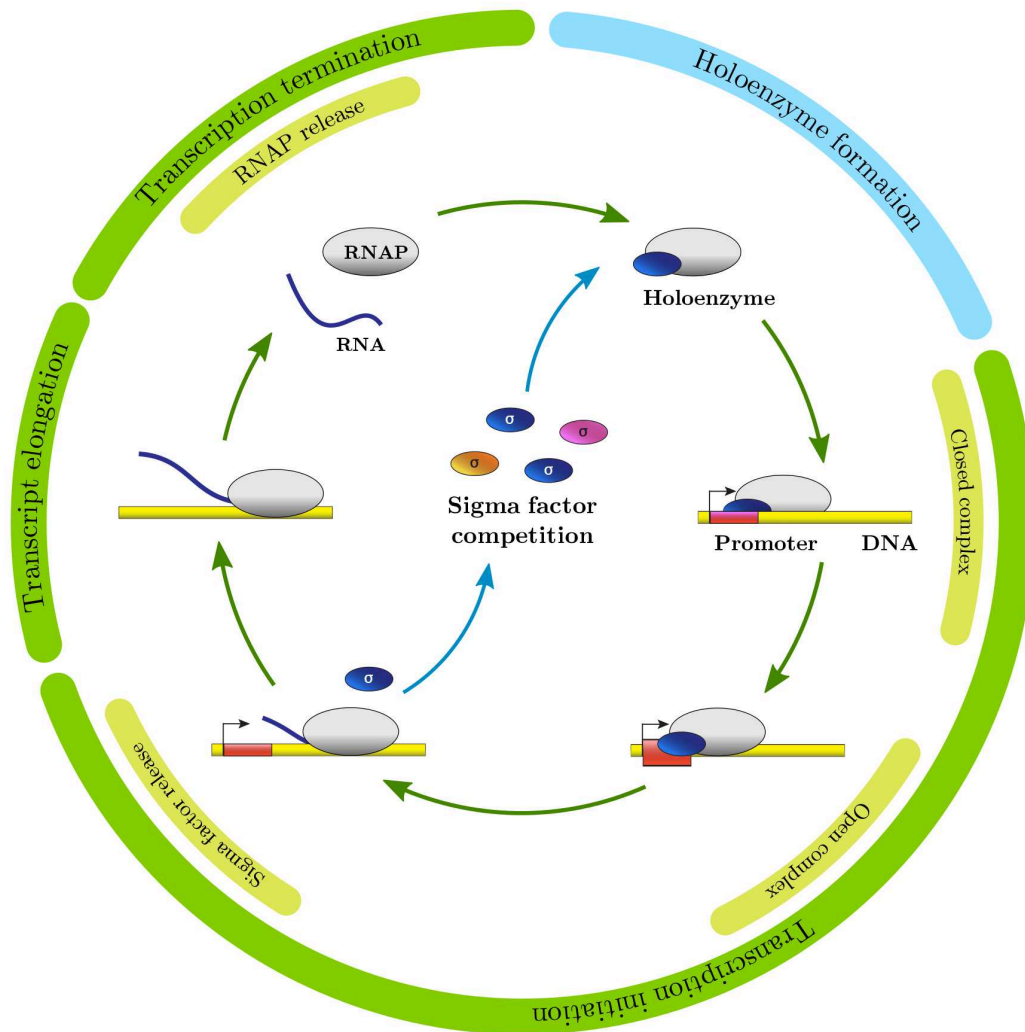


Figure 1.3: The sigma cycle allows the reprogramming of the core RNAP (represented by the grey oval). The illustration shows the main steps of the bacterial transcription cycle. First, sigma factor σ reversibly binds to the core enzyme RNAP to form the holoenzyme, then the holoenzyme recognizes the promoter and eventually after initiation (consisting of closed complex formation, open complex formation, and synthesis of some RNA nucleotides) starts the transcription. Next, during early elongation, the sigma factor is released and the elongation proceeds with the RNAP until a termination sequence. Finally, the RNA, the DNA and the RNAP are separated, and the core enzyme can form a new holoenzyme with a free sigma factor and begin a new transcription event. To form the holoenzyme, different species of sigma factor (colored ovals) have to compete to bind to the core RNAP.

such as growth of flagella (σ^F in *E. coli*) and sporulation ($\sigma^H, \sigma^F, \sigma^E, \sigma^G, \sigma^K$ in *B. subtilis*). In addition, some phages carry genes to code sigma factors that direct transcription to phage genes [5, 6]. The molecules and the regulatory networks involved in the gene regulation process of *Escherichia coli* were extensively studied. For this reason, here we mainly use the notation from this bacterium, although our analysis remains valid for other bacterial species. Specifically, *E. coli* has seven known sigma factors [7, 8]: the vegetative or housekeeping σ^{70} , and six alternative sigma factors activated in response to specific stresses ($\sigma^N, \sigma^F, \sigma^H, \sigma^{FecI}, \sigma^E, \sigma^S$). Their main functions are summarized in Table 1.1.

E. coli sigma factors can be divided in two distinct families [9]: the σ^{70} -class, including all the sigma factor but σ^N , and the structurally different σ^N -class. This second class consists of only σ^N itself, and its holoenzyme recognizes a promoter sequence very different from the one that binds the σ^{70} holoenzyme. Contrasting to σ^{70} , σ^N can bind to certain promoters even in the absence of the core RNAP, however with a reduced affinity. The σ^{70} -holoenzyme can spontaneously start the transcription once it binds to the promoters, while σ^N -driven transcription needs the presence of activators [9, 10].

Sigma factor competition. The number of core RNAPs is limited inside the cell (values ranges from 3000 to 13000 depending on the growth conditions [11, 12, 13]) and, similarly to the number of housekeeping sigma factors, remains constant in the shift from the growth to the stationary phase [12, 11]. During exponential growth, the intracellular concentration of σ^{70} is the highest (between 5000 and 17000 molecules), while the level of the alternative sigma factors vary substantially depending on the kind of inducing stress [14, 12, 11, 15] and in some cases a single species can reach up to two thirds of the core RNAP level (*i.e.* σ^S [12] and σ^E [11]). Thus, the total number of sigma factors is in excess over core RNAP [11, 12] and when more than one species of sigma factors are active in the cell at the same time, they have to compete

σ name	Gene that produces the σ	Main function: σ controls the
σ^{70}, σ^D	rpoD	housekeeping genes
σ^{54}, σ^N	rpoN, glnF	nitrogen regulated genes
σ^{28}, σ^F	fliA	flagellar genes
σ^{32}, σ^H	rpoH	heat shock response
$\sigma^{19}, \sigma^{FecI}$	fecI	ferric citrate uptake
σ^{24}, σ^E	rpoE	heat shock, extracytoplasmic-function
σ^{38}, σ^S	rpoS	stationary phase genes

Table 1.1: The seven *E. coli* sigma factors and their main function in the cell. The number in the name of the sigma factor indicates the molecular weight in kDalton.

to bind to the core to form a specific holoenzyme (highlighted by the blue path in Figure 1.3). Evidence for sigma factor competition in bacterial cells has come from overexpression experiments modulating the level of sigma factors and from mutants with altered sigma-core dissociation constants [16, 17, 18, 19, 20]. Furthermore, sigma factor competition has been demonstrated in *in vitro* transcription assays [21, 22, 8, 5, 6, 18, 23, 24, 25]. In addition to the concentration of sigma subunits, another factor that determines the probability of formation of the holoenzyme is the binding affinity to core RNAP. Each sigma factor species binds to the core with a different affinity and, similarly, different holoenzyme species recognize distinct promoter classes in the genome in order to activate specific adaptive responses. Initially, the holoenzyme and the core adhere weakly to the DNA, due to electrostatic interactions (non-specific binding), and typically slide along the template before dissociating again. However, when the holoenzyme encounters the promoter, the sigma factor has the ability to recognize this region and to bind the RNAP to the DNA template more tightly than to a non-specific site. Generally, neither the free sigma factor (but σ^N) nor the free core are able to recognize the promoter.

Resource distribution and genetic cross talk. The cell uses resource distribution as a global regulatory mechanism to coordinate coupled pathways: reduced availability of a component leads to competition among processes and consequently couples the limited machinery to the global state of the cell. Clear examples are competition between different mRNA species for ribosomes [26], small regulatory RNAs [27], proteases [28] and transcription factor binding [29]. Specifically, sigma factor competition for the finite pool of RNAP is believed to modulate extensively the global transcription profile, which determines the survival of the cell in different environments by distributing the polymerases between housekeeping genes and stress response genes [11, 30].

Modulation of transcription. During situation of nutrient abundance the association of the housekeeping sigma factor with the core RNAP is favored because of its strong binding affinity and higher intracellular level [8, 7]. Upon stress conditions, the limited amount of RNAP must be appropriately redistributed to promote the transcription of genes involved in the maintenance of cell functions. In order to facilitate the alternative holoenzyme-driven transcription, the bacterial cell adopts different strategies [31] to diminish in a reversible manner the dominant influence of the housekeeping sigma factor. An important aiding mechanism is provided by anti-sigma factors [32] that, by binding the cognate sigma factor, prevent the corresponding holoenzyme formation, as shown in the lower panel of Figure 1.4. For example, the Rsd protein has been shown to bind σ^{70} [12] and to favor transcription mediated by alternative sigma factors [21, 23, 33, 34, 35]. The number of Rsd proteins doubles during the shift from exponential growth to stationary phase, to reach approximately the level of σ^{70} and sequester a consistent fraction of housekeeping sigma

factors [12]. Another regulator of the σ^{70} level is the small RNA 6S RNA [36], highly conserved among various bacterial species [37]. 6S RNA, that accumulates during the late stationary phase (increasing even 10-fold from a thousands molecules [38]), binds exclusively to the housekeeping holoenzyme blocking the promoter recognition [38, 36] (lower panel of Figure 1.4). The second column of Table 1.2 summarizes the intracellular abundance as fraction of core RNA polymerase of various molecular species during exponential growth.

1.3 Stringent response

Stringent response. During exponential growth, the cell demands many ribosomes that serve for protein synthesis. For that reason the transcription of ribosomal RNA (rRNA), under the control of the housekeeping holoenzyme that forms the basic structure of ribosomes, sequesters a large fraction of RNA polymerases [42]. This is shown in the upper panel of Figure 1.4, which represents a sketch of the RNAP partitioning during growth phase. Amino acid deprivation induces stringent response [21, 43, 9, 31], a specific nutritional stress response primarily mediated by the RNAP-binding alarmone guanosine (penta-)tetra-phosphate (p)ppGpp and supported by its cohort DksA (here collectively called effectors). Stringent response is characterized by the reduced expression of the growth genes, rapid inhibition of the synthesis of proteins and ribosomal RNA, and increased transcription of the σ^{70} -driven biosynthetic genes

Molecule	Exponential growth molecular abundance as fraction of RNAP	Stringent/stress response molecular abundance as fraction of RNAP
RNAP	1	1
σ^{70} [11, 12]	2	2
Alternative σ [11, 12, 7]	few molecules	2/3
Anti- σ^{70} (Rsd) [12]	1	2
6S RNA [38]	1/10	1
(p)ppGpp [39, 40]	10	300
DksA [41]	20	20

Table 1.2: Intracellular abundance of various molecular species during exponential growth and stringent/stress response in *E. coli*. Values are expressed as fraction of core RNA polymerase. The number of enzyme RNAPs present during growth phase in the cell ranges from 3000 molecules to 13000 molecules depending on the growth conditions and experimental measurements [11, 13]. The amount of RNAP stays constant during the shift from exponential growth to stringent response [12, 11].

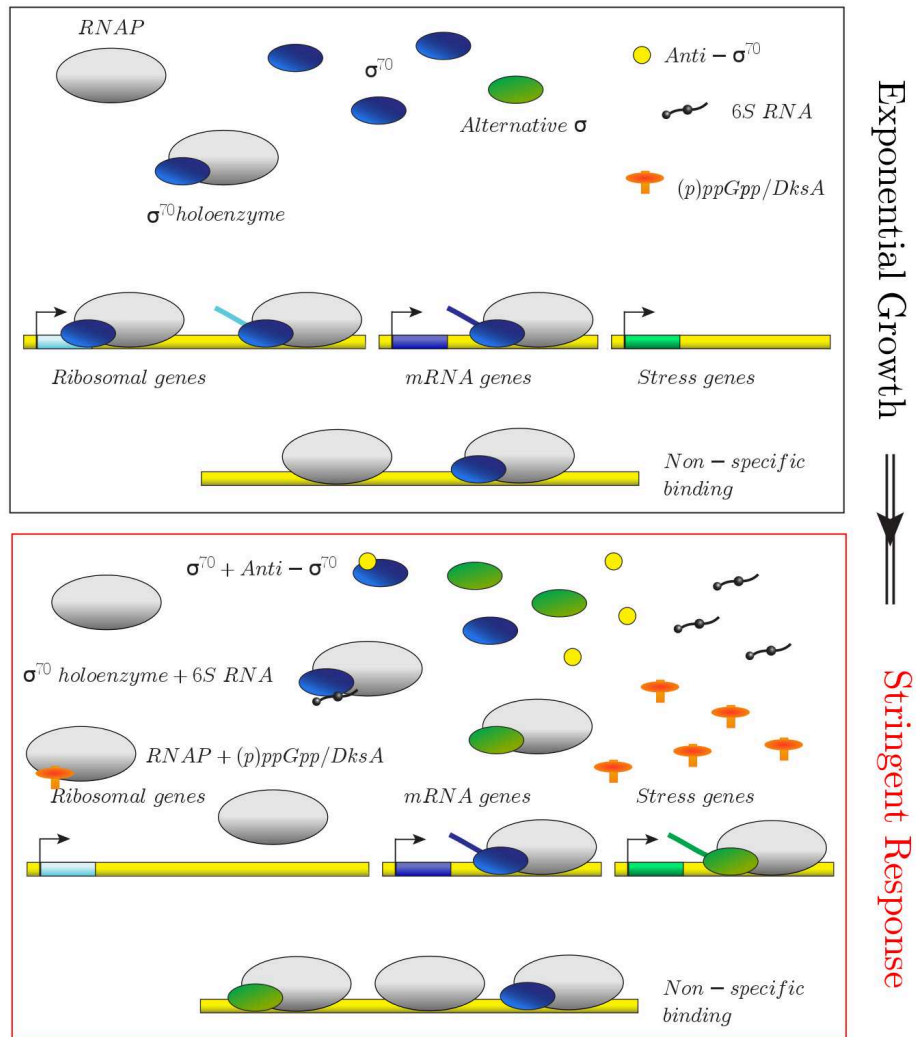


Figure 1.4: Pictorial representation of the redistribution of RNA polymerase during the shift from exponential growth to stringent response in the presence of various molecules involved in the process. The main effect of the RNAP partitioning in stringent phase is the suppression of transcription of the ribosomal promoters and the up-regulation of transcription of the maintenance and survival genes. All the alternative sigma factors are lumped into a single class. The abundance of the different molecules is reported in Table 1.2. (Figure adapted from reference [31]).

[44, 45] and alternative sigma factor-dependent genes [43, 31]. Upon the stop of transcription of the ribosomal RNA many RNA polymerases become available. It has been suggested that the final outcome of (p)ppGpp/DksA is the redistribution of the

RNA polymerase from the ribosomal genes to the survival operons [46]. At the same time, the number of anti- σ^{70} and 6S RNA increases in the shift from growth to famine (displayed in the lower panel of Figure 1.4). The intracellular abundance of the various molecular species acting during exponential growth and stringent/stress response in *E. coli* is summarized in Table 1.2. The different partition of RNAP during stringent response among free, non-specifically bound, sequestered by 6S RNA and transcribing units compared to the exponential growth case [47, 42, 48] is believed to favor the formation of alternative holoenzymes and to indirectly lead to the up-regulation of the survival genes during starvation [31, 21, 23, 49].

Passive and active regulation. This indirect up-regulation of the transcription of the sigma alternative-dependent genes through inhibition of ribosomal promoters represents a passive regulation scenario, supported by experiments with mutants [24, 50]. The effectors can also exert a direct action by altering either the promoter and elongation efficiency or the sigma-core binding affinity [21, 23, 24, 25, 51, 33]. Following these considerations, it has been also proposed, but never directly observed, that ppGpp may have the ability to weaken the affinity between sigma factor and core RNAP [21, 52, 53] in order to facilitate the access of the alternative sigma factors to the limited core RNAPs.

1.4 Motivation and overview

General picture of the processes considered in this thesis. During recent years, much effort has been made to quantitatively characterize gene regulation and regulatory networks [54, 55, 56, 57, 58]. In a reductionist spirit, gene regulation has usually been studied one gene at a time. However, it has become increasingly clear that genes are coupled both to each other and to the state of the cell as a whole through the limiting transcription and translation machinery that they share [59, 60, 61, 26]. Specifically, different sigma factor species compete to bind to the limited amount of RNA polymerase. As a consequence of sigma factor competition, any increase in activity of one sigma factor indirectly represses binding of other sigma factors to core and consequently the transcription of the genes that they control. Such passive regulation was proposed to contribute to the switch of the global gene expression program [49] and to occur in the stringent response and during entry to stationary phase [21, 49, 25, 33, 62]. In both cases, the down-regulation or the stop of transcription of ribosomal RNA represent a major perturbation of the allocation of (core) RNA polymerases to different genes and to different sigma factors. However, a quantitative analysis is required as many cellular parameters change at the same time and may have opposing effects on the genes of interest, so that their net effect may not be obvious.

Model and results. For these reasons, in this thesis we develop a theoretical

thermodynamic model to study quantitatively the global regulation exerted by competition among different species of environmental-sensitive sigma factors for binding to the enzyme RNA polymerase. One of our aims is to provide a valid - and at the same time simple - tool to explain biological and experimental results. Our model is based on and extends previous theoretical work on sigma factor competition by Grigorova *et al.* [11]. In **Chapter 2**, we first use a reduced core model at equilibrium to quantitatively analyze *in vitro* competition experiments from the literature [22, 21, 25] and find good agreement between the model and the data. Then, in **Chapter 3**, we extend the model to include anti-sigma factors and 6S RNA. By regulating the basal level of available sigma factors and housekeeping holoenzymes, these two modulators inhibit the transcription of entire classes of genes. We also analyze the effect of the non-specific DNA binding, which has been shown to buffer against passive effect in σ^{70} -dependent transcription upon an increased RNA polymerase concentration due to the stop of ribosomal RNA transcription [42]. By contrast, we show here that non-specific binding does not buffer alternative σ -dependent transcription against such passive effects, supporting a role for indirect up-regulation of alternative σ -dependent stress response genes. Moreover, we include an explicit description of transcript elongation, which we show to have rather complex effects by modulating the effective sigma-core binding affinity in addition to sequestering RNAP core enzymes. Finally, in **Chapter 4** we apply the model to the increase in the availability of core RNAP during stringent response and show that passive up-regulation should indeed play an important role for alternative sigma-dependent transcription. We determine that under certain conditions the transcription of the stress genes presents a hypersensitive response to the modulation of the RNAP. The up-regulation of products of survival genes is then a direct reflection of the rearrangement of sigma factors and RNAP resources. To show that, we first compared the RNAP distribution during exponential growth as calculated by our model to previous models [47, 42, 48]. We find that the prediction of the RNA synthesis rate matches well with the measure of the synthesis rates *in vivo* [47]. Next, we analyze the RNAP partitioning in the same cell during different scenarios of stringent response. Our simulation suggests that a weakening of the σ^{70} -core binding affinity allows a strong up-regulation of the stress genes. On top of that, we analyze an *in vitro* transcription experiment [21] that - investigated with our model - supports a direct weakening action of the (p)ppGpp on the housekeeping holoenzyme dissociation constant. For a direct comparison of the predictions of our model with real cells, precise determinations of all the relevant physiological cellular parameters are needed. To that end, we collect and discuss in **Appendixes A and E** a selection of experimental and theoretical estimations for the quantities adopted in our analysis. We restrict the quantitative investigation to the well studied *Escherichia coli* bacterium, even though the theoretical analysis stays general for similar systems. Some analytical approximations are presented in **Appendixes B, C and D**.

Chapter 2

Model for sigma factor competition

To analyze sigma factor competition, we have developed a quasi-steady state model inspired by an earlier work by Grigороva *et al.* [11]. Our model, as shown in Figure 2.1, describes the interaction between sigma factors and core RNAPs. Core RNAPs (E) bind to sigma factors (σ^i , where i denotes the type of sigma factor) to form holoenzymes ($E\sigma^i$). The binding is characterized by a dissociation constant $K_{E\sigma^i}$. Holoenzymes specifically recognize a cognate class of promoters, from which they initiate transcription.

In an extended description, discussed in Chapter 3, after initiation of transcription, the sigma factor is released in a stochastic fashion and the core RNAP transcribes until it reaches a termination sequence. This cycle enables the reprogramming of RNAPs by different sigma factors. We also include the effects of additional regulators such as anti-sigma factors, 6S RNA and non-specific binding. In the following we discuss this model step-by-step starting with the core model.

Specifically, in this chapter, first we explain the case of a single sigma factor that binds to the core RNA polymerase. Then, we analyze the case of two sigma factors competing for binding to the core RNAP. We show that the expression of genes driven by the housekeeping holoenzyme can be passively regulated by acting on the availability of the alternative sigma factor. Good agreement between the model and the data from three *in vitro* competition experiments from the literature [22, 21, 25] validates our simplified model.

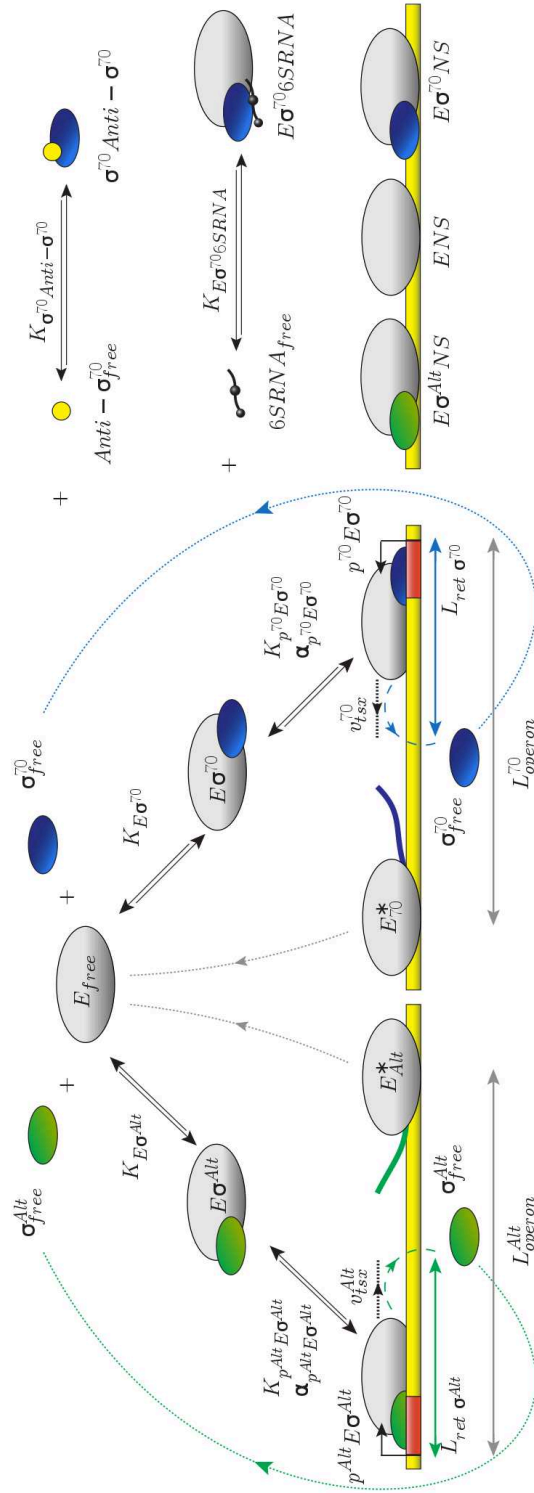


Figure 2.1: Model for sigma factor competition with two types of sigma factors, housekeeping σ^{70} and generic alternative σ^{Alt} , anti- σ^{70} , 6S RNA, and non-specific binding. The model describes binding of σ^{70} or σ^{Alt} to core RNA polymerase (E) to form holoenzymes ($E\sigma^{70}$ and $E\sigma^{Alt}$) as well as transcription (promoter binding, transcription initiation, and elongation) of the cognate genes. Anti- σ^{70} , 6S RNA, and non-specific binding modulate the competition.

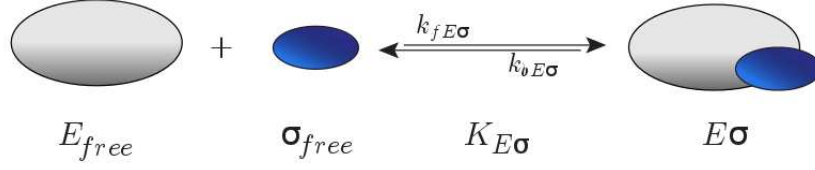


Figure 2.2: Sigma factor σ binds to core RNAP E with a dissociation constant $K_{E\sigma}$.

2.1 One sigma factor species binding to RNAP

Single sigma factor species. We first consider the binding of a single species of sigma factor to core RNAP, presented in Figure 2.2. Sigma-core binding is described by the equilibrium of the reaction



where E , σ , and $E\sigma$ respectively denote the core RNAP, the sigma subunit, and the holoenzyme. The index “free” distinguishes free subunits that are not part of a holoenzyme from total quantities. $k_{fE\sigma}$ and $k_{bE\sigma}$ are the forward and backward rates of holoenzyme formation. To quantitatively describe the kinetics of the process, we introduce the concept of concentration. The molar concentration $[N]$ of a given molecular species N quantifies the numbers of moles n (given by $mol = \text{number of molecules}/N_A$, where N_A is the Avogadro constant) per unit of volume V , *i.e.* $[N] = n/V$ (measured in molar units $M = mol/L$). Thus, one molecule in a cell of volume of 1 fL corresponds to a concentration of ~ 1.7 nM. Molecular concentrations can vary over volume and in time. If we assume that spatial concentration changes over distances that are larger than mean molecular spacing, every small box of volume can be handled like a box with uniform concentration. Besides, we always consider large numbers of molecules (see Table A.1 in Appendix A). These assumptions are enough to suppose homogeneous concentrations and neglect stochastic fluctuations. Time evolution of the concentrations is given by the rate equations

$$\begin{aligned} \frac{d[\sigma_{free}]}{dt} &= -k_{fE\sigma}[E_{free}][\sigma_{free}] + k_{bE\sigma}[E\sigma] \\ \frac{d[E_{free}]}{dt} &= -k_{fE\sigma}[E_{free}][\sigma_{free}] + k_{bE\sigma}[E\sigma] \\ \frac{d[E\sigma]}{dt} &= k_{fE\sigma}[E_{free}][\sigma_{free}] - k_{bE\sigma}[E\sigma]. \end{aligned}$$

The concentrations also fulfill

$$[E] = [E_{free}] + [E\sigma] \quad (2.2)$$

$$[\sigma] = [\sigma_{free}] + [E\sigma], \quad (2.3)$$

where $[N]$ without any index represents the total amount of N subunits.

We adopt an equilibrium approximation to analyze this system. In the cell, this assumption is justified by the fact that the reactions that create holoenzymes are fast and the concentrations of sigma factor, core RNAP, and holoenzyme are supposed to reach equilibrium in a short time and stay constant for a relatively long time; *in vitro*, to obtain equilibrium in such reaction, it is enough to wait the necessary time before acquiring the data [11, 63]. This approximation is also supported by well-established and validated models of gene transcription that assume a quasi-steady-state description [64, 47, 65, 11]. At equilibrium, the concentrations of the molecules involved in Reaction 2.1 fulfill

$$\frac{[E_{free}][\sigma_{free}]}{[E\sigma]} = \frac{k_{bE\sigma}}{k_{fE\sigma}} \equiv K_{E\sigma}. \quad (2.4)$$

In the following, we sometimes refer to the dissociation constant $K_{E\sigma}$ (measured in Molar units) as binding affinity. Since the dissociation constant expresses the probability of unbinding and producing reagents from products, we state that a small dissociation constant (here considered smaller than 10^{-6} M, see Table A.1 in Appendix A) represents a strong binding affinity, and a large dissociation constant (larger than 10^{-6} M) represents a weak binding affinity.

Holoenzyme formation. The amount of holoenzymes in a cell or produced during a binding experiment is an experimentally accessible quantity. From Equations 2.3 – 2.4, the concentration of holoenzymes formed by the equilibrium of the Reaction 2.1 results

$$[E\sigma] = \frac{1}{2} \left(K_{E\sigma} + [E] + [\sigma] - \sqrt{([E] + [\sigma] + K_{E\sigma})^2 - 4[E][\sigma]} \right). \quad (2.5)$$

If the core-sigma affinity $K_{E\sigma}$ is very strong, the holoenzyme concentration reduces to $\min([E], [\sigma])$ and, if the affinity is very weak, to $[E][\sigma]/K_{E\sigma}$. Figure 2.3(a) shows the formation of holoenzyme as a function of sigma factors. Unless specified otherwise, we quantify the amounts of the various molecular species by their absolute number in an average cell. Our reference *E. coli* cell, supposed to have a high growth rate (2.5 dbl/h), has a characteristic volume of 1.32 fL and 11400 core RNAPs [47]. For summary and discussion about the values of the parameters, we refer to Table A.1 in Appendix A.

Transcription rates. Next, we examine the transcription rates. Each holoenzyme species transcribes a set of cognate genes with a transcription rate that depends

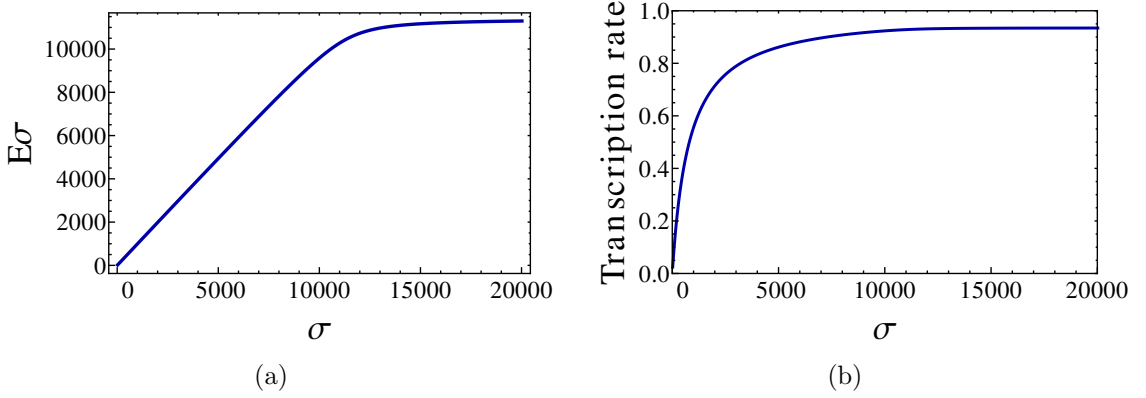


Figure 2.3: Single sigma factor species. (a) Number of holoenzymes as a function of the number of sigma factors in the cell in the presence of a fixed concentration of cores. The steepness of the curve depends on the core-sigma factor dissociation, here $K_{E\sigma} = 10^{-7}$ M. The value of the holoenzymes at saturation is defined by the total amount of available RNAPs, here 11400. (b) Normalized transcription rate of a σ -dependent gene. After its formation, the holoenzyme is able to bind to the cognate promoter with a specific dissociation constant, here $K_{pE\sigma} = 10^{-6}$ M.

on the holoenzyme concentration and on the parameters of the promoter, which is described with a Michaelis-Menten model. If binding is equilibrated before transcription is initiated, the Michaelis constant of the promoter $K_{pE\sigma}$ corresponds to a holoenzyme-promoter dissociation constant. We assume that only a small number of RNAPs are transcribing at any time, so that the pools of non-transcribing holoenzymes and free subunits are not perturbed by transcription. This assumption should be valid for *in vitro* experiments, but may not hold in the cell; the latter case will be discussed in Chapter 3. Besides, we assumed that every holoenzyme-promoter complex gives rise to a product of transcription. The NTPs availability is always thought to be at saturating concentration and not explicitly included. Thus, the rate of transcription of a gene (RNA synthesis rate per cell volume) with a promoter p cognate to $E\sigma$ is

$$J = \alpha_{pE\sigma}[p] \frac{[E\sigma]}{K_{pE\sigma} + [E\sigma]}, \quad (2.6)$$

where $\alpha_{pE\sigma}$ is the maximal initiation rate, $[p]$ the total concentration of the cognate promoter and $K_{pE\sigma}$ the Michaelis constant. In the following, we usually plot the normalized transcription rate per gene (to which we refer simply as “transcription rate”), defined as

$$\tilde{J} = \frac{J}{\alpha_{pE\sigma}[p]} = \frac{[E\sigma]}{K_{pE\sigma} + [E\sigma]}. \quad (2.7)$$

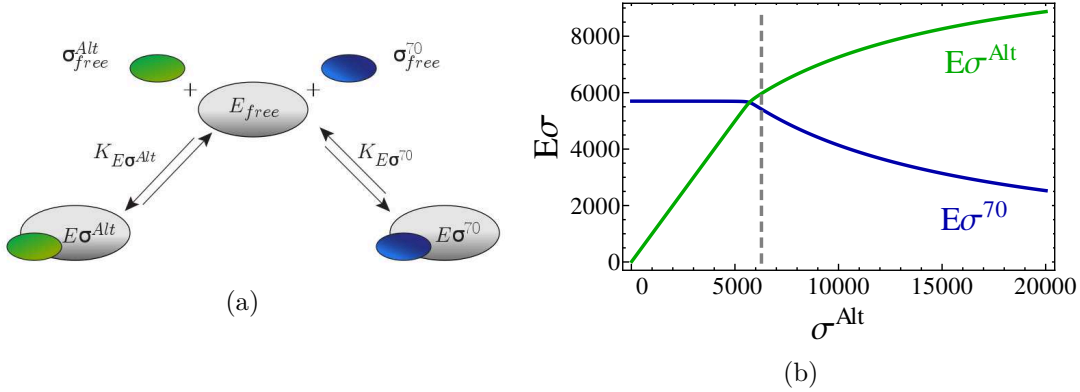


Figure 2.4: Holoenzyme formation. (a) Core model for holoenzyme formation. (b) Number of housekeeping and alternative holoenzymes ($E\sigma^{70}$ and $E\sigma^{Alt}$, respectively) as a function of the number of alternative sigma factors in the cell. The gray dashed line represents the onset of sigma factor competition, here when $[E] \simeq [\sigma^{70}] + [\sigma^{Alt}]$.

Figure 2.3(b) shows the transcription rate compared to the number of sigma factors in the cell. If the holoenzyme binds weakly to the promoter ($K_{pE\sigma} \gg [E\sigma]$), the promoter is in the linear regime and $\tilde{J} \simeq [E\sigma]/K_{pE\sigma}$. While for strong binding affinity ($K_{pE\sigma} \ll [E\sigma]$), the normalized transcription rates saturate to unity. $K_{pE\sigma}$ is equal to the concentration of the holoenzyme at half maximum height of the saturation value.

2.2 Sigma factors competition for binding RNAP

Sigma factor competition. For simplicity, we focus on the case of only two competing sigma factors, the housekeeping sigma factor σ^{70} , and one type of alternative sigma factor σ^{Alt} , as in Figure 2.4(a). This simplification can be interpreted in two ways: it provides a good description of specific stress responses, in which only one specific alternative sigma factor accumulates; or alternatively, it applies to a general stress response, in which most or all alternative sigma factors are induced simultaneously, if these are lumped together into a single group of alternative sigma factors, assuming that their parameters are rather similar. The competition of sigma factors for core RNAP depends on five parameters: the concentrations of cores and sigma factors, and the dissociation constants between them. We model two sigma factors that compete for core RNAPs with





At equilibrium, the reactions above give the equations for the conservation of molecules and the dissociation constants $K_{E\sigma}$ between core and sigma factor:

$$[E] = [E_{free}] + [E\sigma^{70}] + [E\sigma^{Alt}] \quad (2.9)$$

$$[\sigma^{70}] = [\sigma_{free}^{70}] + [E\sigma^{70}] \quad (2.10)$$

$$[\sigma^{Alt}] = [\sigma_{free}^{Alt}] + [E\sigma^{Alt}] \quad (2.11)$$

$$\frac{[E_{free}][\sigma_{free}^{70}]}{[E\sigma^{70}]} = K_{E\sigma^{70}} \quad (2.12)$$

$$\frac{[E_{free}][\sigma_{free}^{Alt}]}{[E\sigma^{Alt}]} = K_{E\sigma^{Alt}}. \quad (2.13)$$

Analytical expressions for the concentrations of the holoenzymes can be found for some special cases (see Appendix B), but in general, we solve these equations numerically.

Now, we consider fixed concentrations of core RNAP and σ^{70} , here 11400 and 5700 molecules, respectively, as in a rapidly growing *E. coli* cell, and modulate the concentration of σ^{Alt} . This situation is accessible to *in vitro* experiments and mimics the accumulation of alternative sigma factors during the transition from exponential to stationary phase. First, we study the formation of holoenzymes in the absence of transcription (*i.e.* no DNA present), as in Figure 2.4(a). Figure 2.4(b) shows the amounts (number per cell) of the two species of holoenzymes as functions of the number of alternative sigma factors. Both sigma factors are taken to bind to core RNAP with equal dissociation constants of 1 nM. As long as the total concentration of sigma subunits is smaller than that of core RNAPs, there are enough cores to bind all sigma factors. In that case, the number of alternative holoenzymes increases linearly in the number of alternative sigma factors, and formation of $E\sigma^{70}$ is unaffected by the increasing concentration of σ^{Alt} , *i.e.* there is no competition for core RNAP or no cross talk between the two branches of the system. Competition sets in, and the formation of $E\sigma^{70}$ gets reduced by the presence of the alternative sigma factor, approximately when the total concentration of sigma factors exceeds the concentration of cores RNAPs, as previously observed in reference [11].

Definition of competition. While the onset of sigma factor competition is abrupt for very strong sigma-core binding, in general, there is a smooth transition. Thus, we define the onset of competition to be the point where the alternative sigma factors cause a 5% reduction of $[E\sigma^{70}]$ compared to the situation without alternative sigma factors, *i.e.* for which

$$\frac{[E\sigma^{70}]_{\sigma^{Alt}=0} - [E\sigma^{70}]_{\sigma^{Alt}\neq 0}}{[E\sigma^{70}]_{\sigma^{Alt}=0}} = \rho \quad (2.14)$$

where $\rho = 5\%$. The starting point of the competition defined in this way is indicated by a grey dashed vertical line in Figure 2.4(b) and in the following plots. Thus, when the total concentration of sigma factors exceeds the concentration of cores, an increase in availability of alternative sigma factors indirectly down-regulates the production of housekeeping holoenzymes, a characteristic common to every system showing competition and one-to-one binding stoichiometry. We note that if the number of housekeeping sigma factors already exceeds that of cores, any small number of alternative sigma factors will be in competition with σ^{70} .

Analytical solution with equally strong core-sigma factor binding affinities. This latter condition can be analytically demonstrated by approximating the holoenzyme concentration. As a matter of fact, a general analytical solution for the problem of two competing sigma factor is not available, but different subsets of the parameters allow simplifications for which the model (as defined by Equations 2.9–2.13) can be solved analytically. A complete set of solutions for all the values of the parameters is given in Appendix B. If the two dissociation constants between core RNAP and sigma factors are equal ($K_{E\sigma^{70}} = K_{E\sigma^{Alt}} \equiv K_{E\sigma}$) and small ($K_{E\sigma} \lesssim 10^{-6} M$), the concentration of the holoenzymes is given by

$$\begin{aligned} [E\sigma^{70}] &\approx \begin{cases} [\sigma^{70}] & [\sigma^{Alt}] \leq [E] - [\sigma^{70}] \\ \frac{[E][\sigma^{70}]}{[\sigma^{70}] + [\sigma^{Alt}]} & [\sigma^{Alt}] > [E] - [\sigma^{70}] \end{cases} \\ [E\sigma^{Alt}] &\approx \begin{cases} [\sigma^{Alt}] & [\sigma^{Alt}] \leq [E] - [\sigma^{70}] \\ \frac{[E][\sigma^{Alt}]}{[\sigma^{70}] + [\sigma^{Alt}]} & [\sigma^{Alt}] > [E] - [\sigma^{70}] \end{cases} . \end{aligned}$$

According to Equation 2.14 sigma factor competition is observed when

$$[\sigma^{Alt}] \geq \begin{cases} [\sigma^{70}] \frac{\rho}{1-\rho} & [E] \leq [\sigma^{70}] \\ \frac{[E] - (1-\rho)[\sigma^{70}]}{1-\rho} & [E] > [\sigma^{70}] \end{cases} \quad (2.15)$$

where ρ is the percentage threshold that we set at 5%. At single particle threshold ($\rho \rightarrow 0$), Inequality 2.15 reduces to

$$[\sigma^{Alt}] \geq \begin{cases} 0 & [E] \leq [\sigma^{70}] \\ [E] - [\sigma^{70}] & [E] > [\sigma^{70}] \end{cases} . \quad (2.16)$$

This expression is equivalent to $[\sigma^{70}] + [\sigma^{Alt}] \geq [E]$, showing that if housekeeping sigma factor is in excess of core, any small number of alternative sigma factor triggers the competition. This approximation is discussed in more detail in case VIII of Appendix B.

Analytical solution with strong but different core-sigma factor binding affinities. The criterion of 5% reduction leads to an additional limiting condition for competition. If the dissociation constants of the two holoenzymes are different,

when varying the availability of core RNAP, the criterion of 5% reduction can result in a competition in an intermediate range of core concentrations. To show it, we first solve Equations 2.9–2.13 with $K_{E\sigma^{70}}/K_{E\sigma^{Alt}} \equiv K < 1$ and both binding affinities taken to be strong. This assumptions reproduce the hierarchy of binding affinities during exponential growth (and many altered conditions), in which the dissociation constant of the housekeeping sigma factor to the core RNAP is believed to be smaller than all the other alternative holoenzyme dissociation constants [8, 66]. Neglecting the pool of free holoenzymes in Equation 2.9 (see case VI in Appendix B), we obtain

$$\begin{aligned} [E\sigma^{70}] &= \min\left([E], [\sigma^{70}], \frac{1}{2(K-1)}\left([E](K-1) - [\sigma^{70}] - K[\sigma^{Alt}] + \right. \right. \\ &\quad \left. \left. + \sqrt{4[E](K-1)[\sigma^{70}] + ([E](1-K) + [\sigma^{70}] + K[\sigma^{Alt}])^2}\right)\right) \\ [E\sigma^{Alt}] &= \min\left([E], [\sigma^{Alt}], \frac{1}{2(K-1)}\left([E](K-1) + [\sigma^{70}] + K[\sigma^{Alt}] + \right. \right. \\ &\quad \left. \left. - \sqrt{4[E](K-1)[\sigma^{70}] + ([E](1-K) + [\sigma^{70}] + K[\sigma^{Alt}])^2}\right)\right). \end{aligned} \quad (2.17)$$

According to Equation 2.14, sigma factor competition sets in when

$$[\sigma^{Alt}] \geq \frac{((1-\rho)m - [E])((1-K)(1-\rho)m - [\sigma^{70}])}{K(1-\rho)m}$$

where $m = \min([E], [\sigma^{70}])$. Solving the last expression with respect to $[E]$, we find that for $[\sigma^{Alt}]/[\sigma^{70}] \leq \rho(K(1-\rho) + \rho)/(K(1-\rho))$ there is no competition, for $\rho(K(1-\rho) + \rho)/(K(1-\rho)) < [\sigma^{Alt}]/[\sigma^{70}] \leq \rho/(K(1-\rho))$ there is sigma factor competition if

$$\frac{[\sigma^{70}]\rho - K[\sigma^{Alt}](1-\rho)}{(1-K)(1-\rho)\rho} \leq [E] \leq \frac{(1-\rho)(K([\sigma^{70}] + [\sigma^{Alt}]) - (K-1)\rho[\sigma^{70}])}{K(1-\rho) + \rho} \quad (2.18)$$

and for $[\sigma^{Alt}]/[\sigma^{70}] \geq \rho/(K(1-\rho))$ if

$$[E] \leq \frac{(1-\rho)(K([\sigma^{70}] + [\sigma^{Alt}]) - (K-1)\rho[\sigma^{70}])}{K(1-\rho) + \rho}$$

Equation 2.18 explains the intermediate range of core concentration for which sigma factor competition is present as a function of cores. If $\rho \rightarrow 0$, the competition region reduces again to $[\sigma^{Alt}] \geq 0$ when $[E] \leq [\sigma^{70}]$ and to $[\sigma^{Alt}] \geq [E] - [\sigma^{70}]$ when $[E] > [\sigma^{70}]$ as in Equation 2.16.

Holoenzyme formation in the presence of N sigma factors. If it is not possible to collect all the alternative sigma factors under the σ^{Alt} label, *e.g.* because the dissociation constants are very different or because we also would like to distinguish small differences in binding affinities, we can rewrite the system of Equations

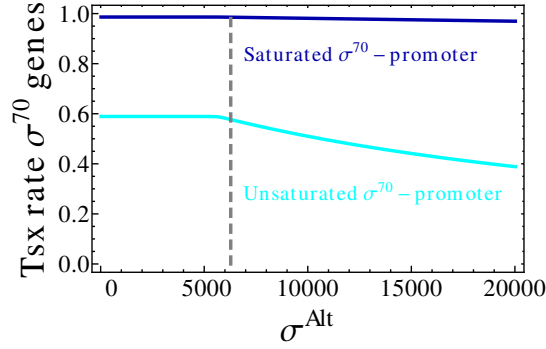


Figure 2.5: Normalized transcription rate \tilde{J} (Equation 2.7) for a σ^{70} -dependent promoter as a function of the number of alternative sigma factors. The numbers of σ^{70} and cores are fixed. The blue line is for a saturated promoter (with $K_{p^{70}E\sigma^{70}} = 10^{-7}$ M) and the cyan line for an unsaturated promoter (with $K_{p^{70}E\sigma^{70}} = 5 \times 10^{-6}$ M). The values of the parameters used in the simulations are summarized in Table A.1 in Appendix A.

2.9–2.13 for N sigma species in the following form:

$$\begin{aligned}
 [E\sigma_j] &= \frac{1}{2} \left([E] + K_{E\sigma_j} + [\sigma_j] - \sum_{i \neq j, i=1}^N [E\sigma_i] + \right. \\
 &\quad \left. - \sqrt{\left([E] + K_{E\sigma_j} + [\sigma_j] - \sum_{i \neq j, i=1}^N [E\sigma_i] \right)^2 + 4[\sigma_j] \left(\sum_{i \neq j, i=1}^N [E\sigma_i] - [E] \right)} \right),
 \end{aligned} \tag{2.19}$$

with $i, j = 1, \dots, N$ and $i \neq j$. It is also true that

$$\frac{[E\sigma_i]}{[E\sigma_j]} = \frac{K_{E\sigma_j} [\sigma_i \text{ free}]}{K_{E\sigma_i} [\sigma_j \text{ free}]} = \frac{K_{E\sigma_j} [\sigma_i] - [E\sigma_i]}{K_{E\sigma_i} [\sigma_j] - [E\sigma_j]}. \tag{2.20}$$

Equation 2.20 shows that the ratio of formation of two kinds of holoenzymes depends on the inverse ratio of the two corresponding dissociation constants, even if other species of sigma factors are involved.

Transcription rate. Figure 2.5 shows the transcription rate of a σ^{70} -dependent promoter as a function of the increasing numbers of σ^{Alt} , again with constant amounts of core RNAPs and σ^{70} . The transcription rate presents a strong dependence on the Michaelis constant of the promoter, $K_{pE\sigma}$. While saturated promoters ($K_{pE\sigma} = 10^{-7}$ M, blue line) are weakly affected by increasing number of σ^{Alt} , the transcription rate from genes depending on unsaturated promoters ($K_{pE\sigma} = 5 \times 10^{-6}$ M, cyan line) directly reflects the holoenzyme concentration of Figure 2.4(b). Upon the onset of competition, transcription from these latter genes is reduced, as the increasing amount

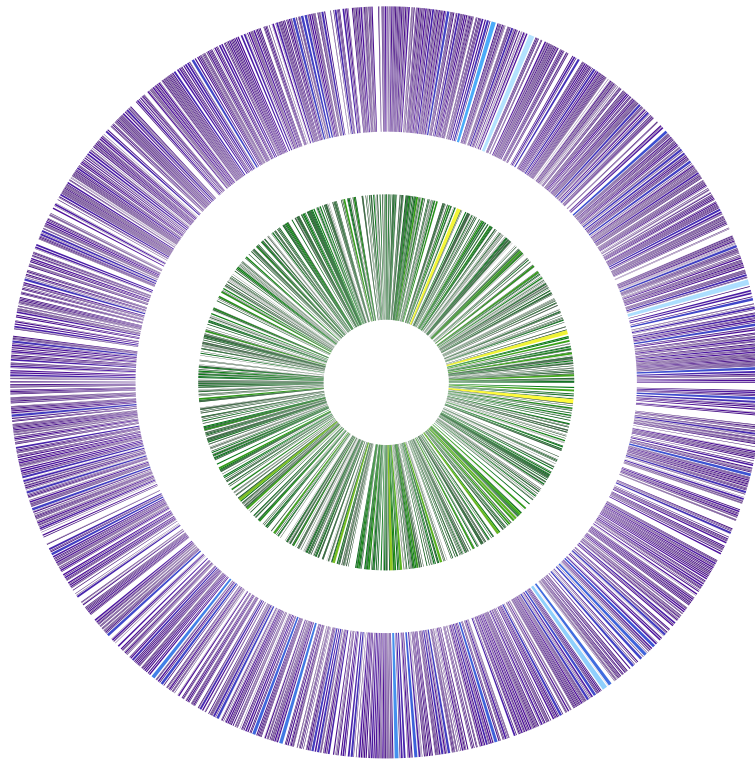


Figure 2.6: Circular gene map of the binding sites of the housekeeping and σ^S -holoenzymes, in blue and green respectively, from a ChIP-chip experiment in *E. coli*, adapted from reference [30]. Each sector represents an operon, whose width is proportional to the operon's length.

of σ^{Alt} diverts core RNAPs to form alternative holoenzymes. Thus, as expected, unsaturated promoters are more sensitive to sigma factor competition than saturated promoters.

Effect of a shared promoter/overlapping promoters on sigma factor competition. ChIP-chip experiments with different sigma factors have shown that many promoters can bind more than one kind of holoenzyme, even though only one type may successfully initiate the transcription of the gene [67, 30]. For example, Figure 2.6 shows a circular genome map of *E. coli* in which it is evident that the housekeeping holoenzyme and of the σ^S -holoenzyme have many shared binding sites (in blue and green, respectively). Each sector represents an operon, whose width is proportional to its length (data adapted from reference [30]). In the instance of a shared promoter, the non-transcribing holoenzyme effectively acts as a transcriptional repressor for the gene, in addition to competing for core RNAP (Figure 2.7(a)). For

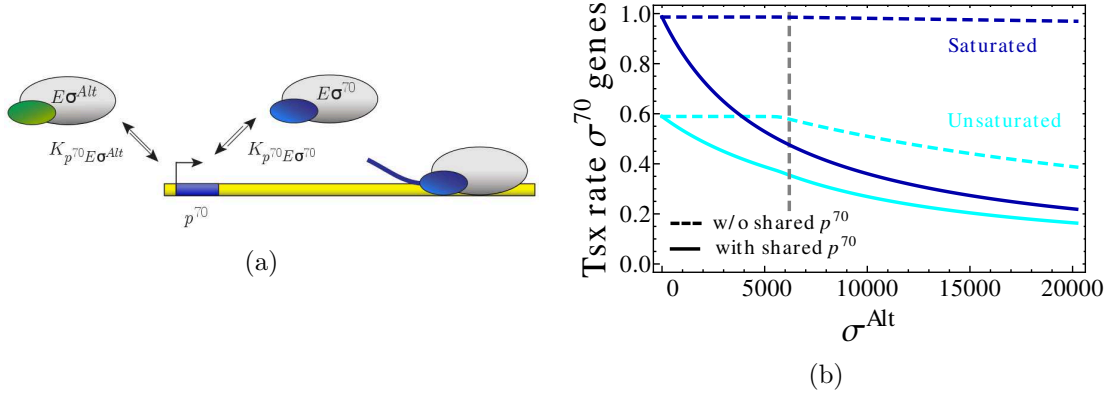


Figure 2.7: Effect of shared promoter/overlapping promoters on sigma factor competition. (a) When a σ^{70} -dependent promoter also binds another type of holoenzyme or overlaps to another promoter, $E\sigma^{Alt}$ also acts as a repressor of the σ^{70} -dependent transcription. (b) Normalized transcription rate of a saturated and unsaturated σ^{70} -dependent promoter as a function of the number of σ^{Alt} (blue and cyan solid lines with $K_{pE\sigma} = 10^{-7}$ M and $K_{pE\sigma} = 5 \times 10^{-6}$ M, respectively). The dashed line shows the corresponding results in the absence of repression by promoter sharing or overlapping.

example, if the gene with the p^{70} promoter only can be transcribed by $E\sigma^{70}$ but also binds $E\sigma^{Alt}$, the transcription rate becomes

$$\tilde{J} = \frac{[E\sigma^{70}]/K_{p^{70}E\sigma^{70}}}{1 + [E\sigma^{70}]/K_{p^{70}E\sigma^{70}} + [E\sigma^{Alt}]/K_{p^{70}E\sigma^{Alt}}}. \quad (2.21)$$

The $E\sigma^{Alt}$ holoenzyme acts as a repressor with binding affinity $K_{p^{70}E\sigma^{Alt}}$ to the p^{70} promoter. The additional function can strongly enhance the negative effect of the alternative sigma factor on σ^{70} -driven transcription. In particular, it also affects saturated promoters that are only weakly affected by sigma factor competition, as shown by the blue line in Figure 2.7(b). Our findings suggest that competition for shared promoters contributes to the repression of transcription of the associated genes, especially in the case where these genes are predominantly transcribed by one of the holoenzyme species binding to the promoter. Evidence for such repression was found in a very recent genome-wide study of sigma factor-promoter binding [30] and qualitatively agrees with the picture resulting from our model: most σ^S -dependent genes were found to be down-regulated by knocking out the genes (a technique by which a gene is disrupted or inactivated) used to code σ^S (*rpoS*). On the contrary those σ^S -dependent genes that are up-regulated were found to be genes that are transcribed by both $E\sigma^{70}$ and $E\sigma^S$ and to which the housekeeping holoenzyme binds more strongly.

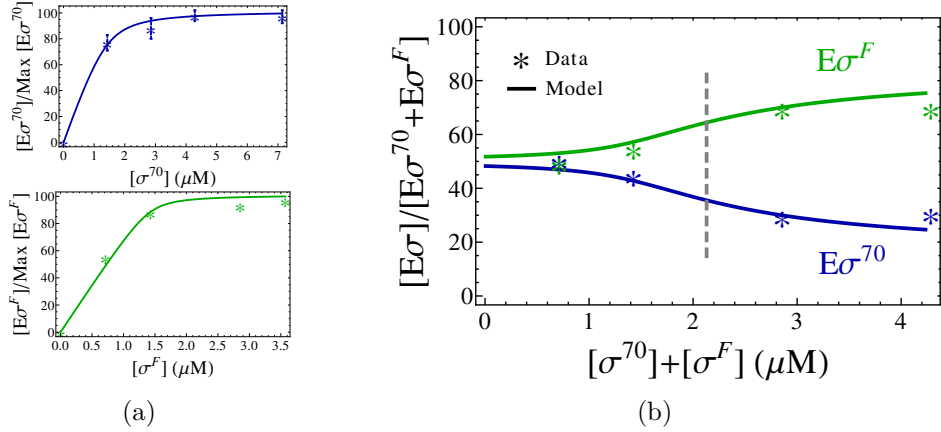


Figure 2.8: Competition experiment *in vitro*. (a) Determination of the sigma-core dissociation constants for σ^{70} and σ^F (see Table 2.1) by fitting the results of binding assays between cores and sigma factors [68, 22] (50 pmol RNAP, volume 35 μL , incubated at 30 $^\circ\text{C}$). Errors in the upper panel are standard deviations of either four or five independent assays. (b) Comparison of model predictions (lines) with an *in vitro* competition experiment [22] with a fixed amount of core and different equimolar amounts of σ^{70} and σ^F (stars) in the same conditions as in (a). The plot shows the percentage of sigma factors bound in holoenzymes as a function of the total sigma factor concentration, $[\sigma^{70}] + [\sigma^F]$.

2.3 Comparison with the experiments

A first competition experiment. We then use the model described so far to analyze some *in vitro* competition experiments, starting with a competition assay between σ^{70} and σ^F . In reference [22], a fixed amount of core RNAP was first mixed with increasing concentrations of either σ^{70} [68] or σ^F [22] to determine the amount of produced holoenzymes. By fitting these data with our model (Equation 2.5), we determine the dissociation constants between core and sigma subunits (Table 2.1 and Figure 2.8(a)). Then, in a competition assay under the same conditions, different equimolar concentrations of σ^{70} and σ^F were mixed with a fixed amount of cores to determine the percentage of corresponding holoenzymes produced by the reaction [22]. The latter experimental results are shown as stars in Figure 2.8(b). Using the dissociation constants determined by the fit together with the known concentrations of sigma factors and core RNAPs, we can quantitatively calculate with our model the holoenzyme percentages in the competition experiment. The results are shown as a solid line in Figure 2.8(b) and well agrees with the experimental data.

To characterize the onset of competition for this case, we need to generalize Definition 2.14 to account for the simultaneous increase in the amount of both sigma factor species. For any number of sigma factor species competing for core RNAP, the

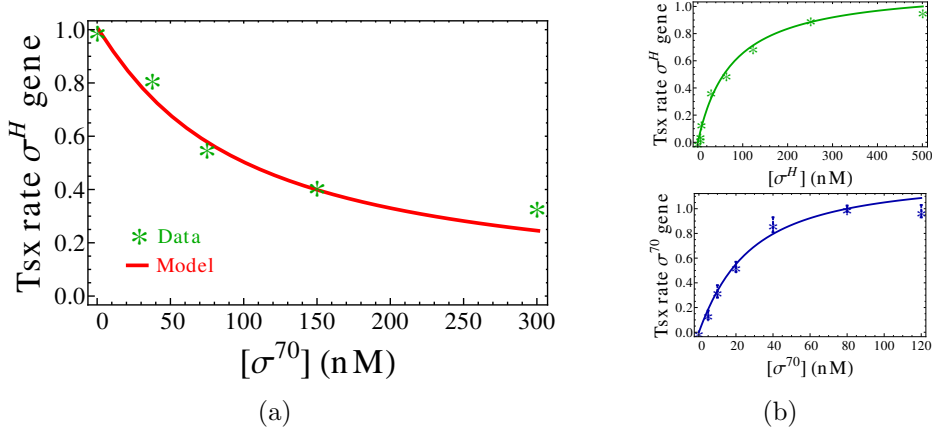


Figure 2.9: Normalized transcription rate of a σ^H -dependent gene as a function of the concentration σ^{70} from a competition experiment *in vitro* [21] (10 mM MgCl₂, pH 7.5, 50 mM KCl, 37°C). (a) The transcription data (stars), obtained in the presence of a fixed amount of core (10 nM) and σ^H (250 nM) and different amounts of σ^{70} , are compared to the prediction of our model (line). To that end, the core-sigma factor and the holoenzyme-promoter dissociation constants are determined by fitting in (b) the results of transcription rate experiments done in the same conditions with a fixed amount of cores, without competition and in the presence of a DNA template containing σ^H -driven [23] and σ^{70} -driven genes [21] (see Table 2.1). Errors and results in the lower panel of (b) are averages of two independent measurements.

competition sets in when the presence of a sigma factor σ^j decreases the formation of a specific holoenzyme $E\sigma^i$ by 5% compared to its maximal value $E\sigma_{max}^i$, that occurs when the sigma factor is σ_{max}^j . That means, when

$$\frac{[E\sigma^i]_{\sigma_{max}^j} - [E\sigma^i]_{\sigma^j > \sigma_{max}^j}}{[E\sigma^i]_{\sigma_{max}^j}} \geq \rho. \quad (2.22)$$

In a generic system, $E\sigma^i$ is chosen to be the holoenzyme whose formation is first affected by competition, *e.g.* the holoenzyme with the weakest binding affinity. Equation 2.22 is used to draw the grey line in Figure 2.8(b). For $\sigma^j = \sigma^{Alt}$, $E\sigma^i = E\sigma^{70}$ and $\sigma_{max}^j = 0$ Equation 2.22 becomes Equation 2.14.

A second competition experiment. The prediction for the transcription rate can be compared to another *in vitro* competition experiment, this time between σ^{70} and σ^H [21]. In this experiment, a DNA template containing the σ^H -dependent PdnaK promoter was mixed with fixed concentrations of RNAPs and σ^H and an increasing concentration of σ^{70} . The measured transcription rates are shown in Figure 2.9(a) as green stars. To reproduce these observations with our model, we need to

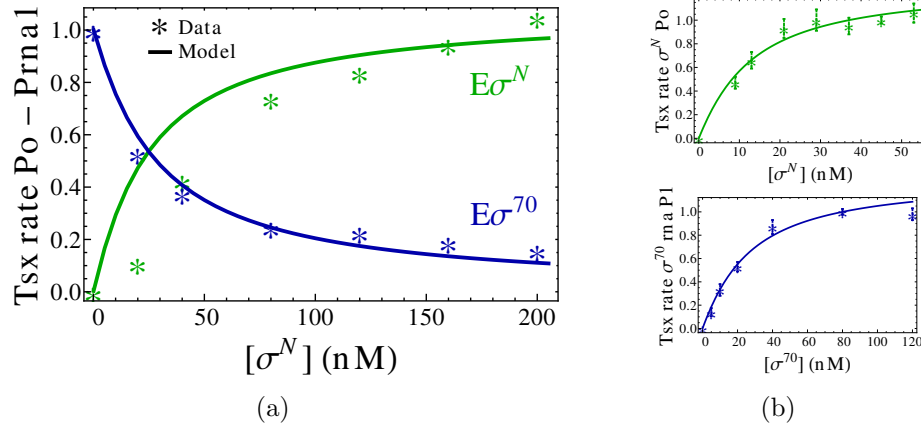


Figure 2.10: Transcription rates of an *in vitro* competition experiment between σ^{70} and σ^N . (a) *In vitro* transcription experiment in the presence of σ^{70} and σ^N [25]. 10 nM core RNAP, 20 nM σ^{70} and a DNA template hosting Prna1 σ^{70} - and Po σ^N -dependent promoters are mixed with an increasing amount of σ^N (pH 7.5, 100 mM NaCl, 10 mM MgCl₂ at 30 °C). Transcription rate is normalized for the Prna1 (blue stars) to transcription levels in the absence of σ^N and presence of 20 nM housekeeping sigma factors, and for the Po (green stars) in the absence of σ^{70} and presence of 160 nM σ^N in same conditions. Solid lines are the theory predictions where we used $K_{E\sigma^{70}}$, $K_{Prna1E\sigma^{70}}$, $K_{E\sigma^N}$ and $K_{PoE\sigma^N}$ obtained from fit of assays without competition. (b) Upper panel: in the same conditions as in (a), 5 nM RNAP cores and a DNA template with Po σ^N -dependent promoter were mixed with variable amounts of σ^N [69]. From the fit of the transcription rate we obtain $K_{E\sigma^N} = 10.8$ nM and $K_{PoE\sigma^N} = 49$ μ M. Lower panel: for description see the lower panel of Figure 2.9(a). From the fit of the transcription rate we obtain $K_{E\sigma^{70}} = 21.1$ nM, $K_{Prna1E\sigma^{70}} = 210$ μ M. Errors and results are averages of two independent measurements. To fit the experimental data we used Equations 2.5 and 2.7 weighted on the errors and normalized on the maximum.

determine the required parameters - the sigma-core dissociation constants $K_{E\sigma^{70}}$ and $K_{E\sigma^H}$, and the holoenzyme-cognate promoter dissociation constant $K_{PdnaK_{E\sigma^H}}$. To that end, we fit two experiments [23, 21] done in the same conditions of the mixing assay, but in the presence of a single-sigma factor species (using Equations 2.5 and 2.7). The results of the fits are summarized in Table 2.1 and in Figure 2.9(b). Once we have all the parameters, we use our model to calculate the transcription rate under conditions of sigma factor competition. The result is plotted as a solid red line in Figure 2.9(a) and well agrees with the experimental data.

A third competition experiment. Now, we compare our model to a second *in vitro* transcription experiment in the presence of competition between σ^{70} and σ^N [25]. A fixed amount of core RNAPs, housekeeping sigma factors and DNA template was mixed with increasing concentrations of σ^N . The DNA contains a σ^{70} -promoter

(Prna1) and a σ^N -dependent promoter (Po). Figure 2.10(a) shows the data of the transcription rate from the Prna1- and Po-dependent genes as blue and green stars, respectively, and as solid lines the prediction of the theory. In order to simulate the observations with our model, we have obtained the binding affinities by fitting results from the same assay in the absence of competition: $K_{E\sigma^N}$, $K_{Po-E\sigma^N}$ from data in reference [69] (stars of the upper panel of Figure 2.10(b)) and, $K_{E\sigma^{70}}$, $K_{Prna1-E\sigma^{70}}$ from data in reference [23] (stars in of the lower panel of Figure 2.10(b)).

Although the correspondence between the simulation of our model and the data is very good, we notice a modest discrepancy in the transcription rate of the Po promoter for low concentrations of σ^N . We can speculate that this could be due to the different mechanism of action of the σ^N compared to the σ^{70} family [9]. Unfortunately, the experiment here analyzed does not provide enough data to include this effect in our theoretical description and test this supposition.

There is a small *caveat* that we need to clarify: while the transcription experiment to obtain $K_{E\sigma^N}$, $K_{Po-E\sigma^N}$ is done in the same conditions as the competition assay (10 mM MgCl₂, pH 7.5, 100 mM NaCl, 30 °C), the transcription experiment to obtain $K_{E\sigma^{70}}$ and $K_{Prna1-E\sigma^{70}}$ had a different salt concentration and temperature (50 mM KCl, 37 °C). First, based on reference [66], where $K_{E\sigma^{70}}$ was measured over a broad range of temperatures, we can exclude that in our situation the temperature could have a major effect on the sigma-core dissociation constants. Secondly, the binding affinities that were registered in reference [70], in which the effect of ionic concentration on the binding affinity was studied, suggest that their variations in are too small to influence our result. The same conclusion can be inferred for the holoenzyme-promoter dissociation constant in different salt and temperature conditions from references [71, 72].

From the analysis above, we can conclude that the quantitative agreements between our calculations and these three experiments provide validation for the modeling approach to sigma factor competition that we use here.

Parameter	Fit value	Reference	Used in Figure
$K_{E\sigma^F}$	25 nM	[22]	2.8(b) [22]
$K_{E\sigma^{70}}$	130 nM	[68]	2.8(b) [22]
$K_{E\sigma^H}$	98.2 nM	[21]	2.9(a) [21]
$K_{PdnaK E\sigma^H}$	24.5 nM	[21]	2.9(a) [21]
$K_{E\sigma^{70}}$	21.1 nM	[23]	2.9(a) [21]
$K_{Prna1 E\sigma^{70}}$	210 μ M	[23]	2.9(a) [21]
$K_{E\sigma^N}$	10.8 nM	[69]	2.10 [25]
$K_{PoE\sigma^N}$	49 μ M	[69]	2.10 [25]

Table 2.1: Summary of the fit values that we use in our simulations.

2.4 Summary

To start transcription, core RNAP reversibly binds to a single sigma factor, an environmental-sensitive unit. The core-sigma factor complex, called holoenzyme, is cognate to a specific class of promoters. While the solely housekeeping sigma factor (σ^{70} in the *E. coli*) is used to transcribe the growth phase genes, during stress phases the cell activates several stress-specific sigma factors that compete with the housekeeping sigma factor to bind to the limited amount of core RNAP. Assuming that the parameters of the alternative sigma factor are similar, they can be lumped into a single class, σ^{Alt} . In this chapter, we have first studied how the modulation of the concentrations of the alternative sigma factors influences the formation of housekeeping and alternative holoenzymes. Since concentrations of cores, sigma factors, and holoenzymes rapidly reach the equilibrium, holoenzyme formation can be characterized by the dissociation constant between cores and sigma factors. We have defined the onset of competition to be the point where the increase of alternative sigma factor causes a 5% reduction in the housekeeping holoenzyme formation compared to the case without σ^{Alt} . For strong binding affinities (small dissociation constants) between core and sigma factors, the onset of the competition is sharp and approximately sets in when the total concentration of sigma factors exceeds the concentration of core RNAPs. Next, we have analyzed the transcription rate of a gene and we have found that unsaturated promoters are more sensitive to sigma factor competition than saturated promoters. Many promoters can bind more than one holoenzyme species, even though only one type may successfully initiate transcription. In this instance the non-transcribing holoenzyme acts as a repressor and because of that during competition even transcription from saturated promoter is largely affected. In the end, we have compared our theory to three different experiments [22, 21, 25], that measure either the holoenzyme formation or the transcription rate during competition of two sigma factor species. The quantitative agreements between our calculations and experiments provide validation for our modeling approach.

Chapter 3

Modulation of sigma factor competition by regulatory factors

Competition between sigma factors can be modulated by additional factors, as shown in Figure 2.1. In this chapter, we use our model to study the influence of two types of such regulators, anti-sigma factors and 6S RNA. Anti-sigma factor binds to the cognate sigma factor [32], either preserving it from degradation or inactivating its functionality. 6S RNA is a small RNA [36] that binds to the housekeeping holoenzyme and impedes the promoter recognition [38, 36]. Anti- σ^{70} and 6S RNA maximally accumulates during stationary phase (Figure 1.4 and Table 1.2) and by reversibly regulating the prevailing role of the housekeeping sigma factor, they promote the transcription of genes under the control of alternative sigma factors.

In addition, the competition may also be affected by non-specific and specific binding of RNA polymerases to DNA, whose effects are discussed in Sections 3.3 and 3.4, respectively. We show that cores and holoenzymes non-specifically bound still play a role in the passive modulation of transcription of the alternative σ -dependent genes. Furthermore, the release of sigma factor from the elongation complex, by adding a second process to dissociate the holoenzyme in addition to the separation in solution, converts the sigma-core binding affinity into an effective dissociation constant, resulting in counter-intuitive behaviors during competition. At the end of the chapter, we explore the effect of introducing transcriptional pauses, transcription factors, the tethering and the rebinding of the sigma factor to the core during the elongation, and regulators of the transcription termination process.

The values chosen for the parameters of the simulations in this chapter are summarized and discussed in Table A.1 of Appendix A. In the following, we refer to “free binding case” as the instance where competition between sigma factors is only for binding to core RNAP, as discussed in Chapter 2. This case is represented by using dashed lines in the plots, unless differently stated. With a “ $E\sigma$ ”, we indicate the holoenzymes that are free in the cell, *i.e.* that are not bound to 6S RNA, not

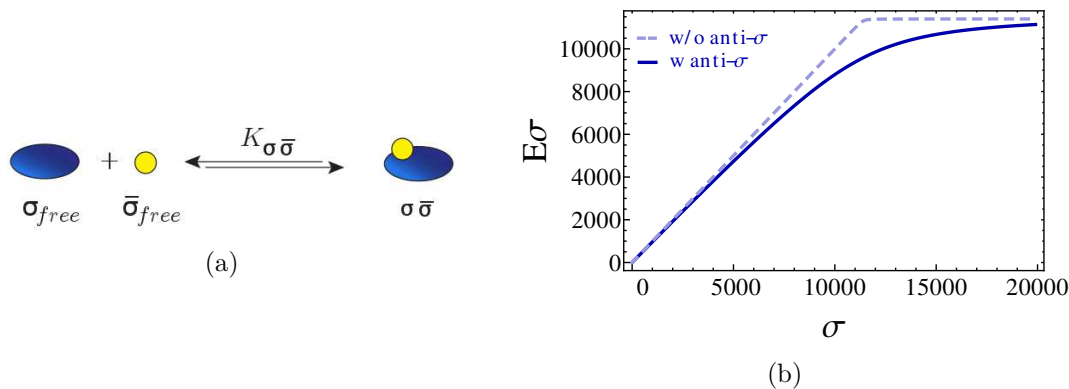


Figure 3.1: Effect of anti-sigma factor. (a) Anti-sigma ($\bar{\sigma}$) sequesters the cognate sigma factor preventing its association with core RNAP. The cell uses anti-sigma factors as a privileged way to modulate the sigma factors availability and readily respond to a changing environment. (b) Holoenzyme formation as a function of sigma factors with a fixed concentration of core RNAPs and anti-sigma factors. For the values adopted in the simulations we always refer to Table A.1 in Appendix A.

non-specifically bound and not engaged in transcription.

3.1 Anti-sigma factors

One strategy towards a more rapid response to environmental changes is to produce alternative sigma factors in advance, and inactivate them if not needed. To that end, the anti-sigma factor creates a complex with the cognate sigma factor, preventing the association with core RNAP [32]. For example, FecR sequesters σ_{FecI} , RseA σ_E , FlgM σ_F , Crl σ_S , and RshA σ_H . Likewise, anti- σ^{70} such as Rsd [21, 23, 34] or AsiA are used to inactivate the housekeeping sigma factor, for example during transition from exponential growth to stationary phase [12, 10]. The interactions between sigma and anti-sigma factors can be quite complex, with different stoichiometries and multiple binding modes [73, 74]. Here, we focus on the simplest case of an anti- σ^{70} (represented as $\bar{\sigma}^{70}$) that binds with one-to-one stoichiometry to σ^{70} with dissociation constant $K_{\sigma^{70}\bar{\sigma}^{70}}$, as in Figure 3.1(a).

3.1.1 Anti-sigma factor binding to cognate sigma factor

Sigma-anti-sigma factor complex formation. We first consider an anti-sigma factor species ($\bar{\sigma}$) in the presence of its cognate sigma factor only. The binding

between these two molecules is described by the reaction



Also taking into accounting the reaction 2.8 that describe the formation of the holoenzyme, the total concentration of the molecules fulfills

$$[E] = [E_{free}] + [E\sigma] \quad (3.1)$$

$$[\sigma] = [\sigma_{free}] + [E\sigma] + [\sigma\bar{\sigma}] \quad (3.2)$$

$$[\bar{\sigma}] = [\bar{\sigma}_{free}] + [\sigma\bar{\sigma}] \quad (3.3)$$

and at equilibrium the following equations are also valid

$$\frac{[E_{free}][\sigma_{free}]}{[E\sigma]} = K_{E\sigma} \quad (3.4)$$

$$\frac{[\sigma_{free}][\bar{\sigma}_{free}]}{[\sigma\bar{\sigma}]} = \frac{k_{b\sigma\bar{\sigma}}}{k_{f\sigma\bar{\sigma}}} \equiv K_{\sigma\bar{\sigma}}. \quad (3.5)$$

Figure 3.1(b) compares the formation of the holoenzymes as a function of the alternative sigma factor in the presence of a fixed number of anti- σ^{70} to the case where there are not anti-sigma factors (solid and dashed lines, respectively). In accordance with the analysis performed in the Introduction (Table 1.2), we suppose to have 19000 anti-housekeeping sigma factors during a generic stress response, almost twice the number of core RNAPs. We choose the anti- σ^{70} - σ^{70} dissociation constant to be larger (50 nM) than the one between σ^{70} and core (1 nM), as suggested by experimental values (see Table A.1 in Appendix A).

Under the replacements $E \rightarrow \sigma^{70}$, $\sigma \rightarrow E$, and $\bar{\sigma} \rightarrow \sigma^{Alt}$, Equations 3.1–3.5 coincide with Equations 2.9–2.13 of Section 2.2. Thus, analytical solutions in the presence of anti-sigma factors are obtained as in Chapter 2 and Appendix B, with suitable substitutions.

3.1.2 Modulation of competition by anti-sigma factor

Concentrations of molecules at equilibrium. To describe the sequestration of the housekeeping sigma factor by anti- σ^{70} factors, we add to Equations 2.9-2.13 the following expressions

$$[\overline{\sigma^{70}}] = [\overline{\sigma^{70}}_{free}] + [\sigma^{70}\overline{\sigma^{70}}] \quad (3.6)$$

$$\frac{[\overline{\sigma^{70}}_{free}][\sigma^{70}_{free}]}{[\sigma^{70}\overline{\sigma^{70}}]} = K_{\sigma^{70}\overline{\sigma^{70}}} \quad (3.7)$$

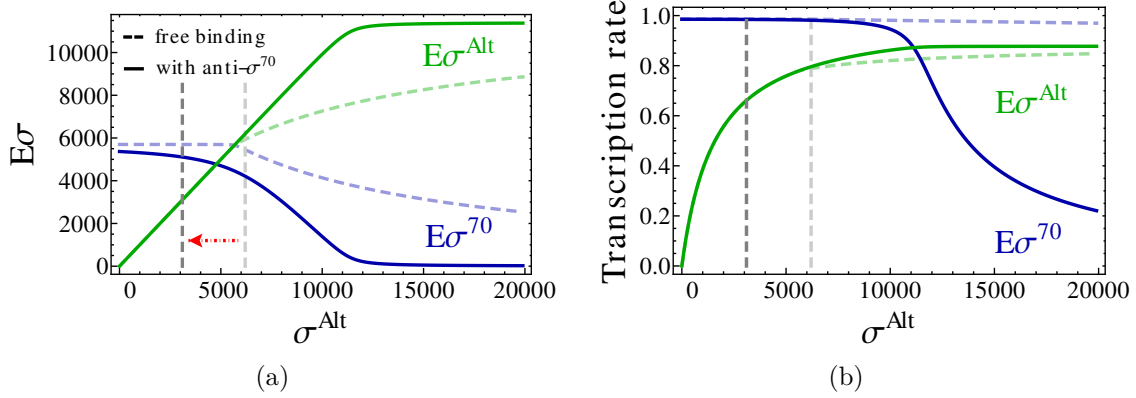


Figure 3.2: Effect of anti-sigma factors during sigma factor competition. (a) Holoenzyme formation as a function of the alternative sigma factor. The dashed lines show the case without anti-sigma factors and the solid lines the case with a fixed amount of anti-sigma factors (19000 molecules); the red arrow highlights the shift of the onset of competition. (b) Normalized transcription rate per promoter. Here and in the following the promoter-holoenzyme dissociation constants are assumed to be $K_{p^{70}E\sigma^{70}} = 10^{-7}$ M and $K_{p^{Alt}E\sigma^{Alt}} = 2 \times 10^{-6}$ M.

and modify Equation 2.10 into $[\sigma^{70}] = [\sigma_{free}^{70}] + [E\sigma^{70}] + [\sigma^{70}\overline{\sigma^{70}}]$.

Holoenzyme formation and transcription rate. Figure 3.2(a) compares the formation of the two holoenzyme species as a function of the alternative sigma factor in the presence of anti- σ^{70} (solid line) to the free binding case (dashed line). A fixed amount of anti- σ^{70} induces competition (whose onset is approximated by Equation C.1 in the Appendix C) for a smaller number of σ^{Alt} , as shown by the red arrow. This shift happens because fewer housekeeping sigma subunits are now available to form holoenzymes compared to the free binding case, thus fewer alternative sigma factors are also needed to outcompete them for the cores. The effect of anti-sigma factors is more pronounced under conditions of competition. As a matter of fact, to the right of the grey line even transcription of a gene with a saturated σ^{70} -dependent promoter is down-regulated, as shown by the solid blue line in Figure 3.2(b). Here and in the following chapters, in order to mimic the effect of strong ribosomal promoters, we assume that the housekeeping holoenzyme binds with a smaller dissociation constant to its cognate promoter ($K_{p^{70}E\sigma^{70}} = 10^{-7}$ M), compared to the alternative holoenzyme dissociation constants ($K_{p^{Alt}E\sigma^{Alt}} = 2 \times 10^{-6}$ M).

3.1.3 Anti-anti-sigma factors

Holoenzyme formation and transcription rate. Anti-anti-sigma factors provide

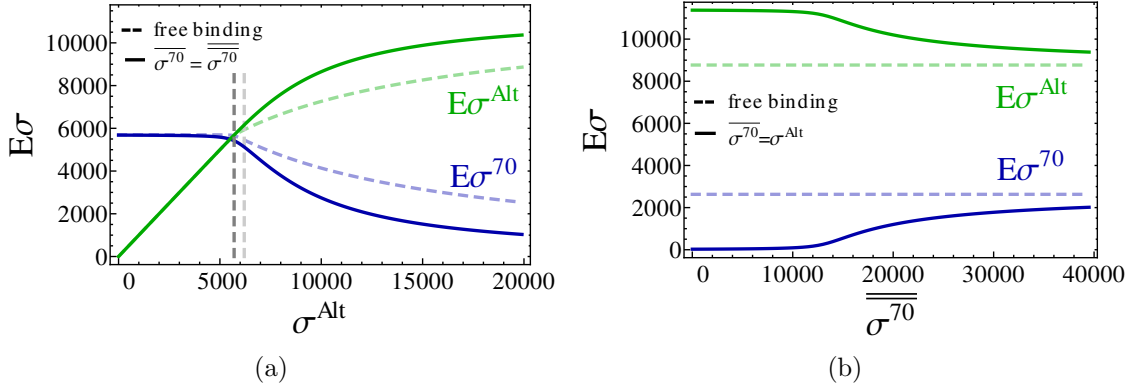


Figure 3.3: Effect of anti-anti- σ^{70} factors. (a) Holoenzyme formation as a function of the number of alternative sigma factors in the presence of the same numbers of anti-anti- σ^{70} and anti- σ^{70} (here 19000) and $K_{\sigma^{70}\overline{\sigma^{70}}} = K_{\overline{\sigma^{70}}\overline{\sigma^{70}}} = 50$ nM (solid lines). (b) Holoenzyme formation as a function of the anti-anti- σ^{70} , in the presence of equal numbers of σ^{Alt} and $\overline{\sigma^{70}}$.

a mechanism to quickly activate or relieve under certain stimuli the effects of anti-sigma factors [32, 75]. Anti-anti-sigma factor ($\overline{\overline{\sigma}}$) binds to cognate anti- σ preventing its interaction with a specific sigma factor. The action of an anti-anti- σ^{70} is described in our model by

$$\begin{aligned} [\overline{\overline{\sigma^{70}}}] &= [\overline{\overline{\sigma^{70}}}_{free}] + [\overline{\sigma^{70}} \overline{\overline{\sigma^{70}}}] \\ \frac{[\overline{\overline{\sigma^{70}}}_{free}][\overline{\sigma^{70}}_{free}]}{[\overline{\sigma^{70}} \overline{\overline{\sigma^{70}}}]} &= K_{\overline{\sigma^{70}} \overline{\overline{\sigma^{70}}}}. \end{aligned}$$

Figure 3.3(a) compares the holoenzyme formation during the free binding case (dashed lines) to a situation where there are equal numbers of anti- σ^{70} and anti-anti- σ^{70} , with the same dissociation constants $K_{\sigma^{70}\overline{\sigma^{70}}} = K_{\overline{\sigma^{70}}\overline{\sigma^{70}}}$ (solid lines). These conditions are not enough to restore the complete functionality of the housekeeping sigma factors, as shown by the difference between solid and dashed lines. Figure 3.3(b) demonstrates that to approach the case of binding without any modulators (dashed lines), a number of anti-anti-sigma factors larger than the number of anti-sigma is needed, because of the sequestration of cores by competing sigma factors. The same result can be achieved by supposing $K_{\overline{\sigma^{70}}\overline{\sigma^{70}}}$ is sufficiently smaller than $K_{\sigma^{70}\overline{\sigma^{70}}}$. The amount of formed housekeeping holoenzymes starts to increase approximately when $\overline{\overline{\sigma^{70}}} = \overline{\sigma^{70}} = 9000$.

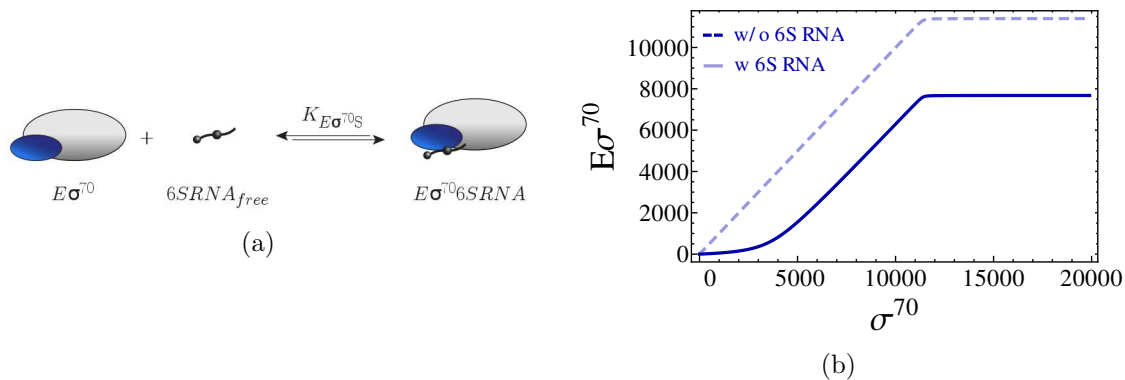


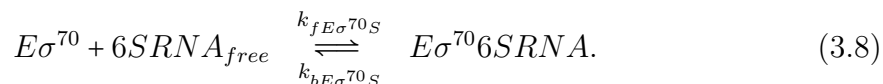
Figure 3.4: Effect of 6S RNA. (a) 6S RNA sequesters $E\sigma^{70}$ holoenzyme preventing the transcription of the associated genes. (b) Number of formed housekeeping holoenzymes as a function of the σ^{70} in the presence of 3800 6S RNA, with $K_{E\sigma^{70}} = 1$ nM and $K_{E\sigma^{70}S} = 200$ nM.

3.2 6S RNA

Another regulator of the availability of RNAP is 6S RNA, a small non-coding RNA transcribed from the *ssrS* gene that binds the active site of housekeeping holoenzyme (Figure 3.4(a)) [36, 31]. In this way, it prevents access to cognate promoters and thus inhibits transcription [76]. 6S RNA maximally accumulates during late stationary phase, where it sequesters many $E\sigma^{70}$ and thereby down-regulates the transcription of the associated genes. This mechanism is believed to enhance the transcription from the promoters dependent on the stationary phase sigma factors, facilitating the shift from an exponential growth to a stationary phase (reviewed in [31]). However, by sequestering $E\sigma^{70}$, 6S RNA also sequesters cores, which are also needed for the formation of the alternative holoenzymes. Therefore, we tested its effects within our model.

3.2.1 Binding of 6S RNA to the housekeeping holoenzyme

6S RNA-housekeeping holoenzyme complex formation. In the presence of the only housekeeping sigma factor, the reaction that describes the association of 6S RNA to the cognate holoenzyme is



From reactions 3.8 and 2.8, we obtain

$$[E] = [E_{free}] + [E\sigma^{70}] + [E\sigma^{70}S] \quad (3.9)$$

$$[\sigma^{70}] = [\sigma_{free}^{70}] + [E\sigma^{70}] + [E\sigma^{70}S] \quad (3.10)$$

$$[S] = [S_{free}] + [E\sigma^{70}S] \quad (3.11)$$

and we define the dissociation constants at equilibrium as

$$\frac{[E_{free}][\sigma_{free}^{70}]}{[E\sigma^{70}]} = K_{E\sigma^{70}} \quad (3.12)$$

$$\frac{[E\sigma^{70}][S_{free}]}{[E\sigma^{70}S]} = \frac{k_{bE\sigma^{70}S}}{k_{fE\sigma^{70}S}} \equiv K_{E\sigma^{70}S}, \quad (3.13)$$

where $[S]$ denotes the 6S RNA concentration. In references [36] and [38], it has been estimated that the quantity of 6S RNA reaches some thousands of units in the cell during the late stationary phase. For that reason, we choose for our simulations the available 6S RNA to be approximately one third of the total RNAP cores, *i.e.* 3800 6S RNA (see Appendix A). As discussed in Table A.1 in Appendix A, by fitting a binding experiment between the housekeeping holoenzyme and 6S RNA, we find that their dissociation constant $K_{E\sigma^{70}S}$ is around 200 nM, usually much larger than the sigma-core dissociation constant. Under this latter assumption, the holoenzyme concentration fulfills

$$[E\sigma^{70}] = \frac{1}{2} \left(-K_{E\sigma^{70}S} - [S] + m + \sqrt{(K_{E\sigma^{70}S} + [S] - m)^2 + 4mK_{E\sigma^{70}S}} \right)$$

where $m = \min([E], [\sigma^{70}])$ (see derivation in Appendix C). This expression well approximates the solid line of Figure 3.4(b), that represents the holoenzyme formation in the presence of a fixed number of 6S RNA. In the same figure, the dashed line shows the free binding case in the absence of modulators; the difference between the two lines roughly gives the number of holoenzymes sequestered by 6S RNA.

3.2.2 Modulation of sigma factor competition by 6S RNA

Effect of 6S RNA during sigma factor competition. Equations 2.11, 2.13 and 3.9–3.13, with the opportune modifications in Equation 3.9 to include the alternative holoenzyme, describe the sequestration of the housekeeping holoenzyme by 6S RNA during sigma factor competition at equilibrium in our model.

Under condition of sigma factor competition, the presence of a fixed amount of 6S RNA reduces the concentrations of both $E\sigma^{70}$ and $E\sigma^{Alt}$, as shown by the solid lines of Figure 3.5(a). The decrease is more pronounced for the housekeeping holoenzymes, which are affected by the sequestration of cores and of σ^{70} . Thus, the formation of alternative holoenzymes relative to total holoenzymes is indeed increased, however, the absolute amount of alternative holoenzymes is typically reduced by the presence of 6S RNA. Only under conditions of no competition (excess of core RNAPs, to the

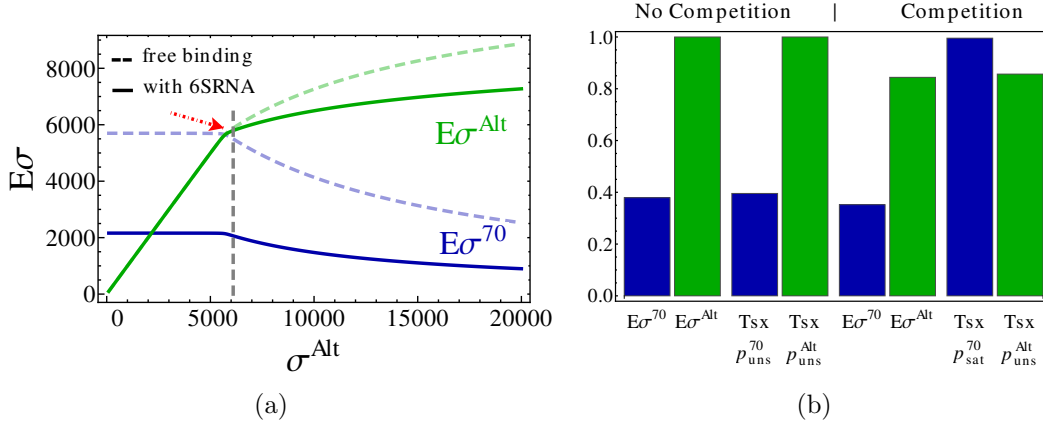


Figure 3.5: Effect of 6S RNA during sigma factor competition. (a) Holoenzyme formation as a function of the alternative sigma factor. Dashed and solid lines show the cases without 6S RNA and with 6S RNA, respectively. The red arrow emphasizes that the initial point of competition is not shifted. (b) The first group of bars (1)–(4) is related to a case with 4000 σ^{Alt} , the second group of bars (5)–(8) to a case with 15000 σ^{Alt} , respectively without and during sigma factor competition in the presence of 3800 6S RNA. Bars (1) and (2), and (5) and (6) show the number of holoenzymes normalized on the holoenzyme formation without 6S RNA. Bars (3) and (4), and (7) and (8) show the transcription rate in the presence of 6S RNA normalized on transcription rate without 6S RNA, with both promoters unsaturated ($K_{p^{70}E\sigma^{70}} = K_{p^{Alt}E\sigma^{Alt}} = 10^{-4}$ M, (3) and (4)) and with σ^{70} -dependent promoters saturated ($K_{p^{70}E\sigma^{70}} = 10^{-8}$ M, $K_{p^{Alt}E\sigma^{Alt}} = 10^{-4}$ M, (7) and (8)), respectively. The blue bars represent the σ^{70} -dependent quantities; the green bars the σ^{Alt} -dependent quantities.

left of the grey dashed line in Figure 3.5(a)), the formation of alternative holoenzymes is unaffected by 6S RNA.

This effect is shown in the bar graph of Figure 3.5(b), in which we normalize the amount of (free) holoenzymes and the transcription rates in the presence of 6S RNA to the case without 6S RNA. The first two bars show the case that we have just discussed, holoenzyme formation without sigma competition, in which alternative holoenzymes are unaffected compared to the free binding case. For unsaturated promoters, the transcription rate proportionally reflects the free holoenzyme concentrations (shown as the third and fourth bar of Figure 3.5(b)), so the same observation made for the holoenzyme formation can be made for the transcription rates. However, if one or both promoters are saturated or close to saturation, the effect of 6S RNA can be much weaker. In particular, under condition of sigma factor competition (15000 σ^{Alt} and holoenzyme formation in fifth and sixth bar) with a saturated σ^{70} -dependent promoter and an unsaturated σ^{Alt} -dependent promoter, as shown by the seventh and eighth bar of Figure 3.5(b), the expected behavior can be inverted: σ^{70} -dependent

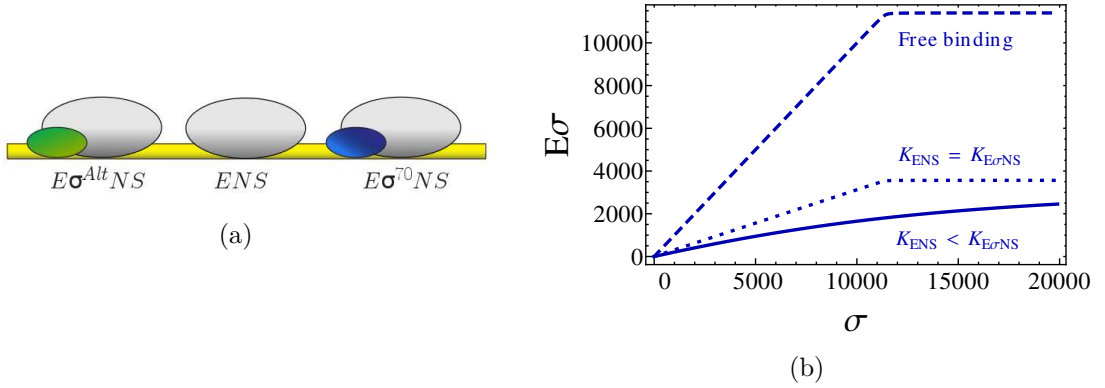


Figure 3.6: Effect of non-specific binding of holoenzymes and cores to DNA. (a) Non-specific binding sequesters both core RNAPs and holoenzymes. (b) Formation of holoenzymes in the presence of one type of sigma factor in the absence of DNA (no non-specific binding, dashed line), in the presence of DNA with equal non-specific binding affinities of cores and holoenzymes ($K_{E\sigma NS} = K_{ENS} = 10^{-2}$ M, dotted line), and with different non-specific binding affinities ($K_{E\sigma NS} = 10^{-2}$ M, $K_{ENS} = 10^{-6}$ M, solid line).

transcription is almost unaffected while σ^{Alt} transcription is reduced.

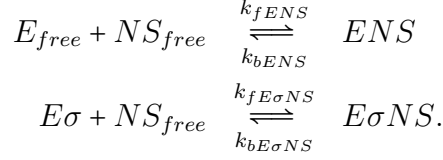
In contrast to the case of anti-sigma factors discussed above, for physiological values of the 6S RNA parameters (weak binding affinity to the housekeeping holoenzyme, numbers of 6S RNA smaller than σ^{70} and excess of cores over 6S RNA, see Tables A.1 and E.2 in Appendix A and E, respectively), the onset of sigma factor competition is not affected by 6S RNA in a detectable manner (highlighted by the red arrow in Figure 3.5(a)). This difference can be understood by considering that by sequestering $E\sigma^{70}$ holoenzymes, 6S RNA equally reduces the numbers of free housekeeping sigma factors and free RNAP cores that participate in the competition.

3.3 Non-specific DNA binding

In addition to their specific binding to promoters, holoenzymes as well as core RNAPs can also bind to DNA non-specifically, in an approximately sequence-independent manner [72]. Despite being weak, non-specific binding may have a strong effect because of the great abundance of non-specific binding sites [54, 42]. Non-specific binding of RNAPs to DNA was proposed to keep weak promoters unsaturated as a prerequisite for the positive control of transcription [11] and to buffer the free RNAP concentration against strong modulation by the stop of transcription of highly expressed genes [42]. Here, we test this effect of the non-specific binding with our model.

3.3.1 Non-specific binding with of one sigma factor species

Holoenzyme formation. Non-specific binding of core RNAP and holoenzymes to DNA (with binding sites NS , Figure 3.6(a)) is described by the reactions



The number of free binding sites largely exceeds the number of occupied binding sites (specific and unspecific, see discussion in Appendix A), hence $[NS] \simeq [NS_{free}]$ and

$$[E] = [E_{free}] + [ENS] + [E\sigma] + [E\sigma NS] \quad (3.14)$$

$$[\sigma] = [\sigma_{free}] + [E\sigma] + [E\sigma] + [E\sigma NS]. \quad (3.15)$$

At equilibrium the following equations are also true

$$\frac{[E_{free}][\sigma_{free}]}{[E\sigma]} = K_{E\sigma} \quad (3.16)$$

$$\frac{[E_{free}][NS_{free}]}{[ENS]} = \frac{k_{bENS}}{k_{fENS}} \equiv K_{ENS} \quad (3.17)$$

$$\frac{[E\sigma][NS_{free}]}{[E\sigma NS]} = \frac{k_{bE\sigma NS}}{k_{fE\sigma NS}} \equiv K_{E\sigma NS}. \quad (3.18)$$

From Equations 3.14 – 3.18, the holoenzyme concentration in the case of a single sigma factor species is given by

$$\begin{aligned} [E\sigma] = & \frac{K_{E\sigma NS}}{2K_{ENS}([NS] + K_{E\sigma NS})^2} \left(K_{E\sigma NS}K_{ENS}(K_{E\sigma} + [E] + [\sigma]) + \right. \quad (3.19) \\ & + [NS](K_{E\sigma}K_{E\sigma NS} + K_{ENS}([E] + [\sigma])) + \\ & - \left(4K_{ENS}K_{E\sigma}K_{E\sigma NS}[E](K_{ENS} + [NS])(K_{E\sigma NS} + [NS]) + \right. \\ & \left. \left. + (K_{ENS}K_{E\sigma NS}(K_{E\sigma} + [\sigma] - [E]) + [NS](K_{E\sigma}K_{E\sigma NS} + K_{ENS}([\sigma] - [E])))^2 \right)^{1/2} \right). \end{aligned}$$

In our model, using parameters expected for the situation in the cell (a relatively large non-specific dissociation constant $K_{NS} \simeq 10^{-3}$ M [54, 42] and a total of 17×10^6 binding sites given by 4.6×10^6 base pairs per genome times 3.8 genome equivalents present in a rapidly growing *E. coli* cell), we find that non-specific binding strongly reduces the concentration of free holoenzymes and, thus, specific binding to promoters. In Figure 3.6(b), in the presence of only one type of sigma factor, the dashed line shows the reference state without non-specific binding, the dotted and solid lines cases with

non-specific binding. If non-specific binding of core RNAPs and holoenzymes are characterized by the same (or approximately the same) dissociation constant (K_{ENS} and $K_{E\sigma NS}$, respectively, dotted line in Figure 3.6(b)), non-specific DNA binding does not affect sigma binding to core, and the total number of holoenzymes is the same as without non-specific binding (dashed line). In that case, the concentration of free holoenzymes is simply rescaled with the probability that a holoenzyme is free in the cytoplasm, $K_{NS}/(K_{NS} + [NS])$, compared to the case without non-specific binding. As a matter of fact, if $K_{E\sigma NS} = K_{ENS} \equiv K_{NS}$, Equation 3.19 can be rewritten as

$$[E\sigma] = \frac{K_{NS}}{2([NS] + K_{NS})} \left(K_{E\sigma} + [E] + [\sigma] - \sqrt{([E] + [\sigma] + K_{E\sigma})^2 - 4[E][\sigma]} \right), \quad (3.20)$$

that divided by Equation 2.5, gives the scaling factor $K_{NS}/([NS] + K_{NS})$ with respect to the free binding case. This property is lost when the non-specific dissociation constants are different (solid line). For example, if core RNAP binds to DNA more strongly than to the holoenzyme, the non-specific DNA competes with σ^{70} for core binding and thereby reduces the concentration of (both total and free) holoenzymes. From an experimental point of view, the dissociation constants for the non-specific binding are dependent on the ionic conditions, due to the electrostatic nature of the non-specific binding, with a stronger dependence for core than for $E\sigma^{70}$ [72] (see discussion in Appendix A). Under physiological high-salt conditions, K_{ENS} and $K_{E\sigma^{70}NS}$ are expected to be rather similar [72], so that the sigma-core binding is not affected by the presence of non-specific DNA. However, a difference in the dissociation constants could affect *in vitro* transcription if different experimental conditions are used.

3.3.2 Modulation of sigma factor competition by non-specific DNA binding

Effect of non-specific binding on sigma factor competition. The situation of two sigma factor species competing to bind to core RNAP in the presence of non-specific DNA binding is described in our model by the following equations:

$$[E] = [E_{free}] + [ENS] + [E\sigma^{70}] + [E\sigma^{70}NS] + [E\sigma^{Alt}] + [E\sigma^{Alt}NS] \quad (3.21)$$

$$[\sigma^{70}] = [\sigma_{free}^{70}] + [E\sigma^{70}] + [E\sigma^{70}] + [E\sigma^{70}NS] \quad (3.22)$$

$$[\sigma^{Alt}] = [\sigma_{free}^{Alt}] + [E\sigma^{Alt}] + [E\sigma^{Alt}] + [E\sigma^{Alt}NS] \quad (3.23)$$

and at equilibrium

$$\frac{[E_{free}][\sigma_{free}^{70}]}{[E\sigma^{70}]} = K_{E\sigma^{70}} \quad (3.24)$$

$$\frac{[E_{free}][\sigma_{free}^{Alt}]}{[E\sigma^{Alt}]} = K_{E\sigma^{Alt}} \quad (3.25)$$

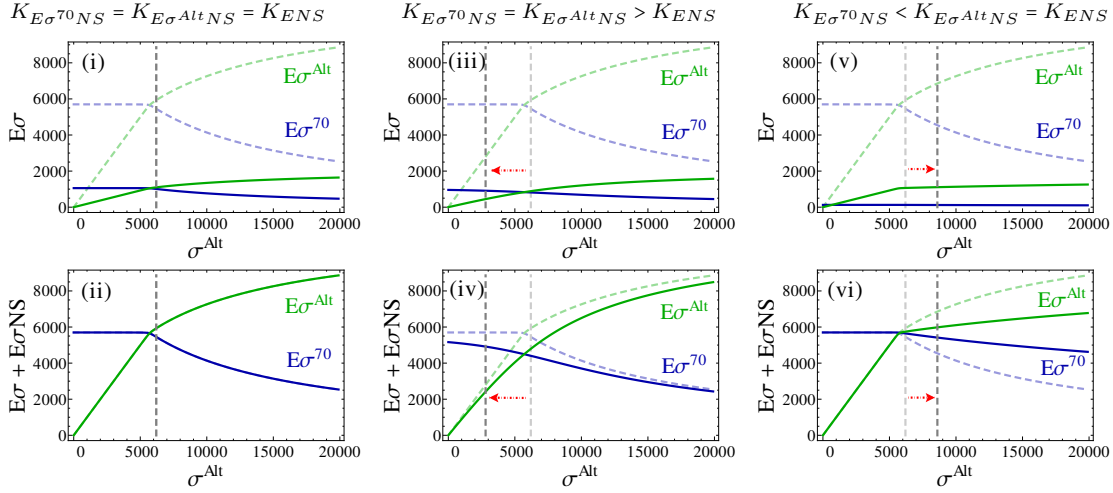


Figure 3.7: Effect of non-specific binding of holoenzymes and cores to DNA during sigma factor competition. Number of free cytoplasmic holoenzymes $E\sigma^{70}$ and $E\sigma^{Alt}$ (upper row) and total number of holoenzymes (free and non-specifically bound, $E\sigma + E\sigma NS$, lower row) as functions of the copy number of alternative sigma factors for three different combinations of non-specific binding affinities: in (i) and (ii) all non-specific dissociation constants are equal ($K_{E\sigma^{70}NS} = K_{E\sigma^{Alt}NS} = K_{ENS} = 5 \times 10^{-3}$ M); in (iii) and (iv) the non-specific dissociation constant for the core is smaller than that for the holoenzymes ($K_{E\sigma^{70}NS} = K_{E\sigma^{Alt}NS} = 5 \times 10^{-3}$ M, $K_{ENS} = 5 \times 10^{-6}$ M); in (v) and (vi) the non-specific dissociation constant for the $E\sigma^{70}$ is smaller than those for $E\sigma^{Alt}$ and core ($K_{E\sigma^{Alt}NS} = K_{ENS} = 5 \times 10^{-3}$ M, $K_{E\sigma^{70}NS} = 5 \times 10^{-4}$ M). The dashed lines in all panels show the reference case without DNA (no non-specific binding).

$$\frac{[E_{free}][NS_{free}]}{[ENS]} = \frac{k_{bENS}}{k_{fENS}} \equiv K_{ENS} \quad (3.26)$$

$$\frac{[E\sigma^{70}][NS_{free}]}{[E\sigma^{70}NS]} = K_{E\sigma^{70}NS} \quad (3.27)$$

$$\frac{[E\sigma^{Alt}][NS_{free}]}{[E\sigma^{Alt}NS]} = K_{E\sigma^{Alt}NS}. \quad (3.28)$$

We can see from Figure 3.7 that if the two holoenzymes and the core RNAPs have the same binding affinity for the non-specific DNA ($K_{E\sigma^{70}NS} = K_{E\sigma^{Alt}NS} = K_{ENS}$, solid lines in panels (i) and (ii)), the non-specific binding does not affect sigma factor competition and free concentrations of holoenzymes are obtained by rescaling the total concentrations of holoenzymes in the absence of DNA (solid and dashed lines in panel (i), respectively). The scaling factor is the same as for the case in the presence of one sigma factor species, *i.e.* $K_{NS}/(K_{NS} + [NS])$. Under these conditions, both free and non-specifically bound core RNAPs participate in sigma factor competition,

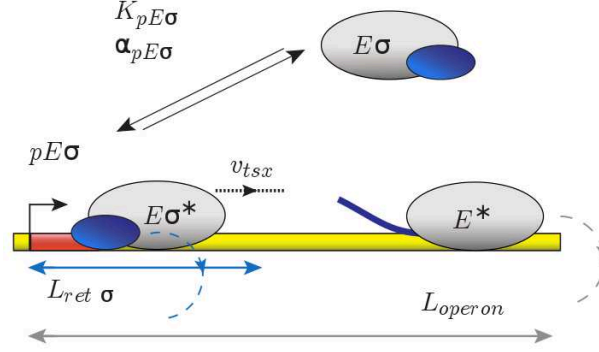


Figure 3.8: Active elongation sequesters core RNAPs for the length of the operon and sigma subunit for some nucleotides.

as shown in panel (ii), where we plot the total number of holoenzymes (free and non-specifically bound). Here, the solid lines (with $K_{ENS} = K_{E\sigma^{70}NS} = K_{E\sigma^{Alt}NS}$) fall on top of the dashed lines, which show the case without non-specific binding. Here, we have assumed equal sigma-core dissociation constants for both sigma factor species. It can be numerically shown that a sufficient condition to obtain a rescaling of the holoenzyme formation in the presence of non-specific binding with respect to the case without DNA is always $K_{E\sigma^{70}NS} = K_{E\sigma^{Alt}NS} = K_{ENS}$, even if $K_{E\sigma^{70}} \neq K_{E\sigma^{Alt}}$. In this case, as noticed, the onset of sigma factor competition is not shifted. When one of the non-specific dissociation constants is different, however, the rescaling property is lost and the onset of sigma factor competition is displaced, as shown by the red arrows and solid lines in panels (iii)–(vi). In panels (iii) and (iv), K_{ENS} is smaller than $K_{E\sigma^{70}NS} = K_{E\sigma^{Alt}NS}$, and the competition (defined by the 5% criterion for the free holoenzymes) starts for a lower number of alternative sigma factors, due to the sequestration of cores. In panels (v) and (vi), $K_{E\sigma^{70}NS}$ is smaller than $K_{ENS} = K_{E\sigma^{Alt}NS}$, and the onset of competition shifts to a larger number of σ^{Alt} because the non-specific binding of $E\sigma^{70}$ enhances the formation of housekeeping holoenzymes, so the competition is biased towards $E\sigma^{70}$. In the cell, non-specific binding of the housekeeping holoenzyme and core are expected to be similar [72] and one can suppose the non-specific binding of alternative sigma factors to be comparable as well. In that case, we can conclude from our results that the presence of DNA does not strongly affect sigma factor competition.

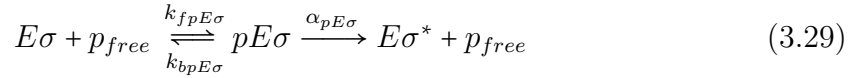
3.4 Transcript elongation

In this section, we consider transcript elongation in more detail. When a holoenzyme binds to a specific promoter (Figure 3.8), it starts to transcribe the associated genes

with the initiation rate $\alpha_{pE\sigma}$. During early elongation, the sigma factor is typically released in a stochastic fashion [77, 3, 78], whereas the core RNAP is committed until it reaches a termination sequence. Thus, transcript elongation sequesters both core RNAPs and sigma factors, but for different amounts of time. The retention length of sigma was estimated to be between 100 [79] and 500 nucleotides [3]. With an elongation speed of 55 nt/sec, an average retention length of 300 nucleotides corresponds to a retention time of ~ 5 seconds. For comparison, core is sequestered for 30–120 seconds, assuming a range of operon lengths of 1500–6000 nucleotides. In the following, we analyze the effect of active elongation on the dissociation constant between core and sigma factor and the effect on the competition.

3.4.1 Transcript elongation with one sigma factor species

Concentrations of holoenzyme, core RNAP and sigma factors busy in transcription. The binding of the holoenzyme to the cognate promoter p and the process of active transcription are described in our model by the reactions



where $\alpha_{pE\sigma}$ is the maximal initiation rate, starred quantities represent the units busy in active elongation with speed v_{tsx} and committed for a retention length L . In the model, we supposed all steps to be reversible apart from transition to the active elongation process. At steady state, we obtain

$$[p] = [p_{free}] + [pE\sigma] \quad (3.32)$$

$$\frac{[p_{free}][E\sigma]}{[pE\sigma]} = \frac{k_{bpE\sigma} + \alpha_{pE\sigma}}{k_{fpE\sigma}} \equiv K_{pE\sigma} \quad (3.33)$$

$$[E\sigma^*] = \frac{\alpha_{pE\sigma}}{k_{ret \ \sigma}} [pE\sigma] \quad (3.34)$$

$$[E^*] = \frac{\alpha_{pE\sigma}}{k_{ret \ E}} [pE\sigma] \quad (3.35)$$

$$\frac{d[RNA]}{dt} = \alpha_{pE\sigma} [pE\sigma]. \quad (3.36)$$

where, for this simple case:

$$[pE\sigma] = [p] \frac{[E\sigma]}{K_{pE\sigma} + [E\sigma]}. \quad (3.37)$$

We also have to modify Equations 2.9–2.13 to conserve the total number of molecules. Equation 3.33 defines the Michaelis-Menten constant $K_{pE\sigma}$ of the promoter. Plugging Equation 3.37 into Equation 3.36 and dividing it by the initiation rate and the promoter concentration, we obtain again Equation 2.7, that we used to define the normalized transcription rate. Concentrations of sigma factors and core RNAPs bound to DNA are, respectively:

$$\begin{aligned} [\sigma]_{DNA} &= [pE\sigma] + [E\sigma^*] = [p] \frac{[E\sigma]}{K_{E\sigma p} + [E\sigma]} \left(1 + \frac{\alpha_{pE\sigma} L_{ret}}{v_{tsx}} \right) \\ [E]_{DNA} &= [pE\sigma] + [E\sigma^*] + [E^*] = [p] \frac{[E\sigma]}{K_{E\sigma p} + [E\sigma]} \left(1 + \frac{\alpha_{pE\sigma} L_{operon}}{v_{tsx}} \right). \end{aligned}$$

Sigma and core retention rates can be estimated from

$$\begin{aligned} k_{ret \sigma} &= \frac{v_{tsx}}{L_{ret \sigma}} \\ k_{ret E} &= \frac{v_{tsx}}{L_{operon} - L_{ret \sigma}}. \end{aligned} \quad (3.38)$$

Effective dissociation constant. In addition to sequestering those cores that are active in elongation, transcription also modulates the binding equilibrium between core and sigma, because the two are actively separated during early elongation. This modulation can be expressed by a binding equilibrium that is characterized by an effective dissociation constant:

$$\frac{[E_{free}][\sigma_{free}]}{[E\sigma]} = K_{E\sigma} + \frac{J/[E\sigma]}{k_{fE\sigma}} = K_{eff} \quad (3.39)$$

with

$$K_{eff} = K_{E\sigma} + \frac{\alpha_{pE\sigma}}{k_{fE\sigma}} \frac{[pE\sigma]}{[E\sigma]} \quad (3.40)$$

that for the model of transcription described by Reactions 3.29–3.31 can be rewritten as

$$K_{eff} = K_{E\sigma} + \frac{\alpha_{pE\sigma}}{k_{fE\sigma}} \frac{[p]}{K_{pE\sigma} + [E\sigma]}. \quad (3.41)$$

The two terms on the right hand side arise from the two pathways for the separation of sigma and core: the first term corresponds to the usual binding equilibrium in solution, and the second term expresses active separation by transcription. Here, $k_{fE\sigma}$ is the sigma-core binding rate (or the formation rate of the holoenzyme) and J (as before) is the transcription rate per volume (initiations per second per volume), which expresses a sigma-core dissociation rate. Indeed, J can be interpreted either as transcription rate per volume of a specific gene *in vitro* or as effective transcription rate of all active genes in the cell volume. In Equation 3.41, we have expressed the

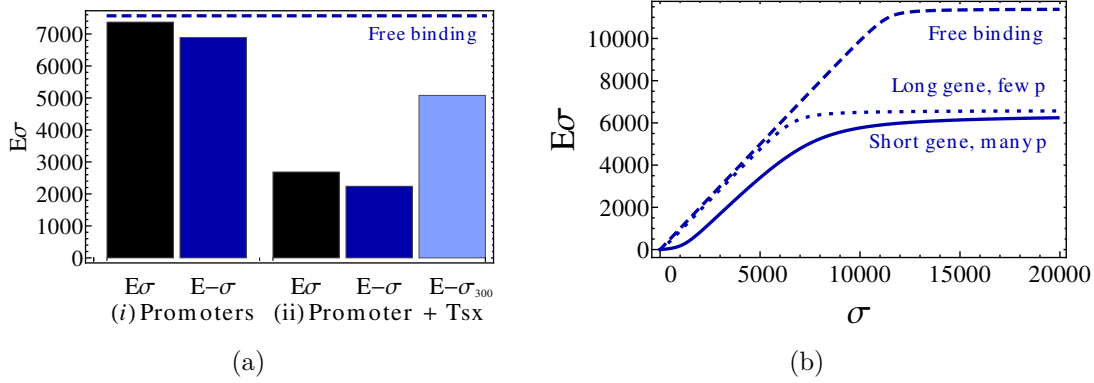


Figure 3.9: Effect of transcript elongation in the presence of one sigma factor species. (a) Formation of holoenzymes in the presence of one type of sigma factor in the absence of DNA (dashed line), in the presence of specific binding to DNA (holoenzymes bind to promoter with $K_{pE\sigma} = 10^{-7}$ M but do not transcribe, case (i)), and in the presence of specific binding to DNA and transcription (case (ii)). The black bars ($E\sigma$) show the case when sigma factor and core unbind as holoenzyme (the binding affinity is described by the equilibrium dissociation constant), the dark blue ($E-\sigma$) and the light blue bars ($E-\sigma_{300}$) show the cases when sigma factor separates from core either after promoter unbinding or gene transcription and after 300 nucleotides, respectively (thus the binding affinity is K_{Eff}). (b) Number of holoenzymes $E\sigma$ as a function of the copy number of sigma factors in the absence of DNA (no specific binding and no transcription with $K_{E\sigma} = 20$ nM, dashed line), with transcription of either a long (20000 nucleotides) but relatively rare gene (20 promoters), as dotted line, or a shorter (2000 nucleotides) but relatively abundant gene (200 promoters), as solid lines. In the latter cases, the cognate genes (holoenzymes bind to promoter with $K_{pE\sigma} = 10^{-7}$ M) with unbinding of sigma factor after 300 nucleotides, core at the end of the operon (thus the binding affinity is K_{Eff}).

transcription rate by the Michaelis-Menten model with the maximal transcription rate $\alpha_{pE\sigma}$ and the Michaelis constant $K_{pE\sigma}$ of the promoter. Equation 3.39 indicates that sigma-core dissociation constants measured in the presence of transcription may not reflect the true binding strength, but rather a weaker effective affinity, because the initiation of transcription provides an additional pathway to dissociate core RNAP and sigma factor. If, however, the transcription rate J is very low or if the transcribed sequence is short, *i.e.* shorter than or comparable to the sigma retention length, as it is often the case in *in vitro* assays, this effect can be neglected and one can use $[E_{free}][\sigma_{free}]/[E\sigma] = K_{E\sigma}$ instead of Equation 3.39.

To disentangle the effects of sequestration of cores and modulation of sigma-core binding by transcript elongation, in Figure 3.9(a) we compare several scenarios for holoenzyme formation and promoter binding in the presence of a single type of sigma

factor. The blue dashed line shows, as reference, the number of holoenzymes formed in the absence of transcription (free binding without DNA). In this case, since the binding between sigma factor and core is quite strong ($K_{E\sigma} = 2 \times 10^{-8}$ M), the number of holoenzymes is approximately given by the smaller one between the numbers of core RNAPs and sigma factors (see Equation 2.5). Thus, here the numbers of sigma factors, because we have 7600 sigma and 11400 cores. Case (i) shows the number of free holoenzymes if holoenzymes can bind to promoters, but do not transcribe. When sigma factor and core RNAP are released together as a holoenzyme when unbinding from the promoter (black bar (i), $E\sigma$), the binding process is characterized by the equilibrium dissociation constant $K_{E\sigma}$. With 200 promoters, $K_{pE\sigma} = 10^{-7}$ M and with the chosen parameters, (essentially) every promoter is occupied and the number of free holoenzymes is reduced by the number of promoters (each promoter sequesters one holoenzyme). If sigma factor and core RNAP are released as separate subunits when unbinding the promoter (blue bar (i), $E - \sigma$), in addition to the sequestration, the binding between sigma and core is also modulated by the supplementary dissociation pathway, and results in the weaker binding characterized by K_{eff} from Equation 3.39. As a consequence, fewer free holoenzymes can be formed than in the previous case. If we include transcript elongation, as shown in case (ii), RNAPs remain sequestered for a longer time, so the free holoenzyme concentration is reduced even more. We consider again the two instances, where core and sigma are released either as holoenzyme (black bar (ii), $E\sigma$, where we used $K_{E\sigma}$) or separately at the end of the operon (blue $E - \sigma$ and light blue $E - \sigma_{300}$ bars (ii), where we used K_{eff}). The latter cases show how the modulation of sigma-core binding plays a prominent role. As a matter of fact, when holoenzyme formation is limited by the availability of sigma factors, the sequestration of sigma factors by transcription slightly reduces holoenzyme formation (compare third and fourth bars). When, instead, the sigma factor is released after 300 nucleotides, the larger pool of free available sigma factors counteracts the weakening effect of K_{eff} (light blue bar).

Figure 3.9(b) shows that the transcription process is dominant over the promoter binding process: the number of formed free holoenzymes $E\sigma$ as a function of sigma factors hardly depends on the number of genes, but rather on the total number of transcribed nucleotides. The number of formed free holoenzymes as a function of sigma factors in the presence of transcription of a long (20000 nucleotides) but relatively rare gene (20 promoters, dotted line) is similar to the one of a shorter (2000 nucleotides) but relatively abundant gene (200 promoters, solid line). As usual, the dashed line represents the free holoenzymes in the absence of DNA.

3.4.2 Modulation of competition by transcript elongation

Transcript elongation during competition. During competition of two sigma factors, the transcription-dependent effective binding affinities can result in complex

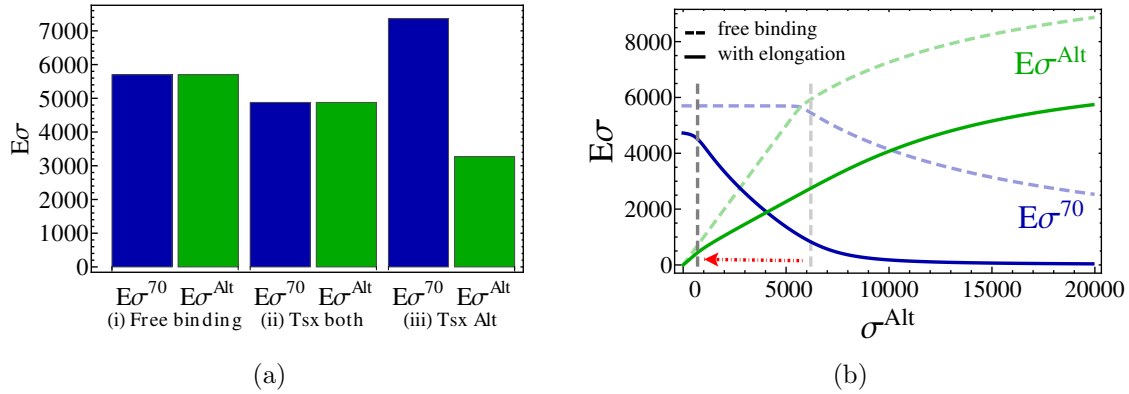


Figure 3.10: Effect of transcript elongation on sigma factor competition. (a) Number of holoenzymes $E\sigma^{70}$ and $E\sigma^{Alt}$ as a function of the copy number of alternative sigma factors in the absence of DNA (case (i)), and with transcription of both σ^{70} - and σ^{Alt} -dependent genes but with unbinding of sigma factor after 300 nucleotides and core at the end of the operon (case (ii)), and with the transcription of the σ^{Alt} -dependent genes only (case (iii)). Values of the parameters are the same as in Figure 3.9(a). (b) Normalized transcription rate for σ^{70} - and σ^{Alt} -dependent promoters as a function of the number of alternative sigma factors, related to the case of Figure 3.10(b) (with $K_{p^{70}E\sigma^{70}} = 100$ nM and $K_{p^{Alt}E\sigma^{Alt}} = 2000$ nM).

counterintuitive behavior. As an example, Figure 3.10(a) shows a scenario in which transcription of housekeeping sigma-dependent genes is abolished. The blue and green bars represent the number of free housekeeping and alternative holoenzymes, respectively, which are characterized by the same parameters, $K_{E\sigma} = 1$ nM, 7600 sigma factors of each species and 11400 core RNAPs. The first two bars (free binding case (i)) show the free binding of sigma factors and cores without transcription. Since the binding affinities are strong and sigma factors are in excess over RNAP, cores are the limiting subunits and, due to the symmetry in the parameters, they are equally divided among the two species of sigma. The same happens in the presence of transcription, again with symmetric parameters, as shown by the second two bars (case (ii) with 200 promoters of each type, gene length of 2000 nucleotides, release of sigma factor and core after 300 nucleotides and at the end of the gene, respectively, and hence equal K_{eff} for both types of sigma factor). The reduction with respect to the free binding case is given by sequestration by transcription and by the effect of K_{eff} . In case (iii), a shut-down of housekeeping genes frees a large number of core RNAPs, and thus one might expect that the production of all holoenzymes is stimulated. However, at the same time the binding between core and σ^{70} effectively becomes more tight, because it is no longer disrupted by the initiation of transcription. As a

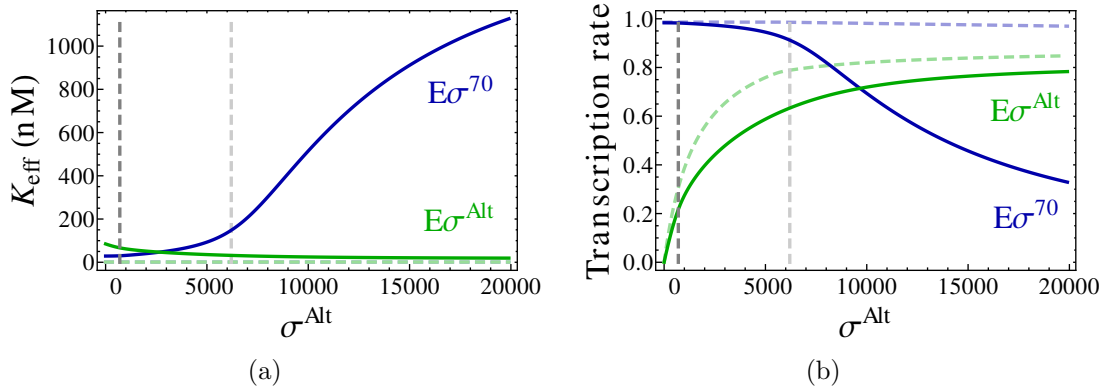


Figure 3.11: Effect of transcript elongation on sigma factor competition. (a) Formation of holoenzymes $E\sigma^{70}$ and $E\sigma^{Alt}$ as a function of the number of alternative sigma factors without DNA (dashed lines) and transcript elongation (solid lines). Modulation of the effective binding affinities K_{eff} by sigma factor competition related to the case of Figure 3.10(b).

consequence, the formation of housekeeping holoenzyme is favored over the formation of alternative holoenzyme, resulting in the counterintuitive decrease of the number of alternative holoenzymes. Note that the excess of sigma factors over core RNAPs allows the formation of more $E\sigma^{70}$ than in the free binding case without transcription.

In Figure 3.10(b), we show how transcript elongation affects sigma factor competition as a function of the increasing concentration of alternative sigma factors. Here, the number of available cores that participate in the competition is effectively reduced by sequestration in transcript elongation, with the effect that competition is already expected to set in for fewer sigma factors. In addition, the effective reduction in binding affinity between sigma and core smoothens the transition to the competition regime, shifting the onset of competition to smaller numbers of sigma factors, as highlighted by the red arrow. The differential release of sigma factor and core is key to this shift: if sigma factors remained bound to core during the entire elongation, the competition would be almost unaffected by the transcription process for a large range of parameters. The modulation of effective binding affinities K_{eff} by the sigma factor competition during alternative sigma increase is shown in Figure 3.11(a). The corresponding transcription rates, with a strong effect on the σ^{70} -dependent promoters, are shown in Figure 3.11(b).

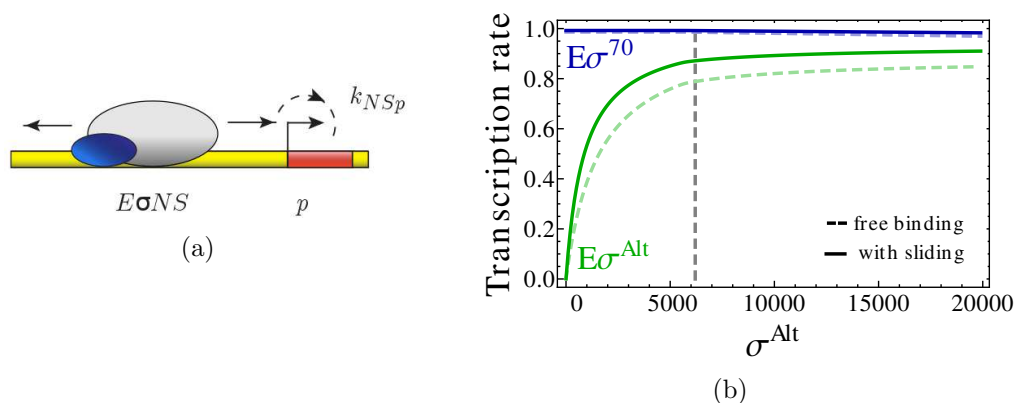


Figure 3.12: Effect of sliding of holoenzyme to find the cognate promoter. (a) The holoenzyme binds non-specifically and diffuses along the DNA strand. During the sliding it may bind specifically to a cognate promoter. (b) Normalized transcription rates in the absence of DNA and in the presence of DNA and RNAP sliding (solid and dashed lines, respectively). Values of the parameters as in Figure 3.7 panel (i) of Section 3.3.

3.5 Transcript elongation - Extensions

So far, to describe the initiation of transcription and the elongation we have used a simplified model that only takes into account the most important steps of the process. In this section, we extend our formulation to obtain a more accurate description of this mechanism. We analyze facilitated binding of holoenzyme to promoter by sliding on the DNA, multi-steps transition from close to open complex, we review the calculations about the effect of shared/overlapping promoters, and we consider the effect of elongation pauses, of transcription factors and of modulation of transcription termination. Besides, it has been demonstrated *in vitro* that housekeeping sigma factors can stay tethered to core after early elongation of some genes [80] and also that free sigma factors are able to rebind the elongating complex [81].

We inspect these effects during sigma factor competition in *in vitro* systems that use physiological values of the parameters and, by estimating their importance *in vivo*, we find that, in the scenarios here analyzed, the simple model of the previous section catches all the necessary features. This happens either because the effect of these modulators can be included into global values of the parameters (*e.g.* the effect of pauses can be included into rates, transcription factors into the number of active promoters, and the modulation of termination into gene lengths) or because experimental evidence shows that their impact is limited or absent *in vivo* (*e.g.* sliding, tethering of sigma to core, sigma rebinding to elongating complex).

3.5.1 RNAP may slide to find the promoter target

RNA polymerase, such as other DNA binding proteins, does not find the promoter target by pure diffusion. However, diffusion is believed to be just one of the possible strategies that can be adopted to achieve the specific binding of the $E\sigma$ to the promoter [82]; among others there are sliding on the DNA, hopping, and intersegmental transfer. So far, we have used parameters for the specific binding (*e.g.* $K_{pE\sigma}$) and non-specific binding (K_{NS}) which already include all the effects of the facilitated diffusion. In this section we disentangle target location by diffusion in the bulk from one-dimensional sliding, which is the most important among facilitated protein transfer mechanisms. However, recent single-molecule experiments of RNAP promoter search in *E. coli* reveal a reduced importance of the facilitated diffusion in the cell [83, 84]. For that reason, we neglect this effect *in vivo* (and *in vitro* because we always use DNA strands that are too short to exhibit any consequence of the facilitated finding).

When RNAP non-specifically binds to DNA, it can slide along the strand for a certain length and eventually undergoes a dissociation event. If during this one-dimensional diffusion, the holoenzyme finds a cognate promoter, it may specifically bind it (we assume irreversibly) with a k_{NSp} rate (as in Figure 3.12(a)):



At equilibrium, this reaction leads to the following modification of the Equations 3.18 and 3.33:

$$\begin{aligned} \frac{[p_{free}][E\sigma]}{[pE\sigma]} &= K_{pE\sigma} - \frac{[E\sigma NS][p_{free}]}{[pE\sigma]} \frac{k_{NSp}}{k_{fpE\sigma}} \\ \frac{[E\sigma][NS]}{[E\sigma NS]} &= K_{E\sigma NS} + [p_{free}] \frac{k_{NSp}}{k_{fE\sigma NS}} \end{aligned}$$

where $k_{fE\sigma NS}$ is the non-specific holoenzyme-DNA binding rate, introduced in Section 3.3. By using values of the parameters expected in the cell (see Table A.1 in Appendix A), the second terms on the right side of both expressions are negligible, thus specific and non-specific dissociation constants to DNA are unmodified by the sliding. Despite that, reaction 3.42 implies that the normalized transcription rate becomes

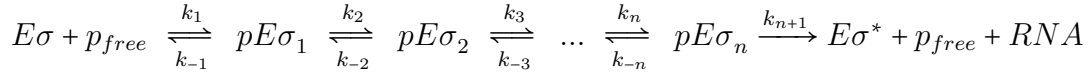
$$\tilde{J} = \frac{[E\sigma] + \frac{k_{NSp}}{k_{fpE\sigma}} [E\sigma NS]}{[E\sigma] + K_{pE\sigma} + \frac{k_{NSp}}{k_{fpE\sigma}} [E\sigma NS]}. \quad (3.43)$$

Equation 3.43 disentangles in the transcription rate the effect of finding the target by pure diffusion from the enhanced one-dimensional search. Figure 3.12(b) shows that the effect of sliding on the transcription rate (solid lines), according to the values of the parameters that we chose (here $k_{NSp} = 2k_{fpE\sigma}$ and $K_{E\sigma NS} = 5 \times 10^{-3}$ M), is negligible compared to the free binding case (dashed lines).

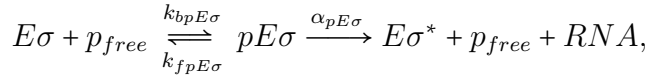
3.5.2 Modulation of transition to open complex

The process of transcription can be roughly divided in three stages: initiation, in which the holoenzyme recognizes the promoter and the RNA synthesis begins; elongation, in which the elongating complex moves along the DNA strand; and termination, in which the RNAP and the RNA product are released. Initiation of transcription can be further divided into several steps. In first approximation, after the promoter recognition, the holoenzyme forms a closed complex, in which the DNA remains double stranded. Next, the enzyme transits to the open complex, it unwinds the DNA to make possible the binding of nucleotides and starts the active elongation. These last passages have been suggested to include several conformationally different steps, whose number depends on the kind of promoter [65, 85]. Here, we generalize this description to any number of steps.

If the process of transition from free holoenzyme to open complex includes n steps, the transcription can be described by



where k_i and k_{-i} are, respectively, forward and backward rates among single steps. The total concentration of promoter is $[p] = [p_{free}] + \sum_{i=1}^n [pE\sigma^i]$. In our model, the initiation of transcription is described by a Michaelis-Menten reaction scheme



which can be considered as a coarse-grained description of the n -step scheme above. This latter can be rewritten in Michaelis-Menten form

$$J = \alpha_{pE\sigma} [p] \frac{[E\sigma]}{K_{pE\sigma} + [E\sigma]} \quad \text{with} \quad K_{pE\sigma} = \frac{k_{bpE\sigma} + \alpha_{pE\sigma}}{k_{fpE\sigma}}$$

via the relations

$$k_{fpE\sigma} = k_1, \quad k_{bpE\sigma} = \frac{k_1}{Z} \sum_{s=1}^n \prod_{\substack{i=1 \\ i \neq s+1}}^{n+1} k_{(-)i} \text{ if } i \leq s,$$

$$\alpha_{pE\sigma} = \frac{\prod_{i=1}^{n+1} k_i}{Z}, \quad Z = \sum_{j=1}^n \sum_{s=1}^j \prod_{\substack{i=1 \\ i \neq j+1}}^{n+1} k_{(-)i} \text{ if } i \leq j \text{ and } s+1 \leq i < n+1.$$

In the subscripts of $(-)$ there are the conditions that request the use of the backward rate. The expressions above generalize the one-step transition of the RNAP from the closed to the open complex. For $n = 4$, this result reduces to the already known multi-step process presented in reference [65].

As an application, we consider the measurement of the kinetic rates involved in the multistep-transcription initiation of a σ^N -holoenzyme in a single molecule experiment [86]. The process of transition from DNA binding to open complex has been divided in three steps, hence, by using the equivalences above with $n = 3$ and the measured rates, we find $K_{pE\sigma} = 1.4$ nM, resulting in a saturated promoter.

3.5.3 Shared promoter/overlapping promoters

In Section 2.2, we have already presented the normalized transcription rate in the presence of a shared promoter/overlapping promoter (Equation 2.21 and Figure 2.7), obtained by neglecting the effect of active elongation and using the usual Michaelis-Menten constant. Here, by considering the active transcription, we see that the competition for binding a promoter effectively tweaks the core-sigma binding affinity.

By taking into account both promoter binding and DNA transcription by holoenzymes, Equation 3.37 modifies to

$$\begin{aligned} [p^i E\sigma^i] &= \frac{[E\sigma^i]/K_{p^i E\sigma^i}}{1 + [E\sigma^i]/K_{p^i E\sigma^i} + [E\sigma^j]/K_{p^i E\sigma^j}} \\ [p^i E\sigma^j] &= \frac{[E\sigma^j]/K_{p^i E\sigma^j}}{1 + [E\sigma^j]/K_{p^i E\sigma^j} + [E\sigma^i]/K_{p^i E\sigma^i}}, \end{aligned}$$

where indexes “ i ” and “ j ” can be either “70” or “*Alt*” and $K_{p^i E\sigma^j} = [E\sigma^j][p_{free}^i]/[p^i E\sigma^j]$. Equations 3.32–3.36 and the effective dissociation constant K_{eff} (Equation 3.40) are changed accordingly. These modifications induce negligible changes both on the holoenzyme formation compared to the case without shared/overlapped promoters (shown in Figure 3.10(b)) and on the transcription rate where we neglected the active elongation (Figure 2.7). These considerations justify the use of Equation 2.21 for the case of shared/overlapping promoters.

3.5.4 Transcriptional pauses and promoter clearance

Active elongation by RNAP is not always a smooth process, in fact it can be suspended by pauses (*e.g.* dependent on the nucleotide sequence, produced by RNAP traffic, by backtracking, by hairpin folding, by (p)ppGpp or promoter-proximal pauses). The duration of the pauses is largely variable and depends on the inducing mechanism: a pause can last from few to many seconds [87]. We notice in this section that pauses of the holoenzyme at the promoter and during transcription also effectively modulate the core-sigma binding affinity. While pauses of the elongating complex reduce the number of free holoenzymes, pauses at the promoters increase this quantity by preventing new bindings. The effect of pauses can be included into core and sigma elongation retention rates.

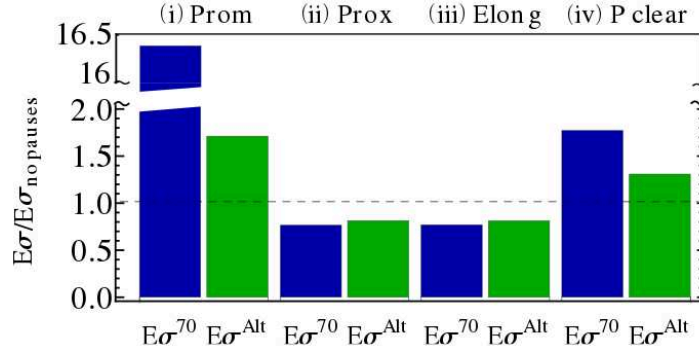


Figure 3.13: Fold increase in the holoenzyme formation in the presence of sigma factor competition (with 15000 σ^{Alt}) with a ten-second-pause at the promoter (case (i)), just after the promoter when the sigma factor is still in complex with the core (case (ii)), during the elongation (case (iii)), and taking into account the RNAP size, compared to the case in the absence of pauses (black line).

We include within our model promoter-proximal pauses of average duration $\langle t_{prox\ pause} \rangle$ by modifying the sigma factor retention rate to

$$k_{ret\ \sigma} = \frac{1}{\frac{L_{ret\ \sigma}}{v_{tsx}} + \langle t_{prox\ pause} \rangle}.$$

We implement elongation pauses through

$$k_{ret\ E} = \frac{1}{\frac{L_{operon}}{v_{tsx}} - \frac{L_{ret\ \sigma}}{v_{tsx}} + \langle t_{elong\ pause} \rangle}$$

and by modifying the initiation rate, we take into account pauses at the promoter:

$$\alpha_{pE\sigma} = \frac{1}{1/\alpha_{pE\sigma\ no\ pause} + \langle t_p\ pause \rangle}. \quad (3.44)$$

Cases (i), (ii), and (iii) of Figure 3.13 show the fold increase in the number of free holoenzymes during sigma factor competition in the presence of pauses of equal duration (10 seconds) at the promoter (case (i)), just after the promoter when the sigma factor is still in complex with the core (case (ii), proximal pauses) and during elongation (case (iii)), compared to the reference case in the absence of pauses (but with transcription, black dashed line). Proximal (case (ii)) and elongation (case (iii)) pauses respectively retain holoenzymes and cores, reducing the number of available cores to form free holoenzymes (and the effective binding affinity is weaker than in the case without pauses). On the contrary, pauses at the promoters act as a bottleneck

for the initiation: they prevent new bindings causing a large increase in the number of free holoenzymes (case (i)) and the effective binding affinity results much stronger than the in case in the absence of pauses.

Till now, we have considered that the RNA polymerase does not spend any time on the promoter. In reality, due to the size of the holoenzyme, the process to free the binding sequence takes some time. A RNA polymerase occupies around 50 nucleotides [88, 89], hence with an average speed on the DNA strand of 55 nucleotides (assumed to be equal to the elongation speed), the holoenzyme spends almost one second on the promoter, enough to increase by 1.5-fold the number of free holoenzymes (case (iv) of Figure 3.13).

Nevertheless, the net effect on the absolute numbers of free holoenzymes is small (matter of few $E\sigma^{70}$ and hundreds of $E\sigma^{Alt}$ units) and transcription rates are almost unaffected by pauses, due to the promoter strength. Moreover, we can still use the model of transcription developed in Section 3.4, provided that the modulation by pauses is taken into account (or included) in the measured retention rates.

3.5.5 Transcription factors: repressors and activators

By specifically binding to DNA, transcription factors regulate the flow of the genetic information at the promoter level either inhibiting (in this case the transcription factor is called repressor) or enhancing (activator) the expression of specific genes [90, 54, 91]. Normally, in the literature, the only effect of the transcription factors is on the transcription rate. Here, we show that by modulating the transcription, they influence also the effective dissociation constant of core and sigma.

At equilibrium, the concentrations of molecules and the dissociation constant of a repressor I that binds the promoter site p according to the reaction



are given by

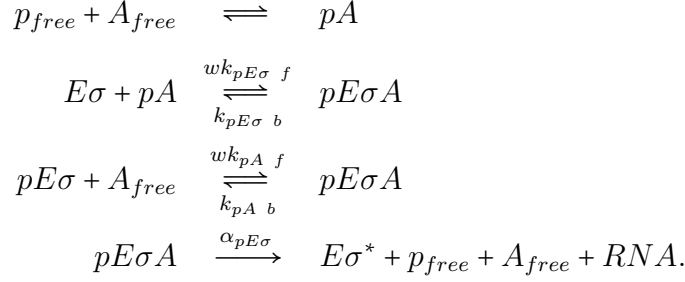
$$\begin{aligned} [I] &= [I_{free}] + [pI] \\ [pI] &= [p] \frac{[I_{free}]/K_{pI}}{1 + [E\sigma]/K_{E\sigma p} + [I_{free}]/K_{pI}} \\ [E\sigma p] &= [p] \frac{[E\sigma]/K_{E\sigma p}}{1 + [E\sigma]/K_{E\sigma p} + [I_{free}]/K_{pI}} \\ \frac{[I_{free}][p_{free}]}{[pI]} &\equiv K_{pI}. \end{aligned}$$

The normalized transcription rate

$$\tilde{J} = \frac{[E\sigma]/K_{E\sigma p}}{1 + [E\sigma]/K_{E\sigma p} + [I_{free}]/K_{pI}}$$

generalizes the overlapping promoter case of Equation 2.21, where the free holoenzyme acts as a repressor.

An A activator helps the cognate promoter recruit the holoenzyme by enhancing their association rate with cooperativity factor w ($w > 1$ [91]):



At equilibrium, the concentrations of the molecules and the dissociation constants fulfill

$$\begin{aligned}
 [A] &= [A_{free}] + [pA] + [pE\sigma A] \\
 \frac{[A_{free}][p_{free}]}{[pA]} &\equiv K_{pA} \\
 \frac{[A_{free}][pE\sigma]}{[pE\sigma A]} &= \frac{k_{pA b}}{wk_{pA f}} \equiv \frac{K_{pA}}{w} \\
 \frac{[E\sigma][pA]}{[pE\sigma A]} &= \frac{k_{pE\sigma b}}{wk_{pE\sigma f}} \equiv \frac{K_{pE\sigma}}{w}
 \end{aligned}$$

and the normalized transcription rate becomes

$$\tilde{J} = \frac{[E\sigma]/K_{pE\sigma} + w[A_{free}]/K_{pA} \cdot [E\sigma]/K_{pE\sigma}}{1 + [E\sigma]/K_{pE\sigma} + [A_{free}]/K_{pA} + w[A_{free}]/K_{pA} \cdot [E\sigma]/K_{pE\sigma}}.$$

Thus in the presence of a transcription factor, the effective binding affinity, that depends on \tilde{J} , changes following Equation 3.40. If we want use the model of transcription in Section 3.4 without any modification, the effect of the transcription factor must be included in the average number of active promoters.

Figure 3.14 compares the scenario of a repressor ($I = 10000$, left panel) and an activator ($A = 10000$, right panel) acting on the housekeeping sigma promoter to the case without any transcription factor (black dashed line), during sigma factor competition (with 15000 alternative sigma factors). The transcription factors are supposed to bind to the promoter with the same strength as the housekeeping holoenzyme. Since the repressor at the σ^{70} -promoter prevents the binding of the cognate holoenzymes, the number of free $E\sigma^{70}$ results is increased (σ^{70} -bar of case (i)), while its transcription rate is diminished (σ^{70} -bar of case (ii)). As a consequence of the sequestration of many cores by the formation of the housekeeping sigma factors, the

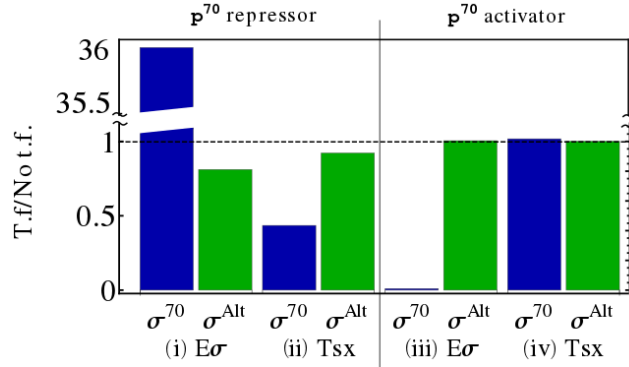


Figure 3.14: Fold increase in the holoenzyme formation (cases (i) and (iii)) and transcription rate (cases (ii) and (iv)) in the presence of sigma factor competition (with 15000 σ^{Alt}) with either a housekeeping sigma factor-dependent promoter repressor (left panel) or promoter activator (right panel), compared to the case in the absence of pauses (black line). The transcription factors bind to the cognate promoter with the same dissociation constant of the housekeeping holoenzyme. Values of the parameters as in Figure 3.10.

activity of the alternative sigma factors is inhibited (σ^{Alt} -bars of cases (i) and (ii)). The right panel shows the effect of an activator acting on the housekeeping sigma factor-dependent promoter. The saturated σ^{70} -promoter (σ^{70} -bar in case (iv)), even in the presence of a strong activator (with cooperativity factor of 100), is obviously unaffected, although the activator procures many holoenzymes that are not longer in the pool of free holoenzymes (shown by the decrease of the σ^{70} -bar of case (iii)). Since many RNAPs are sequestered by the housekeeping genes, the activity of the σ^{Alt} -dependent unsaturated promoter does not change.

3.5.6 Tethered sigma factor to core during elongation

It has been reported from *in vitro* assays that a fraction of σ^{70} can stay tethered to the RNAP core during and hereafter the whole transcription process of some specific genes, with a maximal population of retained sigma factors during stationary phase [78]. Nevertheless, this effect may be mitigated *in vivo* by the presence of the Nus factor that assists the displacement of sigma factor from core [92].

To smoothly switch from the case where all sigma factors are committed up to the end of the operon to the case where all sigma factors are retained just for some nucleotides, we introduce in the following reactions the control parameter λ that represents the fraction of sigma factors tethered to the elongating RNAP for the whole operon:



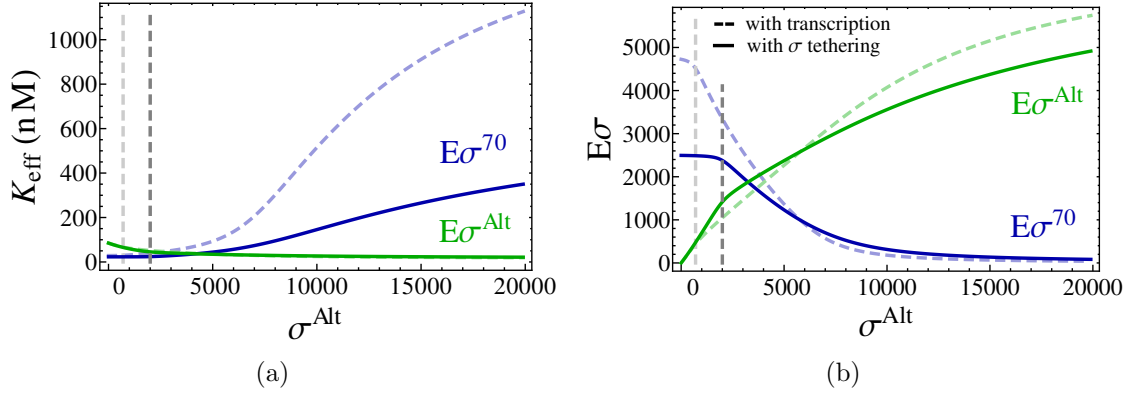
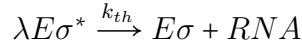


Figure 3.15: Effect of sigma factor tethered to core during elongation. (a) shows the effective binding affinity and (b) the holoenzyme formation as a function of alternative sigma factors with 90% of sigma factors tethered to core RNAPs (solid lines), compared to the case where the sigma factor is retained for 300 nucleotides (dashed lines).



where $0 \leq \lambda \leq 1$. Equations 3.34, 3.35 and 3.39 are replaced by

$$\begin{aligned} [E\sigma^*] &= \frac{\alpha_p E\sigma}{(1-\lambda)k_{ret\sigma} + \lambda k_{th}} [pE\sigma] \\ [E^*] &= \frac{(1-\lambda)k_{ret\sigma}}{k_{retE}} \frac{\alpha_p E\sigma}{(1-\lambda)k_{ret\sigma} + \lambda k_{th}} [pE\sigma] \\ \frac{[E_{free}][\sigma_{free}]}{[E\sigma]} &= K_{E\sigma} + \frac{(1-\lambda)k_{ret\sigma}}{(1-\lambda)k_{ret\sigma} + \lambda k_{th}} \frac{\alpha_p E\sigma}{k_{fE\sigma}} \frac{[pE\sigma]}{[E\sigma]} \equiv K_{eff}. \end{aligned} \quad (3.45)$$

These equations allow to transform the free binding case with the equilibrium constant $K_{E\sigma}$ into the case with the effective binding affinity K_{eff} by tweaking the λ parameter. When $\lambda = 0$, all sigma factors stay associated to the core, even after the termination of elongation. Solid lines of Figure 3.15(a) demonstrate that the value of the effective binding affinity, when 90% of the $E\sigma^{70}$ retain the sigma factor up to the end of the operon, is smaller compared to the case where all sigma factors are sequestered for 300 nucleotides (dashed lines). This stronger housekeeping sigma-core effective binding affinity induces during competition an increase in the formation of $E\sigma^{70}$ at the expenses of the alternative holoenzymes (displayed by the solid lines in Figure 3.15(b)). Figure 3.16, that presents the ratio of the transcription rate with sigma-tethering over the transcription rate without sigma-tethering, shows that the non-dissociation of the holoenzyme complex favors the class of promoters for

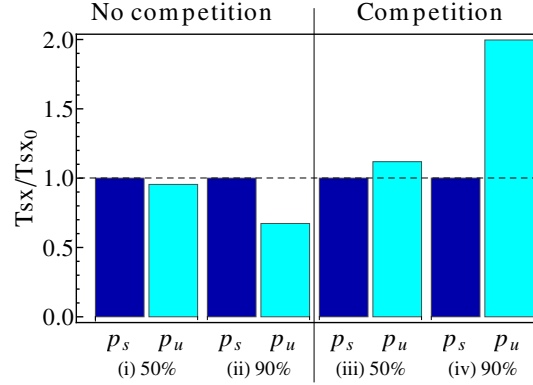


Figure 3.16: Ratio of the transcription rate with sigma-tethering over the transcription rate without sigma-tethering. Blue and cyan bars respectively show the effect of tethering on a saturated promoter ($K_{pE\sigma} = 0.1$ nM) and on an unsaturated promoter ($K_{pE\sigma} = 10000$ nM) in the presence of 50% (cases (i),(iii)) and 90% (cases (ii),(iv)) tethered sigma factors. Left and right panels respectively show the results in the presence (cases (i),(ii) with $1000 \sigma^{Alt}$) and in the absence (cases (iii),(iv) with $15000 \sigma^{Alt}$) of sigma factor competition. Values of the other parameters as in Figure 3.10.

which the sigma-core formation is limiting compared to the holoenzyme-promoter association. While the transcription rate of a saturated promoter (blue bars) is not affected, the transcription of an unsaturated promoter (cyan bars) undergoes a small decrease outside the competition regime (cases (i) and (ii)) and benefits of the stronger K_{eff} during sigma factor competition (cases (iii) and (iv)), particularly for many tethered σ^{70} (case (iv)). In reference [80], it was suggested that the ratio of the binding affinities sigma-core/holoenzyme-promoter determines the enhancement of a promoter transcription in the presence of tethered sigma factors. From our analysis, we find in particular that the transcription is largely influenced by the ratio $\alpha_{pE\sigma}/k_{fE\sigma}$ in the second term of K_{eff} of Equation 3.45.

3.5.7 Sigma factor may rebind to the elongating complex

In vitro experiments with housekeeping sigma factors have proven that even after being released, sigma factors may transiently rebind to the elongating complex with a low binding affinity [80]. Although the *in vivo* concentration of sigma factors suggests that σ^{70} rebinding also occurs in the cell [81], transcription factors (such as Nus factors), that contact the RNAP in a site overlapping the sigma binding site, can reduce its effects [4]. On top of that, here we show that the rebinding becomes relevant, only provided that enough sigma factors are present.

For example, reference [4] assumes from theoretical estimations based on exper-

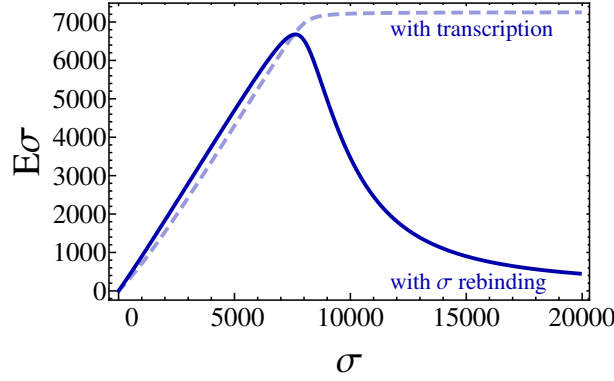
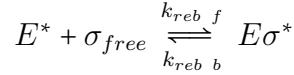


Figure 3.17: Holoenzyme formation in the presence of a single sigma factor species, with $k_{reb\ f} = 2.5 \times 10^7 \text{ M}^{-1} \text{ s}^{-1}$ and $k_{reb\ b} = 2.5 \text{ s}^{-1}$.

imental data that the binding and unbinding rates of housekeeping sigma factors described by the reaction



are $k_{reb\ f} = 2.5 \times 10^7 \text{ M}^{-1} \text{ s}^{-1}$ and $k_{reb\ b} = 2.5 \text{ s}^{-1}$, respectively. Using this reaction at equilibrium with our model, the concentration of transcribing holoenzymes and the rebinding dissociation constant are

$$\begin{aligned} [E\sigma^*] &= \frac{\alpha_{pE\sigma}}{k_{ret\ \sigma} + k_{reb\ b}} [pE\sigma] \left(1 + \frac{k_{reb\ f}}{k_{ret\ E}} [\sigma_{free}] \right) \\ \frac{[E^*][\sigma_{free}]}{[E\sigma^*]} &= \frac{k_{reb\ b}}{k_{reb\ f}} \equiv K_{reb}. \end{aligned}$$

Upon sigma rebinding, the newly formed holoenzyme goes on transcribing some nucleotides. To include in our description the effect of the nucleotides transcribed by this complex, it is enough to modify the sigma factor retention length $L_{ret\ \sigma}$. Here, we neglect this minor change, because we suppose that the binding-unbinding process is fast and thus only few nucleotides are transcribed.

Figure 3.17 shows the number of free holoenzymes (not bound to DNA) that are formed in the cell with a single sigma factor in the presence either of transcription only (dashed line) or of sigma rebinding (solid line). In this latter case, as far as the sigma factors are fewer than the cores, the formation of free holoenzymes is enhanced by the strong core-sigma binding affinity, resulting in the increasing solid line. When all the free polymerases are occupied by a sigma factors, every additional sigma factor binds to the elongating cores, producing an abrupt decrease in the number of free holoenzymes (decreasing solid line). In this situation, both free and elongating cores

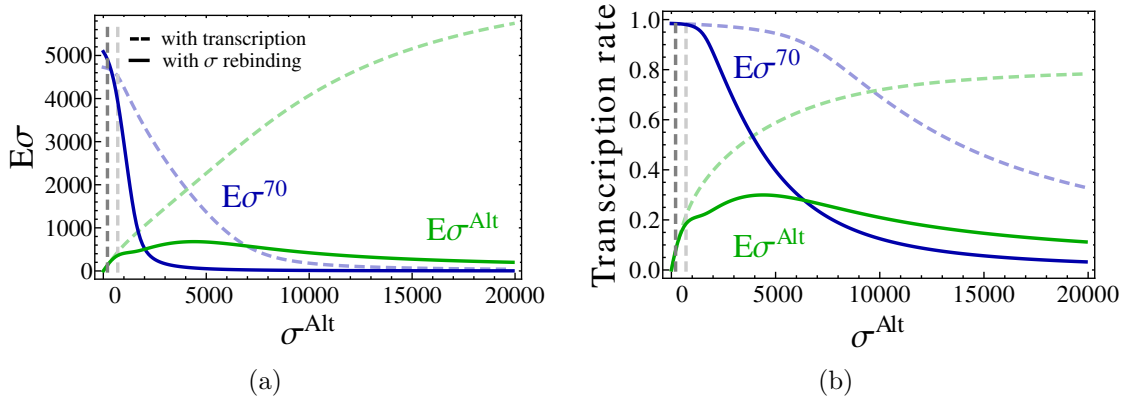


Figure 3.18: Effect of a sigma factor rebinding to the elongating complex. (a)-(b) Holoenzyme formation (in (a)) and transcription rate (in (b)) as a function of alternative sigma factors, with and without sigma factor rebinding (solid and dashed lines, respectively). Values of the parameters as in Figure 3.10.

compete to bind to the free sigma factors. Figure 3.17 clearly highlights that sigma factor rebinding becomes relevant provided that σ concentration is high enough. As a consequence, with two sigma factor species (where we allow every free sigma factor to rebind to any transcribing core) the rebinding effect on the free holoenzymes is more pronounced for large numbers of alternative sigma factors, as shown by the solid lines in Figures 3.18(a) and 3.18(b).

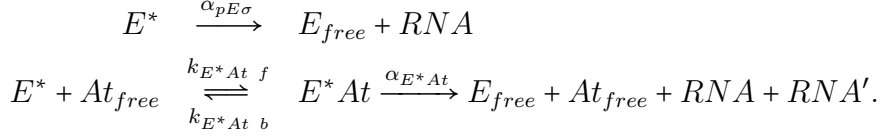
Since the rebinding effect seems to be either small or even not present *in vivo* [4], we neglect in the following this mechanism.

3.5.8 Terminators and anti-terminators of transcription

RNA polymerase synthesizes RNA up to a termination signal, where the enzyme releases the product and dissociates from the DNA strand. Termination events can be categorized in two classes: intrinsic terminations, when a specific termination sequence in the DNA is solely recognized by the RNAP without the requirement of any ancillary cellular factors (these are the cases considered up to here) and rho-dependent terminations, in which a protein called rho factor binds to the nascent RNA strand, relocates along the RNA and interacts with the core enzyme releasing it from the elongation complex. Pausing of the RNA polymerase at the termination site allows the rho factor to reach the core. The fraction of transcripts that are not stopped by the termination sequence are referred to as readthrough events. Furthermore, termination can be prevented by several specific anti-termination factors [2].

In the simplest scenario, when an anti-terminator At interacts with the elongating

RNAP E^* , it induces a readthrough event, that is described in our model by the reactions



RNA is the product of transcription up to the normal termination sequence and RNA' is the piece of RNA transcribed thanks to the anti-termination binding. The concentration of molecules and the dissociation constant at equilibrium fulfill

$$[At] = [At_{free}] + [E^*At] \quad (3.46)$$

$$[E^*At] = [At] \frac{[E^*]}{[E^*] + K_{E^*At}} \quad (3.47)$$

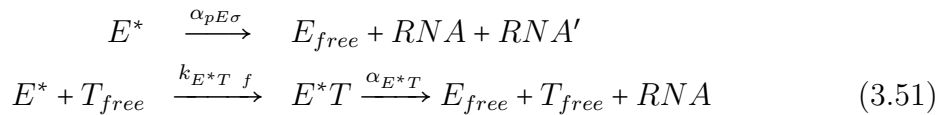
$$\begin{aligned}
 [E^*] &= \frac{1}{2k_{ret\ E}} \left(\alpha_{pE\sigma}[pE\sigma] - \alpha_{E^*At}[At] - K_{E^*At}k_{ret\ E} + \right. \\
 &\quad \left. + \sqrt{(\alpha_{E^*At}[At] + K_{E^*At}k_{ret\ E} + \alpha_{pE\sigma}[pE\sigma])^2 - 4\alpha_{pE\sigma}K_{E^*At}k_{ret\ E}[pE\sigma]} \right) \quad (3.48)
 \end{aligned}$$

$$\frac{[At_{free}][E^*]}{[E^*At]} = \frac{k_{E^*At\ b} + \alpha_{E^*At}}{k_{E^*At\ f}} \equiv K_{E^*At} \quad (3.49)$$

and the transcription rates are given by

$$\begin{aligned}
 \frac{d[RNA]}{dt} &= \alpha_{pE\sigma}[pE\sigma] + \alpha_{E^*At}[E^*At] \\
 \frac{d[RNA']}{dt} &= \alpha_{E^*At}[E^*At].
 \end{aligned} \quad (3.50)$$

The rho-dependent termination can be treated in a similar way. In the reactions



we suppose that the terminator protein rho (T) irreversibly binds to the elongating RNAP and destabilizes the elongating complex. Here, RNA is the product of the transcription terminated with the rho factor and RNA' is the piece transcribed after going through the stop point of the rho-dependent termination (readthrough). To obtain the concentrations of the molecules and the binding affinity, it is enough to substitute At with T in Equations 3.46–3.49 and to change the transcription rate of Equation 3.50 into $d[RNA']/dt = \alpha_{pE\sigma}[pE\sigma]$.

In both terminator and anti-terminator case, the core retention rate $k_{ret\ E}$ depends on a transcribed sequence of length L longer than the operon length and on pauses of

the elongation complex at the termination site of average time $\langle t_{pause} \rangle$ in the following way:

$$k_{ret\ E} = \frac{1}{\frac{L}{v_{tsx}} + \langle t_{pause} \rangle}.$$

If we now suppose the termination to be always rho factor-dependent, the transcription rate is simply $d[RNA]/dt = \alpha_{pE\sigma}[pE\sigma]$ and the concentration of elongating cores is

$$[E^*] = \frac{\alpha_{pE\sigma}}{k_{ret\ E\ eff}}[pE\sigma].$$

In this expression, we have defined an effective retention rate of the elongating complex that depends on the concentration of terminators: $k_{ret\ E\ eff} = k_{E^*T\ f}[T_{free}]$. If the number of rho factors largely exceeds the number of elongating complexes to which the rho can bind, we observe that the number of free terminators is almost equal to the number of total terminators ($[T_{free}] \simeq [T]$) and the $k_{ret\ E\ eff}$ becomes a constant: $k_{E^*T\ f}[T]$. Hence, to describe a rho-dependent termination process, we can still use Equation 3.38 with L_{operon} replaced by

$$L_{ret\ eff} = v_{tsx} \left(\frac{1}{k_{E^*T\ f}[T]} - \langle t_{pause} \rangle \right) \quad (3.52)$$

where we have also included the pauses at the termination site.

From our analysis, we conclude that, generally, when the transcription process needs an adjuvant factor (such as the rho factor), the $k_{ret\ E}$ rate at which free cores are released after sequestration by elongation process becomes an effective rate, dependent on the concentration of the helping protein. This dependence, under some assumptions (here that the amount of terminator factors exceeds the transcribing cores), can be included in some effective quantities, such as in the elongation rate for this last case.

3.6 Competition and regulatory factors

Here, we give a compact formulation for the equations that describe the enhanced model for sigma factor competition of Figure 2.1. We can rewrite the system of equations, whose solutions give the concentration of the molecular species used in our model, as:

$$\begin{aligned} [A^i B^j] &= \frac{[A_{free}^i][B^j] \prod_{l \neq i} K_{A^l B^j} \prod_n K_{C^n B^j}}{\prod_l K_{A^l B^j} \prod_n K_{C^n B^j} + \sum_{X=A,C} \sum_{\{l\}} [X_{free}^1]_j \prod_{m \neq l} K_{X^m B^j} \prod_n K_{A^n B^j}} \\ [D_{free}^j] &= \frac{[D^j] \prod_n K_{C^n D^j}}{\prod_n K_{C^n D^j} + \sum_C \sum_{\{l\}} [C_{free}^1]_j \prod_{m \neq l} K_{C^m D^j}} \end{aligned} \quad (3.53)$$

where we include all the regulatory factors introduced in this chapter (*i.e.* anti-sigma factors, 6S RNA, non-specific binding, and transcript elongation). Indexes run over all the different types of molecules of that species, *e.g.* $\sigma^i = \sigma^{70}, \sigma^S, \sigma^N \dots$ or $p^i = p^{70}, p^S, p^N \dots$ and so forth. We extend the analysis allowing every anti-sigma factor $\overline{\sigma^i}$ to bind to any other species of sigma factor σ^j , every anti-anti-sigma factor $\overline{\overline{\sigma^i}}$ to bind to any other species of anti-sigma factor $\overline{\sigma^j}$, every holoenzyme $E\sigma^i$ to bind to any promoter p^i and transcribing its dependent gene, and supposing the existence of various small RNA S^i able to sequester any holoenzyme species. $A, B, C, \overline{C}, S^i, NS, p^i$ and A, B, C (not D) can be even $E\sigma^i$. In Equation 3.53, C represents the particles that bind to B that are different from A . In all equations, where not specified, indexes can also take the same value. If one complex can not be formed, we set the corresponding concentration to zero: *e.g.* if S^i does not bind to $E\sigma^j$, hence $[E\sigma^j S^i] = 0$, or if $E\sigma^i$ does not bind to promoter p^j , hence $\alpha_{p^j E\sigma^i} = 0$. If a dissociation constant does not exist, *e.g.* K_{AB} , we impose that $K_{AB} = 1$ and $[AB] = 0$. We also introduce the conventions that if $[E\sigma_l]$ binds to p^j , thus $[E\sigma_l]_{p^j} = [E\sigma_l]$, otherwise $[E\sigma_l]_{p^j} = 0$. $\{, \}$ represents a function where every single index appears only once without repetition. In every calculation, we approximate $[NS] \simeq [NS_{free}]$. $[E\sigma^i]$ can be explicitly obtained by solving

$$\frac{[E_{free}][\sigma^i]}{[E\sigma^i]} = K_{E\sigma^i} + \frac{\sum_j \alpha_{p^j E\sigma^i} [p^j E\sigma^i]}{k_{fE\sigma^i} [E\sigma^i]}. \quad (3.54)$$

By using

$$\begin{aligned} [E^*]_{p^i} &= \frac{\sum_j \alpha_{p^i E\sigma^j} [E\sigma^j p^i]}{k_{retp^i E}} \\ [E\sigma^{i*}]_{p^j} &= \frac{\alpha_{p^j E\sigma^i}}{k_{retp^j \sigma^i}} [p^j E\sigma^i] \\ [p^j E\sigma_i] &= [p^j] \frac{[E\sigma_i] \prod_{l \neq i} K_{p^j E\sigma_l}}{\prod_l K_{p^j E\sigma_l} + \sum_{\{l\}} [E\sigma_l]_{p^j} \prod_{m \neq l} K_{p^j E\sigma^m}} \end{aligned}$$

$[E\sigma^i]$ can also be rewritten as

$$[E\sigma^i] = \frac{E_{free} \sigma_{free}^i k_{fE\sigma^i} - \sum_j \alpha_{p^j E\sigma^i} [p^j E\sigma^i]}{K_{E\sigma^i} k_{fE\sigma^i}}.$$

The transcription rate fulfills

$$\frac{d[RNA_{p^i}]}{dt} = \sum_j \alpha_{p^i E\sigma^j} [p^i E\sigma^j].$$

3.7 Summary

In this chapter we have seen how the regulatory factors (represented in Figure 2.1) tune the holoenzyme formation and the transcription rate.

Anti- σ^{70} binds to the cognate sigma factor and, by preventing its association to the core, reduces the amount of housekeeping holoenzymes. The competition typically sets in with less alternative sigma factors compared to the case without any modulator (Figure 3.2(a)), and even saturated σ^{70} -dependent promoters are down-regulated by increasing concentration of alternative sigma factors (Figure 3.2(b)). Anti-anti-sigma factors may eventually neutralize the effect of anti-sigma factors by binding to cognate anti-sigma factors (Figure 3.3).

6S RNA specifically binds to the housekeeping holoenzyme and reduces the concentrations of both $E\sigma^{Alt}$ and, in particular, of $E\sigma^{70}$ (Figure 3.5(a)), which is affected by sequestration of cores and σ^{70} . In this case, the onset of sigma factor competition is not affected in a detectable manner (Figure 3.5(a)).

Non-specific interactions of core RNAPs and holoenzymes with DNA shift the onset of competition according to the imbalance among the non-specific dissociation constants (Figure 3.7). In particular, if the two holoenzymes and the cores have the same binding affinity for non-specific DNA, that is likely to be in physiological conditions, non-specific binding does not affect sigma factor competition, and free concentrations of holoenzymes are obtained by rescaling the total concentrations of holoenzymes of the free binding case. For that reason non-specifically bound holoenzymes play a role similar to their free counterpart in sigma factor competition. Thus, non-specific binding itself neither helps in sequestering excess of free RNAPs after a stop of ribosomal promoters [42] nor promotes an active control [11] by enhancing alternative sigma factor-dependent gene regulation.

Transcript elongation modulates the binding equilibrium between core and sigma, characterized by an effective dissociation constant (Equation 3.39), because the two are actively separated during early elongation. In Section 3.4.2, we have shown that during sigma factor competition, the effective binding affinities can originate complex behaviors that may be counterintuitive. Besides that, the differential release of sigma factor and core shifts the onset of sigma factor competition (Figure 3.10); if sigma factor remained bound to core during elongation, the competition would be almost unaffected by the elongation process for a large range of parameters.

In Section 3.5, we have studied some extensions of the transcription model. In particular, we have analyzed the consequences of the sliding of the holoenzyme on the DNA to find the promoter, we have considered pauses during the elongating process, the effect of transcription factors, of modulation of the transcription termination, of tethering of the sigma factor to the core during and hereafter elongation, and the possibility of rebinding to the elongating complex. We have found that the simplest model of transcription can still be used, provided that the effect of these modulators is

included into the global values of the parameters (*e.g.* effect of pauses can be included into rates, transcription factors into number of active promoters, modulation of termination into gene lengths). σ^N -dependent genes also present abortive transcription, need for activators and poised state of sigma factor to start the transcription process [31, 9, 93]. These effects can be taken into account by effectively lowering the rate of initiation of transcription. As for the facilitated one-dimensional diffusion to find the promoter, the tethering of sigma to core and the sigma rebinding to elongating complex, experimental evidence have shown that their impact *in vivo* is limited or absent.

Chapter 4

Stringent response

In this chapter, we use our model to address the passive up-regulation of genes under the control of alternative sigma factors during stringent response. Stringent response is a cellular program activated by amino acid starvation: shortage of amino acids leads to accumulation of uncharged tRNAs, which induces the synthesis of the signaling nucleotide (p)ppGpp [43, 94]. (p)ppGpp is a global regulator that directly or indirectly affects many processes, but its key regulatory role is to suppress the transcription of ribosomal RNA (rRNA) [95]. Since rRNA transcription accounts for up to 75% of all transcription in rapidly growing bacteria [13, 42], the *rrn* operons encoding the rRNAs sequester large numbers of RNA polymerases. These become free upon the stop of *rrn* transcription and thus become available to transcribe other genes. It has therefore been proposed that the stop or strong suppression of rRNA transcription passively up-regulates genes such as σ^{70} -dependent biosynthesis genes [96, 50] and alternative sigma factor-driven stress response genes [21, 23, 33]. A recent theoretical study has however estimated the effect on biosynthesis genes to be relatively small [42], so that direct activation of these genes by (p)ppGpp (together with DksA) [45] is likely to be the dominant effect. The reason for the moderate effect is a relatively large pool of RNAPs non-specifically bound to DNA that buffers against such strong impact of the rRNA shut-down [42]. This result is in contrast with our findings from Section 3.3 in Chapter 3, where we show that non-specific binding does not affect the competition of sigma factors, so that alternative sigma factor-controlled transcription may not be buffered against the release of core RNAPs from *rrn* operons. Modulation of transcription during stringent (and stress) response is also a reflection of the reallocation of the RNA polymerase in the cell among different classes of genes. Although (p)ppGpp plays a major role in this mechanism, other regulators such as anti-sigma factors and 6S RNA may be necessary to favor the access of alternative sigma factors to cores to reroute the transcriptional program [31, 9]. In the following, we therefore test within our model first the consequences of the stringent response on sigma competition, then the effects of modulators on partitioning of RNAP among

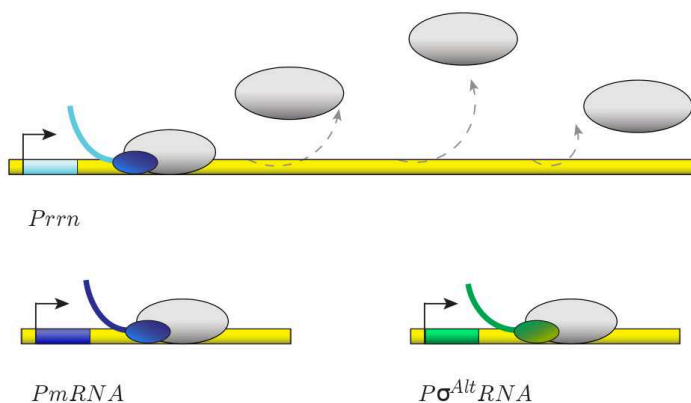


Figure 4.1: Stringent response. During stringent response RNA polymerases involved in rRNA transcription are quickly released and increase the pool of free cores.

different processes in the cell during different stress (stringent) response scenarios. Besides, it was proposed that regulation during stringent response may come from a weakening effect of the (p)ppGpp alarmone on the housekeeping holoenzyme binding affinity [21, 52, 53]. At the end of this chapter, we analyze a competition experiment that supports a possible direct weakening induced by (p)ppGpp on the housekeeping holoenzyme dissociation constant.

4.1 Increased core availability

Parameters of the model. We first inspect the consequences of an increased concentration of core RNAPs due to their release from *rrn* operons (Figure 4.1). We describe the total transcription in the cell by three classes of promoters: ribosomal RNA promoters (P_{rrn}), σ^{70} -dependent mRNA (non-ribosomal) promoters (P_{mRNA}), and alternative sigma-driven promoters ($P_{\sigma^{Alt}RNA}$). The stop of transcription of rRNA frees a large amount of cores (as well as some housekeeping sigma factors) that were sequestered there. For a simplified, but quantitative description of a bacterial cell during stringent response, we first have to choose the parameters of the model: the numbers of cores and housekeeping and alternative sigma factors as well as the dissociation constants. A complete discussion about our choice is provided in Table A.1 of Appendix A and Table E.1 of Appendix E. We start from a previous description [42] based on the data of reference [13] and consider *E. coli* cells growing with a growth rate of 2.5 dbl/h. Such a cell contains on average a total of 11400 RNAPs. Out of these, approximately 1100 are immature assembly intermediates, 2600 are transcribing rRNA, and 700 are transcribing mRNA [42]. The remaining 7000 RNAPs are

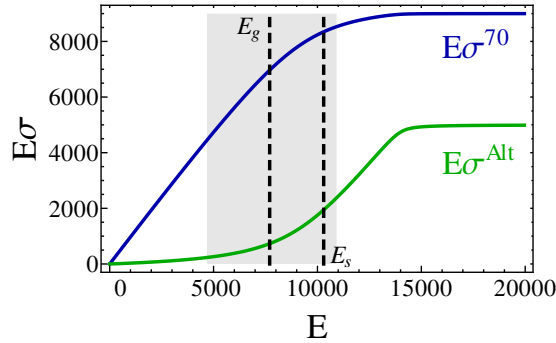


Figure 4.2: Stringent response. Number of holoenzymes $E\sigma^{70}$ and $E\sigma^{Alt}$ as a function of the copy number of core RNAPs. The black dashed lines show the number of available RNAPs during exponential growth state (E_g) and during stringent response state. The gray region shows the range of core RNAP for which there is sigma factor competition.

partitioned among non-specifically bound and free cores. We consider the immediate response to amino acid starvation, which is rapid and occurs on a timescale of ~ 1 minute. On this time scale, synthesis of new proteins is not expected to play an important role, so that the total number of molecular players can be considered as constant; in fact, the numbers of core RNAPs and σ^{70} also do not change much in the transition from exponential growth to stationary phase [12, 97] (although their availability to form holoenzymes may be changed by sequestration, *e.g.* by anti-sigma factor and 6S RNA). Thus, the stop of *rrn* transcription releases 2600 core RNAPs, so that the total number of cores available to transcribe mRNA is increased to ~ 10300 . Interpretation of measurements of the number of σ^{70} molecules per cell is not as easy. While older studies reported an excess of core RNAPs over σ^{70} [97, 14], an 1.3–3-fold excess of the housekeeping sigma factor over core has recently been observed [11, 12]. However, it has been found that the Rsd anti- σ^{70} factor is also comparable in number to σ^{70} [12] and has a strong binding affinity for it [10]. Thus, it is likely that a substantial fraction of the housekeeping sigmas are sequestered by the anti-sigma factor. In the following, we use a plausible value of 9000 available (non-sequestered) σ^{70} molecules per cell. The main alternative sigma factor active during stringent response is σ^S [98]. Below, we are going to consider a wide range of copy numbers of σ^S , but for now we assume that there are 5000 copies present, as estimated from observations during entry to stationary phase (60 % of core [12], few of which are transcribing during growth). Finally, we use dissociation constants $K_{E\sigma^{70}} = 1$ nM and $K_{E\sigma^{Alt}} = 20$ nM, consistent with experimental values as well as a Michaelis constant of $10 \mu\text{M}$ for the binding of either holoenzymes to their cognate promoters.

Holoenzyme numbers as a function of available core numbers. Mimicking the increase in core availability, in Figure 4.2 we plot the numbers of holoenzymes of

both types as functions of the number of core RNAPs. An increased availability of core RNAPs allows the formation of holoenzymes, until all sigma factors are engaged in holoenzymes. Competition between sigma factors occurs in the range of core numbers marked by the grey stripe. The upper limit of this stripe is given approximately by the excess of sigma factors over cores and the lower limit depends on both the difference in sigma-core affinity and the 5% criterion (approximated by Equation 2.18 in Chapter 2). The analytical approximation for the curves describing holoenzyme formation has already been discussed in Section 2.2 of Chapter 2 and is further expanded in case VI of Appendix B. The black dashed lines respectively mark the numbers of available core RNAPs during exponential growth (E_g) and after release of the *rrn*-transcribing cores in stringent response (E_s). Here, both values lie in the region of competition. In the competition region, the number of alternative holoenzymes increases steeply, indicating that alternative sigma holoenzymes, and thus alternative sigma-driven transcription, is quite sensitive to the concentration of available core RNAPs.

4.2 Response factor

4.2.1 Definition

Definition of response factor. We quantify the sensitivity of the alternative sigma-driven transcription to the concentration of available core RNAPs by determining a logarithmic response factor of the dependence of the transcription rate on the core concentration.

In general, the response coefficient R_X [99] characterizes the sensitivity of an observable (here, the normalized transcription rate of the σ^{Alt} -dependent genes) to the change of a control parameter X (here, either the total amount of core RNAPs or alternative sigma factors). The logarithmic response R_X of the transcription rate to a change in X is defined as

$$R_X = \frac{d \log \tilde{J}(X)}{d \log(X)}. \quad (4.1)$$

In the simulations we use a finite version of this factor:

$$R_X = \frac{X}{\tilde{J}(X)} \frac{\tilde{J}(X + \Delta X) - \tilde{J}(X)}{\Delta X},$$

with ΔX being the change in the total amount of the X quantity, assumed to be the change during a simulation step. Equation 4.1, following the definition of the normalized transcription rate \tilde{J} (Equation 2.7 in Chapter 2), can be rewritten as

$$R_X = \frac{K_p^{Alt} E_{\sigma^{Alt}} [X]}{(K_p^{Alt} E_{\sigma^{Alt}} + [E_{\sigma^{Alt}}]) [E_{\sigma^{Alt}}]} \frac{\partial [E_{\sigma^{Alt}}]}{\partial [X]}. \quad (4.2)$$

Properties of the response factor. When $X = 0$ $R_{X=0} = 1$; and R_X goes to zero for a large number of σ^{Alt} or RNAPs (see Proof 1 in Appendix D). Therefore, a necessary and sufficient condition to have an absolute maximum of R_X different from the origin is $R_X > 1$. By using Equation 4.1, this condition can also be rewritten as

$$\frac{\partial \tilde{\mathcal{J}}([X])}{\partial [X]} > \frac{\tilde{\mathcal{J}}([X])}{[X]}$$

or by Equation 4.2 as

$$\frac{\partial [E\sigma^{Alt}]}{\partial [X]} > \frac{(K_{p^{Alt}E\sigma^{Alt}} + [E\sigma^{Alt}])[E\sigma^{Alt}]}{K_{p^{Alt}E\sigma^{Alt}}[X]}. \quad (4.3)$$

If we suppose for a moment $\tilde{\mathcal{J}} = R_0 X^n$ with R_0 a constant, the solution of Equation 4.1 is $R_X = n$, meaning that a value of the response coefficient larger than one denotes that the system is more sensitive to a change in the control parameter than a linear function. This instance is designated as hyper- or ultra-sensitivity. Imposing $R_X > 1$ in Equation 4.2 we find that the transcription rate is an increasing function of X , convex around its maximum X_M (this is a necessary and sufficient condition for hypersensitivity, from Proof 2 in Appendix D). This maximum is found by solving

$$\frac{\partial^2 \tilde{\mathcal{J}}([X])}{\partial [X]^2} = \frac{1}{[X]} \frac{\partial \tilde{\mathcal{J}}([X])}{\partial [X]} \left(\frac{[X]}{\tilde{\mathcal{J}}([X])} \frac{\partial \tilde{\mathcal{J}}([X])}{\partial [X]} - 1 \right)$$

or explicitly, from the definition of $\tilde{\mathcal{J}}$:

$$\frac{\partial^2 [E\sigma^{Alt}]}{\partial [X]^2} = \frac{\partial [E\sigma^{Alt}]}{\partial [X]} \left(\frac{\partial [E\sigma^{Alt}]}{\partial [X]} \frac{K_{p^{Alt}E\sigma^{Alt}} + 2[E\sigma^{Alt}]}{[E\sigma^{Alt}](K_{p^{Alt}E\sigma^{Alt}} + [E\sigma^{Alt}])} - \frac{1}{[X]} \right). \quad (4.4)$$

By imposing again $R_X > 1$ and using Equation 4.4, $[E\sigma^{Alt}]$ results a monotonic increasing function, convex around the maximum (convexity of the holoenzyme concentration is only a necessary but not sufficient condition for the presence of a maximum, see Appendix D, Proof 3).

If the binding affinity between the alternative holoenzyme and cognate promoter is strong ($K_{p^{Alt}E\sigma^{Alt}} \ll [E\sigma^{Alt}]$), from Equation 4.2 the response factor fulfills

$$R_X \simeq \frac{K_{p^{Alt}E\sigma^{Alt}}[X]}{[E\sigma^{Alt}]^2} \frac{\partial [E\sigma^{Alt}]}{\partial [X]}.$$

The condition $R_X > 1$ for the presence of a maximum becomes

$$\frac{\partial [E\sigma^{Alt}]}{\partial [X]} > \frac{[E\sigma^{Alt}]^2}{K_{p^{Alt}E\sigma^{Alt}}[X]}$$

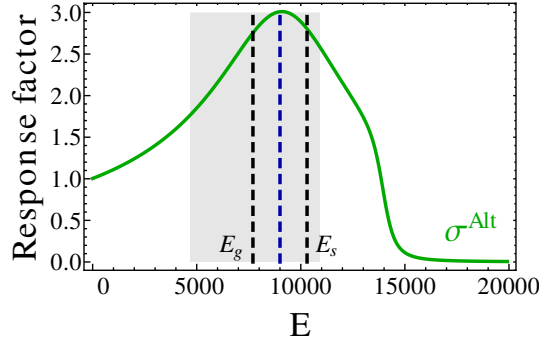


Figure 4.3: Stringent response. Response factor R_E of the alternative sigma factor-dependent gene transcription (with $K_{p^{Alt}E\sigma^{Alt}} = 10^{-5}$ M) to an increase of concentration of RNAPs. The blue dashed line shows the maximal sensitivity, that for strong core-sigma binding is found for $[E] \simeq [\sigma^{70}]$ and lies in the competition region.

and Equation 4.4 reduces to

$$\frac{\partial^2[E\sigma^{Alt}]}{\partial[X]^2} = \frac{\partial[E\sigma^{Alt}]}{\partial[X]} \left(\frac{\partial[E\sigma^{Alt}]}{\partial[X]} \frac{2}{[E\sigma^{Alt}]} - \frac{1}{[X]} \right). \quad (4.5)$$

For very strong dissociation constants ($K_{p^{Alt}E\sigma^{Alt}} \rightarrow 0$), the factor R_X is null and the system does not present any sensitivity. Hence, a necessary condition to efficiently up-regulate the transcription of a gene is that the dissociation constant between the gene's promoter and the cognate holoenzyme can not be too strong (simplifying, the promoter must be unsaturated to be regulated). On the other hand, if the binding affinity between the alternative holoenzyme and cognate promoter is weak ($K_{p^{Alt}E\sigma^{Alt}} \gg [E\sigma^{Alt}]$), we obtain from Equation 4.2

$$R_X \simeq \frac{[X]}{[E\sigma^{Alt}]} \frac{\partial[E\sigma^{Alt}]}{\partial[X]}.$$

By using the last expression, $R_X > 1$ implies

$$\frac{\partial[E\sigma^{Alt}]}{\partial[X]} > \frac{[E\sigma^{Alt}]}{[X]}.$$

The concentration $[X_M]$ for which there is maximal response can be found by solving

$$\frac{\partial^2[E\sigma^{Alt}]}{\partial[X]^2} = \frac{\partial[E\sigma^{Alt}]}{\partial[X]} \left(\frac{\partial[E\sigma^{Alt}]}{\partial[X]} \frac{1}{[E\sigma^{Alt}]} - \frac{1}{[X]} \right). \quad (4.6)$$

4.2.2 Free binding case

We characterize here the response factor for the binding of sigma factor to core RNAP in the absence of DNA and modulators, *i.e.* for the free binding case of Chapter 2.

Strong core-sigma binding affinities. In the presence of two sigma factor species, from the analytical solutions of the free binding case with strong core-sigma binding affinities (Equations 2.17 in Chapter 2), we find that $R_{\sigma^{Alt}}$ never has a maximum, whereas R_E , from Equation 4.4, has a maximum if the approximate condition

$$\frac{K_{E\sigma^{70}}}{K_{E\sigma^{Alt}}} < \frac{r - [\sigma^{70}](K_{p^{Alt}E\sigma^{Alt}} + [\sigma^{Alt}])}{2[\sigma^{Alt}]^2} \quad (4.7)$$

is satisfied. r is given by

$$r = \sqrt{4K_{p^{Alt}E\sigma^{Alt}}[\sigma^{70}][\sigma^{Alt}]^2 + [\sigma^{70}]^2(K_{p^{Alt}E\sigma^{Alt}} + [\sigma^{Alt}])^2}$$

In this case, $R_E > 1$ as long as $E < \sigma^{70} + \sigma^{Alt}$. The right hand side of Equation 4.7 is always smaller than or equal to one and for a small Michaelis constant $K_{p^{Alt}E\sigma^{Alt}}$, as we suppose to have in our simulations (see Table A.1 in Appendix A), it approaches one. Thus, a necessary (but not sufficient) condition for the presence of a maximum of R_E is $K \equiv K_{E\sigma^{70}}/K_{E\sigma^{Alt}} < 1$ (Proofs 4 and 5 in Appendix D). The maximal response, in this case, is found in the competition region around $E = \sigma^{70}$. This case is shown in Figure 4.3, that plots the response factor related to the case of Figure 4.2, where we find values of R_E up to 3, with the maximal sensitivity marked by the dashed blue line.

As a matter of fact, if the binding affinity between the alternative sigma factor and the core is much weaker than the corresponding housekeeping one ($K \ll 1$), the solution given by Equation 2.17 reduces to (see case VI in Appendix B)

$$[E\sigma^{70}] \approx \begin{cases} [E] & [E] \leq [\sigma^{70}] \\ [\sigma^{70}] & [E] > [\sigma^{70}] \end{cases}$$

$$[E\sigma^{Alt}] \approx \begin{cases} 0 & [E] \leq [\sigma^{70}] \\ [E] - [\sigma^{70}] & [\sigma^{70}] < [E] \leq [\sigma^{70}] + [\sigma^{Alt}] \\ [\sigma^{Alt}] & [E] > [\sigma^{70}] + [\sigma^{Alt}] \end{cases} .$$

According to Equation 4.4, $[E] = [\sigma^{70}]$ yields the maximal response factor. It is worth noticing that all the results here presented only depend on the ratio K and not on the specific values of the two holoenzyme binding affinities.

Conditions to obtain a hypersensitive response. The results above can also be generalized for cases in which core-sigma dissociation constants are not small. The necessary condition to obtain hypersensitivity of R_E for the free binding case in the presence of two sigma factor species competing for the core remains $K < 1$

(see Appendix B). On the contrary, $R_{\sigma^{Alt}}$ never has a maximum (from Proof 6 in Appendix D). Generally, the maximum of the response factor R_X (and hence ultrasensitivity) arises near the value where all σ^{70} molecules are sequestered and lies in the competition region, as in the case above. From this point, free alternative sigma factors and cores are available to form alternative holoenzymes, inducing a steep increase in the number of $E\sigma^{Alt}$ and eventually in the cognate transcription rate [100]. In the presence of a single sigma factor, the response factor does not exhibit sensitivity.

Response factor and stringent response. This analysis of the response factor indicates that not only can alternative sigma-dependent transcription be passively induced by the stop of ribosomal RNA transcription, but also that even relatively small changes in core RNAP concentration are amplified into a pronounced increase of the transcription rate. If the number of housekeeping sigma factors (and hence the maximal sensitivity) lies between E_g and E_s , as in Figure 4.3, or it is larger than both E_g and E_s , the σ^{Alt} -dependent gene transcription is enhanced. On the contrary, if the number of σ^{70} factors is smaller than the number of available cores during exponential growth and in the stringent response, hypersensitivity to increased core availability is lost, because the response factor can be in the region where sensitivity is smaller than unity. From this argument we can conclude that if housekeeping sigma factors are indeed in excess over core RNAPs, as suggested by some measurements [11, 12], strong amplification of passive up-regulation of σ^{Alt} -dependent transcription can only be achieved if the housekeeping sigma factors are actively sequestered by some mechanism, such as anti-sigma factors. We thus speculate that such a thing may be a key function of the anti- σ^{70} factor Rsd. If the latter condition is satisfied, our results indicate that an indirect (passive) up-regulation of the alternative sigma-dependent genes is possible, however such passive regulation requires that the system be tuned to work within or near the competition regime.

4.2.3 Response factor in the presence of regulatory factors

Here, we summarize some results about the response factor in the presence of either anti-sigma factors, 6S RNA, non-specific binding, or transcript elongation. The extended analytical calculations and the simulations can be found in Appendix C.

Hypersensitivity in the presence of anti-sigma factor. Numerically, we find that an increase in the number of alternative sigma factors in the presence of two competing sigma species and a fixed number of anti- σ^{70} never presents hypersensitivity. Instead, $R_E > 1$ when $K_{E\sigma^{70}} < K_{E\sigma^{Alt}}$ and $\overline{\sigma^{70}} \leq \sigma^{70}$. The maximal sensitivity is found for $E \simeq \sigma^{70} - \overline{\sigma^{70}}$.

Hypersensitivity in the presence of 6S RNA. Both increasing the number of cores and σ^{70} , the response factor shows always hypersensitivity in the presence of a single sigma factor and 6S RNA. During sigma factor competition, every amount

of 6S RNA produces a sharp hypersensitive response to an increased availability of cores. R_E is larger than one for values of core RNAP whose concentration satisfies Equation C.6 in Appendix C:

$$\begin{aligned}
[E] < & \frac{[S][\sigma^{70}] + K_{E\sigma^{70}S}[\sigma^{Alt}]}{K_{E\sigma^{70}S}[S][\sigma^{Alt}][\sigma^{70}]^2} \\
& \cdot \left([\sigma^{70}] \sqrt{K_{pE\sigma^{Alt}} K_{E\sigma^{70}S} [S][\sigma^{Alt}] ([\sigma^{Alt}][\sigma^{70}] + [\sigma^{Alt}] K_{E\sigma^{70}S})} + \right. \\
& \left. - K_{E\sigma^{70}S} [S][\sigma^{Alt}][\sigma^{70}] - K_{E\sigma^{70}S}^2 [\sigma^{Alt}]^2 \right),
\end{aligned}$$

where $[S]$ represents the concentration of 6S RNA. The maximal response results when the number of cores is around the number of molecules that is less abundant among 6S RNA and housekeeping sigma factors. Besides, if $K_{E\sigma^{70}} < K_{E\sigma^{Alt}}$ and there are fewer 6S RNA than housekeeping sigma factors, R_E displays both maxima in the hypersensitive region ($E \simeq \sigma^{70}$ and $E \simeq$ 6S RNA). If the number of 6S RNA is equal to the number of σ^{70} , R_E has one sharp peak, whose value corresponds to the product of the values of the two single maxima. For these reasons, 6S RNA might be a strong and efficient modulator of the alternative sigma factor-driven transcription. $R_{\sigma^{Alt}}$ has no maxima (excluding the one for $\sigma^{Alt} = 0$).

Hypersensitivity and non-specific binding. For physiological values of the non-specific binding affinities (all non-specific dissociation constants have a similar value K_{NS} , $K_{NS} > K_{E\sigma}$, and $K_{NS} > 10^{-6}$ M), we numerically find that the condition to have a maximum larger than one of R_E in $E \simeq \sigma^{70}$ is $K_{E\sigma^{70}} < K_{E\sigma^{Alt}}$. As for the case with 6S RNA, $R_{\sigma^{Alt}}$ does not present a maximum.

Hypersensitivity and active elongation. From numerical simulations in the presence of transcription, $R_{\sigma^{Alt}}$ never has a maximum. By changing one parameter at a time and by using symmetric values for the quantities related to housekeeping and alternative sigma factors, we find that R_E presents hypersensitivity if one of the following conditions is satisfied: $K_{E\sigma^{70}} < K_{E\sigma^{Alt}}$, $[\sigma^{70}] > [\sigma^{Alt}]$, $[p^{70}] < [p^{Alt}]$, $\alpha_{pE\sigma^{70}} < \alpha_{pE\sigma^{Alt}}$, $v_{tsx \sigma^{70}} < v_{tsx \sigma^{Alt}}$, $L_{ret \sigma^{Alt}} < L_{ret \sigma^{70}}$, $k_{bE\sigma^{70}} > k_{bE\sigma^{Alt}}$.

4.2.4 Response factor R_E

Table 4.1 collects the conditions to have a hypersensitive response as a function of the increasing number of core RNAPs (second column) and the position of its maximum (third column) during sigma factor competition. In this study, we use the physiological values of the parameters as reported in Table A.1 of Appendix A. For example, in the presence of anti- σ^{70} , the response factor as a function of the increasing cores presents a hypersensitive response whenever the number of housekeeping sigma factors exceeds the anti-sigma factors and $K_{E\sigma^{70}}/K_{E\sigma^{Alt}} < 1$. The maximal response is

Effect of	Conditions to have $R_E > 1$	R_E <i>max</i> in $E \simeq$
free, $K < 1$ $\overline{\sigma^{70}}$ (2)	$K < 1$ (1) $\overline{\sigma^{70}} < \sigma^{70}, K < 1$ (3)	σ^{70} $\sigma^{70} - \overline{\sigma^{70}}$
6S RNA (4)	$S < \sigma^{70}$ (5) $S > \sigma^{70}$	S σ^{70}
NS binding (6)	$K < 1, K_{ENS} \simeq K_{E\sigma^{70}NS} \simeq K_{E\sigma^{Alt}NS}$ $K \simeq 1, K_{E\sigma^{70}NS} < K_{ENS} \simeq K_{E\sigma^{Alt}NS}$	σ^{70} σ^{70}
Transcript elongation	$K_{E\sigma^{70}} < K_{E\sigma^{Alt}} \vee [\sigma^{70}] > [\sigma^{Alt}] \vee$ $\vee [p^{70}] < [p^{Alt}] \vee \alpha_{pE\sigma^{70}} < \alpha_{pE\sigma^{Alt}} \vee$ $\vee v_{tsx \sigma^{70}} < v_{tsx \sigma^{Alt}} \vee L_{ret \sigma^{Alt}} < L_{ret \sigma^{70}} \vee$ $\vee k_{bE\sigma^{70}} > k_{bE\sigma^{Alt}} \vee K_{pE\sigma^{Alt}} \ll K_{pE\sigma^{70}}$	$E < \sigma^{70} + \sigma^{Alt}$

Table 4.1: (1) A more stringent condition is given by Equation 4.7. (2) We assume $K_{\overline{\sigma^{70}}\sigma^{70}} \gtrsim K_{E\sigma^{70}}$. (3) If $\overline{\sigma^{70}} = \sigma^{70} = \sigma^{Alt}$ and $K_{\overline{\sigma^{70}}\sigma^{70}} = K_{E\sigma^{70}}, K \ll 1$ is enough to have a maximum. (4) We assume $K_{E\sigma^{70}S} \gtrsim K_{E\sigma^{70}}$. (5) Already when $S = \sigma^{70} = \sigma^{Alt}$ and $K_{E\sigma^{70}S} = K_{E\sigma^{70}} = K_{E\sigma^{Alt}}$, R_E has a maximum. (6) We assume $K_{ENS}, K_{E\sigma^{70}NS}$, and $K_{E\sigma^{Alt}NS}$ larger than both $K_{E\sigma^{70}}$ and $K_{E\sigma^{Alt}}$. (1),(2),(4),(6) The response factor is larger than one as long as $E < \sigma^{70} + \sigma^{Alt}$. The response factor under an increased number of alternative sigma factors $R_{\sigma^{Alt}}$ does not present a hypersensitive response.

reached by driving the number of cores to be equal to the quantity in the last column, in this example when $E \simeq \sigma^{70} - \overline{\sigma^{70}}$.

We point out that hypersensitivity may be a desired property of synthetic gene circuits. To that end, the knowledge of the values of the parameters that lead to hypersensitivity could be a help in their design. On the other hand, in a simple circuit with just one modulator, the maximum of R_E gives some information on the number of active molecules (either housekeeping sigma factors, 6S RNA or anti-sigma factors), in the event that these quantities are not known.

4.3 Cumulative effects of an increased amount of cores and alternative sigma factors on the competition

Alternative holoenzyme formation and response factor. In addition to the release of core polymerases from the ribosomal genes, the response to stress as such as amino acid starvation also involves the accumulation of alternative sigma factors via their increased synthesis and reduced degradation as well as through release of sigma factors sequestered by anti-sigma factors [9]. Hence, we now inspect the effect

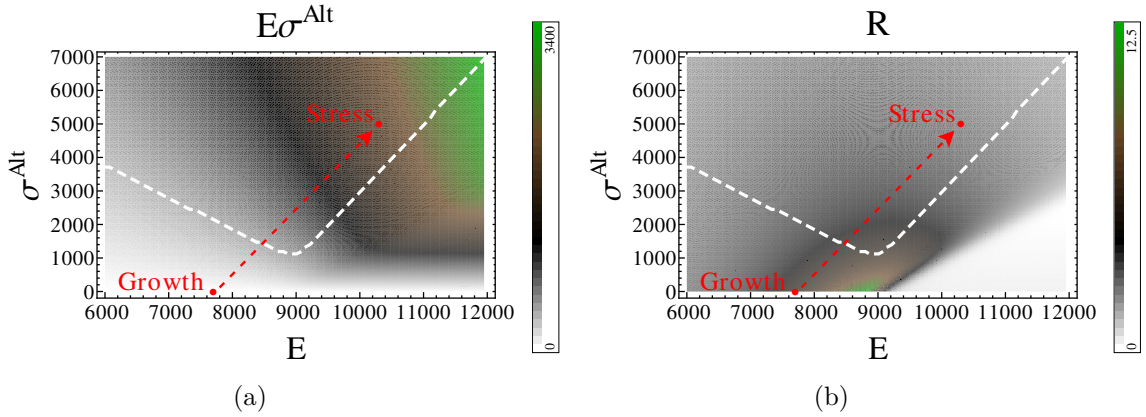


Figure 4.4: Stringent response. (a) Number of alternative holoenzymes and (E) response factor R related to the σ^{Alt} -dependent gene transcription as a function of the number of core RNAPs and alternative sigma factors (with $K_{p^{Alt}E\sigma^{Alt}} = 10^{-5}$ M). The white line encloses the region of sigma factor competition. The endpoints of the red arrow show possible values of cores and alternative sigma factors for a cell in exponential growth state and in stringent state.

of a simultaneous increase in the concentrations of both core RNAPs and alternative sigma factors on the σ^{Alt} -dependent transcription by repeating the analysis above for a wide range of σ^{Alt} concentrations. The shift of the cell from an exponential growth state to a stringent (stress) response state is characterized by an increased number of alternative sigma factors and core polymerases, indicated by the red points in Figures 4.4(a) and 4.4(b). The white dashed lines in these Figures (for which Equation 2.22 in Chapter 2 provides a good analytical approximation) enclose the region of parameter values for which the system exhibits sigma factor competition. Thus, our analysis implies that the stress response drives the cell into a state characterized by sigma factor competition. The formation of alternative holoenzymes in the same condition is shown by the density plot of Figure 4.4(a). It reaches its maximal level, which also corresponds to the maximal σ^{Alt} -dependent transcription, for a large number of core RNAPs and σ^{Alt} factors. However, we would like to point out that the maximal transcription of alternative sigma-dependent genes does not coincide with its maximal response. The response factor of the transcription rate of σ^{Alt} -dependent genes to a cumulative increase of alternative sigma factors and cores RNAPs is shown by the density plot of Figure 4.4(b). This plot shows that to achieve the maximal up-regulation of the alternative sigma factor-dependent genes, the cell can use a small number of σ^{Alt} if the amount of available cores is tuned to $[E] \simeq [\sigma^{70}]$, where the maximal response is obtained. Here, this cumulative response R to the simultaneous increase in the concentration of both alternative sigma factors and core RNAPs on

σ^{Alt} -driven transcription is defined by $R = \sqrt{R_E^2 + R_{\sigma^{Alt}}^2}$ and presents hypersensitive response for values larger than $\sqrt{2}$.

4.4 Synthesis rate

RNA synthesis rate during exponential growth phase. In the previous section, we have investigated the effect of stringent response on the alternative sigma factor transcription starting from a description of the RNAP partition among different processes given in references [42, 13]. Now, we use our complete model (shown in Figure 2.1 of Chapter 2) to evaluate the *in vivo* distribution of the RNA polymerase and, as a consequence, the transcription from different classes of genes during exponential growth and several stringent/stress scenarios. Our complete description includes anti- σ^{70} , 6S RNA, non-specific binding, and active elongation. We remind that during the stringent response the transcription from the *rrn* genes is suppressed and that at the same time, like during generic stress responses, the amounts of σ^S , 6S RNA and anti- σ^{70} Rsd, increase. Now, we do not act any more on the numbers of available RNAP but directly on the activity of the ribosomal promoters, either suppressing them - in this section - or affecting the efficiency of the housekeeping sigma factor - in the next section.

To that end, we first compare the average synthesis rate of the rRNA and mRNA in a rapidly growing *E. coli* cell (2.5 dbl/h) estimated with our model to the one measured by Bremer and collaborators [47]. The rate per minute of synthesis of nucleotides in a cell (nt/min/cell) for every operon is defined as

$$\text{Synthesis rate} = \alpha_{pE\sigma} L_{operon} p \frac{[E\sigma]}{K_{pE\sigma} + [E\sigma]}. \quad (4.8)$$

In the following we consider the total synthesis rate from a class of operons. To compare the predictions of our model to this *in vivo* experiment, we use values of the parameters either directly measured in the same experiment [47], theoretically estimated from it [47, 42], or obtained from experiments performed in the same conditions. These values are summarized in Table E.1 in Appendix E. As a first step, we cluster again the promoters in three classes: ribosomal promoters (P*rrn*), σ^{70} -dependent mRNA (non-ribosomal) promoters (PmRNA), and alternative sigma-driven promoters (P σ^{Alt} RNA). During exponential growth, we suppose that the sigma alternative-driven promoters are not (or negligibly) active (upper row of Figure 4.5(a)). This assumption is justified by the few copies of alternative sigma factors in the cell during the phase of rapid growth. In such a cell, the housekeeping holoenzyme binds more weakly to the ribosomal promoters than to the PmRNA promoters, but with a much higher initiation rate: dissociation constants were measured to be 1.4 μ M

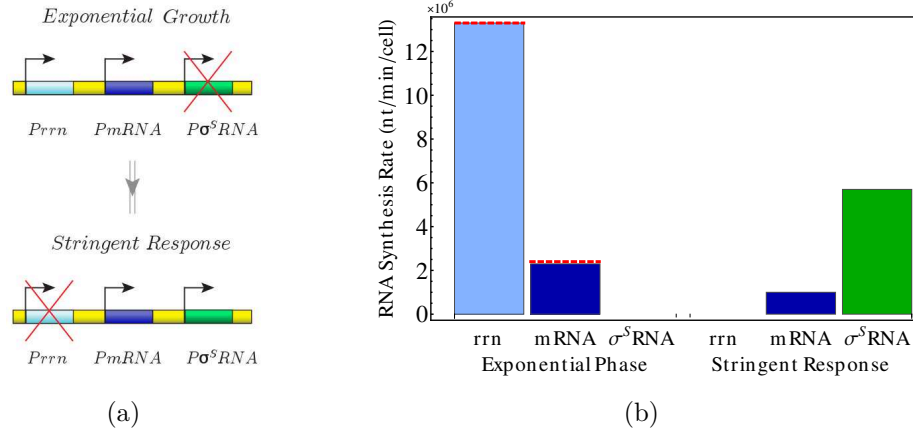


Figure 4.5: Exponential growth and stringent response. (a) During exponential growth phase, rrn and mRNA promoters are active in the cell. Since σ^S is not present, there is no transcription from the cognate genes. Shortage of amino acids induces stringent response, during which transcription from rrn genes is suppressed. At the same time, as during generic stress responses, the amounts of alternative sigma factor, 6S RNA and anti- σ^{70} increase. (b) RNA synthesis rate (nucleotides per minute per cell) during exponential growth and stationary phase. The light blue bar shows the synthesis from the ribosomal genes (rrn), dark blue bars from other σ^{70} -dependent genes (mRNA), and the green bar from σ^S -cognate genes ($\sigma^S RNA$). The red dashed lines represent the experimental values from reference [47]. For a summary of the values obtained during the simulations see Table E.2 in Appendix E.

and $0.7 \mu M$, respectively [47]. References [47, 42] estimated a total of 36 ribosomal promoters, with a quite high initiation rate (110 initiations every minute). With an elongation velocity of 85 nucleotides per second [47] and a total length of 6500 nucleotides per ribosomal gene [42] (which includes the tRNA gene length), the RNAP is sequestered by the rrn genes for 76 seconds. From the number of different types of mRNA in the cell [101], we estimated 64 active PmRNA promoters with an initiation rate of 26 transcriptions per minute [47]. The number of promoters that we use here seems quite small, but we want to emphasize that it represents the average number of active promoters from a steady state analysis, not the total number of possible active σ^{70} -driven promoters; the latter can be much larger. If the average length of the corresponding gene is 2000 nucleotides [42] and the elongation velocity is 45 nucleotides per second [47], the RNAP is sequestered by the elongation process of a PmRNA-cognate gene for 44 seconds. We adopt 300 nucleotides for the retention length of the sigma factors [3]. The total number of σ^{70} and of anti- σ^{70} Rsd during exponential growth phase is almost three times and 1.3 times the total number of RNA polymerases [12], respectively. With 11400 cores [47], this corresponds to almost 32000 σ^{70} and 14500 Rsd. The core-housekeeping sigma factor dissociation

constant (in the absence of transcription) was measured to be 2.8 nM [102] and the σ^{70} -Rsd dissociation constant around 32 nM [10], in conditions similar to the *in vivo* conditions here considered. The total number of non-specific binding sites depends on the total amount of DNA nucleotides and it is given by 3.8 genome equivalents present in a rapidly growing cell times 4.6 Million base pairs per genome. We assume the non-specific dissociation constants to be proportional to the binding sites between the molecule and the DNA: if the core binds non-specifically to the DNA with a dissociation constant of 3100 μ M [42], the holoenzymes bind twice as weakly, because they contact the DNA in roughly half the binding sites of the core RNAP [72]. The number of 6S RNA present in the cell has not been measured precisely [36, 38]. For that reason, we slightly modulate it around the estimated amount of 1000 6S RNA [38] to fine tune the fit of the measured synthesis rate, obtaining an optimum around 1600 6S RNA. Lastly, we use as 6S RNA-housekeeping holoenzyme dissociation constant the one obtained from our fit in Table A.1 in Appendix A (160 nM). In our simulations we also consider the immature RNA polymerases present in the cell [42], expressed by

$$E_{imm} = E(1 - 2^{-\mu\tau}),$$

where μ is the growth rate and τ the maturation time of the core polymerase.

By mimicking the cellular condition during exponential growth with our model and with the values of the parameters here introduced, we plot the RNA synthesis rates in the left panel of Figure 4.5(b) (the light and dark blue bars represent respectively the rRNA and the mRNA synthesis rate). The simulation is in good agreement with the experimental measurements [47] represented by the red lines.

RNA synthesis rate during stringent response. Next, we analyze the same cell during early stringent response, characterized by the complete stop of the transcription of the *rrn* genes and the activation of the alternative sigma factor-dependent genes (second row of Figure 4.5(a)). During response to a generic stress (and also during stringent response), the most abundant alternative sigma factor is σ^S , whose level reaches more than one half of the total number of cores [12], that means 7000 units. The dissociation constant between σ^S and core RNAP is 11 nM [102], weaker than the housekeeping sigma factor-core affinity. We suppose that all the 134 known orthogonal σ^S -driven promoters are now active [103]. We choose all the other σ^S -dependent transcription parameters to be the same as the mRNA's parameters (see Table E.1 in Appendix E). Amounts of anti- σ^{70} Rsd and 6S RNA increase with compared to the situation of pure growth: during a stress response there are 27200 Rsd (obtained by supposing the ratio σ^S /Rsd measured in reference [12] to be constant) and 8000 6S RNA (6S RNA increases five-fold compared to the growth phase [104]).

In this condition, σ^S and σ^{70} compete in the cell, but because of the sequestration of σ^{70} by anti- σ^{70} and 6S RNA, the outcome of transcription is in favor of the sigma alternative-dependent genes that are passively up-regulated, as shown by the green

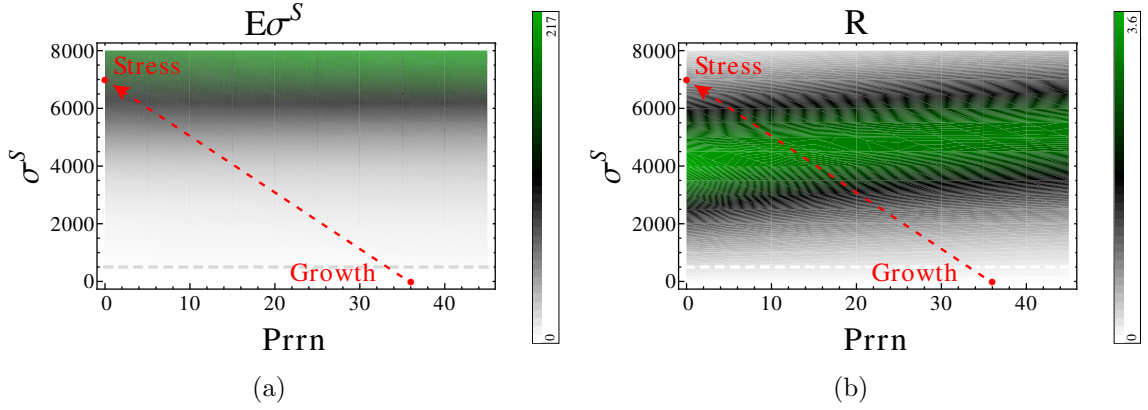


Figure 4.6: Cumulative response factor to an increase of alternative sigma factors and inhibition of ribosomal promoters. (a) $E\sigma^S$ and (b) R competition phase spaces. During stringent response, the stable RNA genes are suppressed and the amount of alternative sigma factors increases. $Prrn$ indicates the total number of ribosomal promoters that are active in a cell. “Growth” refers to a cell that grows at 2.5 dbl/h. The white dashed line represents the onset of the sigma factor competition. The red arrow shows a possible path for the intracellular values of the number of active $Prrn$ and σ^S during the shift from an un-competitive situation to the competition, respectively, in exponential growth and in stringent response. The response of the alternative genes is described by the density plot. During the shift, the amounts of 6S RNA and anti- σ^{70} also increase: we choose to keep the ratios $\sigma^S/6S$ RNA and $\sigma^S/\text{anti-}\sigma^{70}$ fixed. Values of the parameters are as in Table A.1 in Appendix A.

bars of Figure 4.5(b). As expected during a lack of nutrients, the overall synthesis rate is decreased compared to the situation of exponential growth. The second and fourth columns of Table E.2 collect all the quantities obtained in our simulation during growth phase and stringent response.

Cumulative response factor to an increase of alternative sigma factors and inhibition of ribosomal promoters. To quantify the change in the transcription of the alternative sigma factor-driven genes, we analyze the response factor under a simultaneous increase in the number of alternative sigma factors, σ^{70} , 6S RNA, and anti- σ^{70} , while we suppress one-by-one the ribosomal promoters (red path of Figures 4.6(a) and 4.6(b)). To plot this instance, during the simulation we choose to keep the ratios $\sigma^S/6S$ RNA and $\sigma^S/\text{anti-}\sigma^{70}$ fixed. Figure 4.6(a) shows the alternative sigma holoenzyme formation and Figure 4.6(b) the corresponding cumulative response factor $R = \sqrt{R_{\sigma^{Alt}}^2 + R_{Prrn}^2}$. In this case the hypersensitive region is for $R > 1$, because for many and few active ribosomal promoters R_{Prrn} is zero. The white dashed lines enclose the region of the parameter values for which the system exhibits sigma factor

competition. During the shift from exponential growth phase to the early stringent response, the cell crosses the maximal response of the alternative sigma-dependent genes (green region of Figure 4.6(b)), as shown by the red arrow. Numerically, we find that in the range of physiological values of Table E.1 in Appendix E a necessary condition to obtain hypersensitivity is still $K_{E\sigma^{70}} < K_{E\sigma^{Alt}}$.

4.5 Different stringent/stress response scenarios

So far, we have considered a condition of exponential growth (first row of Figure 4.7(a)), where the alternative sigma-driven genes are inactive, and one of stringent response (third row of Figure 4.7(a)), characterized by a complete shut down of the stable RNA promoters. Bars (1) and (3) of Figure 4.7(b) replicate the results of our model for the RNA synthesis rate in these two cases.

Now we modulate the activity of the ribosomal genes. By suppressing the transcription of the rRNA, one may expect the maximal enhancement possible of the σ^S RNA synthesis rate, because more RNAP are now available to form alternative holoenzymes. However, as already noticed in Section 3.4 in which we studied the active elongation, the transcription activity of the *rrn* σ^{70} -genes weakens the effective binding affinity K_{eff} between the housekeeping sigma factor and the core, so the σ^S RNA synthesis in the case of *rrn* suppression results is less than the σ^S RNA synthesis with unsuppressed *rrn* (second row of Figure 4.7(a)), as shown by comparing bars (3) and (2) of Figure 4.7(b), respectively. As a matter of fact, a complete shut down of the stable RNA genes induces a smaller effective $K_{E\sigma^{70}}$ which effect is the suppression of the alternative holoenzyme activity.

So, why should the cell prefer to suppress the transcription of the ribosomal RNA, if the σ^{Alt} -dependent genes are enhanced when the elongation of *rrn* and σ^{Alt} -dependent genes are both active? We can speculate that it is due to a matter of resource saving. During a phase of nutrient deprivation, it is important for the economy of the cell not to produce expensive and useless machinery such as more ribosomes.

What is actually observed *in vivo* is a middle condition between the two extreme cases of complete suppression and unaltered synthesis of the rRNA [106, 39, 43]. Even in conditions of high (p)ppGpp concentration, *in vivo* measurements in *E. coli* [106] demonstrate that the ratio of ribosomal gene activity over total gene activity reaches a constant value (23% of the total RNA synthesis is rRNA, represented by the dashed orange lines in Figure 4.7(b)). In our model this could be obtained, for example, by allowing the simultaneous activity of *rrn*- and σ^S -genes and, at the same time, by weakening the binding affinity either between housekeeping holoenzyme and *rrn* promoters (fourth row of Figure 4.7(a)) or between core and σ^{70} (fifth row of Figure 4.7(a)). The first scenario can just tune the σ^S RNA synthesis rate within the limits given by P_{rrn} - P_{σ^S} RNA coexistence and *rrn* suppression (as shown by bars (4) of

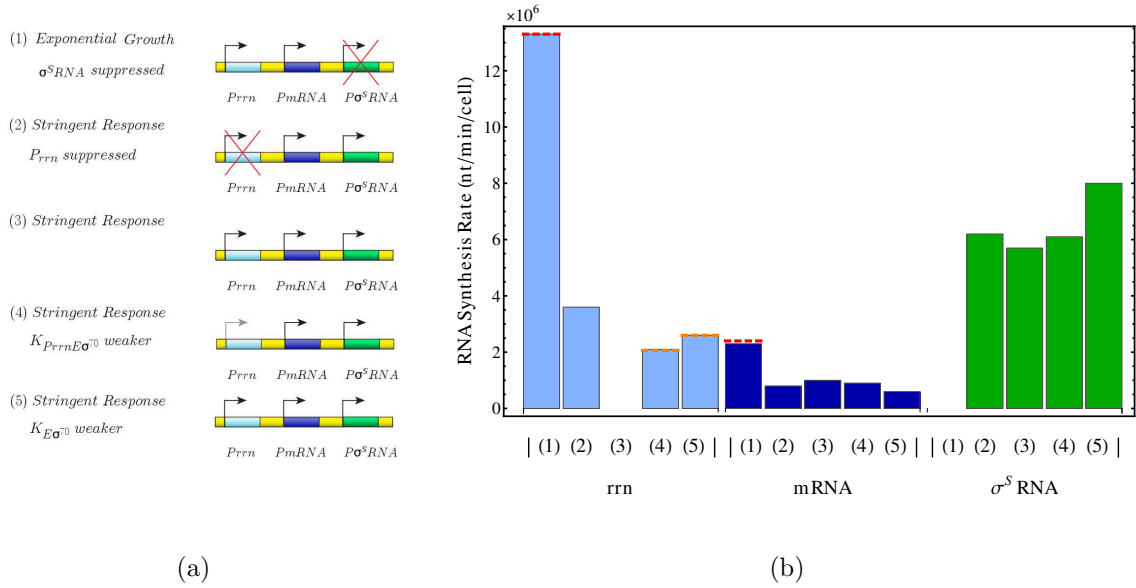


Figure 4.7: RNA synthesis rate in nucleotides per minute per cell of the stable σ^{70} -dependent RNA (rrn), of all the others σ^{70} -cognate genes (mRNA) and of the σ^S -dependent genes (σ^S RNA). (1) Exponential growth with P_{rrn} and P_{mRNA} active; (2) stringent response with P_{mRNA} and $P_{\sigma^S RNA}$ active and P_{rrn} un-suppressed; (3) stringent response with P_{mRNA} and $P_{\sigma^S RNA}$ active but P_{rrn} complete suppressed; (4) stringent response with P_{mRNA} and $P_{\sigma^S RNA}$ active, P_{rrn} un-suppressed but with the binding affinity $K_{P_{rrn}E\sigma^{70}}$ between the housekeeping holoenzyme $E\sigma^{70}$ and the P_{rrn} 2-fold weaker; (5) stringent response with P_{mRNA} and $P_{\sigma^S RNA}$ active, P_{rrn} un-suppressed but with the binding affinity $K_{E\sigma^{70}}$ between the housekeeping sigma factor σ^{70} and the core 3.5-fold weaker. The ratio between the expression of stable RNA and the total mRNA is constant and only depends on the bacterial strain and on the (p)ppGpp concentration [39]. Furthermore, beyond a certain (p)ppGpp threshold, this fraction also becomes independent of the (p)ppGpp amount. In a *E. coli* B/r strain (at 37°C), the ratio stable RNA/total RNA has been shown to decrease from approximately 85% (red line over light blue bar (1) [47, 39]) to 23% (orange lines over light blue bars (4) and (5) [39]) during conditions of growth and stringent response, respectively. We tune the stable RNA synthesis to reach the 23% of the total by using two different approaches: by changing the affinity $K_{P_{rrn}E\sigma^{70}}$ at the promoter (in (4)) and by varying the affinity $K_{E\sigma^{70}}$ (in (5)). The first fit gives a 2-fold weakening of $K_{P_{rrn}E\sigma^{70}}$ (in line with experimental values of 2-5-fold [105]), the latter a 3.5-fold weakening of $K_{E\sigma^{70}}$.

Figure 4.7(b)). The latter can enhance this synthesis, but at the same time keeps the stable RNA transcription (unfavorably) higher (bars (5) of Figure 4.7(b)). We choose the weakening factors of the $K_{P_{rrn}E\sigma^{70}}$ and $K_{E\sigma^{70}}$ binding affinities by tuning them so

that the simulated rRNA synthesis rate equals the *in vivo*-measured rRNA synthesis rate [106]. From these comparisons, the dissociation constant between stable RNA promoter and housekeeping holoenzyme results 2-fold weaker (thus $K_{P_{rrn}E\sigma^{70}} = 2.8 \mu\text{M}$), in line with some experimental estimations of 2-5-fold [105]. The same analysis for the dissociation constant $K_{E\sigma^{70}}$ between core and housekeeping sigma factor yields instead a 3.5-fold weakening (thus $K_{E\sigma^{70}} = 9.8 \text{ nM}$). Theoretically, the two weakening effects can act at the same time and are not the only mechanisms in our simulations capable to balance synthesis rate and costs in the cell. These two options, besides being the easiest ways to overcome the decrease in the expression of the σ^S RNA for the complete stop of synthesis of rRNA without acting on other cellular parameters, were first suggested by experimental results [21, 52, 53].

4.6 RNAP partitioning

Repertition of RNAP among different processes. Figure 1.4 in the Introduction gives an idea of the main players that sequester RNA polymerase during exponential growth and stringent/stress phase. We have used the model of Figure 2.1 in Chapter 2 to quantitatively study all the mechanisms involved in that sketch. Now we finally want to quantify the amount of RNAP involved in every process during exponential growth and stress (or stringent) response.

RNAP partitioning during exponential growth. Figure 4.8 compares the RNAP partitioning among different processes in *Escherichia coli* cells that grow fast (2.5 dbl/h with 37°C) according to our model (bar (1), data and parameters from the previous section), to the models of Bremer *et al.* [47] (bar BDE), to Klumpp and Hwa [42] (bar KH), and to the experimental data of Bakshi *et al.* [48] (bar BDLCW). The first three models are based on experimental values from experiments with minicells (cells that lack the DNA), the last one deduces the RNAP partitioning from an analysis of the single-molecule diffusion *in vivo*.

In Figure 4.8, “Imm” indicates the immature pool of RNAP, “free” the sum of free cores and holoenzymes, “ $E\sigma^{70}6SRNA$ ” the 6S RNA bound to the housekeeping holoenzymes, “NS” the non-specific bound cores and holoenzymes, “ tsx_{rrn} ” the RNAP specifically bound or transcribing ribosomal DNA, “ tsx_{mRNA} ” the RNAP specifically bound or transcribing PmRNA genes, “paused” the non-elongating but specifically bound RNAPs, and “nb” the fraction of RNAP that does not bind to DNA. The analysis of BDE, KH, and our analysis, rely on the same experiments with minicells (summarized in [13, 47]), and for that reason the RNAP partitioning is also similar. Differently from BDE and KH, we include in the model the effect of anti-sigma factors, 6S RNA, and active elongation. The main distinction between our model and the BDE and KH models is the interpretation of the cores non-specifically bound. KH considered the paused RNAPs of BDE as non-specific bound polymerases,

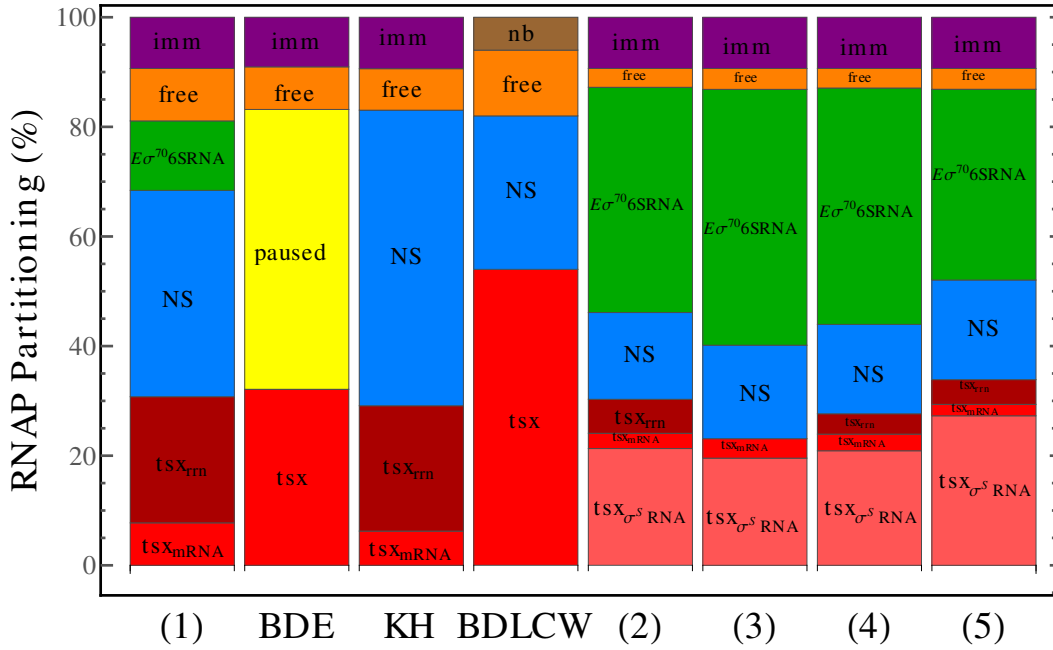


Figure 4.8: RNA polymerase partitioning, as percentage distribution, during exponential growth at 2.5 dbl/h and 37 °C, according to the estimate of: (1) - our model; BDE - reference [47]; KH - reference [42]; and BDLCW reference [48]. “Imm” indicates immature pool of RNAP, “free” the sum of free cores and holoenzymes, “ $E\sigma^{70}6SRNA$ ” 6S RNA bound to housekeeping holoenzymes, “NS” non-specific bound cores and holoenzymes, “ tsx_{rrn} ” RNAP specifically bound or transcribing ribosomal DNA, “ tsx_{mRNA} ” RNAP specifically bound or transcribing PmRNA-genes, and “paused” non-elongating bound RNAPs apart from specifically bound RNAPs. Columns (2)–(5), as explained in Figures 4.7(a) and 4.7(b), show different scenarios of stringent response where “ $tsx_{\sigma^S RNA}$ ” denote RNAP specifically bound or transcribing σ^S -dependent genes. The values used in the simulations are in Table E.1 and the numerical outcome in Table E.2 of Appendix E.

while in the present work we have redistributed them among non-specific and 6S RNA bound RNAPs. The model developed by BDLCW presents a quite larger number of RNAPs engaged in transcription compared to the models based on minicells data. The divergence can be explained by assuming that the different experimental conditions (strains and growing medium), lead for example either to a slow down of the elongation velocity, to underproduction of 6S RNA, to a change in the binding affinities, or to an increased number of active promoters.

RNAP partitioning during stringent/stress phases. Columns (2)–(5) of

Figure 4.8 summarize the RNAP partitioning during the different stringent response scenarios presented in Figures 4.7(a) and 4.7(b). “ $tsx_{\sigma^S RNA}$ ” denotes the RNAP specifically bound or engaged in transcription of the σ^S -dependent genes. During the stringent response, our model predicts an increase of the housekeeping holoenzymes sequestered by 6S RNA, mainly due to more available 6S RNA, and a reduction of the non-specifically bound cores. The total number of transcribing cores stays pretty constant: the reduction of the RNAP transcribing stable RNA (tsx_{rrn}) is compensated by the increase of polymerases on the σ^S -dependent genes ($tsx_{\sigma^S RNA}$). The small reduction of $tsx_{\sigma^S RNA}$ in column (3) is due to the stronger binding affinity between core and housekeeping sigma factor after the suppression of the ribosomal genes. We notice that the pool of cytoplasmic $E\sigma^{70}$ is almost completely sequestered by 6S RNA.

Table E.2 summarizes all the quantities predicted by our model during these different scenarios.

4.7 ppGpp may weaken binding affinity between housekeeping sigma factor and core RNAP

Effect of (p)ppGpp on the housekeeping dissociation constant. Evidence that (p)ppGpp decreases the competitiveness of the housekeeping σ^{70} against alternative sigma factors in binding to the core RNAP has been found *in vitro* thanks to the enhancement of transcription from a σ^H -dependent promoter under conditions of competition between σ^H and σ^{70} [21]. Considerable effort was also dedicated to studying the transcription from the σ^N -driven Po-promoter (a promoter from *Pseudomonas putida*) in the presence of (p)ppGpp and DksA, both *in vivo* and *in vitro*, with opposite results. While the absence of these regulators reduces the Po-dependent transcription *in vivo* [23, 25, 24], they have no effect on *in vitro* systems [25], even during conditions of strong competition between σ^{70} and σ^N [23]. A direct mode of activation was suggested by the stimulation of transcription of σ^E -dependent promoters both *in vivo* and *in vitro* in the presence of (p)ppGpp [51, 33]. Following these considerations, various authors suggested a weakening effect of (p)ppGpp/DksA on the binding affinity between the housekeeping sigma factor and the core RNAP [21, 52, 53]. However, this weakening has never been fully proven. In Figure 4.9, we analyze a transcription assay [21] that supports this direct weakening action of the (p)ppGpp on the housekeeping holoenzyme dissociation constant. In this experiment, Jishage and collaborators [21] used a DNA template containing a σ^H -dependent PdnaK promoter and an orthogonal σ^{70} -dependent Prna1 promoter. We would like to stress that Prna1 is not a ribosomal promoter, therefore nothing can be deduced from this analysis about the (p)ppGpp effect on the ribosomal genes. To study this

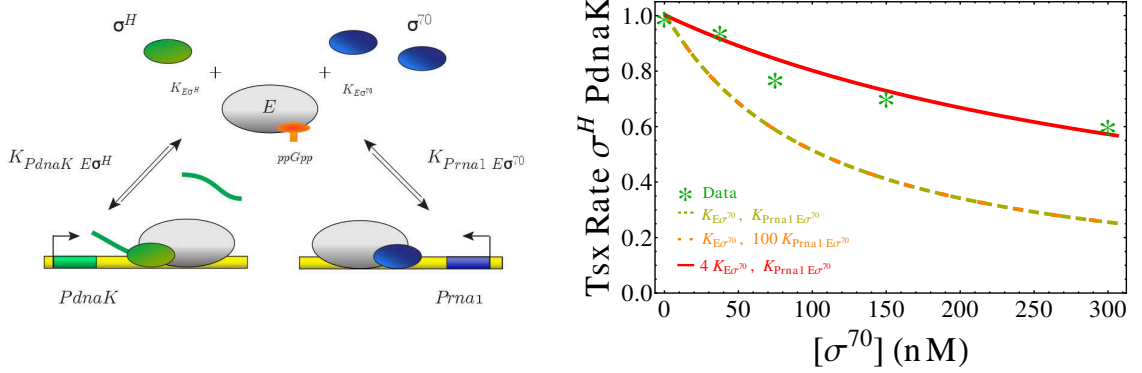


Figure 4.9: Comparison of model prediction (lines) with an *in vitro* competition experiment [21] in the presence of 180 μM of (p)ppGpp and a fixed amount of core RNAPs (10 nM) and σ^H (250 nM) and different amounts of σ^{70} . The plot shows the transcription rate of a σ^H -dependent gene (normalized on the maximal value) as a function of the concentration of σ^{70} . We compare the experimental data (green stars) to different scenarios of action of (p)ppGpp on $K_{E\sigma^{70}}$ and $K_{Prna1 E\sigma^{70}}$ simulated with our model. To that end we used $K_{E\sigma^H} = 98.2$ nM, $K_{PdnaK E\sigma^H} = 24.5$ nM, $K_{E\sigma^{70}} = 21.1$ nM, and $K_{Prna1 E\sigma^{70}} = 210$ μM in the absence of (p)ppGpp, from our fit in Chapter 2. The overlapping yellow and orange lines show simulations with binding affinities as in the absence of (p)ppGpp and a 100-times weaker $K_{Prna1 E\sigma^{70}}$, respectively. A four-fold weaker $K_{E\sigma^{70}}$ reproduces the data (red line).

experiment we obtain first $K_{E\sigma^H}$, $K_{E\sigma^{70}}$, $K_{PdnaK E\sigma^H}$, and $K_{Prna1 E\sigma^{70}}$.

Transcription rates in the absence of (p)ppGpp. We have already obtained those dissociation constants in Chapter 2 from non-competition assays. We remind that Jishage and collaborators [21] have first measured the transcription rates of the σ^H -dependent genes from a binding assay in the absence of (p)ppGpp and in the presence of a fixed amount of core RNAPs and DNA template, and an increasing amount of σ^H factors only. From a fit of their data, we have obtained $K_{E\sigma^H} = 98.2$ nM and $K_{PdnaK E\sigma^H} = 24.5$ nM (upper panel of Figure 2.9(b)). Laurie *et al.* [23] have done the same experiment, in the same conditions, but with σ^{70} only. From a fit of their data, we have obtained $K_{E\sigma^{70}} = 21.1$ nM and $K_{Prna1 E\sigma^{70}} = 210$ μM (lower panel of Figure 2.9(b)).

Then, Jishage and collaborators have performed a competition experiment with increasing σ^{70} , a fixed σ^H , and RNAP. By using the values of the fits, we have found a good agreement between the prediction of our model and this case, as already shown in Figure 2.9(b).

Transcription rates in the presence of (p)ppGpp. Next, they have repeated the competition experiment in the presence of (p)ppGpp after having excluded any effect of (p)ppGpp on the σ^H and $E\sigma^H$ functionality, so that $K_{E\sigma^H}$ and $K_{PdnaK E\sigma^H}$

are unaffected by the presence of (p)ppGpp. Comparing these experimental results with (p)ppGpp (green stars of Figure 4.9) with the transcriptions in the absence of (p)ppGpp, and from the fact that there are not observable effects when σ^H is alone, they deduced that (p)ppGpp must reduce the competitiveness of σ^{70} . We conjecture that this action can be exerted by weakening either the binding affinity between the housekeeping sigma factor and the core RNAP ($K_{E\sigma^{70}}$) or the binding affinity between $E\sigma^{70}$ and the cognate promoter ($K_{Prna1 E\sigma^{70}}$). Therefore we tested these two hypotheses in our model.

Effect of (p)ppGpp on $K_{E\sigma^{70}}$ and $K_{Prna1 E\sigma^{70}}$. To tune $K_{Prna1 E\sigma^{70}}$ under the effect of (p)ppGpp, we also include in the simulation the pool of holoenzymes bound to the promoters. The DNA template used in the experiment is quite short, just 315 base pairs [107], and for that reason we exclude any effect of the non-specific binding and of the differential release of sigma factor and core during early elongation (thus, the dissociation constant is given simply by the equilibrium dissociation constant). To also rule out the effect of the sequestration of the holoenzymes by the elongation process, we simulate with our model the experiments above in the absence of (p)ppGpp, once again including the active transcription. Over a large span of parameters, we do not find any difference in the results. Therefore, we can concentrate our attention just on the modulation of $K_{E\sigma^{70}}$ and $K_{Prna1 E\sigma^{70}}$.

First, we simulate the competition assay with fixed amounts of RNAP, σ^H , DNA template, and an increasing σ^{70} , simply using the binding affinities as given by the fits in the absence of (p)ppGpp ($K_{E\sigma^{70}}$, $K_{PdnaK E\sigma^{70}}$, $K_{E\sigma^H}$, and $K_{PdnaK E\sigma^H}$). We obtain the dark yellow curve in Figure 4.9, far away from the experimental data in the presence of (p)ppGpp (stars). Every simulation with a weakened binding affinity $K_{Prna1 E\sigma^{70}}$ between the housekeeping holoenzyme and its cognate promoter does not reproduce the experimental data, either, as shown by the orange line, where we used a 100 times larger dissociation constant. Instead, we only obtain a good accordance with the data by weakening the housekeeping holoenzyme binding affinity. A four-fold larger dissociation constant $K_{E\sigma^{70}}$ is enough to reproduce the experimental outcome, as demonstrated by the red line. This value is in line with what we have already found in Figure 4.7(b), where a fit has given a 3.5-fold weakening.

This analysis using our model supports, at least for this case, a possible indirect up-regulation of the alternative sigma factor-dependent gene activity through a weakening action on $K_{E\sigma^{70}}$ by (p)ppGpp.

4.8 Summary

In this chapter, we have used our model to examine the effects on the gene expression of an increased amount of alternative sigma factors and core RNAPs, such as in the stringent response, *i.e.* a specific stress response activated upon intracellular

amino acid starvation. Hallmarks of stringent response are the nucleotide alarmone (p)ppGpp and the effector DksA. Interacting directly with the core RNAP, the main role of (p)ppGpp/DksA is the inhibition of the transcription of the ribosomal σ^{70} -dependent genes [108, 109, 110]. Since ribosomal operons are known to sequester a large amount of cores during growth in rich media [13], rapid inhibition of the synthesis of stable RNA results in a quick redistribution of the disengaged RNA polymerases. This process has been proposed to passively up-regulate other genes such as biosynthesis and alternative sigma-driven genes. We have therefore inspected the role of the stringent response on sigma factor competition and passive regulation of transcription within our model.

Hypersensitivity induced by increased core availability. By mimicking the increase of available cores during the shift from exponential growth to early stringent response, we have found that, in the competition region, the number of alternative holoenzymes increases steeply, indicating that the cognate genes are sensitive to the concentration of RNAPs (Figure 4.2). In Figure 4.3 we quantify this sensitivity with the response factor. Our result indicates that the alternative sigma factor-dependent transcription can be passively induced, and that this may present hypersensitivity provided that some conditions are satisfied: the dissociation constant of the housekeeping holoenzyme must be smaller than the dissociation constant of the alternative holoenzyme, and the maximal sensitivity (found when the number of available cores is equal to the number of available housekeeping sigma factors) must lie between, or be larger than, the number of cores available during the exponential growth and the stringent/stationary response. This argument implies that, if the housekeeping sigma factors are in excess over cores (as suggested by some measurements), a passive enhancement of the alternative sigma factor-driven gene transcription can only be achieved if σ^{70} is actively sequestered by some mechanisms, such as anti-sigma factors. In addition to the release of core polymerases from the ribosomal genes, the response to stress involves the accumulation of alternative sigma factors. From our model, we show that by increasing numbers of alternative sigma factors and core polymerases, the cell shifts from exponential growth state to stringent response state (Figure 4.4(b)) entering into a state characterized by sigma factor competition.

Exponential growth and stringent response. Next, we have included the effect of anti- σ^{70} , 6S RNA, non-specific binding, and active elongation, to evaluate the transcription of stable RNA, mRNA and alternative sigma-dependent RNA (σ^S RNA) during exponential growth and different scenarios of stringent (stress) response. Initially, we have compared the RNA synthesis rate predicted by our model during growth condition to the one measured by Bremer and collaborators [47] and we have found a good agreement (Figure 4.5(b)). The RNAP partitioning among different cellular processes predicted by our simulation has proved very similar to the one proposed by Bremer and collaborators [47] and by Klumpp and Hwa [42], but

the transcription activity differs from the one proposed by Bakshi *et al.* [48], most likely because of the different experimental conditions under which the parameters were measured (Figure 4.8). Then, in Figure 4.7(b), we have analyzed the same cell during different scenarios of early stringent response. The activity of the σ^S -dependent genes has resulted higher in the presence of ribosomal RNA transcription than during their suppression (green bars (2) and (3), respectively), due to the weakening effect of the *rrn* elongation on the effective $E - \sigma^{70}$ binding affinity. We have shown that the cell can achieve a middle condition between the two extreme cases of complete suppression and unaltered synthesis of the *rrn* by allowing the activity of *rrn*- and σ^S -genes and, at the same time, by weakening the binding affinity either between housekeeping holoenzyme and *rrn* promoters (fourth row of Figure 4.7(a)) or between core and σ^{70} (fifth row of Figure 4.7(a)), both effects proposed to be induced by (p)ppGpp [21, 52, 53]. The first case tunes the σ^S RNA synthesis between the limits given by P_{rrn} - P_{σ^S} RNA coexistence and *rrn* suppression (bars (4) of Figure 4.7(b)). The second case broadly enhances this synthesis, but at the same time keeps the stable RNA transcription higher (bars (5) of Figure 4.7(b)). This latter condition might be unfavorable during a phase of nutrient deprivation, when it is important for the economy of the cell to produce no more than the needed ribosomes. We have used these two scenarios to fit an *in vivo* experiment with our model [106] (data are the dashed orange lines in Figure 4.7(b)) from which we obtain that (p)ppGpp causes either a 2-fold weakening of the housekeeping holoenzyme-ribosomal promoter binding affinity or a 3.5-fold weakening of core- σ^{70} binding affinity.

(p)ppGpp may weaken the housekeeping holoenzyme dissociation constant. Finally, in Figure 4.9 we have analyzed a transcription experiment [21] that supports a direct weakening action of the (p)ppGpp on the housekeeping holoenzyme dissociation constant. In reference [21] it was found that (p)ppGpp reduces the competitiveness of σ^{70} during a competition transcription assay with σ^H . We have supposed that in such experiment, the influence of (p)ppGpp could only be exerted on the binding affinity either between core and housekeeping sigma factor or between housekeeping holoenzyme and cognate promoter. From the simulation of these two different scenarios with our model, we have found that, at least for this experiment, a possible indirect up-regulation of the alternative sigma factor-dependent gene activity can only come through a weakening of the core- σ^{70} binding affinity.

(p)ppGpp adjusts the asset of the cell. (p)ppGpp is a global regulator during conditions of nutrient starvation, and among its many effects, it is required *in vivo* to induce activity of genes that transcribe σ^S [111, 9, 43]. In our model, the passive effect of (p)ppGpp, whether it causes a repression of the stable RNA promoters or a weakening of the binding affinity between housekeeping sigma factor and core, does not play a major role in enhancing the transcription of the alternative-dependent genes. This is shown by the small differences among green bars (2), (3),

(4), and (5) in Figure 4.7(b). Instead, (p)ppGpp seems to appropriately redistribute the polymerases and, more importantly, to balance costs and benefits in the cell, as presented by the large differences between the light blue bar (1) and bars (2)–(5) in Figure 4.7(b), which respectively represent the exponential growth and the stringent response.

Chapter 5

Summary and outlook

In this thesis we have addressed the effect of sigma factor competition to bind core RNA polymerase on alternative sigma factor-driven transcription. First, we have compared our thermodynamic model to three *in vitro* competition experiments, with which we have found excellent agreement. Then, we have inspected a generic stress response, in which the cell increases the amount of the alternative sigma factors and activates regulators such as anti-sigma and 6S RNA. Finally, including in our description also non-specific binding and active elongation, we have determined that the passive up-regulation of the alternative sigma-dependent transcription is not only possible, but also displays hypersensitivity based on sigma factor competition. Our theoretical analysis supports a significant role of passive control during the global switch of the gene expression program and gives new insights into RNAP partitioning in the cell. Moreover, our model provides a quantitative, complete, and simple characterization of all the main regulatory factors that act on sigma factor competition. This latter analysis may be useful to help design biological devices for synthetic biology.

5.1 Summary and discussion

Bacterial cells react to stress by altering their physiology. Adjustments are characterized by an appropriate and rapid response and display some conserved features regardless of the organism. The reaction to stress is implemented by activation or over-production of specific environment-sensitive sigma factors (σ). These bind to the RNA polymerase (RNAP), form the holoenzyme (composed of the core RNAP and a sigma factor) and modulate the gene expression by changing its affinity to a class of promoters. Referring to the classification in *Escherichia coli*, the vegetative house-keeping σ^{70} is the primary sigma factor during exponential growth; it is the most abundant sigma factor in the cell and largely exceeds the number of core RNAPs

[12, 11]. It has been found that the level of cores and housekeeping sigma factors stays constant in the shift from the exponential growth to the stationary phase, in which different species of sigma factors coexist in the cell [12, 11]. For that reason, pools of different kinds of sigma factors have to compete to bind the limited amount of cores [5, 18]. As a consequence, the outcome of sigma factor competition influences the regulation of transcription of different classes of genes in response to stresses. Furthermore during the stringent response, a stress response to amino acid starvation, the global regulator (p)ppGpp inhibits the transcription of the ribosomal genes [95], which are known to sequester a large amount of RNAPs during rapid growth [13]. The disengagement of these cores has been proposed to passively up-regulate biosynthesis and alternative sigma-driven genes [96, 50, 21, 23, 33].

The reason for this study was the lack of a theory that describes the global effects of sigma factor competition on gene regulation in bacteria. Specifically, in this thesis, we have focused on the “passive” control exerted by sigma factor competition on bacterial transcription either through cross talk among sets of genes that are specifically regulated or through change in the availability of the components of the transcription machinery - core RNAP and sigma factors.

Inspired by a previous work [11], we have developed a theoretical model that describes binding of sigma factors and core RNA polymerase, binding to promoters and transcription initiation and elongation, release of core and sigma factor as well as non-specific binding of the various molecular species to DNA and modulation of molecular availability by anti-sigma factor and 6S RNA. In our thermodynamic model, presented in Figure 2.1, we have focused on the case of two competing sigma factor species, the housekeeping sigma factor σ^{70} , and one type of alternative sigma factor, which we have denoted by σ^{Alt} . This simplification provides either a description of a specific stress responses, in which only one specific alternative sigma factor accumulates or applies to a general stress response, in which different types of alternative sigma factors are induced but lumped together into a single group, assuming that their parameters are rather similar.

In Chapter 2, we have first analyzed the case when competition between sigma factors is for binding to the core RNAP only. In our model, the beginning of the competition is set by the amount of alternative sigma factors necessary to outcompete the housekeeping sigma so as to cause a significant reduction in the production of the housekeeping holoenzymes.

A key condition for competition is that sigma factors are more abundant than core RNAPs. When the binding between sigma factors and core RNAP is strong, as experimentally observed with dissociation constants in the nM range, and the competing sigma factors approximately have the same affinity for the core, this condition is very intuitive: when core is in excess, all sigma factors are found in holoenzymes and no competition is obtained; the competition sets in when the total number of available

sigma factors is larger than the number of available core enzymes (not counting “unavailable” sigma factors and cores that are for example sequestered by anti-sigma factors, 6S RNA, or tied up in transcript elongation). This condition is a general property of systems with one-to-one stoichiometry and competition for binding [27, 112, 28]. The competition gets more complex, when two sigma factors have different affinities for the core. In that case, a stronger-binding sigma factor can start to displace a weak-binding sigma factor even without excess of total sigma factors.

We have found that the transcription of genes with saturated promoters is rather insensitive to such competition. Such promoters bind RNAP strongly, but initiate transcription at a relatively low rate so that they are occupied by RNA polymerase most of the time [113]. The insensitivity against competition may be a mechanism for insulating the transcription of these genes from physiological perturbations related, *e.g.* to stress responses, where sigma factor competition is induced. This comes however at the price of a reduced dynamic range for regulation by transcription factors compared to unsaturated promoters [11]. If, however, promoters are recognized by two species of holoenzymes or promoters depending on different sigma factors overlap, even saturated promoters become affected by sigma factor competition.

The basic formulation of our model presented in Chapter 2 is suitable to describe different processes that deal with molecular competition and/or originates genetic cross talk, such as ribosomes competing for mRNA (see also reference [26]) or competition between enzymes for a substrate.

At the end of Chapter 2, we have used this reduced equilibrium model to describe several *in vitro* experiments [22, 21, 25] which analyze the effects of competition between two species of sigma factors either on the holoenzyme formation, on the transcription rate of one cognate gene or on the transcription rate of two orthogonal promoter families. We have obtained a very good agreement with the experimental data.

In order to reversibly enable the access of alternative sigma factors to cores and to reroute the transcriptional program under stress conditions, the cell adopts several strategies. We have discussed the most relevant regulatory factors in the first part of Chapter 3. Anti-sigma factors act as major regulators of sigma availability [32, 75, 12, 10, 35]. In particular, anti- σ^{70} diminishes the formation of the corresponding holoenzyme by sequestering the housekeeping sigma factors and therefore inhibits the transcription of the cognate genes. Nevertheless, σ^{70} -driven genes with a saturated promoter only exhibit down-regulation when sigma factor competition occurs - moment in which the cell actually needs to tune their expression. On the contrary, transcription from the same genes is almost unaffected by 6S RNA, which forms a specific complex with the housekeeping holoenzyme and prevents promoter binding [36, 76, 38]. While anti- σ^{70} enhances the formation of the alternative holoenzymes, 6S RNA reduces the concentrations of both species of holoenzymes by affecting core

availability. The binding of cores and holoenzymes to the DNA also affects the competition. We have therefore studied the effects of non-specific binding of core RNAPs and holoenzymes to DNA.

If different holoenzymes and/or core RNAP have different non-specific dissociation constants, non-specific binding may in principle interfere with sigma factor competition by shifting the binding equilibrium. If however, these dissociation constants are approximately the same, as it is likely the case under physiological ionic strength [72], cytoplasmic and non-specifically bound components equally participate in sigma factor competition, and the competition is not related to non-specific binding. As a consequence, non-specific binding cannot buffer alternative sigma factor dependent transcription against passive effects due to the increased availability of core RNAPs during stringent response. This conclusion is in contrast to earlier results for the σ^{70} -dependent transcription of biosynthetic operons [42]. The two cases differ in the stage of the transcription initiation pathway during which they are subject to competition. Biosynthetic operon promoters compete with other genes and - more importantly - with non-specific binding sites on the DNA for the binding of holoenzymes. For alternative sigma-dependent transcription, the competition occurs at an earlier stage, namely between the binding of different classes of sigma factors to the core, which is not affected by non-specific binding.

Measured sigma factor dissociation constants exhibit a clear binding hierarchy, with the strongest being for the housekeeping sigma factor [8]. This hierarchy may be altered by the transcriptional activity of the different holoenzymes, because transcription influences sigma factor competition in complex ways. Primarily, transcript elongation sequesters core RNAPs and, to a lesser extent, sigma factors, thus modulating the availability of these components. In addition, transcription also serves as a pathway for the effective dissociation of holoenzymes, effectively increasing their dissociation constant. While these effects are probably of minor importance *in vitro*, they should have a bigger impact *in vivo*, where transcription does perturb the pool of free holoenzymes. As a consequence, it is questionable how relevant the measured equilibrium dissociation constants are for the cell.

So far our model provided a simplified description of the transcription process. At the end of Chapter 3 we have then considered some extensions that may be needed to describe either an *in vitro* or an *in vivo* situation. We have analyzed the one-dimensional diffusion of the holoenzyme along the DNA that may facilitate the promoter finding [82], the tethering of sigma to core during active elongation [78] and the ability of sigma factors to rebind the elongating complex [80]. According to experimental measurements, these mechanisms, which modify our description of the process of transcription *in vitro* may be negligible *in vivo* [83, 84, 78, 4]. The effects of abortive transcriptions, of RNAPs in a paused state, of transcription factors and of termination factors, can be instead included into the average values of some global

parameters (*i.e.* into initiation rate, into elongation rate, into the number of active promoters and gene lengths, respectively). Therefore, concerning the scenario we are interested in, these modulators do not modify our description of transcription.

The regulatory factors studied in Chapter 3 contribute to the redistribution of the RNAPs during the shift from the exponential growth to the stress response phase, which was the focus of our interest in Chapter 4.

According to the observation that non-specific binding does not affect much sigma factor competition, passive up-regulation of alternative sigma factor transcription can be expected during the stringent response, as proposed [25, 33]. During stringent response, the transcription of the ribosomal RNA is rapidly stopped through the action of the alarmone (p)ppGpp. As ribosomal RNA transcription accounts for two third of the total transcription in rapidly growing bacteria [47, 13], a large number of core RNAPs that were sequestered by rRNA transcription become available. Our calculations indicate that not only can this increase in core availability lead to a strong increment in the formation of alternative holoenzymes, and thus the concomitant transcription, but also that alternative sigma factor-dependent transcription may be hypersensitive to such change in core availability. The maximal sensitivity arises when none of the housekeeping sigma is left free. When competition is only among sigma factors for binding the polymerase, if the housekeeping sigma factor binds stronger to core than the alternative sigma factor, the system displays hypersensitivity. In this scenario, the number of cores equal to the number of housekeeping sigma factors yields the maximal response. While sequestration of housekeeping sigma factors by anti-sigma causes hypersensitivity for smaller number of cores, 6S RNA, by sequestering holoenzymes, adjusts the intensity of the response.

As a result of the change in concentration of alternative sigma factors, anti- σ^{70} , and 6S RNA, the core enzyme is redistributed among different cellular processes during the shift from exponential growth to stationary phase.

Therefore, to address this sharing, we first have used our model to analyze the RNAP partitioning and the consequent RNA synthesis rate during the exponential growth by using data from an *in vivo* experiment [47]. To that end, we have divided the genome in three classes: ribosomal genes, housekeeping sigma-driven genes, and alternative sigma-dependent genes. The result of our simulation is very similar to the one obtained in earlier theoretical inspections based on the same data [47, 42]. Instead, it disagrees with the one proposed in a recent paper [48] obtained from a single-molecule diffusion analysis *in vivo*, most likely because of the different experimental conditions under which the parameters were measured. Finally, we have considered the same cell during different scenarios of early stringent response and we have found that the increased availability of alternative sigma factors, anti- σ^{70} , and 6S RNA is enough to passively down-regulate the synthesis of stable RNA.

Counterintuitively, the transcription of the alternative sigma-driven genes appears

higher in the presence of ribosomal RNA transcription than during its suppression, coordinated by (p)ppGpp. This is due to the weakening effect on the effective housekeeping holoenzyme dissociation constant induced by the separation of σ^{70} from cores that elongate the *rrn* genes. This results in the enhancement of the alternative holoenzyme formation. However, in such a case the cell still employs some RNAPs on the stable RNA transcription. Thus, our investigation shows that one task of (p)ppGpp is to appropriately redistribute the polymerases and, importantly, to balance costs and benefits in the cell.

There are some indications (although no definitive evidence) that the decrease of transcription of the ribosomal genes can be modulated by the alarmone (p)ppGpp also actively, acting either on the promoter-holoenzyme affinity or on the affinity of σ^{70} for core RNAP [21, 52, 53]. If this effect is specific to σ^{70} and not present for other sigma factors, it might modulate the sigma factor hierarchy and thereby enhance the competitive success of alternative sigma factors. For that reason, at the end of this thesis we have examined a transcription experiment [21], which analyzed with our model, supports a direct weakening action of the (p)ppGpp on the housekeeping holoenzyme dissociation constant.

5.2 Outlook

In this thesis, we have presented a first description that includes the effects of all the major modulators of the gene expression during exponential growth and early stringent response in a minimal quantitative theory, based on the outcome of the competition between sigma factors to bind to core RNAP. Validated by comparison with *in vitro* [22, 21, 25] and *in vivo* [47] assays, our thermodynamic model can be used to describe the average synthesis rate from a class of genes, the RNAP partitioning among different processes, the sensitivity and cross talk of a (reduced) gene network, and in particular, the modification in transcription of genes depending on the stress-triggered sigma factors during conditions of growth and stress adaptation. Unfortunately, to our knowledge, there are no precise and extensive measurements of all the cellular parameters in different physiological states or in response to different stress conditions. For that reason, it would be useful to perform a systematic *in vivo* study aimed to characterize the same cell in different situations.

Our theory for sigma factor competition can be extended in various directions in order to provide a more complete and realistic description.

First, activation of certain sigma factor species under specific conditions may require an extension of the model by including the effect of some regulators. For example, Crl which specifically binds to σ^S and actively favors the formation of the corresponding holoenzyme [114, 74], or Rsd that *in vitro* has been shown to displace the housekeeping sigma from the holoenzyme [115]. The effect of Crl is important

only when relatively few σ^S are present [116, 117] and at certain temperatures [118], and for that reason we have excluded it from our current analysis.

Secondly, while we have shown that our description is enough to predict a competition experiment *in vitro* [25] in the presence of σ^N and σ^{70} , the possibility of lone binding to cognate promoters, the need of activators and recruiters, and abortive initiations may change our basic model for the transcription of the σ^N -dependent genes *in vivo* [9, 93].

Thirdly, there are other mechanisms that have been shown to affect gene expression *in vivo*. For example, molecular crowding has an important effect also on steady state quantities, by enhancing binding rates and reducing diffusion rates [119]. Even though its impact on the gene network expression *in vivo* has not been completely established, some preliminary results are available for synthetic nanosystems [120]. From the very beginning we have assumed also homogeneous concentrations, nevertheless spatial distribution of molecules and their targets modifies the regulation of the promoters [121].

Furthermore, we have divided sigma factors in two classes only, so that their total number is always large. On the contrary, if we explicitly deal with single species, we have to take into account that some sigma factors are present in the cell with very small numbers, thus variability and noise can play a role that has to be addressed [122, 123, 26]. Moreover, *in vivo* resources are shared with the host cell, so transcription, translation and growth are coupled [124]. Thus, it would be interesting to expand the investigation to larger networks including transcription, translation and growth feedback loops.

Finally, our model can be applied to synthetic biology, and sigma factors have indeed been proposed as versatile components for synthetic gene circuits. Sequestration of sigma factors by anti-sigma factors and competition for core RNAP provide mechanisms for genetic switches [125, 126, 127]. In this context, hyper-sensitive behavior may be a desired property of such switches, and our theory could help tune such systems into the required parameters regime. Recent experimental work in *B. subtilis* has demonstrated interesting pulsing dynamics of a sigma factor, driven by cycles of auto-activation and sequestration [128, 129]. Here, we have only considered steady state situations, but our model can easily be extended to include such driving by coupling our description of the competition of sigma factors to a model for their synthesis.

Appendix A

Values of the parameters used in the simulations

In the following, we discuss the parameters of our model that were experimentally determined and how we choose their values in our calculations. Most of them depend on the physiological condition of the cell and in some cases conflicting values have been reported by different labs or based on different experimental techniques, so that we have used a plausible range of values in our calculations. These values, summarized in Table A.1, are approximation of either *in vivo* or *in vitro* measurements. All quantities are related to *Escherichia coli*. Since most numbers are growth rate dependent, we have assumed values similar to those that a cell has in the early stage of a stress response, after a previous period of rapid growth (here $\mu = 2.5$ dbl/h) - a situation for which the maximal response is expected.

A.1 Average volume

We use an average cell volume of 1.32 fL, in accordance with the average volume given by reference [47] for a growth rate of 2.5 dbl/h (Table A.2). With this choice, concentration of 1 nM corresponds to 0.8 molecules per cell or, alternatively, concentration of ~ 1.26 nM corresponds to one molecule per cell.

A.2 RNAPs and sigma factors

Recent investigations [11, 12] have suggested that the total number of RNAP remains constant during the transition from exponential growth to stationary phase, but it still depends on the growth rate in the exponential phase. In Table A.4, we summarize different measurements for core RNAPs, housekeeping sigma factors and alternative sigma factors, from three different labs.

Quantity	Assumed value
Average cell volume	1.32 fL
E per cell	11400
σ^{70} per cell	5700
σ^{Alt} per cell	from 0 to 20000
$K_{E\sigma^{70}}, K_{E\sigma^{Alt}}$	1 nM
Anti- σ^{70} per cell	19000
$K_{\sigma^{70} Anti-\sigma^{70}}$	50 nM
6S RNA per cell	3800
$K_{\sigma^{70} 6SRNA}$	200 nM
Genome equivalent per cell	3.8
Non-specific binding sites per cell	17.48×10^6
$K_{E\sigma^{Alt} NS}, K_{E\sigma^{70} NS}, K_{ENS}$	from 10^{-6} M to 10^{-2} M
σ -cognate promoters per cell	200
L_{operon}	2000 nt
α_p	40 min^{-1}
v_{tsx}	55 nt/sec
L_{ret}	300 nts
$k_{fE\sigma}$	$10^6 \text{ sec}^{-1} \text{ M}^{-1}$
$K_{p^{70} E\sigma^{70}}, K_{p^{Alt} E\sigma^{Alt}}, K_{p^{70} E\sigma^{Alt}}$	from 10^{-7} M to 10^{-5} M

Table A.1: Values adopted in the simulations.

In our calculations, we used the value of 11400 RNAPs per average cell growing with a growth-rate of $\mu = 2.5$ dbl/h, as estimated by Bremer and Dennis [13]. A larger

Vol (fL)	Conditions	Ref.
0.39	0.45 dbl/h, 37°C	[11]
0.8	1.33 dbl/h, 37°C	[11]
0.63	1 dbl/h, 37°C	[47]
1.2	2.5 dbl/h, 37°C	[47]
0.34	0.6 dbl/h, 37°C	[42]
0.55	1 dbl/h, 37°C	[42]
0.84	1.5 dbl/h, 37°C	[42]
1.11	2 dbl/h, 37°C	[42]
1.32	2.5 dbl/h, 37°C	[42]

Table A.2: Volume of an average cell in different growth conditions.

number has been reported by Grigorova *et al.* [11], which however reflects the larger cell size for cells growing at 30°C compared to cells growing at 37°C. Table A.3 shows in detail more experimental values for the measure of the intracellular concentration of the core RNAP.

E/cell	Conditions	Ref.
2600 ± 1300	0.45 dbl/h, 30 °C	[11]
13000 ± 4000	1.33 dbl/h, 30 °C	[11]
2598 ± 255	1.6 dbl/h, 37 °C	[12]
2574 ± 268	Stat. phase, 37 °C	[12]
3500	1 dbl/h,	[97]
8000	2 dbl/h,	[97]
1500	0.6 dbl/h, 37 °C	[13]
2800	1 dbl/h, 37 °C	[13]
5000	1.5 dbl/h, 37 °C	[13]
8000	2 dbl/h, 37 °C	[13]
11400	2.5 dbl/h, 37 °C	[13]

Table A.3: Average number of RNAP cores per cell. RNAPs was obtained multiplying mass fraction of total protein that is RNAP by mass cell. This latter was quantified through the amount of β and β' RNAP subunits.

The intracellular level of σ^{70} is believed to be higher than the amount of any individual alternative sigma species. According to recent measurements, which we summarize in Table A.4, the housekeeping sigma factor is in excess over core RNAP (1.3-fold from Gross lab [11] and 3-fold from Busby lab [12]), while older measurements in the Ishihama lab [14] found core RNAP in 5-fold excess of σ^{70} . Concentration of housekeeping sigma seems to remain almost constant during the transition from exponential growth to stationary phase [14, 12] but to change with the growth rate [11].

In order to mimic the effects of σ^{70} -sequestration by anti-sigma factors, 6S RNA, and elongating complexes, we set the number of housekeeping sigma factors to be half the number of cores. In our analysis of the stringent response, we estimate the number of housekeeping sigma factors from the RNAP partitioning [42]. Assuming that all free RNAPs, non-specifically bound RNAPs and a fraction of the transcribing RNAPs are housekeeping holoenzymes, the number of housekeeping sigma factors is approximately 9000.

The concentration of alternative sigma factors depend on the cellular condition (see Table A.4). During exponential growth, housekeeping sigma factor is the most abundant. Even though during stationary phase, the amounts of some alternative

Molecules/cell	Gross lab [11, 15]	Busby lab [12]	Ishihama lab [8, 97, 14, 130]
E	2600 ± 1300 (1) 13000 ± 4000 (2)	2598 ± 255 (6) 2574 ± 268 (8)	3500 (9) 8000 (10)
σ^{70}	4700 ± 2400 (1) 17000 ± 4000 (2)	7283 ± 913 (2) 7191 ± 898 (8)	500 – 700 (7) 500 – 700 (8)
σ^{Alt}	$\sigma^E = 3200 \pm 600$ (1) $\sigma^E = 5500 \pm 1200$ (2) $\sigma^H = 20 \pm 5$ (1) $\sigma^H = 120 \pm 34$ (2) $\sigma^H = 50-4850$ (3) $\sigma^H = 850-250$ (4) $\sigma^H = 250$ (5)	$\sigma^S < 1$ (6) $\sigma^S = 1615 \pm 383$ (8)	$\sigma^S < 1$ (7) $\sigma^S = 170 - 230$ (8) 110 σ^N , 30-350 σ^F , few σ^{Fecl}

Table A.4: Average number of RNAP cores and sigma factors per cell from experimental measurements. (1) 0.45 dbl/h, 30°C. (2) 1.33 dbl/h, 30°C. (3) from 1 to 6 minutes after heat shock, 42°C. (4) from 6 to 10 minutes after heat shock, 42°C. (5) over 10 minutes after heat shock, 42°C. (6) 1.6 dbl/h, 37°C. (7) growth phase, 37°C. (8) stationary phase, 37°C. (9) 1 dbl/h. (10) 2 dbl/h. Measurements done using immunoblotting (a technique to detect specific proteins in a sample. Basically, first different proteins of a sample are separated by gel electrophoresis, then are identified with antibodies).

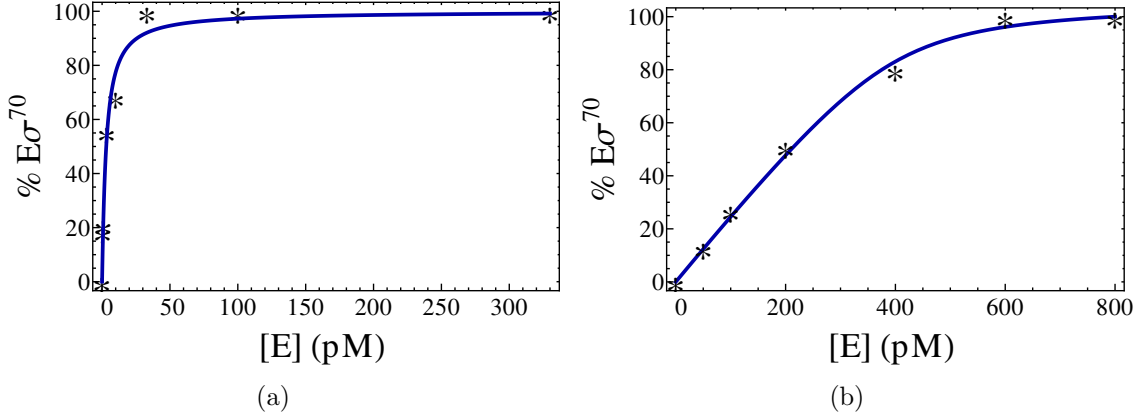


Figure A.1: Binding experiments. A fixed amount of σ^{70} (0.5 nM in (a) and 0.4 nM in (b)) was mixed with increasing concentrations of cores, holoenzymes were counted and normalized on their maximum. From fit of the data with a Michaelis-Menten equation it was obtained $\sigma^{70} = 3.3$ nM [102] and $\sigma^{70} = 0.26$ nM [8], respectively. From a fit with Equation 2.5, we obtained $K_{E\sigma^{70}} = 2.8$ nM for Figure (a) and $K_{E\sigma^{70}} = 0.02$ nM for Figure (b). Data are represented as stars and our fit as solid lines.

sigma factors are increased, the concentration of any single species does not exceed the concentration of total σ^{70} [11]. For example, numbers of σ^N and σ^F were found to be almost constant [14, 12]. By contrast, the concentration of other sigma factors such as σ^H and σ^S is known to considerably increase in altered physiological states [9]. From the data collected in Table A.4, we conclude that the total number of alternative sigma factors (the sum of all sigma species) can exceed the number of core polymerases. In our simulation we increase the concentration of the alternative sigma factor up to 20000 units to mimic either the shift from exponential to stationary phase or *in vitro* experiments with increasing alternative sigma factor concentration.

A.3 Holoenzyme dissociation constants

Sigma-core binding affinity varies with temperature and ionic conditions, as shown in Tables A.7–A.6, where we collect values from the literature. A recent *in vitro* study [66] has systematically investigated these variations for σ^{70} , σ^H , and σ^S and found that different conditions induce variations not only on the absolute binding affinities, but also on the relative binding affinities for the different holoenzymes: $K_{E\sigma^{70}} < K_{E\sigma^S} < K_{E\sigma^H}$ at 20 °C, 150 mM NaCl; $K_{E\sigma^H} < K_{E\sigma^S} < K_{E\sigma^{70}}$ at 20 °C, 100 mM NaCl; $K_{E\sigma^{70}} < K_{E\sigma^S} < K_{E\sigma^H}$ at 30 – 35 °C, irrespective of NaCl concentration and $K_{E\sigma^S} < K_{E\sigma^H} < K_{E\sigma^{70}}$ at 40 °C.

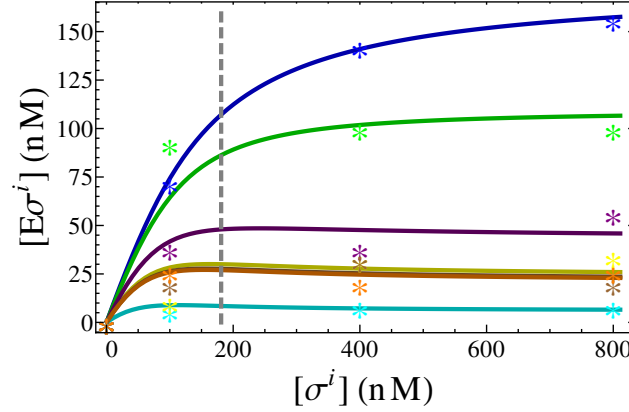


Figure A.2: Mixed holoenzyme reconstruction experiment in the presence of all seven known sigma factors of *E. coli* [8]. An increasing equimolar amount of each sigma factor species was mixed with a fixed amount of core RNAPs (400 nM, 200 mM NaCl, pH 7.6 at 30°C) and the concentration of holoenzymes of every species was counted by gel filtration chromatography (a technique to separate molecules according to their size through filtration in a gel medium). Data represented as stars and our fit as solid lines. Numerical results are in Table A.5. Blue * represents $E\sigma^{70}$, green * $E\sigma^N$, purple * $E\sigma^F$, yellow * $E\sigma^H$, orange * $E\sigma^{FecI}$, brown * $E\sigma^E$, and cyan * $E\sigma^S$. Lines from our fit have the same color but in a darker shade. The gray dashed line of the starting point of the competition is calculated with Equation 2.22 and $i = S$, because $E\sigma^S$ has the weakest binding affinity.

Colland *et al.* [102] measured the affinity between the housekeeping sigma factor and the RNAP core incubating a fixed amount of σ^{70} subunits with increased concentration of core enzymes, and found $K_{E\sigma^{70}} = 3.3 \pm 0.5$ nM. This value was obtained by fitting the binding experiments with a Langmuir isotherm, implicitly assuming a constant concentration of sigma factors available for binding. We have fitted their data again using Equation 2.5 (which in contrast to the Langmuir expression accounts for the reduction of the concentration of free subunits by holoenzymes formation) and have obtained a dissociation constant of 2.8 nM (Figure A.1(a), data as stars and fit as a solid line).

Similarly, Maeda *et al.* [8] reported a dissociation constant of 0.26 nM for the binding of σ^{70} and core RNAP with the same method, in different conditions. We have fitted their data again using Equation 2.5 and have obtained a dissociation constant of 0.02 nM, corresponding to about 10-fold stronger binding (Figure A.1(b)).

In addition, Maeda *et al.* also performed a mixed holoenzyme reconstruction experiment with all seven sigma factors of *E. coli* (at 30°C, 200 mM NaCl). They found that the relative strengths of the dissociation constants, measured using only the saturation condition, was $K_{E\sigma^{70}} < K_{E\sigma^N} < K_{E\sigma^F} < K_{E\sigma^H}, K_{E\sigma^{FecI}} < K_{E\sigma^E} < K_{E\sigma^S}$.

σ^i	$K_{E\sigma^i}/K_{E\sigma^{70}}$ [8]	$K_{E\sigma^i}/K_{E\sigma^{70}}$ our fit
σ^N	1.55	1.59
σ^F	2.85	4.02
σ^H	4.75	7.29
σ^{FecI}	6.65	8.05
σ^E	9.35	8.28
σ^S	16.4	29.59

Table A.5: Dissociation constant between each σ^i and the core RNAP E , relative to $K_{E\sigma^{70}}$, from [8] (second column) and from our fit (third column).

By fitting the complete set of data with our model we obtained almost the same order, $K_{E\sigma^{70}} < K_{E\sigma^N} < K_{E\sigma^F} < K_{E\sigma^H} < K_{E\sigma^E} < K_{E\sigma^{FecI}} < K_{E\sigma^S}$ (Figure A.2). The relative strengths of the dissociation constants are reported in Table A.5. From the same data we also obtained a value of $K_{E\sigma^{70}} = 45.2$ nM, while reference [8] did not report the results of their fit.

We also refit with the same method data from reference [102] to obtain $K_{E\sigma^S} = 11$ nM (Figure A.3), reference [21] to obtain $K_{E\sigma^H} = 98.2$ nM (Figure 2.9(a)), reference [22] to obtain $K_{E\sigma^F} = 25$ nM (Figure 2.8(b)), and reference [69] to obtain $K_{E\sigma^N} = 10.8$ nM (Figure 2.10). In reference [131], it was found $K_{E\sigma^N} = 48$ (100 mM NaCl, pH 8, 30 °C).

Since binding affinities between core and different sigma species are reported to be similarly strong at least *in vitro* [8], we often choose $K_{E\sigma^{70}} = K_{E\sigma^{Alt}}$. In addition we

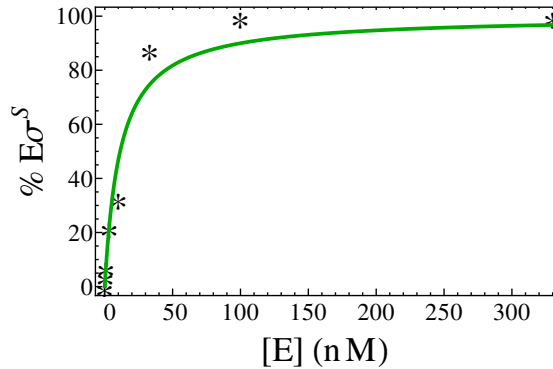


Figure A.3: Binding experiment from reference [102]. A fixed amount of σ^S was mixed with increasing concentration of cores. Data as stars and fit with Equation 2.5 as a solid line. A fit with a Michaelis-Menten function gave $\sigma^S = 15.2 \pm 3.7$ nM [102], while we obtain $K_{E\sigma^S} = 11$ nM.

note that in most cases sigma-core binding is quite strong (nM dissociation constants, see Tables A.6–A.8), which allows us to use approximations in the model such as neglecting free pools of the subunit that is limiting for holoenzyme formation.

In all scenarios, where transcript elongation is described explicitly, we also need the binding rate between sigma and core, as this enters the effective dissociation constants. To our knowledge, this rate has not been measured, but a dissociation rate was measured in reference [74] for the σ^S holoenzyme and found to be around 10^{-3} sec^{-1} . By using this value and a dissociation constant of 1 nM, the holoenzyme formation rate $k_{fE\sigma}$ is obtained as $10^6 \text{ sec}^{-1} \text{ M}^{-1}$. In all calculations, where the equilibrium constant is different from 1 nM, we kept the dissociation rate fixed.

$K_{E\sigma^H}$ (nM)	Conditions	Ref.
28 ± 10	300 mM NaCl, pH 7.9, 20 °C, ⁽³⁾	[132]
0.8	100 mM NaCl, pH 7.9, 22 °C, ⁽²⁾	[70]
0.6	250 mM NaCl, pH 7.9, 22 °C, ⁽²⁾	[70]
2.4	500 mM NaCl, pH 7.9, 22 °C, ⁽²⁾	[70]
0.3	100 mM Kglu, pH 7.9, 22 °C, ⁽²⁾	[70]
1.3	250 mM Kglu, pH 7.9, 22 °C, ⁽²⁾	[70]
2	500 mM Kglu, pH 7.9, 22 °C, ⁽²⁾	[70]
22.5 ± 1.1	10 mM NaCl, pH 7.4, 20 °C, ⁽³⁾	[66]
57.1 ± 2.8	10 mM NaCl, pH 7.4, 25 °C, ⁽³⁾	[66]
72.9 ± 3.4	10 mM NaCl, pH 7.4, 30 °C, ⁽³⁾	[66]
92.9 ± 3.1	10 mM NaCl, pH 7.4, 35 °C, ⁽³⁾	[66]
125 ± 8	10 mM NaCl, pH 7.4, 40 °C, ⁽³⁾	[66]
103 ± 8	150 mM NaCl, pH 7.4, 20 °C, ⁽⁴⁾	[66]
312 ± 21	150 mM NaCl, pH 7.4, 25 °C, ⁽⁴⁾	[66]
614 ± 27	150 mM NaCl, pH 7.4, 30 °C, ⁽⁴⁾	[66]
1720 ± 140	150 mM NaCl, pH 7.4, 40 °C, ⁽⁴⁾	[66]
112 ± 9	100 mM NaCl, pH 7.4, 20 °C, ⁽⁴⁾	[66]
628 ± 32.2	100 mM NaCl, pH 7.4, 30 °C, ⁽⁴⁾	[66]
98.2	50 mM KCl, pH 7.5, 37 °C, ⁽¹⁾	From Table 2.1

Table A.6: Estimates of $K_{E\sigma^H}$. ⁽¹⁾ - ⁽⁴⁾ as in Table A.7. [†] We fit the data from reference [21] as described in Figure 2.9(a) to obtain $K_{E\sigma^H} = 98.2 \text{ nM}$.

$K_{E\sigma^{70}}$ (nM)	Conditions	Ref.
0.26*	200 mM NaCl, pH 7.6, 30 °C, ⁽¹⁾	[8]
$3.3 \pm 0.5^\dagger$	10 mM MgCl ₂ , 100 mM Kglu, pH 8, 37 °C, ⁽¹⁾	[102]
8	100 mM NaCl, pH 7.9, 22 °C, ⁽²⁾	[70]
50	250 mM NaCl, pH 7.9, 22 °C, ⁽²⁾	[70]
300	500 mM NaCl, pH 7.9, 22 °C, ⁽²⁾	[70]
3	100 mM Kglu, pH 7.9, 22 °C, ⁽²⁾	[70]
17	250 mM Kglu, pH 7.9, 22 °C, ⁽²⁾	[70]
21	500 mM Kglu, pH 7.9, 22 °C, ⁽²⁾	[70]
$1.25 \pm 0.22^\ddagger$	10 mM NaCl, pH 7.4, 20 °C, ⁽³⁾	[66]
5 ± 0.66	10 mM NaCl, pH 7.4, 25 °C, ⁽³⁾	[66]
9.09 ± 0.71	10 mM NaCl, pH 7.4, 30 °C, ⁽³⁾	[66]
12.7 ± 1	10 mM NaCl, pH 7.4, 35 °C, ⁽³⁾	[66]
15.8 ± 1.7	10 mM NaCl, pH 7.4, 40 °C, ⁽³⁾	[66]
60 ± 10.4	150 mM NaCl, pH 7.4, 20 °C, ⁽⁴⁾	[66]
201 ± 23	150 mM NaCl, pH 7.4, 25 °C, ⁽⁴⁾	[66]
475 ± 23	150 mM NaCl, pH 7.4, 30 °C, ⁽⁴⁾	[66]
3000 ± 1700	150 mM NaCl, pH 7.4, 40 °C, ⁽⁴⁾	[66]
10.3 ± 1.1	100 mM NaCl, pH 7.4, 20 °C, ⁽⁴⁾	[66]
450 ± 29.2	100 mM NaCl, pH 7.4, 30 °C, ⁽⁴⁾	[66]
130 [‡]	0.2 M KCl, pH 7.8, 30 °C, ⁽¹⁾	From Table 2.1
21.1 [§]	50 mM KCl, 10 mM MgCl ₂ , pH 7.5, 37 °C, ⁽¹⁾	From Table 2.1

Table A.7: Collection of measured values of the σ^{70} -core dissociation constant $K_{E\sigma^{70}}$. ⁽¹⁾ Gel electrophoresis or filtration followed by immunoblotting (techniques to separate and analyze macromolecules according to their charge or size in a gel matrix). ⁽²⁾ Fret/Lret (techniques to measure the kinetics of reactions through light emission). ⁽³⁾ Langmuir - Blodgett trough (in this technique the pressure-area isotherm of a monolayer of molecules (RNAP) is measured with and without adding the ligand (sigma factors), and the the affinity is calculated from their differences). ⁽⁴⁾ Surface plasmon resonance (a technique that measures the variation in dielectric properties of receptors immobilized on a surface layer when they are bound to ligands. The instrument detects the absorbance of the light on the material, which gives a measure of the amount of mass on the surface; when a ligand binds the surface the mass changes). * From our fit in Figure A.1(b), we have found $K_{E\sigma^{70}} = 0.02$ nM. [†] From our fit in Figure A.1(a), we have found $K_{E\sigma^{70}} = 3.3 \pm 0.5$ nM. [‡] In reference [66], two different techniques were used to evaluate the same quantity. Discrepancies in the measurements, as explained in the paper, must be inferred to the intrinsic diversity of the two detection method. Langmuir - Blodgett trough measures directly equilibrium dissociation constants on an equilibrium assay, while the surface plasmon resonance detects on and off rates and affects the RNAP- σ interfaces. [‡] From the fit done in Section 2.2, Figure 2.8(a). [§] From the fit done in Section 2.2, lower panel of Figure 2.9(b).

$K_{E\sigma^S}$ (nM)	Conditions	Ref.
$15.2 \pm 3.7^\dagger$	10 mM MgCl ₂ , 100 mM Kglu, pH 8, 37°C, ⁽¹⁾	[102]
68.2 ± 8.4	25°C, ⁽⁴⁾	[74]
59 ± 3.9	10 mM NaCl, pH 7.4, 20°C, ⁽³⁾	[66]
61.2 ± 4.9	10 mM NaCl, pH 7.4, 25°C, ⁽³⁾	[66]
62.5 ± 5.6	10 mM NaCl, pH 7.4, 30°C, ⁽³⁾	[66]
65.7 ± 4.6	10 mM NaCl, pH 7.4, 35°C, ⁽³⁾	[66]
250 ± 22	150 mM NaCl, pH 7.4, 20°C, ⁽⁴⁾	[66]
325 ± 23	150 mM NaCl, pH 7.4, 25°C, ⁽⁴⁾	[66]
450 ± 22	150 mM NaCl, pH 7.4, 30°C, ⁽⁴⁾	[66]
125 ± 11.3	100 mM NaCl, pH 7.4, 20°C, ⁽⁴⁾	[66]
628 ± 32.2	100 mM NaCl, pH 7.4, 30°C, ⁽⁴⁾	[66]

Table A.8: Collection of measured values of the σ^S -core dissociation constant $K_{E\sigma^S}$. ⁽¹⁾-⁽⁴⁾ as in Table A.7. [†] We refit the data from reference [102] using Equation 2.5 to obtain $K_{E\sigma^S} = 11$ nM (Figure A.3).

A.4 Anti-sigma factors

In the cell both anti- σ^{Alt} (such as FecR/ σ^{FecI} , RseA/ σ^E , FlgM/ σ^F , RshA/ σ^H) and anti- σ^{70} (such as Rsd or AsiA) can be present. They can vary from few units to large numbers, as shown in Table A.9. Piper *et al.* [12] (Busby lab) measured 3300 Rsd per cell in exponential growth phase (1.3-fold core RNAPs) and 6200 per cell in stationary phase (2.5-fold core). We choose anti- σ^{70} factors to be 1.7-fold the core number.

Anti-sigma- σ binding affinities seem to be pretty weak compared to sigma factor-core strength. For example, the couple RseA/ σ^E has a dissociation constant around 100 nM [73], AsiA/ σ^{70} 67 nM, and Rsd/ σ^{70} 32 nM [10]. We assume a $K_{\sigma^{70}Anti-\sigma^{70}}$ in line with these latter values.

A.5 6S RNA

The intracellular number of 6S RNA per cell has never been measured precisely. In references [36] and [38], it was estimate that 6S RNA can increase from hundreds of units during exponential growth to thousands during late stationary phase. Not knowing the exact numbers, we choose the available 6S RNA to be one third of the total RNAP cores.

To have an idea of the dissociation constant between $E\sigma^{70}$ and 6S RNA, we fit an experiment that evaluates the inhibition of 6S RNA on the initiation complex forma-

Quantity	Measured value	Ref.
Rsd /cell during exponential phase ⁽¹⁾	3319 ± 593	[12]
Rsd /cell during stationary phase ⁽¹⁾	6242 ± 895	[12]
RseA /cell during exponential phase ⁽²⁾	200	[73]
RseB /cell during exponential phase ⁽²⁾	40	[73]
RseA /cell during heat shock ⁽²⁾	400	[73]
RseB /cell during heat shock ⁽²⁾	80	[73]
$K_{\sigma^{70} AsiA}$ ⁽³⁾	67 nM	[10]
$K_{\sigma^{70} Rsd}$ ⁽³⁾	32 nM	[10]
$K_{AsiAAsiA}$ ⁽⁴⁾	0.35 μ M	[133]
$K_{AsiAAsiA}$ ⁽⁵⁾	0.6 μ M	[134]
$K_{\sigma^E RseARseB}$ ⁽⁶⁾	50 nM	[73]
$K_{\sigma^E RseA}$ ⁽⁶⁾	100 nM	[73]
$K_{RseARseB}$ ⁽⁷⁾	20-70 nM	[135]

Table A.9: Intracellular number and *in vitro* binding affinity to cognate sigma factors of several anti-sigma factors. ⁽¹⁾ from immunoblotting using K12 MG1655 strain at 37°C. ⁽²⁾ from immunoblotting by using LMG191 and MC4100 strains at 30°C. ⁽³⁾ surface plasmon resonance. ⁽⁴⁾ complexes measured with sedimentation equilibrium, a technique generally used to determine molecular mass. If the monitoring is in real time, it allows to determine formation of complexes, stoichiometry, and as a consequence equilibrium constants. ⁽⁵⁾ sedimentation equilibrium at 20°C. ⁽⁶⁾ immunoblotting. ⁽⁷⁾ fluorescence anisotropy (a technique to measure the kinetics of reactions through light emitted with unequal intensities along different axes of polarization by fluorescent tags).

tion of a σ^{70} -dependent promoter in *E. coli* (Figure S2 in the Supporting Information of [76]). The fit gives $K_{E\sigma^{70}6SRNA} \simeq 156$ nM (Figure A.4), a value that we often approximate to 200 nM.

A.6 Non-specific binding

Every free DNA site can in principle be a non-specific binding site. *E. coli* has approximately 4.6×10^6 base pairs per genome. Thus, with 3.8 genome equivalents per cell at a growth rate of 2.5 dbl/h [13], there are about 17.48×10^6 non-specific binding sites per cell.

The genome equivalent is the average amount of DNA in a cell necessary to guarantee that all genes are present. In Table A.10 we collect some values of genome equivalent corresponding to different growth conditions. Figure A.5 shows the behavior of the average genome equivalent as a function of the growth rate.

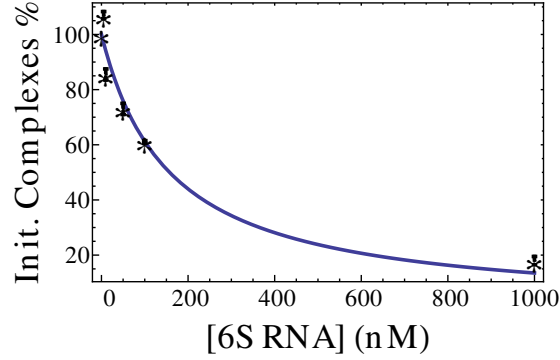


Figure A.4: A fixed amount of housekeeping holoenzyme (3 nM) was mixed with an increasing concentration of 6S RNA in the presence of a cognate promoter and the inhibition on the promoter complex formation was measured [76] (stars). From a fit with Equations 2.5 and 2.7, adapted for 6S RNA, we obtain $K_{E\sigma^{70}6SRNA} = 155.7$ nM. Our fit is represented by the solid line.

In reference [42], the dissociation constant for non-specific binding was estimated to be 3.1×10^{-3} M and in reference [54], 10^{-4} M. *In vitro* experiments [72] with 0.2 M NaCl or KCl found $K_{E\sigma NS} \simeq 10^{-5}$ M and $K_{ENS} \simeq 5 \times 10^{-7}$ M, and with ionic conditions that approximate the physiological conditions (in the presence of 0.01 M $MgCl_2$), the non-specific binding affinities of holoenzyme and core were found to be comparable ($K_{E\sigma NS} \simeq 3 \times 10^{-4}$ and $K_{ENS} \simeq 10^{-4}$). In our calculations, we used values for non-specific binding between 10^{-6} M and 10^{-2} M.

Conditions	Genome equivalent	Ref.
0.45 dbl/h, †	1.4	[11]
0.6 dbl/h, 37°C	1.6	[13]
1 dbl/h, 37°C	1.8	[13]
1.33 dbl/h, †	2.4	[11]
1.5 dbl/h, 37°C	2.3	[13]
2 dbl/h, 37°C	3.0	[13]
2.5 dbl/h, 37°C	3.8	[13]

Table A.10: Genome equivalent content of a cell. † In reference [11] they interpolate their measurements with the data from references [136, 137]. Even if experimental conditions are different (e.g. 37°C and 30°C, in [136, 137] and [11], respectively), the results are in line with the other values given in the table.

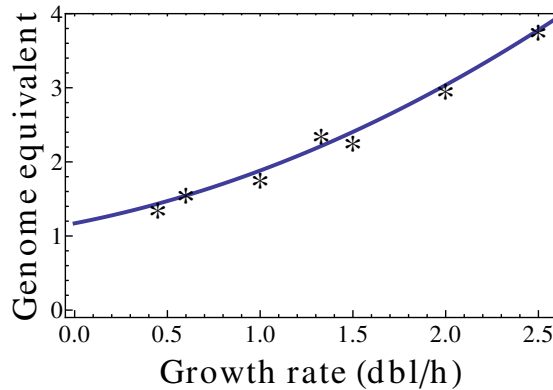


Figure A.5: Graphical representation of the data in Table A.10. The solid line shows the quadratic function obtained from their fit: genome equivalent = $0.2 \text{ growth rate}^2 + 0.5 \text{ growth rate} + 1.2$.

A.7 Specific binding to promoters and elongation

In the *E. coli* genome, around 1800 promoters are under the control of the housekeeping sigma factor and 1300 depend on the alternative sigma factors [103]. However, only fractions of these promoters are active at any time. Also over a third are recognized by more than one holoenzyme species [103]. In addition, the promoter concentration varies during the life cycle of the cell with the replication of the genome, and also with the growth conditions. Here, we used an average number of 200 active promoters/cell.

In the *in vitro* experiments we analyzed, the length of the transcribed sequence is typically short, around 300 nucleotides. To describe *in vivo* situations, we choose an average length of 2000 nucleotides per operon and assume to have one promoter per operon that is recognized by a single holoenzyme species.

The promoters are characterized by the maximal transcription rate (α_p) and the Michaelis constant $K_{pE\sigma}$. For α_p , we take values similar to the *in vivo* values estimated in [137, 42]. $K_{pE\sigma}$ is taken to be comparable to the values reported for the affinities between the RNAP and *rrn* promoters or *lac* promoter [47, 54].

The elongation speed of the transcribing RNA polymerase varies with growth conditions and depends on the transcribed sequence. Here we take an average transcription speed v_{tsx} of 55 nt sec^{-1} , as estimated for mRNA transcription in reference [13]. Based on the measurements of references [3, 79], we adopt a mean sigma factor retention length L_{ret} of 300 nucleotides.

Typical mRNA transcription rates are around $1\text{-}10 \text{ min}^{-1}$. For highly transcribed genes, such as ribosomal genes, they reach $25\text{-}30 \text{ min}^{-1}$ [138, 47]; in some cases even higher values were estimated, as in reference [47] (110 initiations per promoter per minute). We assume a maximal transcription rate similar to the one estimated *in*

in vivo from references [137] and [42].

The average elongation speed of a transcribing RNA polymerase varies with growth and physiological conditions, besides it also depends on the transcribed sequence. We assume an average transcription speed v_{tsx} of 55 nucleotides/sec, as estimated for mRNA genes in reference [13] (values for different growth rates are summarized in Table A.11 [13]).

Parameter	0.6 dbl/h	1 dbl/h	1.5 dbl/h	2 dbl/h	2.5 dbl/h
$v_{tsx} \text{ mRNA}$	39	45	50	52	55
$v_{tsx} \text{ rRNA}$	85	85	85	85	85

Table A.11: Elongation rate in nt/s for mRNA and rRNA [13].

Appendix B

Competition between two sigma factor species to bind to RNAP - Analytical results

A simple general analytical solution for the problem of two competing species of sigma factor is not possible. Nevertheless, every subset of parameters allows simplifications thanks to which the system of Equations 2.9–2.13 of Chapter 2 can be analytically solved. In the main text, we refer to these cases as the “free binding cases”, *i.e.* in the absence of modulators and DNA (when competition between sigma factors is only for binding to core RNAP).

Each of the following cases is obtained by neglecting a term in the set of Equations 2.9–2.13:

- I - $[E\sigma^{70}] \ll [E_{free}] + [E\sigma^{Alt}]$ in Equation 2.9;
- II - $[E\sigma^{70}] \ll [\sigma_{free}^{70}]$ in Equation 2.10;
- III - $[E\sigma^{Alt}] \ll [\sigma_{free}^{Alt}]$ in Equation 2.11;
- IV - $[E\sigma^{Alt}] \ll [E_{free}] + [E\sigma^{70}]$ in Equation 2.9;
- V - $[\sigma_{free}^{Alt}] \ll [E\sigma^{Alt}]$ in Equation 2.11;
- VI - $[E_{free}] \ll [E\sigma^{70}] + [E\sigma^{Alt}]$ in Equation 2.9;
- VII - $[\sigma_{free}^{70}] \ll [E\sigma^{70}]$ in Equation 2.10;
- VIII - if $K_{E\sigma^{70}} = K_{E\sigma^{Alt}}$ the system has an exact solution. In the text, we use this instance (represented with dashed lines in the plots) as basis for comparison to the situations in the presence of modulators and DNA.

$K = K_{E\sigma^{70}}/K_{E\sigma^{Alt}}$	strong $K_{E\sigma^i} \lesssim 10^{-6} \text{ M}$	weak $K_{E\sigma^i} \gtrsim 10^{-6} \text{ M}$
$K \gg 1$	V, VI	I, II
$K = 1$	VIII	VIII
$K \ll 1$	VI, VII	III, IV

Table B.1: Classification of analytical solutions according to the strength of $K_{E\sigma^{70}}$, $K_{E\sigma^{Alt}}$, and K , assuming that the dissociation constants have similar strength and $[\sigma^{70}] < [E]$.

Besides, if we suppose that the amount of available housekeeping sigma factors is less than the amount of core RNAPs (because of the effects of σ^{70} -sequestration by anti-sigma factors, 6S RNA, and elongating complexes) and that the binding affinities $K_{E\sigma^{70}}$ and $K_{E\sigma^{Alt}}$ are either both strong (smaller than 10^{-6} M) or both weak (larger than 10^{-6} M), we can divide the pattern of solutions as in Table B.1, according to the strength of sigma-core binding affinities and the ratio $K = K_{E\sigma^{70}}/K_{E\sigma^{Alt}}$. This is obviously just a possible partition, that reflects the conditions in the cell, justified by the discussion of Table A.1 in Appendix A.

Generally, from the analysis of the single cases, we conclude that the response factor R_E presents hypersensitivity when $K < 1$. The maximum is always found for $E \simeq \sigma^{70}$.

All the following solutions are also valid by swapping the indexes “70” and “Alt”, because System 2.9–2.13 is symmetric under this exchange. The simulations are done with the values of the parameters in Table A.1 in Appendix A, where not differently stated.

B.1 Case I

We can neglect $[E\sigma^{70}]$ in Equation 2.9 either when $[E] < [\sigma^{Alt}]$ and $[E] > [\sigma^{70}] + [\sigma^{Alt}]$ with $K > 1$, when $[E] > [\sigma^{70}] + [\sigma^{Alt}]$ with $K < 1$ or for weak binding affinities and $K \gg 1$. With this approximation, the concentrations of the holoenzymes result

$$\begin{aligned}
[E\sigma^{70}] &= \frac{[\sigma^{70}]}{2([\sigma^{70}](K_{E\sigma^{70}} - K_{E\sigma^{Alt}}) + K_{E\sigma^{70}}(K_{E\sigma^{70}} - K_{E\sigma^{Alt}} - [\sigma^{Alt}]))}. \quad (\text{B.1}) \\
&\cdot \left([E]K_{E\sigma^{70}} - 2[E]K_{E\sigma^{Alt}} - K_{E\sigma^{70}}K_{E\sigma^{Alt}} - K_{E\sigma^{70}}[\sigma^{Alt}] + \right. \\
&\left. + K_{E\sigma^{70}}\sqrt{4[E]K_{E\sigma^{Alt}} + (K_{E\sigma^{Alt}} - [E] + [\sigma^{Alt}])^2} \right) \\
[E\sigma^{Alt}] &= \frac{1}{2} \left([E] + K_{E\sigma^{Alt}} + [\sigma^{Alt}] - \sqrt{4[E]K_{E\sigma^{Alt}} + (K_{E\sigma^{Alt}} - [E] + [\sigma^{Alt}])^2} \right).
\end{aligned}$$

Using Equation 2.14 in Chapter 2 and $K \gg 1$, we find that there is sigma factor competition when

$$[\sigma^{Alt}] \geq \frac{\rho[E](K_{E\sigma^{Alt}} + [E])}{K_{E\sigma^{70}} + \rho[E]}$$

or as a function of the concentration of core RNAPs when

$$[E] \leq \frac{\rho(\sigma^{Alt} - K_{E\sigma^{70}}) + \sqrt{\rho(\rho(K_{E\sigma^{70}} - \sigma^{Alt})^2 + 4K_{E\sigma^{70}}\sigma^{Alt})}}{2\rho}.$$

B.2 Case II

If $[E\sigma^{70}] \ll [\sigma_{free}^{70}]$ in Equation 2.10, the holoenzyme concentrations fulfill

$$\begin{aligned} [E\sigma^{70}] &= \frac{[\sigma^{70}]}{2K_{E\sigma^{70}}(K_{E\sigma^{70}} + [\sigma^{70}])} \left(([E]K_{E\sigma^{70}} - K_{E\sigma^{70}}K_{E\sigma^{Alt}} - K_{E\sigma^{Alt}}[\sigma^{70}] - K_{E\sigma^{70}}[\sigma^{Alt}] + \right. \\ &\quad \left. + \sqrt{4[E]K_{E\sigma^{Alt}}K_{E\sigma^{70}}(K_{E\sigma^{70}} + [\sigma^{70}]) + (K_{E\sigma^{Alt}}[\sigma^{70}] + K_{E\sigma^{70}}(K_{E\sigma^{Alt}} + [\sigma^{Alt}] - [E])^2)} \right) \\ [E\sigma^{Alt}] &= \frac{1}{2K_{E\sigma^{70}}} \left([E]K_{E\sigma^{70}} + K_{E\sigma^{70}}K_{E\sigma^{Alt}} + K_{E\sigma^{Alt}}[\sigma^{70}] + K_{E\sigma^{70}}[\sigma^{Alt}] + \right. \\ &\quad \left. - \sqrt{4[E]K_{E\sigma^{Alt}}K_{E\sigma^{70}}(K_{E\sigma^{70}} + [\sigma^{70}]) + (K_{E\sigma^{Alt}}[\sigma^{70}] + K_{E\sigma^{70}}(K_{E\sigma^{Alt}} + [\sigma^{Alt}] - [E])^2)} \right). \end{aligned}$$

This assumption is valid either when $[E] < [\sigma^{70}] + [\sigma^{Alt}]$ and $K > 1$, when $[E] < |[\sigma^{70}] - [\sigma^{Alt}]|$ and $K < 1$ or for weak binding affinities and $K \gg 1$. Sigma factors compete for binding to the core when

$$[\sigma^{Alt}] \geq \frac{\rho}{1-\rho} (K_{E\sigma^{Alt}}[\sigma^{70}] + K_{E\sigma^{70}}(K_{E\sigma^{Alt}} + [E](1-\rho)))$$

or as a function of the polymerase concentration when

$$[E] \leq \frac{[\sigma^{Alt}]}{\rho} - \frac{K_{E\sigma^{Alt}}(K_{E\sigma^{70}} + [\sigma^{70}])}{K_{E\sigma^{70}}(1-\rho)}.$$

B.3 Case III

If $[E\sigma^{Alt}] \ll [\sigma_{free}^{Alt}]$ in Equation 2.11, the concentrations of the holoenzymes are

$$\begin{aligned} [E\sigma^{70}] &= \frac{1}{2K_{E\sigma^{Alt}}} \left([E]K_{E\sigma^{Alt}} + K_{E\sigma^{70}}K_{E\sigma^{Alt}} + K_{E\sigma^{Alt}}[\sigma^{70}] + K_{E\sigma^{70}}[\sigma^{Alt}] + \right. \\ &\quad \left. - \sqrt{4[E]K_{E\sigma^{Alt}}K_{E\sigma^{70}}(K_{E\sigma^{Alt}} + [\sigma^{Alt}]) + (K_{E\sigma^{Alt}}([\sigma^{70}] - [E]) + K_{E\sigma^{70}}(K_{E\sigma^{Alt}} + [\sigma^{Alt}]))^2} \right) \quad (\text{B.2}) \\ [E\sigma^{Alt}] &= \frac{[\sigma^{Alt}]}{2K_{E\sigma^{Alt}}(K_{E\sigma^{Alt}} + [\sigma^{Alt}])} \left([E]K_{E\sigma^{Alt}} - K_{E\sigma^{70}}K_{E\sigma^{Alt}} - K_{E\sigma^{Alt}}[\sigma^{70}] - K_{E\sigma^{70}}[\sigma^{Alt}] + \right. \\ &\quad \left. + \sqrt{4[E]K_{E\sigma^{Alt}}K_{E\sigma^{70}}(K_{E\sigma^{Alt}} + [\sigma^{Alt}]) + (K_{E\sigma^{Alt}}([\sigma^{70}] - [E]) + K_{E\sigma^{70}}(K_{E\sigma^{Alt}} + [\sigma^{Alt}]))^2} \right). \end{aligned}$$

This approximation is valid either when $[E] < [\sigma^{70}] + [\sigma^{Alt}]$ and $K < 1$, $[E] < |[\sigma^{70}] - [\sigma^{Alt}]|$ and $K > 1$ or with weak binding affinities and $K \ll 1$. The sigma factor competition takes place when

$$[\sigma^{Alt}] \geq \frac{\rho K_{E\sigma^{Alt}}}{2(1-\rho)K_{E\sigma^{70}}} \left(\rho([E] + K_{E\sigma^{70}} + [\sigma^{70}]) + \right. \quad (B.3)$$

$$\left. - (\rho - 2) \sqrt{K_{E\sigma^{70}}^2 + ([E] - [\sigma^{70}])^2 + 2K_{E\sigma^{70}}([E] + [\sigma^{70}])} \right).$$

or as a function of cores:

$$\frac{1}{2\rho(1-\rho)K_{E\sigma^{Alt}}} \cdot \left(K_{E\sigma^{70}}\rho(\rho-1)(2K_{E\sigma^{Alt}} + [\sigma^{Alt}]) + \rho K_{E\sigma^{Alt}}[\sigma^{70}](2 + (\rho-2)\rho) + \right.$$

$$\left. - (\rho-2) \sqrt{4\rho^2 K_{E\sigma^{70}} K_{E\sigma^{Alt}}^2 [\sigma^{70}](\rho-1) + (K_{E\sigma^{70}}[\sigma^{Alt}](\rho-1) + K_{E\sigma^{Alt}}[\sigma^{70}]\rho^2)^2} \right) \leq$$

$$\leq [E] \leq \frac{1}{2\rho(1-\rho)K_{E\sigma^{Alt}}} \cdot$$

$$\cdot \left(K_{E\sigma^{70}}\rho(\rho-1)(2K_{E\sigma^{Alt}} + [\sigma^{Alt}]) + \rho K_{E\sigma^{Alt}}[\sigma^{70}](2 + (\rho-2)\rho) + \right.$$

$$\left. + (\rho-2) \sqrt{4\rho^2 K_{E\sigma^{70}} K_{E\sigma^{Alt}}^2 [\sigma^{70}](\rho-1) + (K_{E\sigma^{70}}[\sigma^{Alt}](\rho-1) + K_{E\sigma^{Alt}}[\sigma^{70}]\rho^2)^2} \right).$$

In this case, R_E displays hypersensitivity and the maximal response occurs for $[E] \simeq K_{E\sigma^{70}} + [\sigma^{70}]$. Figure B.1 shows the cumulative response under an increased number of core RNAPs and alternative sigma factors. The white and red dashed lines represent the onset of the competition respectively obtained from the simulation and analytically with Equation B.3. The red arrow highlights a possible path for the intracellular number of cores and σ^{Alt} during the shift from exponential growth to stress response. For $K \ll 1$, the solutions of Equations B.2 become

$$[E\sigma^{70}] = \frac{1}{2} \left([E] + K_{E\sigma^{70}} + [\sigma^{70}] - \sqrt{4[E]K_{E\sigma^{70}} + (K_{E\sigma^{70}} - [E] + [\sigma^{70}])^2} \right)$$

$$[E\sigma^{Alt}] = \frac{[\sigma^{Alt}]}{2(K_{E\sigma^{Alt}} + [\sigma^{Alt}])} \left([E] - K_{E\sigma^{70}} - [\sigma^{70}] + \sqrt{4[E]K_{E\sigma^{70}} + (K_{E\sigma^{70}} - [E] + [\sigma^{70}])^2} \right).$$

B.4 Union of cases I, II, and III

If the core-sigma binding affinities are very weak (*i.e.* $K_{E\sigma^{70,Alt}} \geq 10^{-3}$), cases I, II, and III can be merged to obtain from Equations 2.9–2.11 the simplified system

$$\begin{aligned} [E] &= [E_{free}] \\ [\sigma^{70}] &= [\sigma_{free}^{70}] \\ [\sigma^{Alt}] &= [\sigma_{free}^{Alt}] \end{aligned}$$

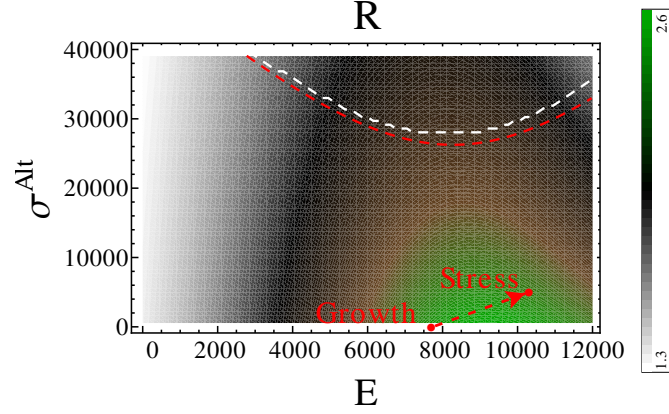


Figure B.1: Case III. Density plot of the response factor R as a function of the number of E cores and alternative sigma factors in the presence of 9000 σ^{70} , $K_{E\sigma^{70}} = 10^{-6}$ M, and $K_{E\sigma^{Alt}} = 10^{-4}$ M. The white and red dashed lines represent the onset of the competition respectively obtained from the simulation and analytically with Equation B.3. The red arrow highlights a possible path for the intracellular number of cores and σ^{Alt} during the shift from the exponential growth to stress response.

and the holoenzyme concentrations can be expressed through the dissociation constants:

$$[E\sigma^{70}] = \frac{[E][\sigma^{70}]}{K_{E\sigma^{70}}}, \quad [E\sigma^{Alt}] = \frac{[E][\sigma^{Alt}]}{K_{E\sigma^{Alt}}}.$$

B.5 Case IV

Under the assumption that $[E\sigma^{Alt}] \ll [E_{free}] + [E\sigma^{70}]$ in Equation 2.9, holoenzyme concentrations are the same as in case I Equations B.1, but with the indexes “Alt” and “70” swapped. This approximation is valid either for $[E] < [\sigma^{70}]$ and $[E] > [\sigma^{70}] + [\sigma^{Alt}]$ with $K < 1$, $[E] > [\sigma^{70}] + [\sigma^{Alt}]$ with $K > 1$ or with weak binding affinities and $K \ll 1$. Here, the housekeeping holoenzyme concentration remains constant. This means that the competition takes place for very large numbers of σ^{Alt} . R_E has a maximum larger than one for $K < 1$, but does not have a simple expression. To explicitly find the maximum, we merge conditions III and IV to obtain

$$[E\sigma^{70}] = \frac{1}{2} \left([E] + K_{E\sigma^{70}} + [\sigma^{70}] - \sqrt{4[E]K_{E\sigma^{70}} + (K_{E\sigma^{70}} - [E] + [\sigma^{70}])^2} \right)$$

$$[E\sigma^{Alt}] = \frac{[\sigma^{Alt}]}{2K_{E\sigma^{Alt}}} \left([E] - K_{E\sigma^{70}} - [\sigma^{70}] + \sqrt{4[E]K_{E\sigma^{70}} + (K_{E\sigma^{70}} - [E] + [\sigma^{70}])^2} \right).$$

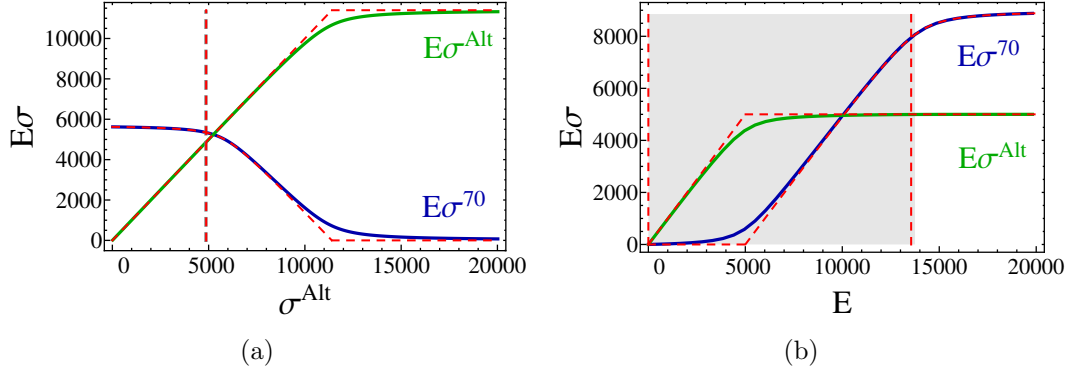


Figure B.2: Case V. Number of holoenzymes as a function of alternative sigma factors in (a) ($E = 11400$ and $\sigma^{70} = 5700$) and cores in (b) ($\sigma^{70} = 9000$ and $\sigma^{Alt} = 5000$) with $K_{E\sigma^{70}} = 10^{-7}$ M and $K_{E\sigma^{Alt}} = 10^{-9}$ M.

Now, the calculation to find the maximum of R_E proceeds as in case III, with the same result: the maximal response is for $[E] \simeq K_{E\sigma^{70}} + [\sigma^{70}]$.

B.6 Case V

Under the assumption that $[\sigma_{free}^{Alt}] \ll [E\sigma^{Alt}]$ in Equation 2.11, the holoenzyme concentrations fulfill

$$\begin{aligned}
 [E\sigma^{70}] &= \frac{1}{2} \left(K_{E\sigma^{70}} - m + [E] + [\sigma^{70}] - \sqrt{4K_{E\sigma^{70}}([E] - m) + (K_{E\sigma^{70}} + m - [E] + [\sigma^{70}])^2} \right) \\
 [E\sigma^{Alt}] &= \min([E], [\sigma^{Alt}]) \equiv m.
 \end{aligned} \tag{B.4}$$

This assumption is valid either when $[E] > [\sigma^{70}] + [\sigma^{Alt}]$ and $K < 1$, $[E] \neq [\sigma^{Alt}]$ and $K > 1$ or generally for strong binding affinities and $K > 1$. Sigma factors are in competition when

$$\begin{aligned}
 [\sigma^{Alt}] &\geq \frac{\rho}{2(K_{E\sigma^{70}}(\rho - 1) + \rho([\sigma^{70}] + [E](\rho - 1)))} \\
 &\left(K_{E\sigma^{70}}(\rho - 1) + ([\sigma^{70}] + [E](\rho - 1))([E](\rho + 1) + \right. \\
 &\quad \left. - (\sqrt{K_{E\sigma^{70}} + ([E] - [\sigma^{70}])^2 + 2K_{E\sigma^{70}}([E] + [\sigma^{70}])} - [\sigma^{70}])) + \right. \\
 &\quad \left. + K_{E\sigma^{70}}(\rho - 1)(2[\sigma^{70}] - \sqrt{K_{E\sigma^{70}} + ([E] - [\sigma^{70}])^2 + 2K_{E\sigma^{70}}([E] + [\sigma^{70}])} + [E](\rho + 2))) \right)
 \end{aligned} \tag{B.5}$$

as shown by Figures B.2(a) and B.2(b), where the solid lines represent the results of the simulations and the red dashed lines the analytical approximations. Equations

B.4 in the case of very strong binding affinities fulfill

$$\begin{aligned} [E\sigma^{70}] &= \frac{1}{2}([E] - m + [\sigma^{70}] - |m - [E] + [\sigma^{70}]|) \\ [E\sigma^{Alt}] &= \min([E], [\sigma^{Alt}]) \end{aligned}$$

and Inequality B.5 becomes

$$[\sigma^{Alt}] \geq \begin{cases} \rho[E] & [E] < [\sigma^{70}] \\ [E] - (1 - \rho)[\sigma^{70}] & [E] \geq [\sigma^{70}] \end{cases}.$$

B.7 Case VI

By neglecting the pool of free holoenzymes in the system of Equations 2.9–2.13 - a simplification that is valid for strong binding affinities - the concentrations of the holoenzymes are

$$\begin{aligned} [E\sigma^{70}] &= \min\left([E], [\sigma^{70}], \frac{1}{2(K-1)}\left([E](K-1) - [\sigma^{70}] - K[\sigma^{Alt}] + \right. \right. & \text{(B.6)} \\ &\quad \left. \left. + \sqrt{4[E](K-1)[\sigma^{70}] + ([E](1-K) + [\sigma^{70}] + K[\sigma^{Alt}])^2}\right)\right) \\ [E\sigma^{Alt}] &= \min\left([E], [\sigma^{Alt}], \frac{1}{2(K-1)}\left([E](K-1) + [\sigma^{70}] + K[\sigma^{Alt}] + \right. \right. \\ &\quad \left. \left. - \sqrt{4[E](K-1)[\sigma^{70}] + ([E](1-K) + [\sigma^{70}] + K[\sigma^{Alt}])^2}\right)\right). \end{aligned}$$

In this case, there is sigma factor competition if

$$[\sigma^{Alt}] \geq \frac{((1-\rho)m - [E])((1-K)(1-\rho)m - [\sigma^{70}])}{K(1-\rho)m} \quad \text{(B.7)}$$

where $m = \min([E], [\sigma^{70}])$. For $\rho = 5\%$ this expression traces the white dashed boundaries of Figures 4.4(a) and 4.4(b) in Chapter 4. By solving Inequality B.7 as a function of $[E]$, we find that for $[\sigma^{Alt}]/[\sigma^{70}] \leq \rho(K(1-\rho) + \rho)/(K(1-\rho))$ there is no competition, while for $\rho(K(1-\rho) + \rho)/(K(1-\rho)) < [\sigma^{Alt}]/[\sigma^{70}] \leq (\rho)/(K(1-\rho))$ the competition is between

$$\frac{[\sigma^{70}]\rho - K[\sigma^{Alt}](1-\rho)}{(1-K)(1-\rho)\rho} \leq [E] \leq \frac{(1-\rho)(K([\sigma^{70}] + [\sigma^{Alt}]) - (K-1)\rho[\sigma^{70}])}{K(1-\rho) + \rho}$$

which approximates the boundaries of the grey region of Figure 4.2 in Chapter 4. For $[\sigma^{Alt}]/[\sigma^{70}] \geq (\rho)/(K(1-\rho))$ there is sigma factor competition when

$$[E] \leq \frac{(1-\rho)(K([\sigma^{70}] + [\sigma^{Alt}]) - (K-1)\rho[\sigma^{70}])}{K(1-\rho) + \rho}.$$

If $\rho \rightarrow 0$, there is competition when $[\sigma^{Alt}] \geq 0$ if $[E] \leq [\sigma^{70}]$ and when $[\sigma^{Alt}] \geq [E] - [\sigma^{70}]$ if $[E] > [\sigma^{70}]$. For $K < 1$, we know from the analysis of the response factor that R_E has a maximum whose value is larger than one. As a matter of fact, if the binding affinity between the alternative sigma factor and the core is much weaker than the corresponding housekeeping one ($K \ll 1$), Equations B.6 can be rewritten as

$$\begin{aligned} [E\sigma^{70}] &= \begin{cases} [E] & [E] \leq [\sigma^{70}] \\ [\sigma^{70}] & [E] > [\sigma^{70}] \end{cases} \\ [E\sigma^{Alt}] &= \begin{cases} 0 & [E] \leq [\sigma^{70}] \\ [E] - [\sigma^{70}] & [\sigma^{70}] < [E] \leq [\sigma^{70}] + [\sigma^{Alt}] \\ [\sigma^{Alt}] & [E] > [\sigma^{70}] + [\sigma^{Alt}] \end{cases} \end{aligned} \quad (\text{B.8})$$

and the maximum of the response factor is $[E] \simeq [\sigma^{70}]$ and lies in the competition region. The value of R_E in this maximum is approximately

$$R_{E \text{ max}} = \frac{2K_{pE\sigma^{Alt}}(K-1)^2[\sigma^{70}]\left(K([\sigma^{Alt}] - [\sigma^{70}]) + r\right)}{r\left(r - K([\sigma^{Alt}] + [\sigma^{70}])\right)\left(\left(r - K([\sigma^{Alt}] + [\sigma^{70}])\right) - 2(K-1)K_{pE\sigma^{Alt}}\right)}$$

where

$$r = \sqrt{K(K([\sigma^{70}] - [\sigma^{Alt}])^2 + 4[\sigma^{70}][\sigma^{Alt}])}.$$

B.8 Case VII

If it is true that $[\sigma_{free}^{70}] \ll [E\sigma^{70}]$ in Equation 2.10, the concentrations of the holoenzymes are given by Equation B.4 of case V with the indexes ‘‘Alt’’ and ‘‘70’’ swapped. This approximation is valid for strong binding affinities and either $[E] > [\sigma^{70}] + [\sigma^{Alt}]$ with $K > 1$ or $[E] \neq [\sigma^{70}]$ with $K < 1$. The housekeeping holoenzyme concentration is a constant, which means that the competition takes place for very large values of alternative sigma factors or cores. R_E has a maximum larger than one when $K < 1$. To find the value of this maximum, we merge conditions VI and VII to obtain the system of Equations B.8, from which we find that $[E] \simeq [\sigma^{70}]$ yield the maximal response.

B.9 Union of cases V, VI, and VII

If the binding affinities are very strong (*i.e.* $K_{E\sigma^{70,Alt}} \geq 10^{-8}$), cases V, VI, and VIII can be merged to obtain the holoenzyme concentrations

$$\begin{aligned} [E\sigma^{70}] &= \min([E], [\sigma^{70}]) \\ [E\sigma^{Alt}] &= \min([E], [\sigma^{Alt}]). \end{aligned}$$

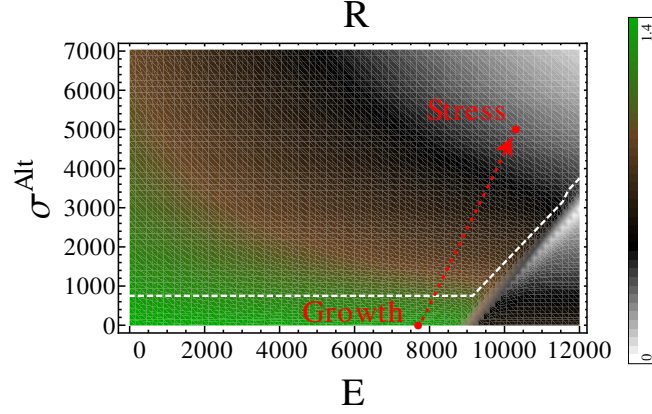


Figure B.3: Case VIII. Density plot of the response factor R as a function of the number of E cores and alternative sigma factors in the presence of 9000 σ^{70} , $K_{E\sigma^{70}} = K_{E\sigma^{Alt}} = 1$ nM. The white dashed line represents the onset of the competition from Equation B.9. The red arrow highlights a possible path for the intracellular number of cores and σ^{Alt} during the shift from exponential growth to stress response.

B.10 Case VIII

If $K_{E\sigma^{70}} = K_{E\sigma^{Alt}} \equiv K_{E\sigma}$, the system of Equations 2.9–2.13 has an exact analytical solution for the concentration of the holoenzymes:

$$[E\sigma^{70}] = \frac{[\sigma^{70}](K_{E\sigma} + [E] + [\sigma^{70}] + [\sigma^{Alt}] - \sqrt{4K_{E\sigma}[E] + (K_{E\sigma} - [E] + [\sigma^{70}] + [\sigma^{Alt}])^2})}{2([\sigma^{70}] + [\sigma^{Alt}])}$$

$$[E\sigma^{Alt}] = \frac{[\sigma^{Alt}](K_{E\sigma} + [E] + [\sigma^{70}] + [\sigma^{Alt}] - \sqrt{4K_{E\sigma}[E] + (K_{E\sigma} - [E] + [\sigma^{70}] + [\sigma^{Alt}])^2})}{2([\sigma^{70}] + [\sigma^{Alt}])}$$

These are the solutions plotted in Figure 2.4(b) in Chapter 2. There is sigma factor competition when

$$[\sigma^{Alt}] \geq \frac{-\rho}{2(\rho - 1)(K_{E\sigma}(\rho - 1) + ([\sigma^{70}] + [E](\rho - 1))\rho)} \quad (\text{B.9})$$

$$\cdot \left(K_{E\sigma}^2(\rho - 1) + ([\sigma^{70}] + [E](\rho - 1)) \left(\sqrt{K_{E\sigma}^2 + ([E] - [\sigma^{70}])^2 + 2K_{E\sigma}([E] + [\sigma^{70}])} + ([E] + [\sigma^{70}](2\rho - 1)) \right) + K_{E\sigma} \left(\sqrt{K_{E\sigma}^2 + ([E] - [\sigma^{70}])^2 + 2K_{E\sigma}([E] + [\sigma^{70}])}(\rho - 1) + (2[E](\rho - 1) + [\sigma^{70}](3\rho - 2)) \right) \right).$$

We use this expression to trace the white dashed line in Figure B.3. The response, here, does not show hypersensitivity.

Thanks to the exact solution given by Inequality B.9, we can inspect how the onset of competition changes as a function of several parameters. Figure B.4(a) presents the number of alternative sigma factors necessary to obtain sigma factor competition with $\rho = 5\%$ as a function of the $K_{E\sigma}$ when the number of housekeeping sigma factors is lower than the number of cores. In this instance, the onset of competition exhibits a minimum. Figure B.4(b) shows that, with a fixed amount of alternative sigma factors, there is a maximal value of cores as a function of the dissociation constants for which the competition sets in. Finally, Figure B.4(c) demonstrates that the 5% criterion has an additional boundary on the number of σ^{Alt} necessary to induce sigma factor competition as a function of the number of σ^{70} .

If $\rho \rightarrow 0$, the onset of competition becomes $[\sigma^{Alt}] = 0$, thus there is competition for any small number of alternative sigma factors. For small values of the core-sigma factor dissociation constants, the concentrations of holoenzymes fulfill

$$\begin{aligned} [E\sigma^{70}] &= \begin{cases} [\sigma^{70}] & [\sigma^{Alt}] \leq [E] - [\sigma^{70}] \\ \frac{[E][\sigma^{70}]}{[\sigma^{70}] + [\sigma^{Alt}]} & [\sigma^{Alt}] > [E] - [\sigma^{70}] \end{cases} \\ [E\sigma^{Alt}] &= \begin{cases} [\sigma^{Alt}] & [\sigma^{Alt}] \leq [E] - [\sigma^{70}] \\ \frac{[E][\sigma^{Alt}]}{[\sigma^{70}] + [\sigma^{Alt}]} & [\sigma^{Alt}] > [E] - [\sigma^{70}] \end{cases} \end{aligned}$$

and the competition condition can be rewritten as

$$[\sigma^{Alt}] \geq \begin{cases} [\sigma^{70}] \frac{\rho}{1-\rho} & [E] \leq [\sigma^{70}] \\ \frac{[E] - (1-\rho)[\sigma^{70}]}{1-\rho} & [E] > [\sigma^{70}] \end{cases} \quad (\text{B.10})$$

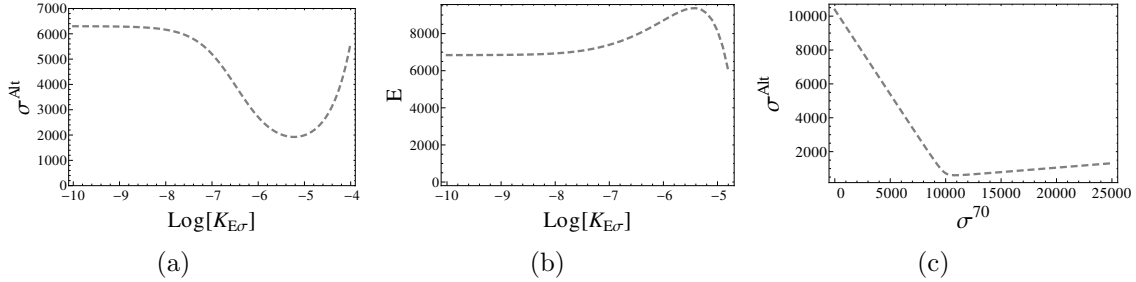


Figure B.4: Consequences of the 5% threshold criterion on the onset of competition. (a) Number of alternative sigma factors for which there is onset of competition as a function of the holoenzyme dissociation constants $K_{E\sigma^{70}} = K_{E\sigma^{Alt}} \equiv K_{E\sigma}$. Here, there are 11400 RNAPs and 5700 housekeeping sigma factors. (b) Onset of competition for the core RNAP as a function of the dissociation constants $K_{E\sigma}$ with 5700 σ^{70} and 1500 σ^{Alt} . (c) Onset of competition for the alternative sigma as a function of housekeeping sigma factors with 10000 cores.

Appendix C

Analytical results in the presence of regulatory factors

Here, we obtain the analytical results relevant for physiological values of the parameters in the presence of regulatory factors, such as anti-sigma factors, 6S RNA, non-specific binding and transcript elongation.

C.1 Anti-sigma factor

C.1.1 Anti-sigma factor during sigma factor competition

According to Table A.1 in Appendix A, the dissociation constant between anti-sigma factor and its cognate sigma factor ($K_{\sigma^{70}\overline{\sigma^{70}}}$) is usually similar or larger than the core-sigma dissociation constant (here, $K_{E\sigma^{70}} = K_{E\sigma^{Alt}} \equiv K_{E\sigma}$). For that reason, here we focus on the following two cases with small $K_{E\sigma}$ and $K_{\sigma^{70}\overline{\sigma^{70}}} (< 10^{-6} \text{ M})$ and with

- I - the number of anti-housekeeping sigma factors larger than number of housekeeping sigma factors;
- II - the number of anti-housekeeping sigma factors smaller than number of housekeeping sigma factors.

For sake of completeness, we study also the instance where

- III - $K_{E\sigma}$ is larger than $K_{\sigma^{70}\overline{\sigma^{70}}}$.

Case I

If $K_{\sigma^{70}\overline{\sigma^{70}}}$ and $K_{E\sigma}$ are both small, $[\overline{\sigma^{70}}] \geq [\sigma^{70}]$, and $[\sigma^{Alt}] < [E]$, we can respectively neglect $[\sigma_{free}^{70}]$ and $[\sigma_{free}^{Alt}]$ in Equations 2.10 and 2.11 (in Chapter 2 adapted to include

the dependence on anti-sigma). Thus, the holoenzyme concentrations result

$$\begin{aligned}
[E\sigma^{70}] &= \frac{1}{2(K_{E\sigma} - K_{\sigma^{70}\overline{\sigma^{70}}})} \left(K_{E\sigma}([\sigma^{70}] - [\overline{\sigma^{70}}]) - K_{\sigma^{70}\overline{\sigma^{70}}}([E] + [\sigma^{70}] - [\sigma^{Alt}]) \right) + \\
&+ (K_{E\sigma}^2([\overline{\sigma^{70}}] - [\sigma^{70}])^2 + K_{\sigma^{70}\overline{\sigma^{70}}}^2([\sigma^{Alt}] + [\sigma^{70}] - [E])^2 + \\
&+ 2K_{E\sigma}K_{\sigma^{70}\overline{\sigma^{70}}}([\overline{\sigma^{70}}]([E] + [\sigma^{70}] - [\sigma^{Alt}]) - [\sigma^{70}]([\sigma^{70}] + [\sigma^{Alt}] - [E])))^{1/2} \\
[E\sigma^{Alt}] &= [\sigma^{Alt}].
\end{aligned}$$

While, if $[\sigma^{Alt}] \geq [E]$, we can neglect $[E_{free}]$, $[E\sigma^{70}]$, and $[\sigma_{free}^{70}]$ in Equations 2.9 and 2.10, respectively. The concentrations fulfill

$$\begin{aligned}
[E\sigma^{70}] &= \frac{1}{2([\overline{\sigma^{70}}] - [\sigma^{70}])} \left(([E] - [\sigma^{Alt}])([\overline{\sigma^{70}}] - [\sigma^{70}]) - K_{\sigma^{70}\overline{\sigma^{70}}}[\sigma^{70}] \right) + \\
&+ \sqrt{4K_{\sigma^{70}\overline{\sigma^{70}}}[E][\sigma^{70}]([\overline{\sigma^{70}}] - [\sigma^{70}]) + (K_{\sigma^{70}\overline{\sigma^{70}}}[\sigma^{70}] + [\sigma^{70}] - [\overline{\sigma^{70}}])([E] - [\sigma^{Alt}])^2} \\
[E\sigma^{Alt}] &= [E].
\end{aligned}$$

Because of the concentrations of the holoenzymes are approximated by two different expressions for small and large numbers of alternative sigma factors, in order to calculate the onset of competition, we have to consider the instances with small and large percentage threshold. For small values of ρ , there is sigma factor competition when

$$\begin{aligned}
[\sigma^{Alt}] &\geq \frac{\rho}{2K_{\sigma^{70}\overline{\sigma^{70}}}(K_{\sigma^{70}\overline{\sigma^{70}}}([\sigma^{70}] + [E](\rho - 1))\rho + K_{E\sigma}([\overline{\sigma^{70}}](\rho - 1) - \rho[\sigma^{70}]))}. \quad (C.1) \\
&\cdot \left(K_{E\sigma}([\overline{\sigma^{70}}] - [\sigma^{70}])^2 + K_{\sigma^{70}\overline{\sigma^{70}}}([\sigma^{70}] + [E](\rho - 1)) \left(K_{\sigma^{70}\overline{\sigma^{70}}}([E] - [\sigma^{70}] + \right. \right. \\
&+ \rho([E] - [\sigma^{70}])) - r \right) + K_{E\sigma} \left(([\sigma^{70}] - [\overline{\sigma^{70}}])r + K_{\sigma^{70}\overline{\sigma^{70}}}([\overline{\sigma^{70}}](\rho - 1)(2[\sigma^{70}] + \right. \\
&+ [E](\rho + 2)) + [\sigma^{70}](2[\sigma^{70}](1 - \rho) + [E](\rho - \rho^2 - 2))) \left. \right)
\end{aligned}$$

where

$$\begin{aligned}
r &= (\rho - 1) \left((K_{\sigma^{70}\overline{\sigma^{70}}}[\overline{\sigma^{70}}] + K_{\sigma^{70}\overline{\sigma^{70}}}[E])^2 - 2(K_{E\sigma} - K_{\sigma^{70}\overline{\sigma^{70}}})[\sigma^{70}] \right) \cdot \\
&\cdot (K_{E\sigma}[\overline{\sigma^{70}}] - K_{\sigma^{70}\overline{\sigma^{70}}}[E]) + (K_{E\sigma} - K_{\sigma^{70}\overline{\sigma^{70}}})^2[\sigma^{70}]^2)^{1/2}.
\end{aligned}$$

For large values of the threshold ρ the competition takes place if

$$[\sigma^{Alt}] \geq \frac{([E] - \rho)(K_{\sigma^{70}\overline{\sigma^{70}}}[\sigma^{70}] + \rho([\overline{\sigma^{70}}] - [\sigma^{70}]))}{\rho([\overline{\sigma^{70}}] - [\sigma^{70}])}.$$

The holoenzyme concentrations and the onset of competitions above - valid for $K_{\sigma^{70}\overline{\sigma^{70}}}$ that is different from $K_{E\sigma}$ - are the analytical approximations of the simulation of Figure 3.2(a) in Chapter 3. If $K_{\sigma^{70}\overline{\sigma^{70}}} = K_{E\sigma}$, the holoenzyme formations result approximately

$$\begin{aligned} [E\sigma^{70}] &= \begin{cases} \frac{[\sigma^{70}]([E] - [\sigma^{Alt}])}{[E] - [\sigma^{Alt}] + [\overline{\sigma^{70}}]} & [\sigma^{Alt}] < [E] \\ 0 & [\sigma^{Alt}] \geq [E] \end{cases} \\ [E\sigma^{Alt}] &= \begin{cases} [\sigma^{Alt}] & [\sigma^{Alt}] < [E] \\ [E] & [\sigma^{Alt}] \geq [E] \end{cases} \end{aligned}$$

and sigma factor competition arises when

$$[\sigma^{Alt}] \geq \frac{\rho[E]([\overline{\sigma^{70}}] + [E])}{[\overline{\sigma^{70}}] + \rho[E]}.$$

Case II

If $K_{\sigma^{70}\overline{\sigma^{70}}}$ and $K_{E\sigma}$ are both small and $[\overline{\sigma^{70}}] < [\sigma^{70}]$, for a number of alternative sigma factors larger than the number of housekeeping sigma factors, the concentrations of the holoenzymes and the onset of competition are the same of case I. For fewer alternative sigma factors, by respectively neglecting $[E_{free}]$ and $[\overline{\sigma^{70}}]_{free}$ in Equations 2.9 and 3.6, we obtain:

$$\begin{aligned} [E\sigma^{70}] &= \begin{cases} \frac{[\sigma^{70}]([E] - [\sigma^{Alt}])}{[E] + [\overline{\sigma^{70}}] - [\sigma^{Alt}] } & [\sigma^{Alt}] \leq [E] - [\sigma^{70}] + [\overline{\sigma^{70}}] \\ \frac{[E]([\overline{\sigma^{70}}] - [\sigma^{70}])}{[\overline{\sigma^{70}}] - [\sigma^{70}] - [\sigma^{Alt}] } & [\sigma^{Alt}] > [E] - [\sigma^{70}] + [\overline{\sigma^{70}}] \end{cases} \\ [E\sigma^{Alt}] &= \begin{cases} [\sigma^{Alt}] & [\sigma^{Alt}] \leq [E] - [\sigma^{70}] + [\overline{\sigma^{70}}] \\ \frac{[E][\sigma^{Alt}]}{[\overline{\sigma^{70}}] + [\sigma^{Alt}] - [\sigma^{70}] } & [\sigma^{Alt}] > [E] - [\sigma^{70}] + [\overline{\sigma^{70}}] \end{cases}. \end{aligned}$$

If $[E] \leq [\sigma^{70}] - [\overline{\sigma^{70}}]$, there is sigma factor competition when

$$[\sigma^{Alt}] \geq \frac{\rho}{(\rho - 1)} ([\overline{\sigma^{70}}] - [\sigma^{70}])$$

and if $[E] > [\sigma^{70}] - [\overline{\sigma^{70}}]$, when

$$[\sigma^{Alt}] \geq \begin{cases} \frac{\rho[E]([\overline{\sigma^{70}}] + [E])}{[\overline{\sigma^{70}}] + \rho[E]} & \rho \leq \frac{[\overline{\sigma^{70}}] ([E] - [\sigma^{70}] + [\overline{\sigma^{70}}])}{[E][\sigma^{70}]} \\ \frac{([\overline{\sigma^{70}}] - [\sigma^{70}])([E] + (\rho - 1)[\sigma^{70}] + [\overline{\sigma^{70}}])}{(\rho - 1)[\sigma^{70}]} & \rho > \frac{[\overline{\sigma^{70}}] ([E] - [\sigma^{70}] + [\overline{\sigma^{70}}])}{[E][\sigma^{70}]} \end{cases}.$$

Case III

If $K_{\sigma^{70}\overline{\sigma^{70}}} \ll K_{E\sigma}$ and both dissociation constants small, we can neglect the pool of free anti-sigma in Equation 3.6. In this case, the holoenzyme concentrations fulfill

$$[E\sigma^{70}] = \begin{cases} [\sigma^{70}] - m & [\sigma^{Alt}] \leq m + [E] - [\sigma^{70}] \\ \frac{[E](m - [\sigma^{70}])}{m - [\sigma^{70}] - [\sigma^{Alt}]} & [\sigma^{Alt}] > m + [E] - [\sigma^{70}] \end{cases}$$

$$[E\sigma^{Alt}] = \begin{cases} [\sigma^{Alt}] & [\sigma^{Alt}] \leq m + [E] - [\sigma^{70}] \\ \frac{[E][\sigma^{Alt}]}{[\sigma^{70}] + [\sigma^{Alt}] - m} & [\sigma^{Alt}] > m + [E] - [\sigma^{70}] \end{cases}$$

where $m = \min([\sigma^{70}], [\overline{\sigma^{70}}])$. The definition of sigma factor competition (Equation 2.14 in Chapter 2) depends on the concentration of the housekeeping holoenzymes. Since this concentration as a function of the alternative sigma factor for $[\sigma^{Alt}] \leq m + [E] - [\sigma^{70}]$ results a constant, the approximation above is not useful to find the onset of competition. To that end, we find the analytical expression for the line that connects the approximate solution with zero alternative sigma factors to the solution with $[\sigma^{Alt}] > m + [E] - [\sigma^{70}]$. We obtain

$$[E\sigma^{70}] = \frac{[\sigma^{Alt}]}{m - [\sigma^{70}] + [E]} ([\sigma^{70}] - m - c) + c$$

where

$$c = \frac{1}{2(K_{E\sigma} - K_{\sigma^{70}\overline{\sigma^{70}}})} \left(- (K_{\sigma^{70}\overline{\sigma^{70}}}([\overline{\sigma^{70}}]_t) - [\sigma^{70}]) + K_{\sigma^{70}\overline{\sigma^{70}}}([E] + [\sigma^{70}]) + (4K_{\sigma^{70}\overline{\sigma^{70}}}K_{E\sigma}([\overline{\sigma^{70}}] - [\sigma^{70}] + [E])[\sigma^{70}] + ([\overline{\sigma^{70}}]K_{E\sigma} + K_{\sigma^{70}\overline{\sigma^{70}}}[E]) - (K_{\sigma^{70}\overline{\sigma^{70}}} + K_{E\sigma})[\sigma^{70}])^2)^{1/2} \right).$$

By using this concentration, the competition sets in when

$$[\sigma^{Alt}] \geq \begin{cases} \frac{\rho([\sigma^{70}] - m)}{1 - \rho} & [E] \leq [\sigma^{70}] - m \wedge \rho \leq \frac{[\sigma^{70}] - m}{c} \\ m - [\sigma^{70}] + \frac{[E]}{1 - \rho} & [E] > [\sigma^{70}] - m \wedge \rho \leq \frac{[\sigma^{70}] - m}{c} \\ \frac{c\rho(m + [E] - [\sigma^{70}])}{c + m - [\sigma^{70}]} & \rho > \frac{[\sigma^{70}] - m}{c} \end{cases}.$$

Onset of competition and response factor

Figure C.1(a) shows the onset of competition for the number of alternative sigma factors as a function of the number of anti- σ^{70} , for different dissociation constants $K_{\sigma^{70}\overline{\sigma^{70}}}$. The grey lines are drawn by numerical simulations and the red lines by analytical approximation from the cases above. When the dissociation constant between anti- σ^{70} - σ^{70} is smaller than $K_{E\sigma}$ (here, 1 nM), the onset presents a maximum, as for

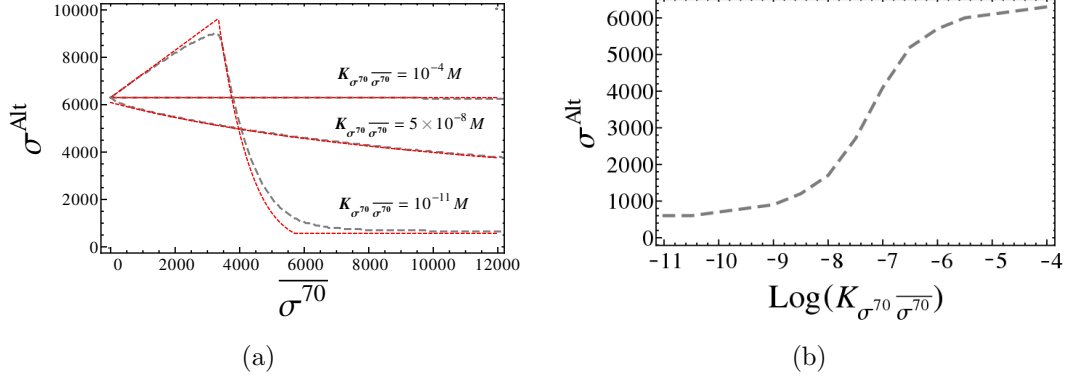


Figure C.1: Onset of competition for the alternative sigma factors as a function of either anti-housekeeping sigma factors (in (a)) with different values of $K_{\sigma^{70}\overline{\sigma^{70}}}$ or $K_{\sigma^{70}\sigma^{70}}$ (in (b)) with 19000 anti- σ^{70} , with 11400 cores, 5700 housekeeping sigma factors and $K_{E\sigma} = 1$ nM.

the case with $K_{\sigma^{70}\overline{\sigma^{70}}} = 10^{-2}$ nM. This onset drops to zero for $[\overline{\sigma^{70}}] = [\sigma^{70}]$. Figure C.1(b) displays the onset of sigma factor competition as a function of $K_{\sigma^{70}\overline{\sigma^{70}}}$.

Numerically, we find that R_E in the presence of two competing sigma species and a fixed number of anti- σ^{70} , the response factor presents hypersensitivity when $K_{E\sigma^{70}} < K_{E\sigma^{Alt}}$ and $\overline{\sigma^{70}} \leq \sigma^{70}$. The maximal sensitivity is found for $E \simeq \sigma^{70} - \overline{\sigma^{70}}$.

C.2 6S RNA

C.2.1 6S RNA in the presence of the only σ^{70}

If $K_{E\sigma^{70}S} \gg K_{E\sigma^{70}}$, we can neglect in turn $[E_{free}]$ and $[\sigma_{free}^{70}]$ in Equations 3.9–3.13, to obtain

$$[E\sigma^{70}] = \frac{1}{2} \left(-K_{E\sigma^{70}S} - [S] + m + \sqrt{(K_{E\sigma^{70}S} + [S] - m)^2 + 4mK_{E\sigma^{70}S}} \right) \quad (C.2)$$

where $m = \min([E], [\sigma^{70}])$ and $[S]$ represents the concentration of 6S RNA. Following the same procedure of Appendix D, we find from Condition 4.3 of Chapter 4 that the response factor $R_{\sigma^{70}}$ produces a hypersensitive response if

$$K_{E\sigma^{70}S} < \frac{(\sqrt{[S](4K_{pE\sigma^{70}} + [S])} - [S])}{2} \quad (C.3)$$

and

$$[\sigma^{70}] < \frac{\sqrt{K_{E\sigma^{70}S}K_{pE\sigma^{70}}[S]^3(K_{E\sigma^{70}S} + [S])^3} - K_{E\sigma^{70}S}[S](K_{E\sigma^{70}S} + [S])^2}{K_{E\sigma^{70}S}[S]^2}. \quad (C.4)$$

From Equation 4.4 of Chapter 4, we find that when $[S] < [E]$, the maximal response is in

$$\begin{aligned}
 [\sigma^{70}] &\simeq \frac{1}{2(K_{pE\sigma^{70}} - 2K_{E\sigma^{70}S})} \cdot \\
 &\cdot K_{E\sigma^{70}S}(K_{E\sigma^{70}S} - K_{pE\sigma^{70}} + 2[S]) + (K_{pE\sigma^{70}} - K_{E\sigma^{70}S}) \cdot \\
 &\cdot \sqrt{K_{E\sigma^{70}S}^2 + 4K_{E\sigma^{70}S}[S] + 4[S]([S] - K_{pE\sigma^{70}})}.
 \end{aligned}$$

For small holoenzyme dissociation constant this condition is simplified to $[\sigma^{70}] \simeq [S]$. When $[S] \leq [E]$, the maximum is instead for $[\sigma^{70}] \simeq [E]$. Thus, in general, $[\sigma^{70}] \simeq \min([E], [S])$ yields the maximal response. Finally, we numerically find that $R_{\sigma^{70}}$ has a hypersensitive response if $K_{E\sigma^{70}S} \ll K_{E\sigma^{70}}$.

A similar analysis shows that the response factor R_E presents hypersensitivity if Equations C.3 and C.4 (with $[\sigma^{70}]$ and $[E]$ switched) are satisfied. In this instance, the maximal response is for $[E] \simeq \min([\sigma^{70}], [S])$. Since Equations C.3 and C.4 are always satisfied for the values of the parameters in Table A.1 (Appendix A), we conclude that 6S RNA in the presence of a single sigma factor induces always hypersensitivity both in R_E and $R_{\sigma^{70}}$.

C.2.2 6S RNA during sigma factor competition

From Table A.1 in Appendix A, the dissociation constant $K_{E\sigma^{70}S}$ between 6S RNA and the housekeeping holoenzyme results larger than the core-sigma dissociation constant (here, $K_{E\sigma^{70}} = K_{E\sigma^{Alt}} \equiv K_{E\sigma}$) and the number of 6S RNA is smaller than the number of housekeeping sigma factors. For these reasons, we look for approximate analytical solution of the system of Equations 2.10–2.13 and 3.9–3.13 (from Chapters 2 and 3, with Equations adapted to include the dependence on 6S RNA) only in the cases that $K_{E\sigma^{70}S} > K_{E\sigma}$ and

- I - the number of cores that is larger than the number of both 6S RNA and σ^{70} ;
- II - the number of cores that is between the number of 6S RNA and σ^{70} ;
- III - the number of cores that is smaller than the number of both 6S RNA and σ^{70} .

Case I

If $[\sigma^{Alt}] \leq [E] - [\sigma^{70}]$ and the number of cores exceeds both numbers of 6S RNA and σ^{70} , we can respectively neglect $[\sigma_{free}^{70}]$ and $[\sigma_{free}^{Alt}]$ in Equations 2.10 and 2.11. The

holoenzyme concentrations fulfill

$$\begin{aligned} [E\sigma^{70}] &= \frac{1}{2} \left([\sigma^{70}] - [S] - K_{E\sigma^{70}S} + r \right) \\ [E\sigma^{Alt}] &= [\sigma^{Alt}] \end{aligned}$$

where $r = \sqrt{([\sigma^{70}] - [S] - K_{E\sigma^{70}S})^2 + 4K_{E\sigma^{70}S}[\sigma^{70}]}$. If $[\sigma^{Alt}] > [E] - [\sigma^{70}]$, we neglect $[E_{free}]$ and to simplify the calculations, we suppose $[E\sigma^{70}S] \equiv c$ to be constant. With these assumptions, the holoenzyme concentrations result

$$\begin{aligned} [E\sigma^{70}] &= \frac{1}{[S] - [\sigma^{70}] - [\sigma^{Alt}]} \left(([E] - c)([S] - [\sigma^{70}]) + K_{E\sigma^{70}S}([\sigma^{70}] + [\sigma^{Alt}]) + \right. \\ &\quad - \left(([S] - [\sigma^{70}])([E] - c) + K_{E\sigma^{70}S}([\sigma^{70}] + [\sigma^{Alt}]) \right)^2 + \\ &\quad \left. + 4([E] - c)K_{E\sigma^{70}S}[\sigma^{70}]([\sigma^{70}] + [\sigma^{Alt}] - [S]) \right)^{1/2} \\ [E\sigma^{Alt}] &= \frac{1}{[S] - [\sigma^{70}] - [\sigma^{Alt}]} \left(([E] - c)([S] - [\sigma^{70}] - 2[\sigma^{Alt}] - K_{E\sigma^{70}S}([\sigma^{70}] + [\sigma^{Alt}])) + \right. \\ &\quad + \left(([S] - [\sigma^{70}])([E] - c) + K_{E\sigma^{70}S}([\sigma^{70}] + [\sigma^{Alt}]) \right)^2 + \\ &\quad \left. + 4([E] - c)K_{E\sigma^{70}S}[\sigma^{70}]([\sigma^{70}] + [\sigma^{Alt}] - [S]) \right)^{1/2}. \end{aligned}$$

with $c = \frac{1}{2} (K_{E\sigma^{70}S} + [\sigma^{70}] + [\sigma^{Alt}] - r)$. There is sigma factor competition when

$$\begin{aligned} [\sigma^{Alt}] &\geq \frac{1}{2K_{E\sigma^{70}S}(\rho - 1)(\rho K_{E\sigma^{70}S} + (1 - \rho)(\rho[\sigma^{70}] - [S]))}. \quad (C.5) \\ &\cdot \left(\rho(\rho - 1)([\sigma^{70}] - [E])([S] - [\sigma^{70}])^2 + \rho K_{E\sigma^{70}S} \left(r([\sigma^{70}] - [E]) + (1 - \rho)[S] \right) + \right. \\ &\quad + K_{E\sigma^{70}S} \left((1 - 2\rho)[\sigma^{70}] - [E] + (\rho - 1)[S] \right) + \left(r\rho(\rho - 1)([S] - [\sigma^{70}])([\sigma^{70}] - [E]) + \right. \\ &\quad + K_{E\sigma^{70}S} (2[S]([E] - [\sigma^{70}]) - \rho[S]([S] + 2[E] - 3[\sigma^{70}]) + \rho^2([S] - [\sigma^{70}])) \cdot \\ &\quad \left. \left. \cdot ([S] - [E] + 3[\sigma^{70}]) + 2\rho^3[\sigma^{70}]([\sigma^{70}] - [S]) \right) \right). \end{aligned}$$

These results are the analytical approximations of the simulation of Figures 3.5(a) in Chapter 2, where we pointed out that the onset of sigma factor competition was not shifted compared to the free binding case. Indeed, if $[S] \ll [\sigma^{70}]$ in Equation C.5, we obtain again Equation B.10 that describes the free binding instance. The analysis of this case I is valid also for $[\sigma^{70}] < [E] < [S]$.

Case II

If $K_{E\sigma} < K_{E\sigma^{70}S}$ and $[S] < [E] < [\sigma^{70}]$, we respectively neglect $[\sigma_{free}^{70}]$ and $[S_{free}]$ in Equations 2.10 and 3.11. Thus, the holoenzyme formations result

$$\begin{aligned} [E\sigma^{70}] &= \frac{[\sigma^{Alt}]([E] - [S])}{[\sigma^{70}] + [\sigma^{Alt}] - [S]} \\ [E\sigma^{Alt}] &= \frac{([S] - [\sigma^{70}])([S] - [E])}{[\sigma^{70}] + [\sigma^{Alt}] - [S]}. \end{aligned}$$

There is sigma factor competition when

$$[\sigma^{Alt}] \geq \frac{\rho([\sigma^{70}] - [S])}{1 - \rho}.$$

Case III

If $K_{E\sigma} < K_{E\sigma^{70}S}$ and the number of cores is less than both of the number of 6S RNA and housekeeping sigma factors, we neglect $[E_{free}]$ and $[E\sigma^{70}]$ in Equation 2.9, $[E\sigma^{70}S]$ and $[E\sigma^{70}]$ in Equation 2.9 and $[E\sigma^{Alt}]$ in Equation 2.11 to obtain

$$\begin{aligned} [E\sigma^{70}] &= \frac{1}{2[\sigma^{Alt}]} \left([\sigma^{70}]([E] - [S]) - K_{E\sigma^{70}S}[\sigma^{Alt}] + \right. \\ &\quad \left. + \sqrt{([\sigma^{70}]([E] - [S]) - K_{E\sigma^{70}S}[\sigma^{Alt}])^2 + 4K_{E\sigma^{70}S}[E][\sigma^{70}][\sigma^{Alt}]} \right) \\ [E\sigma^{Alt}] &= \frac{1}{2[\sigma^{70}]} \left([\sigma^{70}]([E] - [S]) - K_{E\sigma^{70}S}[\sigma^{Alt}] + \right. \\ &\quad \left. + \sqrt{([\sigma^{70}]([E] - [S]) - K_{E\sigma^{70}S}[\sigma^{Alt}])^2 + 4K_{E\sigma^{70}S}[E][\sigma^{70}][\sigma^{Alt}]} \right). \end{aligned}$$

There is sigma factor competition if

$$[\sigma^{Alt}] \geq \frac{\rho([\sigma^{70}] - [S])(([S] - [E])[\sigma^{70}] + K_{E\sigma^{70}S}[E](1 - \rho))}{(1 - \rho)K_{E\sigma^{70}S}(\rho[E] - [S])}.$$

Response factor and onset of competition

From case II and Condition 4.3, we find that in the presence of 6S RNA the response factor R_E presents hypersensitivity when

$$[E] < \frac{[S][\sigma^{Alt}] + \sqrt{K_{pE\sigma^{Alt}}[S][\sigma^{Alt}]^2 + K_{pE\sigma^{Alt}}[S][\sigma^{Alt}][\sigma^{70}] - K_{pE\sigma^{Alt}}[S]^2[\sigma^{Alt}]}}{[\sigma^{Alt}]}.$$

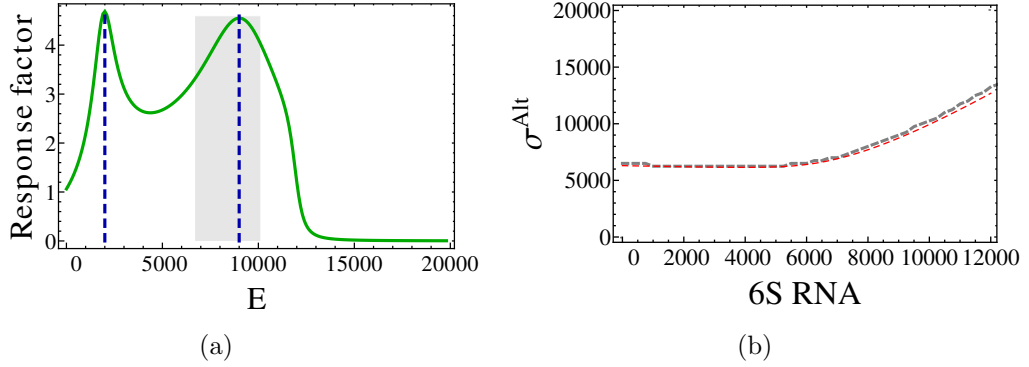


Figure C.2: (a) Response factor R_E with 9000 housekeeping sigma factors, 3000 σ^{Alt} and 2000 6S RNA. The maxima are for $E \simeq 6S \text{ RNA}$ and $E \simeq \sigma^{70}$ is shown by the blue dashed line. Here $K_{E\sigma^{70}} = 1 \text{ nM}$, $K_{E\sigma^{Alt}} = 20 \text{ nM}$ and $K_{E\sigma^{70}S} = 50 \text{ nM}$. (b) Onset of competition for the number of alternative sigma factors as a function of the 6S RNA. As red line the analytical approximation from case I. Values of the parameter as in Figure 3.5(a) with 5700 σ^{70} .

This condition is valid if $[S] < [\sigma^{70}]$. The maximal response results for $[E] = [S]$. Numerically, we find also that when $[S] > [\sigma^{70}]$, R_E has always a maximum around $E = \sigma^{70}$.

By applying the same analysis to the solutions of case III, we find a different (more general but complex) condition for the hypersensitivity of R_E , valid when $K_{E\sigma^{70}} < K_{E\sigma^{70}S}$:

$$\begin{aligned}
 [E] &< \frac{[S][\sigma^{70}] + K_{E\sigma^{70}S}[\sigma^{Alt}]}{K_{E\sigma^{70}S}[S][\sigma^{Alt}][\sigma^{70}]^2} \quad (\text{C.6}) \\
 &\cdot \left([\sigma^{70}] \sqrt{K_{pE\sigma^{Alt}} K_{E\sigma^{70}S} [S][\sigma^{Alt}] ([\sigma^{Alt}][\sigma^{70}] + [\sigma^{Alt}] K_{E\sigma^{70}S}) +} \right. \\
 &\quad \left. - K_{E\sigma^{70}S} [S][\sigma^{Alt}][\sigma^{70}] - K_{E\sigma^{70}S}^2 [\sigma^{Alt}]^2 \right).
 \end{aligned}$$

On top of that, when $K_{E\sigma^{70}} < K_{E\sigma^{Alt}}$ and the number of 6S RNA is less than the number of housekeeping sigma factors, R_E displays two maxima in the hypersensitive region ($E \simeq \sigma^{70}$ and $E \simeq 6S \text{ RNA}$), as shown in Figure C.2(a). If the number of 6S RNA is equal to the number of σ^{70} , R_E has one sharp peak, whose value corresponds to the product of the values of the two single maxima.

We noticed in the main text that in the presence of 6S RNA the onset of sigma factor competition does not shift in a visible manner with respect to the onset in the absence of 6S RNA provided that the number of 6S RNA is less than the number of σ^{70} , a condition supposed to be fulfilled in the cell. On the contrary, when the number of 6S RNA exceeds both the number of housekeeping sigma factors and

core RNAPs, because of the weak binding affinity between 6S RNA and the cognate holoenzyme, this onset shifts (shown in Figure C.2(b) in which the red line is the analytical approximation given by the case I with 5700 σ^{70}).

C.3 Non-specific binding

C.3.1 Response factor with one sigma factor species

By using physiological values of the parameters (*i.e.* great abundance of non-specific binding sites and $K_{E\sigma} < K_{E\sigma NS}$, from Table A.1 in Appendix A) from numerical simulations, we find that neither R_E nor $R_{\sigma^{Alt}}$ have a maximum.

C.3.2 Non-specific binding during sigma factor competition

Holoenzyme concentrations and sigma factor competition. An analytical solution of the system of Equation 3.21–3.28 in Chapter 3 is possible only when $K_{E\sigma^{70}} = K_{E\sigma^{Alt}} \equiv K_{E\sigma}$ and $K_{E\sigma^{70}NS} = K_{E\sigma^{Alt}NS} \equiv K_{NS}$. In this case the holoenzyme concentrations fulfill

$$[E\sigma^{70}] = \frac{K_{NS}[\sigma^{70}]}{2K_{ENS}([NS] + K_{NS})^2([\sigma^{70}] + [\sigma^{Alt}])} \left(K_{ENS}[NS]([E] + [\sigma^{70}] + [\sigma^{Alt}]) + K_{NS}([NS]K_{E\sigma} + K_{ENS}(K_{E\sigma} + [E] + [\sigma^{70}] + [\sigma^{Alt}])) - (4K_{E\sigma}K_{ENS}K_{NS} \cdot ([NS] + K_{NS})([NS] + K_{ENS})[E] + (K_{NS}K_{ENS}(K_{E\sigma} - [E] + [\sigma^{70}] + [\sigma^{Alt}])) + [NS](K_{E\sigma}K_{NS} + K_{ENS}(-[E] + [\sigma^{70}] + [\sigma^{Alt}]))^2)^{1/2} \right)$$

$$[E\sigma^{Alt}] = \frac{[E\sigma^{70}][\sigma^{Alt}]}{[\sigma^{70}]}.$$

By imposing also $K_{ENS} = K_{NS}$, the previous expressions become

$$[E\sigma^{70}] = \frac{K_{NS}[\sigma^{70}]}{2([NS] + K_{NS})([\sigma^{70}] + [\sigma^{Alt}])} \cdot \left(K_{E\sigma} + [E] + [\sigma^{70}] + [\sigma^{Alt}] - \sqrt{4K_{E\sigma}[E] + (K_{E\sigma} - [E] + [\sigma^{70}] + [\sigma^{Alt}])^2} \right) \quad (C.7)$$

$$[E\sigma^{Alt}] = \frac{[E\sigma^{70}][\sigma^{Alt}]}{[\sigma^{70}]} \quad (C.8)$$

and if $K_{E\sigma}$ is very small they are further simplified to

$$\begin{aligned} [E\sigma^{70}] &= \begin{cases} \frac{K_{NS}[\sigma^{70}]}{[NS]+K_{NS}} & [\sigma^{Alt}] \leq [E] - [\sigma^{70}] \\ \frac{K_{NS}[E][\sigma^{70}]}{([NS]+K_{NS})([\sigma^{70}]+[\sigma^{Alt}])} & [\sigma^{Alt}] > [E] - [\sigma^{70}] \end{cases} \\ [E\sigma^{Alt}] &= \begin{cases} \frac{K_{NS}[\sigma^{Alt}]}{[NS]+K_{NS}} & [\sigma^{Alt}] \leq [E] - [\sigma^{70}] \\ \frac{K_{NS}[E][\sigma^{Alt}]}{([NS]+K_{NS})([\sigma^{70}]+[\sigma^{Alt}])} & [\sigma^{Alt}] > [E] - [\sigma^{70}] \end{cases}. \end{aligned}$$

If we divide Equations C.7 and C.8 by Equation 2.5, we obtain the same scaling factor obtained in the presence of one sigma factor species only (Section 3.3): $K_{NS} ([NS] + K_{NS})$. The onset of the sigma factor competition is for

$$[\sigma^{Alt}] = \frac{[E] - (1 - \rho)[\sigma^{70}]}{1 - \rho}$$

that is the same expression of Equation B.10 for the free binding case (case VIII, where $K_{E\sigma^{70}} = K_{E\sigma^{Alt}}$). Thus, the competition's onset is not shifted with respect to the case in the absence of DNA binding, as we have shown in panel (i) of Figure 3.7.

Hypersensitivity. Numerically, we find that the condition $R_E > 1$ is satisfied if $K_{E\sigma^{70}} < K_{E\sigma^{Alt}}$, with a maximal response for $E \simeq \sigma^{70}$.

C.4 Transcript elongation

C.4.1 Holoenzyme formation with one sigma factor species

Holoenzyme concentration. An approximate analytical expression for the concentration of holoenzyme in the presence of the transcript elongation can be provided just for small $K_{E\sigma}$ and small $K_{pE\sigma}$. We neglect in turn the terms $[\sigma_{free}]$ and $[E_{free}]$ in the equations of Section 3.4. With this approximation, the holoenzyme concentration results

$$[E\sigma] = \begin{cases} 0 & [\sigma] \leq a \\ [\sigma] - a & a < [\sigma] \leq [E] - \frac{\alpha_{pE\sigma}[p]}{v_{tsx}}(L_{operon} - L_{ret} \sigma) \\ [E] - \frac{[p]}{v_{tsx}}(v_{tsx} + \alpha_{pE\sigma}L_{operon}) & [\sigma] > [E] - \frac{\alpha_{pE\sigma}[p]}{v_{tsx}}(L_{operon} - L_{ret} \sigma) \end{cases}$$

where $a = [p]/(v_{tsx})(v_{tsx} + \alpha_{pE\sigma}L_{ret} \sigma)$.

Response factor. For some values of the parameters, the number of holoenzymes is a convex function of the sigma factor amount. We recall from Chapter 2, that this feature is just a necessary but not sufficient condition to have a maximum of the response coefficient R_σ . The necessary condition is given by the convexity of the transcription rate, that in this case never is satisfied. As a matter of fact, through a numerical inspection, we find that for a physiological range of the parameters, both R_E and R_σ do not have any maximum.

C.4.2 Transcript elongation during sigma factor competition

If we suppose that all the parameters with index “70” and “*Alt*” have the same values and that the holoenzyme-promoter dissociation constant and the core-sigma dissociation constant are very strong, from the equations of Section 3.4, the holoenzyme concentrations fulfill

$$[E\sigma^{70}] = \frac{(k_{fpE\sigma}([E] + 3[\sigma^{70}] - [\sigma^{Alt}]) - 4[p]v_{tsx} - 2\alpha_{pE\sigma}(L_{operon} + L_{ret\sigma})[p]) - c}{4v_{tsx}k_{fpE\sigma}}$$

$$[E\sigma^{Alt}] = \frac{(k_{fpE\sigma}([E] - [\sigma^{70}] + 3[\sigma^{Alt}]) - 4[p]v_{tsx} - 2\alpha_{pE\sigma}(L_{operon} + L_{ret\sigma})[p]) - c}{4v_{tsx}k_{fpE\sigma}}$$

where

$$c = \sqrt{k_{fpE\sigma}(8\alpha_{pE\sigma}v_{tsx}^2[p] + k_{fpE\sigma}(2\alpha_{pE\sigma}(L_{operon} - L_{ret\sigma})[p] + ([\sigma^{70}] + [\sigma^{Alt}] - [E])v_{tsx}^2))}.$$

In this case, there is competition for any small number of alternative sigma factors.

Hypersensitivity. From numerical inspection, $R_{\sigma^{Alt}}$ has never a maximum in the presence of transcription. By changing one parameter at a time and by using symmetric values for the quantities related to housekeeping and alternative sigma factors, we find that R_E is hypersensitive if one of the following condition is satisfied: $K_{E\sigma^{70}} < K_{E\sigma^{Alt}}$, $[\sigma^{70}] > [\sigma^{Alt}]$, $[p^{70}] < [p^{Alt}]$, $\alpha_{pE\sigma^{70}} < \alpha_{pE\sigma^{Alt}}$, $v_{tsx\sigma^{70}} < v_{tsx\sigma^{Alt}}$, $L_{ret\sigma^{Alt}} < L_{ret\sigma^{70}}$, $k_{bE\sigma^{70}} > k_{bE\sigma^{Alt}}$.

C.5 Onset of sigma factor competition

Table C.1 summarizes the effects of the modulators on the onset of sigma factor competition. The table describes how the onset of sigma factor competition is shifted with compared to the free binding case. The second and third column characterize this shift when increasing number of alternative sigma factors and core RNAP are considered, respectively. We use (physiological) values of the parameters as in Table A.1 in Appendix A. The arrows indicate the shift of the onset of competition, the cross specifies that the onset is unaltered and the two lines in the third column remind that there is competition for a range of cores.

For example, if the dissociation constant of the housekeeping holoenzyme results smaller than the corresponding alternative dissociation constant ($K \equiv K_{E\sigma^{70}}/K_{E\sigma^{Alt}} < 1$), the onset of competition sets in for a larger number of alternative sigma factor (second column) and the range of cores for which there is competition is reduced (third column).

Effect of	Shift of the onset of competition as a function of the σ^{Alt} (1)	Shift of the onset of competition as a function of the E (1)
free, $K < 1$ $\overline{\sigma^{70}}$ (2)	\rightarrow	$\mapsto \leftarrow$
6S RNA (3)	\leftarrow $S < E, S < \sigma^{70}: \times$ other cases: \rightarrow	$S < \sigma^{70}, \sigma^{Alt} < \sigma^{70}: \mapsto \times$ $S < \sigma^{70}, \sigma^{Alt} > \sigma^{70}: \times \times$ $S > \sigma^{70}, \sigma^{Alt} < S: \mapsto \leftarrow$ $S > \sigma^{70}, \sigma^{Alt} > S: \times \leftarrow$
NS binding (4)	$K_{ENS} = K_{E\sigma^{70}NS} = K_{E\sigma^{Alt}NS}: \times$ $K_{ENS} < K_{E\sigma^{70}NS} = K_{E\sigma^{Alt}NS}: \leftarrow$ (5) $K_{E\sigma^{70}NS} < K_{ENS} = K_{E\sigma^{Alt}NS}: \rightarrow$ (5) $K_{E\sigma^{Alt}NS} < K_{ENS} = K_{E\sigma^{70}NS}: \leftarrow$ (5)	$K_{ENS} = K_{E\sigma^{70}NS} = K_{E\sigma^{Alt}NS}: \times \times$ $K_{ENS} < K_{E\sigma^{70}NS} = K_{E\sigma^{Alt}NS}: \mapsto \leftarrow$ (5) $K_{E\sigma^{70}NS} < K_{ENS} = K_{E\sigma^{Alt}NS}: \mapsto \leftarrow$ (5) $K_{E\sigma^{Alt}NS} < K_{ENS} = K_{E\sigma^{70}NS}: \leftarrow \mapsto$ (5)
Transcript elongation	\leftarrow	$\leftarrow \mapsto$

Table C.1: (1) The reference case is the scenario in the absence of regulatory factors and with $K_{E\sigma^{70}} = K_{E\sigma^{Alt}}$ (called the free binding case, represented in Figures 2.4(b) and 4.2). \rightarrow : the onset of the competition is shifted to the right compared to the free binding case, \leftarrow : is shifted to the left, \times : in unmodified, $\|$: the range of values of cores for which there is competition is among the two lines or symbols. (2) We assume $K_{\overline{\sigma^{70}}, \sigma^{70}} < K_{E\sigma^{70}}$. If $K_{\overline{\sigma^{70}}, \sigma^{70}} \gtrsim K_{E\sigma^{70}}$, the onset of competition as a function of alternative sigma factors shifts to the opposite direction. (3) We assume $K_{E\sigma^{70}S} < K_{E\sigma^{70}}$. If $K_{E\sigma^{70}S} \gtrsim K_{E\sigma^{70}}$, the onset of competition as a function of alternative sigma factors shifts to the opposite direction. (4) We assume $K_{ENS}, K_{E\sigma^{70}NS}$ and $K_{E\sigma^{Alt}NS}$ larger than both $K_{E\sigma^{70}}$ and $K_{E\sigma^{Alt}}$. (5) The effect on the onset of competition in the presence of non-specific binding is the opposite if the inequalities between the non specific binding affinities are reversed.

Appendix D

Response factor

In this Appendix, we give the proof of some results regarding the response factor introduced in Chapter 4.

We first recall that $[E\sigma]$ is an increasing function of both alternative sigma factor and core concentration, hence $\partial[E\sigma]/\partial[X] \geq 0$, where X is either σ^{Alt} or E . This can be seen, for example, directly from Equation 2.5 in Chapter 2. If $[E\sigma]$ is an increasing (decreasing) function of $[X]$, the transcription rate is also an increasing (decreasing) function of $[X]$, thus $\partial\tilde{J}/\partial[X] \geq 0$. From Definition 2.7 in Chapter 2, it is also true that $\tilde{J}/[X] \leq 1$.

D.1 R_X

Proof 1. We first inspect the behavior of the response factor for small and large number of X molecules. If ϵ is a small positive number, when $X \rightarrow \epsilon$, the transcription rate fulfills $[\epsilon]/K_{p^{Alt}E\sigma^{Alt}}$. Thus, when $[\epsilon] \rightarrow 0$ the response factor becomes

$$R_{X=0} = \lim_{[\epsilon] \rightarrow 0} \frac{[\epsilon]}{\tilde{J}([\epsilon])} \frac{\partial\tilde{J}([\epsilon])}{\partial[\epsilon]} = 1.$$

For a large number of σ^{Alt} or RNAPs, the transcription rate reaches a constant maximum given by either the core or the alternative sigma availability (since the maximum of $[E\sigma^{Alt}]$ is given by the $\min([E], [\sigma^{Alt}])$) and has a null derivative with respect to X . Thus, according to Definition 4.1 in Chapter 4, when X is large R_X goes to zero.

Proof 2. A necessary and sufficient condition for hypersensitivity is the convexity of the transcription rate around the maximum X_M . As a matter of fact, around X_M , the derivative of the response factor must be null:

$$\left. \frac{\partial R_X}{\partial[X]} \right|_{X \simeq X_M} = \left((1 - R_X) \frac{\partial\tilde{J}([X])}{\partial[X]} + [X] \frac{\partial^2\tilde{J}([X])}{\partial[X]^2} \right) \Big|_{X \simeq X_M} \simeq 0$$

that can be rewritten as

$$R_{X \approx X_M} = 1 + [X] \left(\frac{\partial \tilde{J}([X])}{\partial [X]} \right)^{-1} \frac{\partial^2 \tilde{J}([X])}{\partial [X]^2}.$$

To fulfill the hypersensitivity condition $R_X > 1$, the second derivative of the transcription rate in this latter expression must be positive, which implies the convexity around the maximum X_M of the transcription rate. From the same proof, we also derive the converse implication.

Proof 3. From the convexity of the transcription rate, it follows also that $[E\sigma^{Alt}]$ is a convex function around the maximum. Imposing $\partial^2 \tilde{J}([X]) / \partial [X]^2 > 0$, from the definition of transcription rate follows that

$$\frac{\partial^2 [E\sigma^{Alt}]}{\partial [X]^2} > \frac{2}{K_{p^{Alt}E\sigma^{Alt}} + [E\sigma^{Alt}]} \left(\frac{\partial [E\sigma^{Alt}]}{\partial [X]} \right)^2 \quad (\text{D.1})$$

that is always positive. Thus, it must also be true that

$$\frac{\partial^2 [E\sigma^{Alt}]}{\partial [X]^2} > 0. \quad (\text{D.2})$$

This argument can not be inverted: Inequality D.1 gives a necessary and sufficient condition for the presence of a maximum alternative to Equation 4.3, and Inequality D.2 represents a necessary but not sufficient condition for the presence of that maximum.

D.2 R_E during sigma factor competition

Proof 4. Here, we study inequality $R_E > 1$ for the free binding case of Chapter 2. To analytically solve Equations 2.9–2.13, we keep one variable (*e.g.* $[E_{free}]$) in the solutions. Under this assumption, the alternative sigma factor holoenzyme concentration fulfills

$$[E\sigma^{Alt}] = \frac{1}{2(K-1)} \left(([E] - [E_{free}])(K-1) + [\sigma^{70}] + K[\sigma^{Alt}] + \sqrt{((K-1)([E] - [E_{free}]) - [\sigma^{70}] - K[\sigma^{Alt}])^2 + 4(K-1)([E] - [E_{free}])([\sigma^{70}])} \right), \quad (\text{D.3})$$

where $K = K_{E\sigma^{70}} / K_{E\sigma^{Alt}}$. From this expression, by imposing Condition D.2, we find that $K < 1$ is a necessary (but not sufficient) condition to have a maximum of the response factor.

Proof 5. A more stringent (sufficient and necessary) condition to have a maximum of R_E could be worked out directly from the request $R_E > 1$, equivalent to Condition 4.3

$$\frac{\partial[E\sigma^{Alt}]}{\partial[X]} > \frac{(K_{p^{Alt}E\sigma^{Alt}} + [E\sigma^{Alt}])[E\sigma^{Alt}]}{K_{p^{Alt}E\sigma^{Alt}}[X]} \quad (\text{D.4})$$

and also to Inequality D.1. Unfortunately, these expressions are not solvable analytically. Thus, to obtain the situations for which there is a maximum of R_E , we follow a different approach. We first compare the exact condition given by Inequality D.1 to the relaxed condition given by Inequality D.2. The cases where the two differ, are the instances from which we can work out the most stringent conditions to yield a maximum.

Since the holoenzyme concentration is always sublinear to $\min([E], [\sigma^{Alt}])$, also $\partial[E\sigma^{Alt}]/\partial[E]$ in Inequality D.1 is always much smaller than one. Hence the right term of Inequality D.1 can be very different from zero only when $2/(K_{p^{Alt}E\sigma^{Alt}} + [E\sigma^{Alt}])$ is large. This happens for very small values of $K_{p^{Alt}E\sigma^{Alt}}$ and $[E\sigma^{Alt}]$. But, when the holoenzyme-promoter dissociation constant is very small, we already know that R_E has not a maximum. Thus Inequality D.1 and Inequality D.2 differ only when $[E\sigma^{Alt}] \simeq 0$. We must focus our investigation on this instance.

$[E\sigma^{Alt}]$ approaches zero either when the cores are few, when the alternative sigma are few, or when the binding affinity between them is very weak. We first analyze the case with strong binding, then the case with weak binding. In that way we will find two conditions for the presence of a maximum of R_E , valid under different approximations.

When $K_E\sigma^{Alt}$ is strong, the concentration of alternative holoenzymes is given by Equation B.6 (case VI in Appendix B):

$$[E\sigma^{Alt}] = \min\left([E], [\sigma^{Alt}], \frac{1}{2(K-1)}\left([E](K-1) + [\sigma^{70}] + K[\sigma^{Alt}] + \sqrt{4[E](K-1)[\sigma^{70}] + ([E](1-K) + [\sigma^{70}] + K[\sigma^{Alt}])^2}\right)\right). \quad (\text{D.5})$$

For few σ^{Alt} in this expression, we also know from the study in Appendix B that R_E has not a maximum larger than one. Instead, since for few cores R_E may be larger than one, we expand the holoenzyme concentration of Equation D.5 and its derivative around $E = 0$ and insert their expressions in Condition D.4:

$$\left.\frac{\partial[E\sigma^{Alt}]}{\partial[E]}\right|_{E=0} = \frac{K[\sigma^{Alt}](([\sigma^{70}] + K[\sigma^{Alt}])^2 - 2(K-1)[E][\sigma^{70}])}{([\sigma^{70}] + K[\sigma^{Alt}])^3} + O(E^2)$$

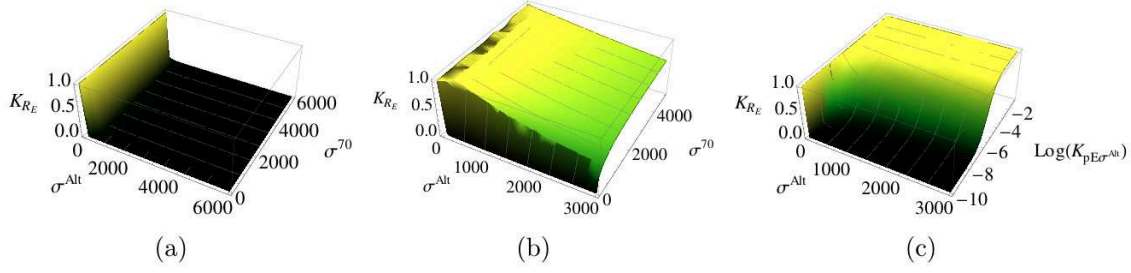


Figure D.1: Values of K_{R_E} (Equation D.6) as a function of the number of σ^{Alt} and either housekeeping sigma factors (in (a) and (b)) or $\text{Log}(K_{p^{Alt} E \sigma^{Alt}})$ (in (c)). When K_{R_E} is very different from one, hypersensitivity is given by Condition D.6 and not by the approximate condition $K < 1$. In (a) $K_{p^{Alt} E \sigma^{Alt}}$ is small (10 nM), and in (b) is larger (10^{-5} M), similarly to the dissociation constant in the cell that we use in all the simulations. In (c) there are 9000 housekeeping sigma factors.

$$\begin{aligned} & \left. \frac{(K_{p^{Alt} E \sigma^{Alt}} + [E \sigma^{Alt}])[E \sigma^{Alt}]}{K_{p^{Alt} E \sigma^{Alt}} [E]} \right|_{E=0} = \frac{1}{K_{p^{Alt} E \sigma^{Alt}} ([\sigma^{70}] + K[\sigma^{Alt}])^3} \cdot \\ & \cdot \left(K[\sigma^{Alt}](K[E][\sigma^{Alt}]([\sigma^{70}] + K[\sigma^{Alt}]) + \right. \\ & \left. + K_{p^{Alt} E \sigma^{Alt}}([E] - ([\sigma^{70}] - K[\sigma^{Alt}]) + ([\sigma^{70}] + K[\sigma^{Alt}])^2)) \right) + O(E^2). \end{aligned}$$

By using these results into Condition D.4, we find that R_E has a maximum if K satisfies

$$\begin{aligned} K & < \frac{\sqrt{4K_{p^{Alt} E \sigma^{Alt}}[\sigma^{70}][\sigma^{Alt}]^2 + [\sigma^{70}]^2(K_{p^{Alt} E \sigma^{Alt}} + [\sigma^{Alt}])^2} - [\sigma^{70}](K_{p^{Alt} E \sigma^{Alt}} + [\sigma^{Alt}])}{2[\sigma^{Alt}]^2} \\ & \equiv K_{R_E}. \end{aligned} \tag{D.6}$$

We find also that the response factor presents hypersensitivity as long as $E < \sigma^{70} + \sigma^{Alt}$.

From Inequality D.2 we have obtained the relaxed condition to have a maximum of R_E , *i.e.* $K < 1$. A more precise condition is now given by $K < K_{R_E}$. Thus, when K_{R_E} is very different from one, hypersensitivity is given by Condition D.6 and not by the approximate condition $K < 1$. In Figures D.1(a), D.1(b), and D.1(c) we compare for which values of the parameters the two approximation differ. If the dissociation constant $K_{p^{Alt} E \sigma^{Alt}}$ is small, the right term K_{R_E} of Inequality 4.7 is only different from zero when $K_{p^{Alt} E \sigma^{Alt}} \ll [\sigma^{Alt}]$. On the contrary, when $K_{p^{Alt} E \sigma^{Alt}} \gg [\sigma^{Alt}]$, the relaxed condition $K < 1$ is always well approximated. According to the values of Table A.1 in Appendix A, the scenario with a large $K_{p^{Alt} E \sigma^{Alt}}$ is almost always satisfied in the cases that we study here, which is why we can always use the $K < 1$ to prove the

presence of a maximum of the response factor R_E during sigma factor competition of the free binding case.

By following the same procedure as above we now study the case with a weak sigma-core dissociation constant. From the union of case III and IV in Appendix B), we find a set of conditions to obtain a maximum of R_E that are also valid when E_{free} is far from being zero:

$$K_{E\sigma^{70}} < \frac{\sqrt{([\sigma^{Alt}][\sigma^{70}])^2 + 4K_{E\sigma^{Alt}}K_{p^{Alt}E\sigma^{Alt}}[\sigma^{Alt}][\sigma^{70}] - [\sigma^{Alt}][\sigma^{70}]}{2[\sigma^{Alt}]} \wedge K < 1.$$

This instance also solve the case with very few σ^{Alt} .

D.3 $R_{\sigma^{Alt}}$ during sigma factor competition

Proof 6. By imposing Inequality 4.7 with the alternative holoenzyme concentration given by Equation D.3, $R_{\sigma^{Alt}}$ in the presence of more than one sigma factor species never shows any maximum.

Appendix E

Values of the parameters used in the simulations of the shift from exponential growth to stationary phase

In this Appendix, we discuss the values of the parameters that we have used in Chapter 4 to simulate the exponential growth case and the stress/stringent response of an *Escherichia coli* cell. Table E.1 collects the values of the parameters adopted in the simulations of Figures 4.5 and 4.7(b). For the growth phase, we analyzed experiments on *E. coli* B/r minicells growing at 2.5 dbl/h in rich medium at 37°C from Bremer *et al.* [47]. The parameters not measured in the same experimental set-up are determined from assays performed in similar conditions. Next, we have assumed that the cell quickly shifts to an early stage of a stringent response, so that many parameters are unchanged (“=” in the table). During this stage, we have considered a shut down of the stable RNA transcription, indicated by the “X” in the table. We speculate that the quantities related to the alternative-driven operons are the same of the mRNA genes. Table E.2 reports the outcomes of the simulations.

Quantity	Exponential	Stringent	Reference
Temperature	37°C	=	[47]
Growth rate	2.5 dbl/h	X	[47]
Average cell volume	1.2 fL	=	[47]
E maturation time	3.4 min	=	[42]
Genome equivalent	3.8	=	[47]
E per cell	11400	=	See below [47]
σ^{70} per cell	31920	=	See below [12]
σ^S per cell	0	7000	See below [12]
$K_{E\sigma^{70}}$	2.8 nM	=	See below [102]
$K_{E\sigma^S}$	11 nM	=	See below [102]
anti- σ^{70} Rsd per cell	14500	27200	See below [12]
$K_{\sigma^{70}Rsd}$	32 nM	=	[10]
6SRNA per cell	1600	8000	See below [38]
$K_{\sigma^{70}6SRNA}$	160 nM	=	See below [76]
$L_{operon} rrrn$	6500 nt	=	[42]
L_{operon} mRNA	2000 nt	=	[47]
$L_{operon} \sigma^S$ RNA	2000 nt	=	[47]
$K_{PrrnE\sigma^{70}}$	1.4 μ M	=	See below [47]
$K_{PmRNAE\sigma^{70}}$	0.7 μ M	=	See below [47]
$K_{P\sigma^SE\sigma^S}$	0.7 μ M	=	See below [47]
Total $Prrn$ per cell	36	X	[47]
Total $PmRNA$ per cell	64	=	See below [101]
Total $P\sigma^S$ RNA/genome eq.	134	=	See below [103]
NS Binding sites/genome eq.	4.6×10^6	=	[139]
α_{Prrn}	110 min^{-1}	=	[47]
α_{PmRNA}	26 min^{-1}	=	[137]
$\alpha_{P\sigma^S RNA}$	26 min^{-1}	=	[137]
$v_{tsx} rrrn$	85 nt/sec	=	[47]
v_{tsx} mRNA	45 nt/sec	=	[47]
$v_{tsx} \sigma^S$ RNA	45 nt/sec	=	[47]
$L_{ret} \sigma$	300 nt	=	[3]
$k_{bE\sigma}$	10^{-3} sec^{-1}	=	[74]
K_{ENS}	3100 μ M	=	[42]
$K_{E\sigma NS}$	6200 μ M	=	See below [42]

Table E.1: Data used in the simulations of Figure 4.5 and 4.7(b) for a bacterial cell during exponential growth and stringent phase. “=” indicates an unchanged value and “X” a suppression.

E.1 RNAPs and sigma factors

We assume to have 11400 core RNAP as suggested by measurements of Bremer and collaborators [47]. Piper *et al.* [12] reported that numbers of core RNAPs and housekeeping sigma factors per cell are unaltered in the shift from exponential growth (*E. coli* MG1655 cell at 37°C in LB medium, 1.6 dbl/h) to the stationary phase. Moreover, they measured the amount of RNAP, σ^{70} , σ^S and Rsd during these two conditions (see Tables A.4 and A.9). We obtained the number of sigma factors and Rsd by assuming the same proportions between housekeeping sigma factors and cores and between Rsd and cores that they found in their measures in the two phases, but with 11400 cores.

We exclude the strong influence of the transcriptional regulator Crl (a σ^S activator) that is supposed to be absent at 37°C [118]. This point is still under debate: for example, reference [117] reports minor presence, but not an absence, of Crl at 37°C.

Colland *et al.* [102] determined the dissociation constants of σ^{70} and σ^S to the core RNAP at 37°C. We refit their curves in Figures A.1(a) and A.3 and obtain $K_{E\sigma^{70}} = 2.8$ nM (Table A.7) and $K_{E\sigma^S} = 11$ nM (Table A.8).

E.2 6S RNA

During exponential growth, Wassarman and Storz [38] estimated approximately 1000 6S RNA copies per cell using *E. coli* K12 at 37°C growing in LB medium. We fine tuned this value to reach 1600 units to better reproduce the synthesis rate of Figure 4.5(b) measured by Bremer and collaborator [47]. Figure 2D of reference [104] shows that, after entering the stationary phase, the 6S RNA cell content increases 5-fold compared to the growth condition, for that reason we adopt a value of 8000 6S RNA in the stationary phase. The dissociation constant between 6S RNA and the housekeeping holoenzyme comes from the fit in Figure A.4.

E.3 Specific binding to promoters and elongation

Unlike us, Bremer and collaborators [47] divide the *Prrn* promoters in two classes, P1 and P2, according to their kinetics parameters. The transcription rate of the sum of their two classes must be the same as the transcription rate of our single *Prrn* class:

$$\tilde{J} = \frac{[E\sigma^{70}]}{[E\sigma^{70}] + K_{P1rrn}} + \frac{[E\sigma^{70}]}{[E\sigma^{70}] + K_{P2rrn}} \simeq \frac{[E\sigma^{70}]}{[E\sigma^{70}] + \frac{K_{P1rrn}K_{P2rrn}}{K_{P1rrn} + K_{P2rrn}}}.$$

The approximation of the last line is valid if $[E\sigma_{free}^{70}] \ll K_{P1rrn}, K_{P2rrn}$. As a matter of fact, according to the measurements of reference [47], $K_{P1rrn} = 2.1$ μ M, $K_{P2rrn} = 4.4$

μM and $[E\sigma_{free}^{70}] \simeq 1.2 \mu\text{M}$. On top of that anti-sigma factors, 6S RNA and non-specific binding, as already discussed, are supposed to sequester a large pool of σ^{70} and cores. These considerations validate the approximation, then we fix $K_{P_{rrn}E\sigma^{70}} \equiv (K_{P_{1rrn}}K_{P_{2rrn}})/(K_{P_{1rrn}} + K_{P_{2rrn}}) = 1.4 \text{ nM}$. We also suppose $K_{P_{\sigma^S}E\sigma^S}$ to be equal to $K_{P_{mRNA}E\sigma^{70}}$, that according to reference [47] is 0.7 nM .

On an average *E. coli* cell there are 221 σ^S -dependent promoters [139], but the number of known orthogonal σ^S -driven promoters is 134 [103].

In the cell, not all promoters are active at the same time, *e.g.* activation may depend on transcription factors. Supposing all of them are in an active state would largely overestimate $[P_{mRNA}]$. For that reason, we evaluate the total mean number of active PmRNA promoters in an average cell from the number of different mRNA copies in a *E. coli* B/r cell growing with 1.5 dbl/h at 37°C measured in reference [101] and then we make a proportion to find the value at $\mu_2 = 2.5 \text{ dbl/h}$. To find the number of active PmRNA promoters, we basically first reduce the dimension of our complete system by fixing one free variable, here $[pE\sigma]$, through the known number of different mRNA copies in the cell at 1.5 dbl/h. Then we find the corresponding expression of $[pE\sigma]$ at 2.5 dbl/h as a function of the values at 1.5 dbl/h, and finally we run the simulation of the system to find the number of active PmRNA at 2.5 dbl/h. To that end, we first suppose the total number of mRNA to be at equilibrium with a degradation rate of $\omega=0.5/\text{min}$ [140]. At steady state, imposing that every PmRNA promoter has one copy per genome equivalent, the average number of different active promoters $p_{d \mu_1}$ in a cell is

$$p_{d \mu_1} = \frac{\omega \text{ mRNA}_{\mu_1}}{\alpha g_{\mu_1} f_{\mu_1}}, \quad (\text{E.1})$$

where α is the maximal transcription rate, g the genome equivalent, mRNA the total mRNA amount, μ_1 the growth rate, and $f_{\mu_1} = E\sigma_{free}/(K_{pE\sigma_{free}} + E\sigma_{free})$. f_{μ_1} indicates that the number of active promoters depends on the number of holoenzymes that are transcribing it and μ_1 shows that the quantities are growth-dependent. The maximal transcription rate α of the mRNA is approximately independent of the growth rate [47] and the degradation rate ω is approximately constant for a large set of growth rates (Figure 1c of [140]). The number of total active promoters is simply given by the number of different active promoters per genome times the genome equivalent: $p_{\mu_1} = p_{d \mu_1} g_{\mu_1}$. At $\mu_2 = 2.5 \text{ dbl/h}$ we have the same expressions, in which the index μ_1 is replaced by μ_2 . The two cases can be related supposing that the number of total active promoters is proportional to the genome equivalent:

$$\frac{p_{\mu_1}}{g_{\mu_1}} = \frac{p_{\mu_2}}{g_{\mu_2}}. \quad (\text{E.2})$$

Equation E.2 expresses the simple idea that the more genome content we have in the

cell, the more promoters are also present on it. From Equations E.1 and E.2, we find

$$p_{\mu_2} = g_{\mu_2} \frac{\omega mRNA_{\mu_1}}{\alpha g_{\mu_1} f_{\mu_1}} \quad (\text{E.3})$$

In our model, p is connected to the amount of holoenzymes that are specifically bound: $[pE\sigma] = [p] \frac{[E\sigma]}{K_{pE\sigma} + [E\sigma]}$. Using Equation E.3, this expression can be rewritten as

$$[pE\sigma]_{\mu_2} = g_{\mu_2} \frac{\omega [mRNA_{\mu_1}] f_{\mu_2}}{\alpha g_{\mu_1} f_{\mu_1}}. \quad (\text{E.4})$$

Now, we can also suppose that $f_{\mu_1} \simeq f_{\mu_2}$, which means that the more promoters are present, the more specific bound holoenzymes there are. This assumption, with Equation E.4, leads to

$$\frac{[pE\sigma]_{\mu_1}}{[pE\sigma]_{\mu_2}} = \frac{[p_{\mu_1}] f_{\mu_1}}{[p_{\mu_1}] f_{\mu_2}} \simeq \frac{g_{\mu_1}}{g_{\mu_2}}.$$

In this way, $[pE\sigma]_{\mu_2}$ is a constant.

This procedure serves basically to replace in our simulation the unknown $[pE\sigma]_{\mu_2}$ with the total number of known mRNA in the cell from reference [101] and reduce the dimensionality of the system to find PmRNA. As a matter of fact, by using $\omega = 0.5/\text{min}$, $mRNA_{\mu_1} = 1380$ [101], $g_{\mu_{1.5}} = 2.3$, and $g_{\mu_{2.5}} = 3.8$ [13] and all the parameters of the second column of Table E.1, we obtain from our simulation $E\sigma_{free}$, that reinserted in Equation E.3 gives $p_{\mu_{2.5}} = 64$ active PmRNA promoters in the cell.

E.4 Non-specific binding

An estimate for the non-specific binding affinity of the core to the DNA can be found in reference [42]: $K_{ENS} = 3100 \mu\text{M}$. We suppose the strength of the binding affinity to be roughly proportional to the number of contact sites between the DNA and the non-specific bound particle (supposition supported also by the finding of reference [72]). Cores and holoenzymes respectively contact the DNA in 30 and 12 nucleotides [105], thus $K_{E\sigma NS} \simeq 2K_{ENS} = 6200 \mu\text{M}$.

E.5 Results of the simulations

Table E.2 shows the results of the simulations of Figures 4.7(b) and 4.8.

Quantity	1	2	3	4	5
E_{free}	11	72	65	70	99
$E\sigma_{free}^{70}$	1085	163	230	184	114
σ_{free}^{70}	10416	454	279	378	846
σ_{rrn}^{70*}	121	32	0	19	24
σ_{mRNA}^{70*}	126	45	58	49	34
E_{rrn}^*	2611	702	0	421	510
$PrrnE\sigma^{70}$	19	5	0	3	4
E_{mRNA}^*	841	301	385	329	226
$PmRNAE\sigma^{70}$	44	16	20	17	12
$E\sigma_{free}^S$	0	156	139	152	218
σ_{free}^S	0	5770	5889	5798	5333
$\sigma_{\sigma^S RNA}^{S*}$	0	346	318	340	444
$E_{\sigma^S RNA}^*$	0	2309	2119	2265	2957
$P\sigma^S RNAE\sigma^S$	0	120	120	118	154
$E\sigma^{70}NS$	4231	637	896	719	444
$E\sigma^S NS$	0	608	544	593	852
ENS	82	560	504	547	776
$E\sigma^{70}6SRNA$	1412	4685	5322	4916	3968
$6SRNA_{free}$	188	3315	2678	3084	4032
$\sigma^{70}Anti - \sigma^{70}$	14468	25882	25116	25663	26476
$Anti - \sigma_{free}^{70}$	32	1318	2084	1567	724
E_{imm}	1066	1066	1066	1066	1066
$Anti - \sigma_{free}^{70}$	32	1318	2084	1567	724
rRNA synt. rate (nt/min/cell/ 10^6)	13.3	3.6	0	2.1	2.6
mRNA synt. rate (nt/min/cell/ 10^6)	2.3	0.8	1	0.9	0.6
σ^S RNA synt. rate (nt/min/cell/ 10^6)	0	6.2	5.7	6.1	8

Table E.2: Quantities in absolute numbers per cell from the simulation of Figures 4.5 and 4.7(b). Explanation of the columns as in Figure 4.7(b). The initial values are given in Table E.1.

List of symbols

$[X]$	Concentration of the molecular species X , measured in molar.
$\alpha_{p^i E \sigma^j}$	Maximal initiation rate of transcription from the promoter p^i , recognized by the holoenzyme $E \sigma^j$.
ΔX	Change in the amount of the quantity X .
λ	Fraction of sigma factors tethered to the elongating RNAP during the entire transcription process.
$\langle X \rangle$	Mean value of X .
$\min(X, Y)$	Smallest value between X and Y .
μ	Growth rate of a culture of cells, measured in doublings per hour.
$\overline{\overline{\sigma^i}}$	Anti-anti sigma factor of the anti- σ^i .
$\overline{\sigma^i}$	Anti-sigma factor of the σ^i .
ρ	Threshold of the onset of sigma factor competition.
σ^i	Sigma factor of the i type.
σ^{70}	Housekeeping sigma factor.
σ^{Alt}	Alternative sigma factor.
τ	Maturation time of the core polymerase, measured in minutes.
A	Activator.
At	Anti-terminator.
dbl	Doublings.
E	Core RNAP enzyme.

$E\sigma^i$	Holoenzyme with the sigma factor σ^i .
eff	Effective.
$elong$	Elongation.
I	Inhibitor or repressor.
Imm	Immature RNAPs.
J	Transcription rate per volume (Equation 2.6), measured in initiations per second per volume.
K	$K \equiv K_{E\sigma^{70}}/K_{E\sigma^{Att}}$.
k_i	A forward rate in a reaction.
k_{-i}	A backward rate in a reaction.
k_{bXY}	Dissociation, or backward, rate of the reaction $X + Y \rightleftharpoons XY$.
K_{eff}	Effective dissociation constant (Equation 3.39).
k_{fXY}	Association, or forward, rate of the reaction $X + Y \rightleftharpoons XY$.
$K_{p^i E\sigma^j}$	Michaelis-Menten constant of the promoter p^i that binds to a holoenzyme $E\sigma^j$.
$k_{ret X}$	Rate of retention: inverse of the time during which X is engaged in the elongation process.
K_{XY}	Dissociation constant obtained from the equilibrium of the reaction $X + Y \rightleftharpoons XY$, measured in molar. We refer to it also as the “binding affinity”.
L_{gene}	Length of a gene, measured in nucleotides.
L_{operon}	Length of an operon, measured in nucleotides.
$L_{ret X}$	Length for which X is retained by the transcription process, measured in nucleotides.
M	Molar, where $M = mol/L$.
min	Minutes.

<i>mol</i>	Moles, where $mol = \text{number of molecules}/N_A$.
N_A	Avogadro constant.
<i>NS</i>	Non-specific.
<i>nt</i>	Nucleotides.
p^i	Promoter p that usually is recognized only by the holoenzyme with the sigma factor σ^i .
$P\sigma^{Alt}RNA$	Alternative sigma-driven promoters.
$PmRNA$	σ^{70} -dependent mRNA (non-ribosomal) promoters.
<i>prox</i>	Proximal.
$Prrn$	Ribosomal RNA promoters.
R	Cumulative response factor to a simultaneous increase of two quantities X and Y , defined by $R = \sqrt{R_X^2 + R_Y^2}$.
R_X	Logarithmic response factor (Equation 4.1).
<i>reb</i>	Rebinding.
<i>ret</i>	Retention.
RNA'	Piece of RNA transcribed thanks to an anti-termination event.
RNA_{p^i}	RNA product of the transcription of the gene whose promoter is p^i .
<i>rrn</i>	Ribosomal operon. We include in this definition all the set of genes that transcribe stable RNA.
S	6S RNA.
<i>sec</i>	Seconds.
T	Rho factor.
t	Time.
<i>th</i>	Tethered.
<i>tsx</i>	Transcription.
V	Volume.

v_{tsx}	Elongation speed, measured in nucleotides/second.
w	Either cooperativity factor in the main text or degradation rate in the Appendixes.
X	Total number of X molecules .
X^*	Unit X engaged in active elongation.
X_M	Value of X for which the response factor R_X has a maximum.
X_{free}	Free or not bound X .
$X_{p^i}^*$	X that transcribes a gene that has p^i as promoter.
X_Y	X bound to Y , where Y is DNA, NS or p^i .
\tilde{J}	Normalized transcription rate per gene (Equation 2.7).

Acknowledgements

Acknowledgements

I would like to thank my supervisor Dr. Stefan Klumpp for the continuous support, encouragement and suggestions during these years, my group members Pintu, Mamata, Michael, Rahul, David, Veronica, Bahareh and Livnat for the nice time spent together, Prof. Lipowsky for giving me the opportunity to work in such a nice environment, all the group leaders and colleagues for their help. Finally, I thank my family and especially Chiara for having been always present.

Ringraziamenti

Per prima cosa, i ringraziamenti in lingua madre. Vorrei cominciare ringraziando mio nonno Carlo, che non ha potuto ricevere - almeno fisicamente - la notizia del mio dottorato. A lui un grandissimo grazie e un abbraccio per tutto il tempo che ha speso con me e tutto quello che mi ha insegnato. Non credo ci siano parole adatte per descrivere quanto mi manca e quanto mi sia stato sempre vicino. Questa tesi, scritta durante il periodo in cui si trovava in ospedale, è dedicata soprattutto a lui. Durante il periodo del mio dottorato è venuto a mancare anche il mio gatto Pallino, che per lungo tempo mi ha fatto compagnia nello studio. Un abbraccio ad entrambi. Grazie.

Voglio ringraziare anche e soprattutto la mia famiglia, mio papà Fausto, mia mamma Patrizia, mia sorella Federica, la mia gatta Cina e le mie nonne Maria e Mina. Mi avete sempre supportato come potevate, chi economicamente, chi stando alzata la notte a correggere il mio inglese e chi accendendo ceri o chi miagolando, ma tutti con il vostro amore, grazie mille anche a voi. E grazie delle torte! Ringrazio anche la mia Chiara, che con i suoi sorrisi e il suo spronarmi continuo mi ha permesso di arrivare alla fine di questo percorso. Grazie per essere venuta così spesso a trovarmi, grazie delle belle giornate passate assieme, delle vacanze e dei giochi, grazie di tutto adesso e sempre (e come sai, ti idem!). Di viaggi stupendi e fotografie scattate in questi anni ce ne sono molti, dall'America all'India, da Israele all'Egitto. E siamo solo all'inizio! Grazie anche alla famiglia di Chiara che ha condiviso con noi questi

quattro anni, grigliando ottime zucchine e dispensando consigli. Un saluto speciale anche a Mangroviotta, Cippo, Rana rossa, Drillo e Lilla. Un altro immenso grazie ai miei amici italiani Giulio e Marta, Leo e Elisa, Cinzia, grazie delle vacanze passate assieme, dei viaggi e delle belle chiacchierate.

Un grazie speciale anche alle città di Potsdam e Berlino, con il castello di Sanssouci e il lago, i musei, la Lego, i ristoranti e le mille attività che hanno riempito le Domeniche mie e di Chiara. Un grazie sentito anche a Specchio e ai suoi aiutanti!

I would also like to thank my flatmates, among all of them Jens, Dirtje, Luis, Pawlok, Sassi, Djamil and Anna-Lena and all their friends. I really enjoyed staying here in Potsdam in our super-cozy painted kitchen. Nevertheless, my German is very bad. This is not for sure fault of Kay, my super great German teacher. Thank you for making every lesson enjoyable. I want to make a special thank to the people that supported me in my institute, we had great time and I hope to see and meet you also later, especially Pintu, Michael, Bahareh, Livnat, David, Mamata, Rahul, Chenyu, Bat-El, Kenny and Maria Antonietta and all my office mates (Janina, Bartosz, Vasil, Tom) and colleagues (Sophia, Celine, Vroni, Flo, Carlus, Thomas, Marius, Russi, Carola, Marko, Corina, Andrea, Ana and many more). Pintu, beside all the exchanges of ideas during these years, thank you to have given me the possibility to come to your marriage in India, it was probably the best trip that Chiara and me had. A hug also to Arpita and her family that made us feel like at home. Thank to the people that during these years visited me (especially to Sara and Peter). Thanks for all the support from my supervisor Stefan, the best I could have ever hoped to have. You made the environment very relaxed and have transmitted the joy to learn, go on and make efforts to improve. Thank you for everything inside and outside the MPI. I should also mention all the other people that supported my work, they are so many...I will just mention Prof. Reinhard Lipowsky, Susann, Dr. Angelo Valleriani (thank you for all the nice and helpful chats), Prof. Thomas Weikl, Prof. Wilhelm Huisinga and Renè.

This is just a quick and small list of all the people that I would like to thank, please forgive me if I forgot someone. I am sure that everyone already knows how helpful he/she has been during this beautiful period.

Bibliography

- [1] F. Crick et al. Central dogma of molecular biology. *Nature*, 227(5258):561–563, 1970.
- [2] J. E. Krebs, E. S. Goldstein, and S. T. Kilpatrick. *Lewin's genes X*. Jones and Bartlett Publishers, 2011.
- [3] M. Raffaele, E. I. Kanin, J. Vogt, R. R. Burgess, and A. Z. Ansari. Holoenzyme switching and stochastic release of sigma factors from RNA polymerase in vivo. *Mol Cell*, 20(3):357–66, November 2005.
- [4] R. A. Mooney, S. A. Darst, and R. Landick. Sigma and RNA polymerase: an on-again, off-again relationship? *Mol. Cell*, 20(3):335–45, November 2005.
- [5] S. Malik, K. Zalenskaya, and A. Goldfarb. Competition between sigma factors for core RNA polymerase. *Nucleic acids research*, 15(20):8521–8530, 1987.
- [6] S. Kolesky, M. Ouhammouch, E. N. Brody, and E. P. Geiduschek. Sigma competition: the contest between bacteriophage T4 middle and late transcription. *Journal of molecular biology*, 291(2):267–281, 1999.
- [7] A. Ishihama. Functional modulation of Escherichia coli RNA polymerase. *Annual Reviews in Microbiology*, 54(1):499–518, 2000.
- [8] H. Maeda, N. Fujita, and A. Ishihama. Competition among seven Escherichia coli sigma subunits: relative binding affinities to the core RNA polymerase. *Nucleic Acids Res*, 28(18):3497–503, September 2000.
- [9] S. Österberg, T. del Peso-Santos, and V. Shingler. Regulation of alternative sigma factor use. *Annu Rev Microbiol*, 65:37–55, 2011.
- [10] U. K. Sharma and D. Chatterji. Differential mechanisms of binding of anti-sigma factors Escherichia coli Rsd and bacteriophage T4 AsiA to E. coli RNA polymerase lead to diverse physiological consequences. *J Bacteriol*, 190(10):3434–43, May 2008.

-
- [11] I. L. Grigorova, N. J. Phleger, V. K. Mutalik, and C. A. Gross. Insights into transcriptional regulation and sigma competition from an equilibrium model of RNA polymerase binding to DNA. *Proc Natl Acad Sci U S A*, 103(14):5332–7, apr 2006.
- [12] S. E. Piper, J. E. Mitchell, D. J. Lee, and S. J. W. Busby. A global view of Escherichia coli Rsd protein and its interactions. *Mol Biosyst*, 5(12):1943–7, December 2009.
- [13] H. Bremer and P. P. Dennis. *Modulation of chemical composition and other parameters of the cell by growth rate*. Escherichia coli and Salmonella. ASM Press, Washington, D.C., 1996.
- [14] M. Jishage, A. Iwata, S. Ueda, and A. Ishihama. Regulation of RNA polymerase sigma subunit synthesis in Escherichia coli: intracellular levels of four species of sigma subunit under various growth conditions. *J Bacteriol*, 178(18):5447–51, September 1996.
- [15] D. B. Straus, W. A. Walter, and C. A. Gross. The heat shock response of E. coli is regulated by changes in the concentration of sigma 32. *Nature*, 329(6137):348–51, September 1987.
- [16] Y. N. Zhou and C. A. Gross. How a mutation in the gene encoding sigma 70 suppresses the defective heat shock response caused by a mutation in the gene encoding sigma 32. *J Bacteriol*, 174(22):7128–37, November 1992.
- [17] Y. N. Zhou, W. A. Walter, and C. A. Gross. A mutant sigma 32 with a small deletion in conserved region 3 of sigma has reduced affinity for core RNA polymerase. *J Bacteriol*, 174(15):5005–12, August 1992.
- [18] A. Farewell, K. Kvint, and T. Nyström. Negative regulation by RpoS: a case of sigma factor competition. *Mol Microbiol*, 29(4):1039–51, August 1998.
- [19] K. A. Hicks and A. D. Grossman. Altering the level and regulation of the major sigma subunit of RNA polymerase affects gene expression and development in Bacillus subtilis. *Mol Microbiol*, 20(1):201–12, April 1996.
- [20] T. Osawa and T. Yura. Effects of reduced amount of RNA polymerase sigma factor on gene expression and growth of Escherichia coli: studies of the rpoD40 (amber) mutation. *Molecular and General Genetics MGG*, 184(2):166–173, 1981.
- [21] M. Jishage, K. Kvint, V. Shingler, and T. Nyström. Regulation of sigma factor competition by the alarmone ppGpp. *Genes Dev*, 16(10):1260–70, May 2002.

-
- [22] T. K. Kundu, S. Kusano, and A. Ishihama. Promoter selectivity of *Escherichia coli* RNA polymerase sigmaF holoenzyme involved in transcription of flagellar and chemotaxis genes. *J Bacteriol*, 179(13):4264–9, jul 1997.
- [23] A. D. Laurie, L. M. D. Bernardo, C. C. Sze, E. Skarfstad, A. Szalewska-Palasz, T. Nyström, and V. Shingler. The role of the alarmone (p)ppGpp in sigma N competition for core RNA polymerase. *J Biol Chem*, 278(3):1494–503, January 2003.
- [24] A. Szalewska-Palasz, L. U. M. Johansson, L. M. D. Bernardo, E. Skärfstad, E. Stec, K. Brännström, and V. Shingler. Properties of RNA polymerase bypass mutants: implications for the role of ppGpp and its co-factor DksA in controlling transcription dependent on sigma54. *J. Biol. Chem.*, 282(25):18046–56, June 2007.
- [25] L. M. D. Bernardo, L. U. M. Johansson, D. Solera, E. Skärfstad, and V. Shingler. The guanosine tetraphosphate (ppGpp) alarmone, DksA and promoter affinity for RNA polymerase in regulation of sigma-dependent transcription. *Mol. Microbiol.*, 60(3):749–64, May 2006.
- [26] W. H. Mather, J. Hasty, L. S. Tsimring, and R. J. Williams. Translational cross talk in gene networks. *Biophys. J.*, 104(11):2564–72, June 2013.
- [27] E. Levine, Z. Zhang, T. Kuhlman, and T. Hwa. Quantitative characteristics of gene regulation by small RNA. *PLoS biology*, 5(9):e229, 2007.
- [28] N. A. Cookson, W. H. Mather, T. Danino, O. Mondragón-Palomino, R. J. Williams, L. S. Tsimring, and J. Hasty. Queueing up for enzymatic processing: correlated signaling through coupled degradation. *Molecular systems biology*, 7(1), 2011.
- [29] R. C. Brewster, F. M. Weinert, H. G. Garcia, D. Song, M. Rydenfelt, and R. Phillips. The Transcription Factor Titration Effect Dictates Level of Gene Expression. *Cell*, 2014.
- [30] B. Cho, D. Kim, E. M. Knight, K. Zengler, and B. O. Palsson. Genome-scale reconstruction of the sigma factor network in *Escherichia coli*: topology and functional states. *BMC Biol.*, 12:4, 2014.
- [31] U. K. Sharma and D. Chatterji. Transcriptional switching in *Escherichia coli* during stress and starvation by modulation of sigma activity. *FEMS Microbiol Rev*, 34(5):646–57, September 2010.

- [32] K. T. Hughes and K. Mathee. The anti-sigma factors. *Annu Rev Microbiol*, 52:231–86, 1998.
- [33] A. Costanzo, H. Nicoloff, S. E. Barchinger, A. B. Banta, R. L. Gourse, and S. E. Ades. ppGpp and DksA likely regulate the activity of the extracytoplasmic stress factor σE in *Escherichia coli* by both direct and indirect mechanisms. *Molecular microbiology*, 67(3):619–632, 2008.
- [34] M. Jishage and A. Ishihama. Transcriptional organization and in vivo role of the *Escherichia coli* *rsd* gene, encoding the regulator of RNA polymerase sigma D. *J Bacteriol*, 181(12):3768–76, June 1999.
- [35] J. E. Mitchell, T. Oshima, S. E. Piper, C. L. Webster, L. F. Westblade, G. Karimova, D. Ladant, A. Kolb, J. L. Hobman, S. J. W. Busby, et al. The *Escherichia coli* regulator of sigma 70 protein, Rsd, can up-regulate some stress-dependent promoters by sequestering sigma 70. *Journal of bacteriology*, 189(9):3489–3495, 2007.
- [36] K. M. Wassarman. 6S RNA: a small RNA regulator of transcription. *Curr Opin Microbiol*, 10(2):164–8, April 2007.
- [37] A. E. Trotochaud and K. M. Wassarman. A highly conserved 6S RNA structure is required for regulation of transcription. *Nature structural & molecular biology*, 12(4):313–319, 2005.
- [38] K. M. Wassarman and G. Storz. 6S RNA regulates *E. coli* RNA polymerase activity. *Cell*, 101(6):613–23, June 2000.
- [39] J. Ryals, R. Little, and H. Bremer. Control of rRNA and tRNA syntheses in *Escherichia coli* by guanosine tetraphosphate. *J. Bacteriol.*, 151(3):1261–8, September 1982.
- [40] M. Cashel, D. Gentry, V. J. Hernandez, and D. Vinella. *The stringent response*. ASM Press, Washington, second edition, 1996.
- [41] S. T. Rutherford, J. J. Lemke, C. E. Vrentas, T. Gaal, W. Ross, and R. L. Gourse. Effects of DksA, GreA, and GreB on transcription initiation: insights into the mechanisms of factors that bind in the secondary channel of RNA polymerase. *Journal of molecular biology*, 366(4):1243–1257, 2007.
- [42] S. Klumpp and T. Hwa. Growth-rate-dependent partitioning of RNA polymerases in bacteria. *Proc Natl Acad Sci U S A*, 105(51):20245–50, December 2008.

- [43] K. Potrykus and M. Cashel. (p)ppGpp: still magical? *Annu. Rev. Microbiol.*, 62:35–51, 2008.
- [44] L. Krásný and R. L. Gourse. An alternative strategy for bacterial ribosome synthesis: *Bacillus subtilis* rRNA transcription regulation. *EMBO J.*, 23(22):4473–83, November 2004.
- [45] B. J. Paul, M. B. Berkmen, and R. L. Gourse. DksA potentiates direct activation of amino acid promoters by ppGpp. *Proceedings of the National Academy of Sciences*, 102(22):7823–7828, 2005.
- [46] B. Gummesson, L. U. Magnusson, M. Lovmar, K. Kvint, Ö. Persson, M. Ballesteros, A. Farewell, and T. Nyström. Increased RNA polymerase availability directs resources towards growth at the expense of maintenance. *The EMBO journal*, 28(15):2209–2219, 2009.
- [47] H. Bremer, P. Dennis, and M. Ehrenberg. Free RNA polymerase and modeling global transcription in *Escherichia coli*. *Biochimie*, 85(6):597–609, June 2003.
- [48] S. Bakshi, R. Dalrymple, W. Li, H. Choi, and J. Weisshaar. Partitioning of RNA Polymerase Activity in Live *Escherichia coli* from Analysis of Single-Molecule Diffusive Trajectories. *Biophysical journal*, 105(12):2676–2686, 2013.
- [49] T. Nyström. Growth versus maintenance: a trade-off dictated by RNA polymerase availability and sigma factor competition? *Mol Microbiol*, 54(4):855–62, November 2004.
- [50] M. M. Barker, T. Gaal, and R. L. Gourse. Mechanism of regulation of transcription initiation by ppGpp. II. Models for positive control based on properties of RNAP mutants and competition for RNAP. *Journal of molecular biology*, 305(4):689–702, 2001.
- [51] A. Costanzo and S. E. Ades. Growth phase-dependent regulation of the extracytoplasmic stress factor, σ_E , by guanosine 3, 5-bispyrophosphate (ppGpp). *Journal of bacteriology*, 188(13):4627–4634, 2006.
- [52] L. U. Magnusson, A. Farewell, and T. Nyström. ppGpp: a global regulator in *Escherichia coli*. *Trends Microbiol.*, 13(5):236–42, May 2005.
- [53] A. Szalewska-Palasz, G. Wegrzyn, and A. Wegrzyn. Mechanisms of physiological regulation of RNA synthesis in bacteria: new discoveries breaking old schemes. *J. Appl. Genet.*, 48(3):281–94, 2007.

-
- [54] L. Bintu, N. E. Buchler, H. G. Garcia, U. Gerland, T. Hwa, J. Kondev, and R. Phillips. Transcriptional regulation by the numbers: models. *Curr Opin Genet Dev*, 15(2):116–24, April 2005.
- [55] I. Golding, J. Paulsson, S. M. Zawilski, and E. C. Cox. Real-time kinetics of gene activity in individual bacteria. *Cell*, 123(6):1025–1036, 2005.
- [56] T. Kuhlman, Z. Zhang, M. H. Saier, and T. Hwa. Combinatorial transcriptional control of the lactose operon of *Escherichia coli*. *Proceedings of the National Academy of Sciences*, 104(14):6043–6048, 2007.
- [57] S. Kaplan, A. Bren, A. Zaslaver, E. Dekel, and U. Alon. Diverse two-dimensional input functions control bacterial sugar genes. *Molecular cell*, 29(6):786–792, 2008.
- [58] N. J. Guido, X. Wang, D. Adalsteinsson, D. McMillen, J. Hasty, C. R. Cantor, T. C. Elston, and J. J. Collins. A bottom-up approach to gene regulation. *Nature*, 439(7078):856–860, 2006.
- [59] S. Klumpp. A superresolution census of RNA polymerase. *Biophys. J.*, 105:2613–2614, 2013.
- [60] M. Scott, C. W. Gunderson, E. M. Mateescu, Z. Zhang, and T. Hwa. Interdependence of cell growth and gene expression: origins and consequences. *Science*, 330(6007):1099–1102, 2010.
- [61] D. Chu, D. J. Barnes, and T. von der Haar. The role of tRNA and ribosome competition in coupling the expression of different mRNAs in *Saccharomyces cerevisiae*. *Nucleic acids research*, 39(15):6705–6714, 2011.
- [62] A. D. Grossman, W. E. Taylor, Z. F. Burton, R. R. Burgess, and C. A. Gross. Stringent response in *Escherichia coli* induces expression of heat shock proteins. *Journal of molecular biology*, 186(2):357–365, 1985.
- [63] L. Michaelis and M. L. Menten. Die kinetik der invertinwirkung. *Biochem. z.*, 49(333-369):352, 1913.
- [64] P. H. Von Hippel, A. Revzin, C. A. Gross, and A. C. Wang. Non-specific DNA binding of genome regulating proteins as a biological control mechanism: 1. The lac operon: equilibrium aspects. *Proceedings of the National Academy of Sciences*, 71(12):4808–4812, 1974.
- [65] P. P. Dennis, M. Ehrenberg, and H. Bremer. Control of rRNA synthesis in *Escherichia coli*: a systems biology approach. *Microbiol. Mol. Biol. Rev.*, 68(4):639–68, December 2004.

- [66] A. Ganguly and D. Chatterji. A Comparative Kinetic and Thermodynamic Perspective of the sigma-Competition Model in *Escherichia coli*. *Biophys J*, 103(6):1325–33, September 2012.
- [67] J. T. Wade, D. C. Roa, D. C. Grainger, D. Hurd, S. J. W. Busby, K. Struhl, and E. Nudler. Extensive functional overlap between sigma factors in *Escherichia coli*. *Nat. Struct. Mol. Biol.*, 13(9):806–14, September 2006.
- [68] S. Kusano, Q. Ding, N. Fujita, and A. Ishihama. Promoter selectivity of *Escherichia coli* RNA polymerase E sigma 70 and E sigma 38 holoenzymes. Effect of DNA supercoiling. *J Biol Chem*, 271(4):1998–2004, January 1996.
- [69] L. M. D. Bernardo, L. U. M. Johansson, E. Skärfstad, and V. Shingler. sigma54-promoter discrimination and regulation by ppGpp and DksA. *J. Biol. Chem.*, 284(2):828–38, January 2009.
- [70] B. T. Glaser, V. Bergendahl, L. C. Anthony, B. Olson, and R. R. Burgess. Studying the salt dependence of the binding of sigma70 and sigma32 to core RNA polymerase using luminescence resonance energy transfer. *PLoS One*, 4(8):e6490, 2009.
- [71] P. T. Singer and C. W. Wu. Kinetics of promoter search by *Escherichia coli* RNA polymerase. Effects of monovalent and divalent cations and temperature. *J. Biol. Chem.*, 263(9):4208–14, March 1988.
- [72] P. L. deHaseth, T. M. Lohman, R. R. Burgess, and M. T. Record. Nonspecific interactions of *Escherichia coli* RNA polymerase with native and denatured DNA: differences in the binding behavior of core and holoenzyme. *Biochemistry*, 17(9):1612–22, May 1978.
- [73] B. Collinet, H. Yuzawa, T. Chen, C. Herrera, and D. Missiakas. RseB binding to the periplasmic domain of RseA modulates the RseA:sigmaE interaction in the cytoplasm and the availability of sigmaE.RNA polymerase. *J Biol Chem*, 275(43):33898–904, October 2000.
- [74] P. England, L. F. Westblade, G. Karimova, V. Robbe-Saule, F. Norel, and A. Kolb. Binding of the unorthodox transcription activator, Crl, to the components of the transcription machinery. *J Biol Chem*, 283(48):33455–64, November 2008.
- [75] J. D. Helmann. Anti-sigma factors. *Curr Opin Microbiol*, 2(2):135–41, April 1999.

- [76] N. Gildehaus, T. Neusser, R. Wurm, and R. Wagner. Studies on the function of the riboregulator 6S RNA from *E. coli*: RNA polymerase binding, inhibition of in vitro transcription and synthesis of RNA-directed de novo transcripts. *Nucleic Acids Res*, 35(6):1885–96, 2007.
- [77] N. Shimamoto, T. Kamigochi, and H. Utiyama. Release of the sigma subunit of *Escherichia coli* DNA-dependent RNA polymerase depends mainly on time elapsed after the start of initiation, not on length of product RNA. *J Biol Chem*, 261(25):11859–65, September 1986.
- [78] A. N. Kapanidis, E. Margeat, T. A. Laurence, S. Doose, S. O. Ho, J. Mukhopadhyay, E. Kortkhonjia, V. Mekler, R. H. Ebright, and S. Weiss. Retention of transcription initiation factor sigma70 in transcription elongation: single-molecule analysis. *Mol Cell*, 20(3):347–56, November 2005.
- [79] N. B. Reppas, J. T. Wade, G. M. Church, and K. Struhl. The transition between transcriptional initiation and elongation in *E. coli* is highly variable and often rate limiting. *Mol. Cell*, 24(5):747–57, December 2006.
- [80] G. Bar-Nahum and E. Nudler. Isolation and characterization of sigma(70)-retaining transcription elongation complexes from *Escherichia coli*. *Cell*, 106(4):443–51, August 2001.
- [81] R. A. Mooney and R. Landick. Tethering sigma70 to RNA polymerase reveals high in vivo activity of sigma factors and sigma70-dependent pausing at promoter-distal locations. *Genes Dev.*, 17(22):2839–51, November 2003.
- [82] S. E. Halford and J. F. Marko. How do site-specific DNA-binding proteins find their targets? *Nucleic Acids Res.*, 32(10):3040–52, 2004.
- [83] F. Wang, S. Redding, I. J. Finkelstein, J. Gorman, D. R. Reichman, and E. C. Greene. The promoter-search mechanism of *Escherichia coli* RNA polymerase is dominated by three-dimensional diffusion. *Nature structural & molecular biology*, 20(2):174–181, 2013.
- [84] L. J. Friedman, J. P. Mumm, and J. Gelles. RNA polymerase approaches its promoter without long-range sliding along DNA. *Proceedings of the National Academy of Sciences*, 110(24):9740–9745, 2013.
- [85] R. M. Saecker, O. V. Tsodikov, K. L. McQuade, P. E. Schlax, M. W. Capp, and M. T. Record. Kinetic studies and structural models of the association of *E. coli* sigma(70) RNA polymerase with the lambdaP(R) promoter: large scale conformational changes in forming the kinetically significant intermediates. *J. Mol. Biol.*, 319(3):649–71, June 2002.

- [86] L. J. Friedman and J. Gelles. Mechanism of transcription initiation at an activator-dependent promoter defined by single-molecule observation. *Cell*, 148(4):679–689, 2012.
- [87] T. Rajala, A. Häkkinen, S. Healy, O. Yli-Harja, and A. S. Ribeiro. Effects of transcriptional pausing on gene expression dynamics. *PLoS computational biology*, 6(3):e1000704, 2010.
- [88] P. Schickor, W. Metzger, W. Werel, H. Lederer, and H. Heumann. Topography of intermediates in transcription initiation of E.coli. *EMBO J.*, 9(7):2215–20, July 1990.
- [89] R. T. Kovacic. The 0 degree C closed complexes between Escherichia coli RNA polymerase and two promoters, T7-A3 and lacUV5. *J. Biol. Chem.*, 262(28):13654–61, October 1987.
- [90] M. A. Shea and G. K. Ackers. The OR control system of bacteriophage lambda. A physical-chemical model for gene regulation. *J. Mol. Biol.*, 181(2):211–30, January 1985.
- [91] L. Bintu, N. E. Buchler, H. G. Garcia, U. Gerland, T. Hwa, J. Kondev, T. Kuhlman, and R. Phillips. Transcriptional regulation by the numbers: applications. *Curr. Opin. Genet. Dev.*, 15(2):125–35, April 2005.
- [92] S. C. Gill, S. E. Weitzel, and P. H. von Hippel. Escherichia coli sigma70 and NusA proteins: I. Binding interactions with core RNA polymerase in solution and within the transcription complex. *Journal of molecular biology*, 220(2):307–324, 1991.
- [93] X. Zhang, M. Chaney, S. R. Wigneshweraraj, J. Schumacher, P. Bordes, W. Cannon, and M. Buck. Mechanochemical ATPases and transcriptional activation. *Molecular microbiology*, 45(4):895–903, 2002.
- [94] C. Condon, C. Squires, and C. L. Squires. Control of rRNA transcription in Escherichia coli. *Microbiological reviews*, 59(4):623–645, 1995.
- [95] H. D. Murray, D. A. Schneider, and R. L. Gourse. Control of rRNA expression by small molecules is dynamic and nonredundant. *Molecular cell*, 12(1):125–134, 2003.
- [96] Y. N. Zhou and D. J. Jin. The rpoB mutants destabilizing initiation complexes at stringently controlled promoters behave like “stringent” RNA polymerases in Escherichia coli. *Proceedings of the National Academy of Sciences*, 95(6):2908–2913, 1998.

-
- [97] A. Ishihama and R. Fukuda. Autogenous and post-transcriptional regulation of RNA polymerase synthesis. *Mol Cell Biochem*, 31(3):177–96, August 1980.
- [98] R Hengge-Aronis. The general stress response in *Escherichia coli*. In G. Storz and R. Hengge-Aronis, editors, *Bacterial stress response*, pages 161–179. ASM Press, 2000.
- [99] D. D. Vos, F. J. Bruggeman, H. V. Westerhoff, and B. M. Bakker. How molecular competition influences fluxes in gene expression networks. *PLoS ONE*, 6(12):e28494, 2011.
- [100] Q. Zhang, S. Bhattacharya, and M. E. Andersen. Ultrasensitive response motifs: basic amplifiers in molecular signalling networks. *Open Biol*, 3(4):130031, April 2013.
- [101] F. C. Neidhardt and R. Curtiss, editors. *Escherichia coli and Salmonella: Cellular and Molecular Biology*. ASM Press, Washington, second edition, 1996.
- [102] F. Colland, N. Fujita, A. Ishihama, and A. Kolb. The interaction between sigmaS, the stationary phase sigma factor, and the core enzyme of *Escherichia coli* RNA polymerase. *Genes Cells*, 7(3):233–47, March 2002.
- [103] S. Gama-Castro et al. RegulonDB version 7.0: transcriptional regulation of *Escherichia coli* K-12 integrated within genetic sensory response units (Gensor Units). *Nucleic Acids Res*, 39(Database issue):D98–105, January 2011.
- [104] T. Neusser, N. Gildehaus, R. Wurm, and R. Wagner. Studies on the expression of 6S RNA from *E. coli*: involvement of regulators important for stress and growth adaptation. *Biol. Chem.*, 389(3):285–97, March 2008.
- [105] T. Kolmsee, D. Delic, T. Agyenim, C. Calles, and R. Wagner. Differential stringent control of *Escherichia coli* rRNA promoters: effects of ppGpp, DksA and the initiating nucleotides. *Microbiology (Reading, Engl.)*, 157(Pt 10):2871–9, October 2011.
- [106] R. Little, J. Ryals, and H. Bremer. Physiological characterization of *Escherichia coli* rpoB mutants with abnormal control of ribosome synthesis. *J. Bacteriol.*, 155(3):1162–70, September 1983.
- [107] R. K. Karls, D. J. Jin, and T. J. Donohue. Transcription properties of RNA polymerase holoenzymes isolated from the purple nonsulfur bacterium *Rhodobacter sphaeroides*. *Journal of bacteriology*, 175(23):7629–7638, 1993.

- [108] D. Chatterji, Y. Ogawa, T. Shimada, and A. Ishihama. The role of the omega subunit of RNA polymerase in expression of the *relA* gene in *Escherichia coli*. *FEMS Microbiol Lett*, 267(1):51–5, February 2007.
- [109] I. Artsimovitch, V. Patlan, S. Sekine, M. Vassylyeva, T. Hosaka, K. Ochi, S. Yokoyama, and D. Vassylyev. Structural basis for transcription regulation by alarmone ppGpp. *Cell*, 117(3):299–310, April 2004.
- [110] C. W. Lennon, T. Gaal, W. Ross, and R. L. Gourse. *Escherichia coli* DksA binds to Free RNA polymerase with higher affinity than to RNA polymerase in an open complex. *J Bacteriol*, 191(18):5854–8, September 2009.
- [111] Z. D. Dalebroux and M. S. Swanson. ppGpp: magic beyond RNA polymerase. *Nat Rev Microbiol*, 10(3):203–12, March 2012.
- [112] N. E. Buchler and F. R. Cross. Protein sequestration generates a flexible ultra-sensitive response in a genetic network. *Molecular systems biology*, 5(1), 2009.
- [113] A. Hatoum and J. Roberts. Prevalence of RNA polymerase stalling at *Escherichia coli* promoters after open complex formation. *Molecular microbiology*, 68(1):17–28, 2008.
- [114] A. Bougdour, C. Cunning, P. J. Baptiste, T. Elliott, and S. Gottesman. Multiple pathways for regulation of σ S (RpoS) stability in *Escherichia coli* via the action of multiple anti-adaptors. *Molecular microbiology*, 68(2):298–313, 2008.
- [115] L. L. Ilag, L. F. Westblade, C. Deshayes, A. Kolb, S. J. W. Busby, and C. V. Robinson. Mass Spectrometry of *Escherichia coli* RNA Polymerase: Interactions of the Core Enzyme with sigma 70 and Rsd Protein. *Structure*, 12(2):269–275, 2004.
- [116] V. Robbe-Saule, M. D. Lopes, A. Kolb, and F. Norel. Physiological effects of Crl in *Salmonella* are modulated by σ S level and promoter specificity. *Journal of bacteriology*, 189(8):2976–2987, 2007.
- [117] A. Typas, C. Barembruch, A. Possling, and R. Hengge. Stationary phase re-organisation of the *Escherichia coli* transcription machinery by Crl protein, a fine-tuner of σ s activity and levels. *The EMBO journal*, 26(6):1569–1578, 2007.
- [118] A. Bougdour, C. Lelong, and J. Geiselmann. Crl, a low temperature-induced protein in *Escherichia coli* that binds directly to the stationary phase sigma subunit of RNA polymerase. *J. Biol. Chem.*, 279(19):19540–50, May 2004.
- [119] M. J. Morelli, R. J. Allen, and P. Rein ten Wolde. Effects of macromolecular crowding on genetic networks. *Biophysical journal*, 101(12):2882–2891, 2011.

-
- [120] C. Tan, S. Saurabh, M. P. Bruchez, R. Schwartz, and P. LeDuc. Molecular crowding shapes gene expression in synthetic cellular nanosystems. *Nature nanotechnology*, 8(8):602–608, 2013.
- [121] T. E. Kuhlman and E. C. Cox. Gene location and DNA density determine transcription factor distributions in *Escherichia coli*. *Molecular systems biology*, 8(1), 2012.
- [122] J. Paulsson. Models of stochastic gene expression. *Physics of life reviews*, 2(2):157–175, 2005.
- [123] A. Sanchez, S. Choubey, and J. Kondev. Regulation of noise in gene expression. *Annual review of biophysics*, 42:469–491, 2013.
- [124] S. Klumpp and T. Hwa. Bacterial growth: global effects on gene expression, growth feedback and proteome partition. *Curr. Opin. Biotechnol.*, 28C:96–102, February 2014.
- [125] D. Chen and A. P. Arkin. Sequestration-based bistability enables tuning of the switching boundaries and design of a latch. *Molecular systems biology*, 8(1), 2012.
- [126] V. A. Rhodius, T. H. Segall-Shapiro, B. D. Sharon, A. Ghodasara, E. Orlova, H. Tabakh, D. H. Burkhardt, K. Clancy, T. C. Peterson, C. A. Gross, et al. Design of orthogonal genetic switches based on a crosstalk map of σ_s , anti- σ_s , and promoters. *Molecular systems biology*, 9(1), 2013.
- [127] J. Shin and V. Noireaux. An *E. coli* cell-free expression toolbox: application to synthetic gene circuits and artificial cells. *ACS synthetic biology*, 1(1):29–41, 2012.
- [128] A. Tiwari, J. C. J. Ray, J. Narula, and O. A. Igoshin. Bistable responses in bacterial genetic networks: designs and dynamical consequences. *Mathematical biosciences*, 231(1):76–89, 2011.
- [129] J. C. W. Locke, J. W. Young, M. Fontes, M. J. H. Jiménez, and M. B. Elowitz. Stochastic pulse regulation in bacterial stress response. *Science*, 334(6054):366–369, 2011.
- [130] H. Maeda, M. Jishage, T. Nomura, N. Fujita, and A. Ishihama. Two extracytoplasmic function sigma subunits, sigma(E) and sigma(FecI), of *Escherichia coli*: promoter selectivity and intracellular levels. *J Bacteriol*, 182(4):1181–4, February 2000.

- [131] D. J. Scott, A. L. Ferguson, M. T. Gallegos, M. Pitt, M. Buck, and J. G. Hoggett. Interaction of sigma factor sigmaN with Escherichia coli RNA polymerase core enzyme. *Biochem J*, 352 Pt 2:539–47, December 2000.
- [132] V. Bergendahl and R. Burgess. Studying sigma-core interactions in Escherichia coli RNA polymerase by electrophoretic shift assays and luminescence resonance energy transfer. *Meth. Enzymol.*, 370:192–205, 2003.
- [133] J. M. Gilmore, R. J. B. Urbauer, L. Minakhin, V. Akoyev, M. Zolkiewski, K. Severinov, and J. L. Urbauer. Determinants of affinity and activity of the anti-sigma factor AsiA. *Biochemistry*, 49(29):6143–54, July 2010.
- [134] L. J. Lambert, V. Schirf, B. Demeler, M. Cadene, and M. H. Werner. Flipping a genetic switch by subunit exchange. *EMBO J.*, 20(24):7149–59, December 2001.
- [135] B. O. Cezairliyan and R. T. Sauer. Inhibition of regulated proteolysis by RseB. *Proc. Natl. Acad. Sci. U.S.A.*, 104(10):3771–6, March 2007.
- [136] H. Bremer and S. Lin-Chao. Analysis of the physiological control of replication of ColE1-type plasmids. *J. Theor. Biol.*, 123(4):453–70, December 1986.
- [137] S. Liang, M. Bipatnath, Y. Xu, S. Chen, P. Dennis, M. Ehrenberg, and H. Bremer. Activities of constitutive promoters in Escherichia coli. *J Mol Biol*, 292(1):19–37, September 1999.
- [138] S. Klumpp and T. Hwa. Stochasticity and traffic jams in the transcription of ribosomal RNA: Intriguing role of termination and antitermination. *Proc. Natl. Acad. Sci. U.S.A.*, 105(47):18159–64, November 2008.
- [139] I. M. Keseler et al. EcoCyc: fusing model organism databases with systems biology. *Nucleic Acids Res.*, 41(Database issue):D605–12, January 2013.
- [140] S. Klumpp, Z. Zhang, and T. Hwa. Growth Rate-Dependent Global Effects on Gene Expression in Bacteria. *Cell*, 139(7):1366–1375, December 2009.